Study of the Influence of Extreme Environmental Conditions on the Behavior of Macrosynthetic Fiber Reinforced Concretes

DOCTORAL THESIS

Author: Marta Caballero Jorna

Thesis directors:
Prof. Pedro Serna Ros
Dr. Marta Roig Flores

Valencia, Spain
May 2024

UNIVERSITAT POLITÈCNICA DE VALÈNCIA
PROGRAMA DE DOCTORADO EN INGENIERÍA DE LA CONSTRUCCIÓN

Study of the Influence of Extreme Environmental Conditions on the Behavior of Macrosynthetic Fiber Reinforced Concretes

Estudio de la influencia de condiciones ambientales extremas en el comportamiento de hormigones reforzados con macrofibras sintéticas

by

MARTA CABALLERO JORNA

Submitted in fulfillment of the requirements for the degree of Doctor of Philosophy in Building Engineering from the Departamento de Ingeniería de la Construcción y Proyectos de Ingeniería Civil of the Universitat Politècnica de València

Supervisors:

Prof. Pedro Serna

Dr. Marta Roig Flores

Departamento de Ingeniería de la Construcción y Proyectos de Ingeniería Civil

Instituto de Ciencia y Tecnología del Hormigón (ICITECH)

External evaluation committee:

Thesis committee:

UNIVERSITAT POLITÈCNICA DE VALÈNCIA
Valencia, Spain

May 2024

A mis padres,

Acknowledgments

Es de bien nacidos ser agradecidos, por eso, aprovecho este espacio para dedicar unas palabras de agradecimiento a todas las personas que me han acompañado y alentado en este gran reto durante estos años de mi vida.

En primer lugar, doy gracias inmensas a mis tutores. Pedro, Marta (R), gracias por haber sido guía y apoyo (tanto personal como académico) durante esta andadura. Tengo claro que no hubiera llegado hasta aquí sin vosotros. Gracias por todo el tiempo de calidad que me habéis brindado, por todo lo compartido y por todo lo aprendido. Asimismo, quiero agradecer a mi tutora en colaboración de prácticas docentes, Ester Giménez, su compromiso desinteresado y a Concha Pacheco, por haber apostado por mi desde mis inicios.

En segundo lugar, gracias a mis amigos del grupo de investigación NNRG que me ofrecieron su apoyo y su ayuda de forma incondicional. A Paco y a todo el equipo técnico que ha estado conmigo al pie del cañón, sin el cual el trabajo experimental hubiera sido mucho más duro. A Sidi, Aitor, Edu, David, Ronny, Michela, Ger, Francisco, Majid, Kiran, Pardis, Nacho, gracias a todos. En especial, quiero agradecerle a Hesam, el haber caminado conmigo de la mano desde el principio. Te deseo toda la suerte del mundo en esta nueva etapa que también comienza para ti, Doostkami. Igualmente, me gustaría dar las gracias a los compañeros de BLA BLA CIRI, que hicieron de mi estancia en Bolonia una experiencia magnífica y como no, a todos los compañeros (y ahora amigos) del ICI-TECH.

En tercer lugar, a mis amigos, por motivarme a seguir siempre hacia adelante, a levantarme cuando me he caído, a perseverar y a confiar en mí. En especial, a M.ª Carmen, por ser y estar y a Carlos y a Paola, por el sprint final. Me gustaría poder enumerar a todos y cada uno de ellos, pero se haría interminable. Estoy muy agradecida por toda la gente que está a mi lado; a todos aquellos que han puesto de su parte para que pudiera finalizar esta tesis doctoral, GRACIAS.

Y, por último, pero no por ello menos importante, quiero agradecer a mi familia, por estar incluso en la distancia. Papá, al final, te hice caso. A mi madre, a mi tita, a mis hermanos Dani y Alberto, no tengo palabras para vosotros, os quiero.

Abstract

Adding fibers into concrete-matrix has been a common practice since the sixties to enhance the properties of traditional concretes. Over time, advancements in construction sector have led to the introduction of various fiber types into the market, resulting on different types of Fiber Reinforced Concretes (FRCs). Unlike steel fibers, macrosynthetic fibers are a more recent addition. Despite studies on their behavior, there has not been investigated deeply how temperature affects macrosynthetic fiber reinforced concrete (MSFRC). The use of MSFRC could be promoted as long as further investigations into their behavior were carried out to verify their performance and mitigate mistrust.

The purpose of this Thesis comes from the need to understand the mechanical behavior of MSFRC under non-standard temperatures and to clarify certain implications, as pre-cracking state of MSFRC elements in terms of aging (by temperature). This work analyzes the short- (3 days of exposure) and long-term (90 and 180 days of exposure) behavior of three types of MSFRCs and one steel fiber reinforced concrete (SFRC) at different extreme environmental conditions (temperatures ranging from -15 to 60 °C). Additionally, the behavior of a commercial macro synthetic fiber is evaluated at single-fiber level (from -30 to 140 °C) and the interaction between fiber and matrix is also studied at mesoscale (from -30 to 40 °C). Different methodologies have been used to investigate herein: compression tests in 150 mm side cubes and three-point bending tests in 150 × 150 × 600 mm beams, uniaxial tests on individual fibers and on notched cylinders of 150 × Ø 125 mm. All these tests were performed in specimens at service conditions, that is, tested at the target temperatures, making a total of 186 cubes, 434 beams, 210 fibers and 30 cylinders.

The results show that properties of the studied fiber are dependent on temperature. Additionally, temperature and time of exposure affect mechanical properties of MSFRCs, but their effects are not to a great extent. These results are supported by a statical study which, in turn, have allowed to develop a simple numerical approach to the mechanical properties of FRC when designing for extreme environmental conditions over time. This Thesis advances the understanding of the FRCs, particularly MSFRCs, which may be improved their use in some civil engineering applications.

Resumen

La adición de fibras a la matriz cementicia ha sido una práctica común desde los años sesenta para mejorar las propiedades de los hormigones tradicionales. Con el tiempo, los avances en la tecnología han llevado a la introducción de varios tipos de fibras en el mercado, dado lugar a diferentes tipos de hormigones reforzados con fibras (FRC). En comparación con las fibras de acero, las macro-fibras sintéticas han aparecido recientemente. A pesar de los estudios sobre su comportamiento, no se ha estudiado exhaustivamente cómo la temperatura afecta al hormigón reforzado con macro-fibras sintéticas (MSFRC). El uso de MSFRC podría promoverse siempre y cuando se llevaran a cabo más investigaciones sobre su comportamiento para verificar su desempeño.

El propósito de esta Tesis surge de la necesidad de comprender el comportamiento mecánico del MSFRC bajo temperaturas y aclarar ciertas implicaciones, como el efecto de la prefisuración en su envejecimiento (por temperatura). Este trabajo analiza el comportamiento a corto (3 días de exposición) y largo plazo (90 y 180 días de exposición) de tres tipos de MSFRCs y un hormigón reforzado con fibras de acero (SFRC) bajo diferentes condiciones ambientales extremas (temperaturas que oscilan entre -15 y 60 °C). Además, se evalúa el comportamiento de una macro-fibra sintética comercial, a nivel de filamento (de -30 a 140 °C) y también se estudia la interacción entre la fibra y la matriz a meso-escala (de -30 a 40 °C). Para su investigación, se han utilizado diferentes metodologías: compresión en cubos de 150 mm de lado y ensayos de flexión a tres puntos en vigas de 150 × 150 × 600 mm, ensayo uniaxial en fibras y en cilindros entallados de 150 × Ø125 mm. Todos estos ensayos se realizaron bajo las temperaturas objetivo.

Los resultados muestran que las propiedades de la fibra estudiada dependen de la temperatura. Además, la temperatura y del tiempo de exposición afectan las propiedades mecánicas analizadas de los MSFRCs, pero estos efectos no son muy importantes. Estos resultados están respaldados por un estudio estadístico que, a su vez, ha permitido desarrollar una aproximación numérica simple a las propiedades mecánicas del FRC cuando se diseña para condiciones ambientales extremas a lo largo del tiempo. Esta Tesis promueve la comprensión de los FRCs, particularmente los MSFRCs, mejorando la confianza en su aplicación en proyectos de ingeniería civil.

Resum

L'addició de fibres a la matriu cimentosa ha sigut una pràctica comuna des dels anys seixanta per a millorar les propietats dels formigons tradicionals. Amb el temps, els avanços en la tecnologia han portat a la introducció de diversos tipus de fibres en el mercat, resultant en diferents tipus de formigons reforçats amb fibres (FRC). En comparació amb les fibres d'acer, les macro- fibres sintètiques han aparegut recentment. Malgrat els estudis sobre el seu comportament, no s'ha estudiat exhaustivament com la temperatura afecta al formigó reforçat amb macro-fibres sintètiques (MSFRC). L'ús de MSFRC podria promoure's sempre que es dugueren a terme més investigacions sobre el seu comportament per a el seu acompliment.

El propòsit d'esta Tesi sorgix de la necessitat de comprendre el comportament mecànic del MSFRC sota temperatures no estàndard i aclarir unes certes implicacions, com a elements MSFRC prefissurats i no prefissurats, en termes d'envelliment (per temperatura). Este treball analitza el comportament a curt (3 dies d'exposició) i llarg termini (90 i 180 dies d'exposició) de tres tipus de MSFRCs i un formigó reforçat amb fibres d'acer (SFRC) baix diferents condicions ambientals extremes (temperatures que oscil·len entre -15 i 60 °C). A més, s'avalua el comportament d'una fibra comercial tipus II, a nivell de filament (de -30 a 140 °C) i també s'estudia la interacció entre la fibra i la matriu a meso-escala (de -30 a 40 °C). Per al seu investigació, s'han utilitzat diferents metodologies: compressió en cubs de 150 mm de costat i assajos de flexió en tres punts en bigues de 150 × 150 × 600 mm, assaig uniaxial en fibres i en cilindres dentats de 200 × Ø125 mm. Tots estos assajos es van realitzar en condicions de servici, és a dir, a les temperatures objectiu.

Els resultats mostren que les propietats de la fibra estudiada depengen de la temperatura. A més, la temperatura i el temps de exposició són factors importants en les propietats mecàniques analitzades dels MSFRCs. Estos resultats estan recolzats per un estudi estadístic que, al seu torn, ha permés desenvolupar una aproximació numèrica simple a les propietats mecàniques del FRC quan es dissenya per a condicions ambientals extremes al llarg del temps. Esta Tesi promou la comprensió dels FRC, particularment els MSFRC, que poden millorar la confiança en l'aplicació de MSFRC en projectes d'enginyeria civil.

Index

Acknowledgments vii
Abstract ix
Resumen xi
Resum xiii
List of Figures xxvii
List of Tables xxxiii
Glossary xl
Chapter 1. Introduction 1
  1.1. Context 1
  1.2. Objectives 4
  1.3. Structure of the Document 5
Chapter 2. State of the Art 7
  2.1. Fiber Reinforced Concrete 8
    2.1.1. Origin and Concept 8
    2.1.2. Types of FRCs 9
  2.2. Macrosynthetic Fiber Reinforced Concrete (MSFRC) 11
    2.2.1. Types of Synthetic Fibers 12
      a) Micro vs macro fibers 12
      b) Material of the fiber 13
        i) PP fibers 14
    2.2.2. Fresh and Hardened State Properties of MSFRC 16
      a) Fresh state properties 17
      b) Hardened state properties 17

i) Tests for the evaluation of flexural strengths in MSFRC..... 18
2.2.3. MSFRC Applications.. 19
2.3. Durability based on the Influence of Extreme Environmental Conditions on the Behavior of MSFRCs.. 21
2.3.1. Influence of Temperature on Synthetic Fibers 22
a) Critical properties 23
b) Durability of PP fibers.. 25
i) Chemical and aggressive agents 25
ii) Creep.. 26
iii) Temperature 27
c) Comparison of methodologies.. 28
2.3.2. Influence of Temperature on Plain Concrete and on FRCs 29
a) Compressive strength 29
i) Studies at elevated temperatures....................................... 29
ii) Studies at low and sub-zero temperatures 30
iii) Studies regarding to humidity content 32
iv) Summary on compressive strength under extreme environmental conditions.. 32
b) Tensile and flexural strengths 33
i) Studies at elevated temperatures....................................... 33
ii) Studies at low and sub-zero temperatures 34
iii) Long-term studies at temperatures.................................... 36
iv) Comparison of methodologies.. 37
v) Summary on tensile and flexural strength at temperatures 40
2.3.3. Influence of Temperature on the Fiber-matrix Interface........... 40
a) Fiber-matrix interface structure at nano- and micro- scale......... 41
b) Fiber-matrix interface properties in meso- scale 42
i) Comparison of methodologies.. 44
2.4. Design Specifications of MSFRC 47
2.4.1. Fib Model Code... 47
2.4.2. International Recommendations, Codes and Standards.......... 49

2.5. Critical Summary 49
Chapter 3. Experimental Program and Methodology 51
3.1. Outline of the Research Activity 52
3.1.1. First Study: Short-term Exposure 52
3.1.2. Second Study: Long-term Exposure 53
3.2. Experimental Program 54
3.2.1. First Study: Short-term Exposure 54
a) First experimental campaign: single fiber tensile strength 54
b) Second experimental campaign: FRC compressive strength 55
c) Third experimental campaign: FRC flexural tensile strength 56
d) Fourth experimental campaign: FRC direct tensile strength 57
3.2.2. Second Study: Long-term Exposure 57
a) First experimental campaign: FRC compressive strength 58
b) Second experimental campaign: FRC flexural tensile strengths 58
3.3. Materials 59
3.3.1. Fibers used 59
3.3.2. Concrete Mix Design used 61
a) Experimental campaigns on compressive and flexural tensile strengths 61
i) Characterization tests 63
b) Experimental campaign on direct tensile strength 64
i) Characterization tests 66
3.4. Methodology 66
3.4.1. Simulation of Extreme Environmental Conditions 66
a) Fiber level 66
b) Material level 67
3.4.2. Selection of the Time of Exposure 69
3.4.3. Testing Properties at Temperatures 70
a) Fiber level 71
b) Material level: compressive, flexural and direct tensile strengths 72
i) Compressive strengths 72

ii) Flexural tensile strengths 73
iii) Influence of an existing pre-crack 75
iv) Direct tensile strength 76
3.4.4. Temperature Control During the Tests 79
Chapter 4. Behavior of MSFRCs under Different Environmental Conditions at Short-term Exposure 81
4.1. Influence of Environmental Conditions on Fiber's Behavior 82
4.2. Influence of Environmental Conditions on Compressive Strengths 89
4.3. Influence of Environmental Conditions on Flexural Strengths 93
4.3.1. Combined Effect of Pre-cracking and Temperature on Flexural Tensile Strengths 98
4.3.2. Effect of Number of Fibers on Flexural Tensile Strengths 102
a) Study of the number of fibers present in the cross-section 102
b) Effect of number of fibers on flexural strengths at temperature 107
4.4. Influence of Environmental Conditions on Direct Tensile Strengths 109
4.4.1. Effect of the Number of Fibers present in the Cross-section on Direct Tensile Strengths at Temperatures 113
4.4.2. Study on the Fiber Breakage (inside concrete-matrix) at Temperatures 115
4.5. General Discussion 116
4.5.1. Single-fiber Level: Discussion 116
4.5.2. Material Level: Discussion 117
a) Compression behavior 117
b) Flexural behavior 118
c) Tensile behavior 121
4.5.3. Comparison between the Study Levels 122
4.5.4. Summary of the Results 123
Chapter 5. Behavior of MSFRCs after Long-term Exposure under Different Environmental Conditions 125
5.1. Influence of Environmental Conditions on Compressive Strengths 126
5.1.1. Compressive Strength's Results after 90 days of exposure 126

5.1.2. Compressive Strength's Results after 180 days of exposure. 128

5.1.3. Analysis of Aging: Comparison between 3, 90 vs 180 Days' Compression Results under Temperatures.. 130

5.2. Influence of Environmental Conditions on Flexural Strengths 133

5.2.1. Effect of Temperature on Flexural Tensile Strengths in Non-Pre-Cracked State at long-term 134

a) Flexural strength's results after 90 days of exposure 134

b) Flexural strength's results after 180 days of exposure 136

c) Analysis of aging: comparison between short- and long-term bending results under extreme environmental conditions.................. 141

5.2.2. Combined Effect of Pre-cracking and Temperature on Flexural Tensile Strengths at long-term 144

a) Flexural strength's results after 90 days of exposure 144

b) Flexural strength's results after 180 days of exposure 146

c) Comparison between non-pre-cracked and pre-cracked state bending results under extreme environmental conditions.................. 149

5.2.3. Effect of Number of Fibers on Flexural Tensile Strengths at Extreme Environmental Conditions 151

a) Study of the number of fibers present in the fracture surface... 152

b) Flexural strength's results considering N after 90 days of exposure 156

c) Flexural strength's results considering N after 180 days of exposure 157

d) Analysis of aging: comparison between short- and long-term residual flexural results (considering N) under extreme environmental conditions 159

5.3. General Discussion 170

5.3.1. Compressive Behavior 170

5.3.2. Flexural Behavior 171

5.3.3. Aging 174

5.3.4. General Summary 179

Chapter 6. Statistical Analysis of the Results of the FRC Flexural Behavior under extreme environmental conditions over time 181

6.1. Introduction to the Exploratory Data Analysis performed............. 181

6.2. Statistical Study of the Influence of “State” factor on Flexural Strengths of FRCs at Extreme Environmental Conditions 184
6.2.1. f_{R3} 184
6.2.2. f_{R3}/N 185
6.2.3. Summary of Results of Statistical Analysis for State............. 185
6.3. Statistical Study of Flexural Strengths of MSFRC (PF1) at Extreme Environmental Conditions.. 185
6.3.1. f_{LOP} 186
a) Inter-groups variability – short-term vs. long-term effects 186
b) Inter-groups variability – temperature effects 187
6.3.2. f_{R1} 188
a) Inter-groups variability – short-term vs. long-term effects 189
6.3.3. f_{R1}/N 189
a) Inter-groups variability – short-term vs. long-term effects 190
6.3.4. f_{R3} 191
a) Inter-groups variability – short-term vs. long-term effects 191
b) Inter-groups variability – temperature effect............................ 191
6.3.5. f_{R3}/N 192
a) Inter-groups variability – short-term vs. long-term effects 193
b) Inter-groups variability – temperature effects 193
6.3.6. Summary of Results of Statistical Study for MSFRC-PF1...... 194
6.4. Statistical Study of Flexural Strengths of MSFRC (PF2) at Extreme Environmental Conditions.. 195
6.4.1. f_{LOP} 196
a) Inter-groups variability – temperature effects 196
6.4.2. f_{R1} 197
a) Inter-groups variability – temperature effects 197
6.4.3. f_{R1}/N 198
6.4.4. f_{R3} 198
a) Inter-groups variability – temperature effect............................ 199
6.4.5. f_{R3}/N 199

a) Inter-groups variability – temperature effects 200
6.4.6. Summary of Results of Statistical Analysis for MSFRC-PF2.. 200
6.5. Statistical Study of Flexural Strengths of MSFRC (PF3) at Extreme Environmental Conditions 201
6.5.1. f_{LOP} 201
a) Inter-groups variability – temperature effects 202
6.5.2. f_{R1} 202
a) Inter-groups variability – temperature effects 203
6.5.3. f_{R1}/N 203
a) Inter-groups variability – temperature effects 204
6.5.4. f_{R3} 204
a) Inter-groups variability – temperature effect 205
6.5.5. f_{R3}/N 205
a) Inter-groups variability – temperature effects 206
6.5.6. Summary of Results for MSFRC-PF3 206
6.6. Statistical Study of Flexural Strengths of SFRC at Extreme Environmental Conditions 207
6.6.1. f_{LOP} 207
a) Inter-groups variability – short-term vs. long-term effects......... 207
b) Inter-groups variability – temperature effects 208
6.6.2. f_{R1} 209
a) Inter-groups variability – short-term vs. long-term effects......... 209
6.6.3. f_{R1}/N 210
a) Inter-groups variability – short-term vs. long-term effects......... 211
6.6.4. f_{R3} 211
6.6.5. f_{R3}/N 212
6.6.6. Summary of Results for SFRC-SF 212
6.7. General Summary of the Statistical Study of Flexural Strengths of FRCs at Extreme Environmental Conditions over Time............................ 212
6.7.1. Effects of Extreme Environmental Conditions (temperature) . 213
6.7.2. Other effects 213

6.8. Proposal of Simple Numerical Equations for Flexural Behavior of FRCs under Different Extreme Environment Conditions 214
6.8.1. Numerical Equations for Flexural Behavior of MSFRC-PF1 .. 215
a) f_{LOP} 215
b) f_{R1} 216
c) f_{R1}/N 217
d) f_{R3} 217
e) f_{R3}/N 218
6.8.2. Numerical Equations for Flexural Behavior of MSFRC-PF2 .. 219
a) f_{LOP} 219
b) f_{R1} 219
b) f_{R1}/N 220
d) f_{R3} 221
e) f_{R3}/N 221
6.8.3. Numerical Equations for Flexural Behavior of MSFRC-PF3 .. 222
a) f_{LOP} 222
b) f_{R1} 223
c) f_{R1}/N 223
d) f_{R3} 224
e) f_{R3}/N 225
6.8.4. Numerical Equations for Flexural Behavior of SFRCs 225
a) f_{LOP} 225
b) f_{R1} 226
c) f_{R1}/N 227
d) f_{R3} 227
e) f_{R3}/N 228
6.9. General Summary of the Regression Study 229
6.9.1. Response Surfaces 231
Chapter 7. Conclusions and Future Research 239
7.1. Conclusions 239

7.1.1. Conclusions Derived from Short-term Experimental Campaigns 239
7.1.2. Conclusions Derived from Long-term Experimental Campaigns 241
7.1.3. Conclusions Derived from the Statistical Analysis 242
7.2. Future Research 243
7.3. Publications Derived from this Thesis 244
References 247

List of Figures

Figure 1. Comparison of publications and citations in SFRC and MSFRC........ 2
Figure 2. Publication and Citation Report on MSFRCs and temperature. 3
Figure 3. Outline of the Chapter 2. 8
Figure 4. Regimes of fiber content in FRCs [23]. 11
Figure 5. Different effect on plain concrete of micro and macro fibers [56]. 13
Figure 6. Typical shapes of PP fibers used as mortars and concretes reinforcement with different sections (from left to right): square embossed, circle corrugate and twisted [23]. 15
Figure 7. Diagram of two kinds of fiber-cement paste interface in FRC (steel fiber above and synthetic fiber below) [68].. 16
Figure 8. Typical stress-CMOD curve for FRC obtained by EN 14651 [82]..... 18
Figure 9. MSFRC applications: (a) General paving for Palo Verde Wastewater Reclamation Facility Expansion, in USA; (b) Shotcrete ground support for Brisbane Cross River Rail Shotcrete Lining, in Australia; (c) Concrete topping for Scheldt Bridge, in Belgium and (d) Segmental lining for Pista Nueva Malaga Rail Tunnel project, in Spain [103]. 20
Figure 10. Continuous operating temperature for plastics [115]...................... 22
Figure 11. Temperature-dependence on PP fibers [118]. 23
Figure 12. Cracking due to incompatibility of thermal deformation between steel fibers and concrete-matrix [121]... 24
Figure 13. Thermal expansion coefficients of different materials at ambient temperature... 24
Figure 14. Comparison of the Poisson's ratio for different materials at standard temperature... 25
Figure 15. Polypropylene photo-oxidation (degradation) scheme [124]. 26
Figure 16. (a) Stress-strain curves and (b) Single fiber tensile creep behavior from -10 to 60 °C [131]... 27
Figure 17. Compressive strength results in terms of temperature [138]. 30
Figure 18. Experimental values of modulus of elasticity and compressive strength of plain concrete vs temperature—expressed as a percentage of the values measured at 20 °C [145]... 31
Figure 19. Relationship between compressive strength and the strength classes in plain concrete at positive and negative temperatures [148]. 31

Figure 20. Measured values of compressive strength of water-saturated and partially dried concrete vs temperature— expressed as a percentage of the values measured at 20°C [145]. 32
Figure 21. Effective fracture toughness for plain concrete exposed to dry environments under different temperatures [154]. 33
Figure 22. Comparison of (a) MSFRC (PP fibers), and (b) SFRC at varying temperatures, in terms of flexural strength at various CMOD [155]. 34
Figure 23. Flexural strength results in terms of temperature [138]. 34
Figure 24. Effect of low temperatures on (a) tensile strength and (b) fracture energy of concrete [159]. 35
Figure 25. Mean values of f_{R1} and f_{R3} of the different MSFRCs under low temperatures [162]. 36
Figure 26. Different methodologies used to evaluate temperature factor: (a) [178]; (b) [162]; (c) [167]; (d) [177]; (e) [148]; and (f) [179]. 39
Figure 27. Schematic representation of the fiber-matrix interface of an FRC [185]. 41
Figure 28. Pull out – test rig [155]. 43
Figure 29. Representation of the multiscale structure of FRC and the typical test means [187]. 45
Figure 30. Differences between the approaches to determine the tensile properties of MSFRCs [199]. 46
Figure 31. Fibers used: (a) PF1; (b) PF2; (c); PF3 and (d) SF. 61
Figure 32. (a) P375T08 planetary concrete mixer used; (b) adding water to the mixing; (c) FRC cubes after pouring and compacting and (d) FRC beams after pouring and compacting. 63
Figure 33. Photos of some of the characterization tests performed: (a) slump; (b) air content; (c) fresh density, and (d) compressive tests. 64
Figure 34. (a) Vibrating the concrete poured into the moulds and (b) FRC specimens after pouring and compacting. 65
Figure 35. Example of some of the characterization tests performed: (a) slump, and (b) compression tests. 66
Figure 36. MTS 651 Environmental Chamber. 67
Figure 37. Simulation of conditions during the experimental interface study... 69
Figure 38. Location of the thermocouple (T) in concrete beams in the core (all dimensions in mm). 69
Figure 39. Location of the thermocouple in concrete cylinders in the core (all dimensions in cm). 70
Figure 40. Photos of fiber tensile test procedure: (a) Aluminum plates used to hold fiber during the test; and (b), (c) Tightening of plates to prevent fiber slip. 71
Figure 41. Set-up for direct tensile test on fibers at low temperatures. Nitrogen liquid incorporated to the MTS 651 environmental chamber. 71

Figure 42. (a) Fiber test set-up inside temperature chamber; (b) Zoomed view of fiber and plates in position before testing. 72
Figure 43. Insulation system used during compression test. 73
Figure 44. Insulation system used during 3PBTs. 74
Figure 45. (a) Dividing the specimens into two halves after testing to produce fracture surfaces (b) Examples of fracture surfaces for specimens reinforced with macro synthetic (above) and steel fibers (with the thirds marked). 75
Figure 46. CMOD-Stress diagram: (a) first stage at standard temperature and (b) complete procedure. 76
Figure 47. Phases of the cylinder coring. 77
Figure 48. (a) Scheme of the process of coring; (b) Preparation of the cylinders. 77
Figure 49. (a) Set-up for tensile direct tests on cylinders at temperature; (b) Cylinder after testing under tensile direct. 78
Figure 50. Difference between slipped and broken fibers in a cross-section tested. 79
Figure 51. Results obtained from the thermocouple installed in the core of the beams for each temperature during the performance of the flexural test. 79
Figure 52. Checking surface temperature after testing and removing the insulation system on: (a) a warmed beam (at 40 °C) and (b) a cooled cube (at -15 °C). 80
Figure 53. Outline of the Chapter 4. 82
Figure 54. Average UTS vs. Stress rate at different temperatures. 85
Figure 55. Average E-Modulus vs. Stress rate at different temperatures. 87
Figure 56. Comparison of the mean stress-strain curves of the target fiber at temperatures at 9 MPa/s. 88
Figure 57. Curves obtained in compression tests at temperatures at short-term for: (a) PF1 cubes; (b) PF2 cubes; (c) PF3 cubes and (d) SF cubes. 91
Figure 58. Compressive strengths after 3 days of conservation at different temperatures for the studied FRCs. 92
Figure 59. Debonded paste aggregate at 60 °C. 93
Figure 60. Flexural behavior of MSFRC-PF1 at non-pre-cracked state: (a) at -15 °C; (b) at 5 °C; (c) at 20 °C; (d) at 20 °C, in water immersion; (e) at 40 °C, and (f) at 60 °C, in water immersion. 95
Figure 61. Flexural behavior of MSFRC-PF2 at non-pre-cracked state: (a) at -15 °C; (b) at 20 °C; and (c) at 60 °C, in water immersion. 96
Figure 62. Flexural behavior of MSFRC-PF3 at non-pre-cracked state: (a) at -15 °C; (b) at 20 °C; and (c) at 60 °C, in water immersion. 97
Figure 63. Flexural behavior of SFRC at non-pre-cracked state: (a) at -15 °C; (b) at 20 °C; (c) at 20 °C, in water immersion; and (d) at 60 °C, in water immersion. 98

Figure 64. Flexural behavior of MSFRC (with PF1 fibers) and SFRC in pre-cracked specimens: (a) at -15 °C; (b) at 5 °C; (c) at 20 °C; (d) at 20 °C, in water immersion; (e) at 40 °C, and (f) at 60 °C, in water immersion. 101
Figure 65. Average stress-CMOD curves of pre-cracked and non-pre-cracked specimens: (a) PF1-N; (b) PF1-P; (c) SF-N and (d) SF-P. 102
Figure 66. The total number of fibers at the cross-section for each type of fiber according to the number of events (N. Events): (a) non-pre-cracked and (b) pre-cracked specimens. 104
Figure 67. Linear regressions trend of residual flexural strength f_{R1} as a function of the number of fibers and temperatures for MSFRC-PF1 in pre-cracked specimens: (a) fibers in the lower third and (b) total number of fibers.... 106
Figure 68. Linear regressions trend of residual flexural strength f_{R3} as a function of the number of fibers and temperatures for MSFRC-PF1 in pre-cracked specimens. 107
Figure 69. Normalized residual flexural strength f_{R1} and f_{R3} after short-term exposure at the target environmental conditions: (a) f_{R1}/N for non-pre-cracked specimens; and (b) f_{R3}/N for non-pre-cracked specimens. 108
Figure 70. Normalized residual flexural strength f_{R3}/N after short-term exposure at the target environmental conditions for pre-cracked specimens. 109
Figure 71. Comparison of the mean stress-COD curves of cylinders at temperatures. 111
Figure 72. (a): Maximum stress values after the first peak (second peak) versus target temperatures, and (b): COD values corresponding to the second peak versus target temperatures. 112
Figure 73. Linear regression trend of residual strengths as a function of the total number of fibers: (a) f_{R1}*;(b) f_{R2}*; (c) f_{R3}* and (d) f_{R4}*. 113
Figure 74. Example of a cylinder with a non-homogeneous distribution of fiber on its fracture surface. 114
Figure 75. Comparison of the mean stress-COD curves, considering N, of cylinders at temperatures. 115
Figure 76. Correlation between the ratio number of broken fibers (N_{broken}) divided by the total number of fibers (N), depending on the temperature. 116
Figure 77. Comparison of the obtained results for all the levels of study (fiber and material) in this work at different temperatures (-30 to 40 °C)......... 122
Figure 78. Outline of the Chapter 5. 126
Figure 79. Curves obtained in compression tests at temperatures for: (a) PF1 cubes; and (b) SF cubes, after 90 days subjected to -15 and 60 °C in immersion. 128
Figure 80. Curves obtained in compression tests at temperatures for: (a) PF1 cubes; (b) PF2 cubes; (c) PF3 cubes and (d) SF cubes, after 180 days of exposure. 130
Figure 81. Comparison between 3, 90 vs 180 days' compression results under temperatures for: (a) PF1, (b) PF2, (c) PF3 and (d) SF. 133

Figure 82. Flexural behavior of MSFRC-PF1 at non-pre-cracked state after 90 days: (a) at -15 °C; (b) at 20 °C, and (c) at 60 °C, in water immersion... 135
Figure 83. Flexural behavior of SFRC at non-pre-cracked state after 90 days: (a) at -15 °C; (b) at 20 °C, and (c) at 60 °C, in water immersion. 136
Figure 84. Flexural behavior of MSFRC-PF1 at non-pre-cracked state after 180 days: (a) at -15 °C; (b) at 5 °C; (c) at 20 °C; (d) at 20 °C, in water immersion; (e) at 40 °C, and (c) at 60 °C, in water immersion................................. 138
Figure 85. Flexural behavior of MSFRC-PF2 at non-pre-cracked state after 180 days: (a) at -15 °C; (b) at 20 °C; (c) at 40 °C, and (d) at 60 °C, in water immersion. 139
Figure 86. Flexural behavior of MSFRC-PF3 at non-pre-cracked state after 180 days: (a) at -15 °C; (b) at 20 °C; (c) at 40 °C, and (d) at 60 °C, in water immersion. 140
Figure 87. Flexural behavior of SFRC at non-pre-cracked state after 180 days: (a) at -15 °C; (b) at 20 °C; (c) at 20 °C, in water immersion, and (d) at 60 °C, in water immersion. 141
Figure 88. Flexural behavior of MSFRC (with PF1 fibers) and SFRC in pre-cracked specimens after 90 days: (a) at -15 °C and (b) at 60 °C, in water immersion. 146
Figure 89. Flexural behavior of MSFRC (with PF1 fibers) and SFRC in pre-cracked specimens after 180 days: (a) at -15 °C; (b) at 20 °C; (c) at 20 °C, in water immersion and (d) at 60 °C, in water immersion...................... 148
Figure 90. Average stress-CMOD curves of non-pre-cracked and pre-cracked specimens: (a) PF1-N; (b) PF1-P; (c) SF-N and (d) SF-P, after 90 days of exposition at different temperatures.. 150
Figure 91. Average stress-CMOD curves of non-pre-cracked and pre-cracked specimens: (a) PF1-N; (b) PF1-P; (c) SF-N and (d) SF-P, after 180 days of exposition at different temperatures.. 151
Figure 92. The total number of fibers at the cross-section for each type of fiber according to the number of events (N. Events) for (a) non-pre cracked specimens and (b) for pre-cracked specimens at 90 days.................... 154
Figure 93. The total number of fibers at the cross-section for each type of fiber according to the number of events (N. Events) for (a) non-pre cracked specimens and (b) pre-cracked specimens at 180 days. 155
Figure 94. Normalized residual flexural strength f_{R1} and f_{R3} after long-term exposure (90 days) at the target environmental conditions: (a) f_{R1}/N for non-pre-cracked specimens; and (b) f_{R3}/N for non-pre-cracked specimens.. 156
Figure 95. Normalized residual flexural strengt f_{R3}/N for pre-cracked specimens. 157
Figure 96. Normalized residual flexural strength f_{R1} and f_{R3} after long-term exposure (180 days) at the target environmental conditions: (a) f_{R1}/N for non-pre-cracked specimens; and (b) f_{R3}/N for non-pre-cracked specimens. 158

Figure 97. Normalized residual flexural strength f_{R3}/N for pre-cracked specimens. 159
Figure 98. Evolution of residual strengths of the different types of FRCs studied at -15 °C: (a) MSFRC-PF1 in non-pre-cracked specimens; (b) MSFRC-PF1 in pre-cracked specimens; (c) MSFRC-PF2 in non-pre-cracked specimens; (d) MSFRC-PF3 in non-pre-cracked specimens; (e) SFRC-SF in non-pre-cracked specimens and (f) SFRC-SF in pre-cracked specimens. 162
Figure 99. Evolution of residual strengths of the different types of FRCs studied at 20 °C: (a) MSFRC-PF1 specimens; (b) SFRC-SF specimens; (c) MSFRC-PF2 in non-pre-cracked specimens, and (d) MSFRC-PF3 in non-pre-cracked specimens. 164
Figure 100. Evolution of residual strengths of the different types of FRCs studied at 60 °C, in immersion: (a) MSFRC-PF1 in non-pre-cracked specimens; (b) MSFRC-PF1 in pre-cracked specimens; (c) MSFRC-PF2 in non-pre-cracked specimens; (d) MSFRC-PF3 in non-pre-cracked specimens; (e) SFRC-SF in non-pre-cracked specimens and (f) SFRC-SF in pre-cracked specimens. 167
Figure 101. Comparison of the results from 3PBT for MSFRC reinforced with PF1: (a) at 3 days in non-pre-cracked state; (b) at 180 days in non-pre-cracked state; (c) at 3 days in pre-cracked state and (d) at 180 days in pre-cracked state. 177
Figure 102. Comparison of the results from 3PBT for MSFRC reinforced with PF2: (a) at 3 days in non-pre-cracked state, and (b) at 180 days in non-pre-cracked state. 178
Figure 103. Comparison of the results from 3PBT for MSFRC reinforced with PF3: (a) at 3 days in non-pre-cracked state, and (b) at 180 days in non-pre-cracked state. 178
Figure 104. Comparison of the results from 3PBT for SFRC reinforced with SF: (a) at 3 days in non-pre-cracked state; (b) at 180 days in non-pre-cracked state; (c) at 3 days in pre-cracked state and (d) at 180 days in pre-cracked state. 179
Figure 105. Response surface for MSFRC-PF1 over time: (a) f_{LOP}, (b) f_{R1}, and (c) f_{R3}. 232
Figure 106. Response surface for MSFRC-PF2 over time: (a) f_{LOP}, (b) f_{R1} and (c) f_{R3}. 233
Figure 107. Response surface for MSFRC-PF3 over time: (a) f_{LOP}, (b) f_{R1} and (c) f_{R3}. 234
Figure 108. Response surface for SFRC over time: (a) f_{LOP} (b) f_{R1} and (c) f_{R3}. 235

List of Tables

Table 1. Properties of the most common fibers, extracted from [23]. 10
Table 2. Synthetic fiber reinforcement and their properties, adapted from [23]. 14
Table 3. Experimental program implemented in this Thesis. 52
Table 4. Summary of the number and specimen type, their dimensions and the type of test performed at short-term. 54
Table 5. Stress Rate according to [205]. 55
Table 6. Experimental study at single fiber level on tensile strength of fibers at short-term, including Nº of specimens performed. 55
Table 7. Exposure conditions used and their codes. 56
Table 8. Number of cubes at FRC level on compressive strength on FRCs at 3 days of exposure. 56
Table 9. Number of beams tested at the FRC level on flexural tensile strengths on FRCs at 3 days of exposure. 57
Table 10. Experimental campaign on direct tensile strength on MSFRC-PF1 at 3 days of exposure, including Nº of specimens performed. 57
Table 11. Outline of the number and specimen type, their dimensions and the type of test performed at long-term. 58
Table 12. Number of cubes at FRC level on compressive strength on FRCs at 90 days of exposure. 58
Table 13. Number of cubes at FRC level on compressive strength on FRCs at 180 days of exposure. 58
Table 14. Number of beams at FRC level on flexural strength on FRCs at 90 days of exposure. 59
Table 15. Number of beams at FRC level on flexural strength on FRCs at 180 days of exposure. 59
Table 16. Properties of fibers used in this work. 60
Table 17. Dosage of FRC used in compression and flexural tests. 62
Table 18. Dosage of FRC used in direct tensile tests. 65
Table 19. Programed Extreme Environmental Conditions in this study. 68
Table 20. The average UTS results for low temperatures (below and up to 0°C). 83
Table 21. The average E-modulus results for low temperatures (below and up to 0°C). 83

Table 22. The average UTS results for moderate high temperatures (between 20 - 80 °C). 84
Table 23. The average E-modulus results for moderate high temperatures (between 20 – 80 °C). 84
Table 24. Compressive strengths for the studied FRC at short-term under the extreme environmental conditions. 90
Table 25. Compressive strengths for the studied plain concrete at the extreme defined conditions. 90
Table 26. Results of the f_{LOP} and the residual flexural strengths obtained at defined extreme conditions for non-pre-cracked specimens. 94
Table 27. Results of f_{LOP} he and the residual flexural strengths for pre-cracked specimens. 99
Table 28. Total number of fibers (N) and number of fibers in lower third ($N_{1/3}$) in the cross-section per series for non-pre-cracked specimens. 103
Table 29. Total number of fibers (N) and number of fibers in lower third ($N_{1/3}$) in the cross-section per series for pre-cracked specimens. 103
Table 30. Results for direct tensile tests on MSFRC cylinders at temperatures from -30 to 40 °C. 110
Table 31. Verification of compliance with the structural requirements for the studied FRCs in non-pre-cracked state after 3 days of exposure. 120
Table 32. Verification of compliance with the structural requirements for the studied FRCs in pre-cracked state after 3 days of exposure. 120
Table 33. Results of compression tests after 90 days of exposure at temperature for MSFRC and SFRC. 127
Table 34. Results of compression tests after 180 days of exposure at temperature for MSFRCs and SFRC. 129
Table 35. Comparison of compression results of FRC at 3, 90 and 180 days at different temperatures. 132
Table 36. Results of the f_{LOP} and the residual flexural strengths obtained at defined extreme conditions for non-pre-cracked specimens after 90 days of exposure. 134
Table 37. Results of the f_{LOP} and the residual flexural strengths obtained at defined extreme conditions for non-pre-cracked specimens after 180 days of exposure. 137
Table 38. Evaluation of degradation by temperature of the flexural strengths results of MSFRC-PF1 between 3 and 180 days. 142
Table 39. Evaluation of degradation by temperature of the flexural strengths results of MSFRC-PF2 between 3 and 180 days. 143
Table 40. Evaluation of degradation by temperature of the flexural strengths results of MSFRC-PF3 between 3 and 180 days. 143
Table 41. Evaluation of degradation by temperature of the flexural strengths results of SFRC-SF between 3 and 180 days. 144

Table 42. Results of the f_{LOP} and the residual flexural strengths obtained at defined extreme conditions for pre-cracked specimens after 90 days of exposure. 145
Table 43. Results of the f_{LOP} and the residual flexural strengths obtained at defined extreme conditions for pre-cracked specimens after 180 days of exposure. 147
Table 44. Total number of fibers (N) and number of fibers in lower third ($N_{1/3}$) in the fracture surface per series for non-pre-cracked specimens. 152
Table 45. Total number of fibers (N) and number of fibers in lower third ($N_{1/3}$) in the fracture surface per series for pre-cracked specimens. 153
Table 46. Comparison of the average residual strengths results of MSFRC-PF1 at 3, 90 and 180 days at -15 °C. 160
Table 47. Comparison of the average of the residual strengths results of MSFRC-PF2 at 3 and 180 days at -15 °C. 161
Table 48. Comparison of the average of the residual strengths results of MSFRC-PF3 at 3 and 180 days at -15 °C. 161
Table 49. Comparison of the average of the residual strengths results of SFRC-SF at 3, 90 and 180 days at -15 °C. 161
Table 50. Comparison of the average of the residual strengths results of MSFRC-PF1 at 3, 90 and 180 days at 20 °C. 163
Table 51. Comparison of the average of the residual strengths results of MSFRC-PF2 at 3 and 180 days at 20 °C. 163
Table 52. Comparison of the average of the residual strengths results of MSFRC-PF3 at 3 and 180 days at 20 °C. 163
Table 53. Comparison of the average of the residual strengths results of SFRC-SF at 3, 90 and 180 days at 20 °C. 164
Table 54. Comparison of the average of the residual strengths results of MSFRC-PF1 at 3, 90 and 180 days at 60 °C, in immersion. 165
Table 55. Comparison of the average of the residual strengths results of MSFRC-PF2 at 3 and 180 days at 60 °C, in immersion. 165
Table 56. Comparison of the average of the residual strengths results of MSFRC-PF3 at 3 and 180 days at 60 °C, in immersion. 166
Table 57. Comparison of the average of the residual strengths results of SFRC-SF at 3, 90 and 180 days at 60 °C, in immersion. 166
Table 58. Evaluation of degradation by temperature of the normalized residual strengths results of MSFRC-PF1 between 3 and 180 days in non-pre-cracked state. 168
Table 59. Evaluation of degradation by temperature of the normalized residual strengths results of MSFRC-PF1 between 3 and 180 days in pre-cracked. 168
Table 60. Evaluation of degradation by temperature of the normalized residual strengths results of MSFRC-PF2 between 3 and 180 days in non-pre-cracked state. 169

Table 61. Evaluation of degradation by temperature of the normalized residual strengths results of MSFRC-PF3 between 3 and 180 days in non-pre-cracked state. ... 169
Table 62. Evaluation of degradation by temperature of the normalized residual strengths results of SFRC-SF between 3 and 180 days in non-pre-cracked state. ... 169
Table 63. Evaluation of degradation by temperature of the normalized residual strengths results of SFRC-SF between 3 and 180 days in pre-cracked state. ... 170
Table 64. Verification of compliance with the structural requirements for the studied FRCs after 90 days of exposure. ... 172
Table 65. Verification of compliance with the structural requirements for the studied FRCs after 180 days of exposure. ... 173
Table 66. Verification of compliance with the structural requirements for the studied FRCs in pre-cracked state after 90 days of exposure. ... 173
Table 67. Verification of compliance with the structural requirements for the studied FRCs in pre-cracked state after 180 days of exposure. ... 174
Table 68. Outline of the ANOVA tests carried out in this Thesis. ... 183
Table 69. ANOVA for f_{R3} to identify the influence on "State". ... 185
Table 70. ANOVA for f_{R3}/N to identify the influence on "State". ... 185
Table 71. Analysis of Variance for f_{LOP}. ... 186
Table 72. Multi-Range Test for f_{LOP} per "Time". ... 186
Table 73. Results from Method: 99.0 % Duncan. ... 187
Table 74. Multi-Range Test for f_{LOP} per "Temperature". ... 187
Table 75. Results from Method: 99.0 % Duncan. ... 188
Table 76. Analysis of Variance for f_{R1}. ... 188
Table 77. Analysis of Variance for f_{R1}. ... 188
Table 78. Multi-Range Test for f_{R1} per "Time". ... 189
Table 79. Results from Method: 99.0 % Duncan. ... 189
Table 80. Analysis of Variance for f_{R1}/N. ... 189
Table 81. Analysis of Variance for f_{R1}/N. ... 190
Table 82. Multi-Range Test for f_{R1}/N per "Time". ... 190
Table 83. Results from Method: 99.0 % Duncan. ... 190
Table 84. Analysis of Variance for f_{R3} ... 191
Table 85. Multi-Range Test for f_{R3} per "Time". ... 191
Table 86. Results from Method: 99.0 % Duncan. ... 191
Table 87. Multi-Range Test for f_{R3} per "Temperature". ... 192
Table 88. Results from Method: 99.0 % Duncan. ... 192
Table 89. Analysis of Variance for f_{R3}/N. ... 193
Table 90. Multi-Range Test for f_{R3}/N per "Time" ... 193
Table 91. Results from Method: 99.0 % Duncan. ... 193
Table 92. Multi-Range Test for f_{R3}/N per "Temperature". ... 194
Table 93. Results from Method: 99.0 % Duncan. ... 194

Table 94. Summary of statistical results for MSFRC-PF1. 195
Table 95. Comparison of significance of pairs of means of f_{R3} and f_{R3}/N per "Temperature". 195
Table 96. Analysis of Variance for f_{LOP} 196
Table 97. Multi-Range Test for f_{LOP} per "Temperature". 196
Table 98. Results from Method: 99.0 % Duncan. 196
Table 99. Analysis of Variance for f_{R1}. 197
Table 100. Multi-Range Test for f_{R1} per "Temperature". 197
Table 101. Results from Method: 99.0 % Duncan. 197
Table 102. Analysis of Variance for f_{R1}/N. 198
Table 103. Analysis of Variance for f_{R1}/N. 198
Table 104. Analysis of Variance for f_{R3}. 198
Table 105. Multi-Range Test for f_{R3} per "Temperature". 199
Table 106. Results from Method: 99.0 % Duncan. 199
Table 107. Analysis of Variance for f_{R3}/N. 199
Table 108. Multi-Range Test for f_{R3}/N per "Temperature". 200
Table 109. Results from Method: 99.0 % Duncan. 200
Table 110. Summary of the results of Statistical Analysis for MSFRC-PF2. . 201
Table 111. Analysis of Variance for f_{LOP}. 201
Table 112. Multi-Range Test for f_{LOP} per "Temperature". 202
Table 113. Results from Method: 99.0 % Duncan. 202
Table 114. Analysis of Variance for f_{R1}. 202
Table 115. Multi-Range Test for f_{R1} per "Temperature". 203
Table 116. Results from Method: 99.0 % Duncan. 203
Table 117. Analysis of Variance for f_{R1}/N. 203
Table 118. Multi-Range Test for f_{R1}/N per "Temperature". 204
Table 119. Results from Method: 99.0 % Duncan. 204
Table 120. Analysis of Variance for f_{R3}. 204
Table 121. Multi-Range Test for f_{R3} per "Temperature". 205
Table 122. Results from Method: 99.0 % Duncan. 205
Table 123. Analysis of Variance for f_{R3}/N. 205
Table 124. Multi-Range Test for f_{R3}/N per "Temperature". 206
Table 125. Results from Method: 99.0 % Duncan. 206
Table 126. Summary of the results of Statistical Analysis for MSFRC-PF3. . 207
Table 127. Analysis of Variance for f_{LOP}. 207
Table 128. Multi-Range Testing for f_{LOP} per "Time". 208
Table 129. Results from Method: 99.0 % Duncan. 208
Table 130. Results of Multi-Range Test for f_{LOP} per temperature. 208
Table 131. Results from Method: 99.0 % Duncan. 208
Table 132. Analysis of Variance for f_{R1}. 209
Table 133. Analysis of Variance for f_{R1}. 209
Table 134. Results of Multi-Range Test for f_{R1} per "Time". 210
Table 135. Results from Method: 99.0 % Duncan. 210

Table 136. Analysis of Variance for f_{R1}/N. 210
Table 137. Analysis of Variance for f_{R1}/N. 210
Table 138. Results of Multi-Range Test for f_{R1}/N per “Time”......................... 211
Table 139. Results from Method: 99.0 % Duncan.. 211
Table 140. Analysis of Variance for f_{R3}. 211
Table 141. Analysis of Variance for f_{R3}/N. 212
Table 142. Summary of the results of Statistical Analysis for SFRC-SF. 212
Table 143. Percentage of reduction at 60 °C for f_{R3}. 213
Table 144. Estimation of coefficients and significance test (Equation (7)). ... 216
Table 145. Analysis of Variance of the simple model presented in Equation (7). 216
Table 146. Estimation of coefficients and significance test (Equation (8)). ... 216
Table 147. Analysis of Variance of the model presented in Equation (8). 217
Table 148. Estimation of coefficients and significance test (Equation (9)). ... 217
Table 149. Analysis of Variance of the model presented in Equation (9). 217
Table 150. Estimation of coefficients and significance test (Equation (10)). . 218
Table 151. Analysis of Variance of the model presented in Equation (10). ... 218
Table 152. Estimation of coefficients and significance test (Equation (11)). . 218
Table 153. Analysis of Variance of the model presented in Equation (11). ... 218
Table 154. Estimation of coefficients and significance test (Equation (12)). . 219
Table 155. Analysis of Variance of the simple model presented in Equation (12). 219
Table 156. Estimation of coefficients and significance test (Equation (13)). . 220
Table 157. Analysis of Variance of the model presented in Equation (13). ... 220
Table 158. Estimation of coefficients and significance test (Equation (14)). . 220
Table 159. Analysis of Variance of the model presented in Equation (14). ... 220
Table 160. Estimation of coefficients and significance test (Equation (15)). . 221
Table 161. Analysis of Variance of the model presented in Equation (15). ... 221
Table 162. Estimation of coefficients and significance test (Equation (16)). . 222
Table 163. Analysis of Variance of the model presented in Equation (16). ... 222
Table 164. Estimation of coefficients and significance test (Equation (17)). . 222
Table 165. Analysis of Variance of the model presented in Equation (17). ... 223
Table 166. Estimation of coefficients and significance test (Equation (18)). . 223
Table 167. Analysis of Variance of the model presented in Equation (18). ... 223
Table 168. Estimation of coefficients and significance test (Equation (19)). . 224
Table 169. Analysis of Variance of the model presented in Equation (19). ... 224
Table 170. Estimation of coefficients and significance test (Equation (20)). . 224
Table 171. Analysis of Variance of the model presented in Equation (20). ... 225
Table 172. Estimation of coefficients and significance test (Equation (21)). . 225
Table 173. Analysis of Variance of the model presented in Equation (21). ... 225
Table 174. Estimation of coefficients and significance test (Equation (22)). . 226
Table 175. Analysis of Variance of the model presented in Equation (22). ... 226
Table 176. Estimation of coefficients and significance test (Equation (23)). . 227

Table 177. Analysis of Variance of the model presented in Equation (23). ... 227
Table 178. Estimation of coefficients and significance test (Equation (24))... 227
Table 179. Analysis of Variance of the model presented in Equation (24). ... 227
Table 180. Estimation of coefficients and significance test (Equation (25))... 228
Table 181. Analysis of Variance of the model presented in Equation (25). ... 228
Table 182. Estimation of coefficients and significance test (Equation (26))... 228
Table 183. Estimation of coefficients and significance test (Equation (26))... 228
Table 184. Summary of the equations obtained for f_{LOP}, f_{R1} and f_{R3} for the different types of FRCs. 229
Table 185. Summary of the equations obtained for f_{R1} and f_{R3} (considering N) for the different types of FRCs. 230
Table 186. Summary of the predicted variation (in %) experienced by flexural and residuals strengths due to temperature for the different types of FRCs, according to the obtained equations. 236

Glossary

ACI	American Concrete Institute
ANOVA	Analysis of variances
ASTM	American Society of Testing Materials
CFRC	Carbon Fiber Reinforced Concrete
CMOD	Crack Mouth Opening Displacement
COD	Crack Opening Displacement
CoV	Coefficient of variation
CTE	Thermal expansion coefficient
DICAM	Department of Civil, Chemical, Environmental, and Material Engineering
EBSD	Electron Backscattered Diffraction
EDA	Exploratory Data Analysis
EDS	Energy Dispersive Spectrometer
δ	Misfit produced by dimensional changes
ε_{crit}	Critical failure strain by creep
f_C	Compressive strength
FRC	Fiber Reinforced Concrete
F_L	Applied force
f_{LOP}	Flexural strength at peak load
f_{LOP}^{*}	Tensile strength at peak load
f_{Ri}	Residual flexural strength, i = 1, 2, 3 or 4
f_{Ri}^{*}	Residual tensile strength, i = 1, 2, 3 or 4
GFRC	Glass Fiber Reinforced Concrete
ICITECH	Instituto de Ciencia y Tecnología del Hormigón
ISO	International Organization for Standardization
ITA	International Tunnel Association
L_e	Embedded length

LEFM	Limit Elements Finite Method
LOP	Limit of Proportionality
MAS	Maximum aggregate size
MC 2010	Model Code 2010
MSFA	Macro Synthetic Fiber Association
MSFRC	Macro Synthetic Fiber Reinforced Concrete
NFRC	Natural Fiber Reinforced Concrete
PA	Polyamide
PAN	Acrylic
PE	Polyethylene
PES	Polyester
PP	Polypropylene
PVA	Polyvinyl alcohol
RH	Relative Humidity
RRT	Round-Robin Test
SEM	Scanning Electron Microscopy
SFRC	Steel Fiber Reinforced Concrete
SLS	Service Limit State
SNFRC	Synthetic Fiber Reinforced Concrete
t	Time of exposure
T	Temperature
T_g	Glass transition temperature
TEM	Transmission Electron Microscopy
T_m	Melting point
UHPFRC	Ultra-High Performance Fiber Reinforced Concrete
ULS	Ultimate Limit State
USA	United States of America
UTS	Ultimate tensile strength
UV	Ultraviolet
3PBT	Three-point bending test

Chapter 1
Introduction

Chapter 1 provides a general overview of the problem that gives rise to this Thesis, which is presented in Section 1.1. Furthermore, the objectives and the scope of this work are defined in Section 1.2, and lastly, in Section 1.3, the document's structure is also explained, where the content of each chapter is specified.

1.1. Context

The first experimental works on Fiber Reinforced Concrete (FRCs), specifically with synthetic fibers, date from 1980s. In this decade, micro synthetic fibers were introduced into the concrete-matrix with the aim of minimizing the cracks produced by early-age plastic shrinkage but, these first micro synthetic fibers did not improve the load-deflection response of concrete and they could not enhance [1]. Macro synthetic fibers have gained attention specifically approximately 20 years ago to improve the flexural toughness and thus, Macro Synthetic Fiber Reinforced Concrete (MSFRC) performance [2].

In fact, they are currently the most commonly fiber used in paving applications. In a survey conducted in December 2016 [3], it was found that 94 % of the FRC overlays in United States of America (USA) were constructed with macro synthetic fibers and only 6 % were constructed with steel fibers (mostly in Illinois). Additionally, the International Tunnel Association (ITA) has compiled study cases on MSFRC used in tunnel segments and lining worldwide in several reports [4,5] and their use in these applications is being well-accepted recently.

In spite of MSFRC increasing trend in some applications, most of the studies up today are focused on Steel Fiber Reinforced Concretes (SFRCs). Figure 1 shows a comparison of scientific publications and citations related to both, SFRC and MSFRC (as topic), from 2000 to 2023 (extracted from Web of Science). As can be seen, the popularity on the research of MSFRC has increased in the last decades (noticeably in the last one) simultaneously with the rise of the use of macro synthetic fibers in the industry. This indicates that there is a clear market demand for such products as alternative solutions for steel fibers and reinforcements. Comparing both FRCs, assumptions and conclusions obtained for SFRC cannot be directly extrapolated for MSFRC due to the differences in the properties of the fibers (*e.g.*, synthetic fibers present both lower Young's modulus and ultimate tensile strength).

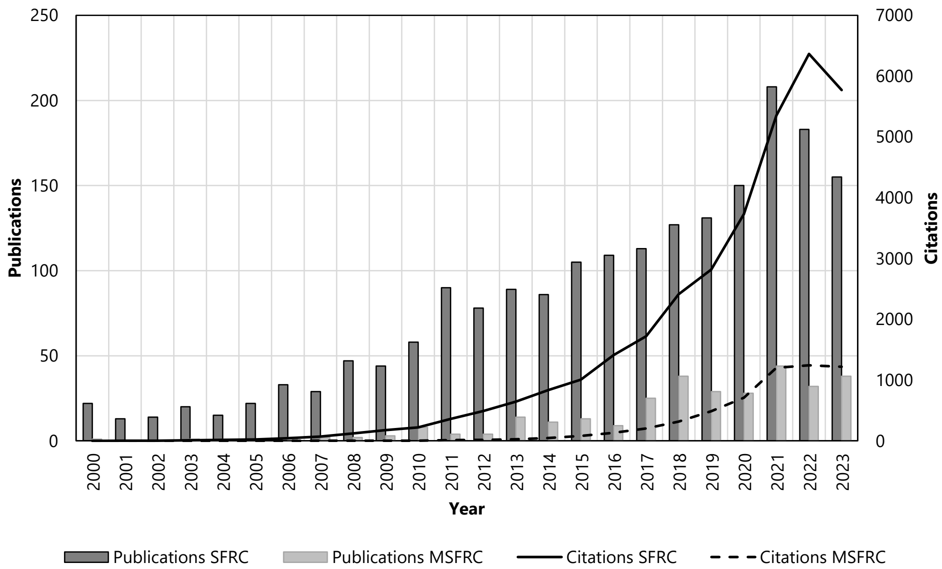

Figure 1. Comparison of publications and citations in SFRC and MSFRC.

An analysis of the existing literature (see Chapter 2) showed that macro synthetic and steel fibers can perform equally when they reinforce concrete-matrix in balanced dosages [6]. MSFRC has proven its technical and economic potential, overcoming various disadvantages of SFRC (*e.g.*, corrosion, density) [7], reducing the life-time maintenance and improving the infrastructure sustainability [8]. However, this analysis also revealed an important lack of information around some uncertainties and MSFRC weaknesses, by which MSFRC are usually criticized [9]. These issues raise concerns on the applicability of macro synthetic fibers to reinforce concrete, generating mistrust in the community, despite their common use in some applications. One of these issues is the influence of extreme environmental conditions on MSFRCs. Extreme environmental conditions involve variations of temperature and relative humidity (RH) which may also induce changes in the material (*e.g.*, seasonal climate changes, occasional fluctuations or the environment described in some applications as industrial tanks or plants). These conditions could pose a risk for safety conditions, service life and serviceability in MSFRC structures.

Temperature and RH effects are already known on plain concrete, given that in practice, concrete is put in service at a wide variety of environmental conditions [10,11]. It is also well proven that macro synthetic fibers are sensible to hygro-thermal phenomena since their properties are thermally dependent [12]. Therefore, MSFRC is expected to be affected by these extreme environmental conditions, but only a relatively small number of studies have focused on analyzing and quantifying this effect. In addition, from those scarce studies published, there is no clear consensus. Figure 2 shows the number of publications and citations produced in this topic in the last 20 years. The Boolean search was done using the keywords “MSFRC” and “temperature” as topic on Web of Sciences, making a total of 40 publications.

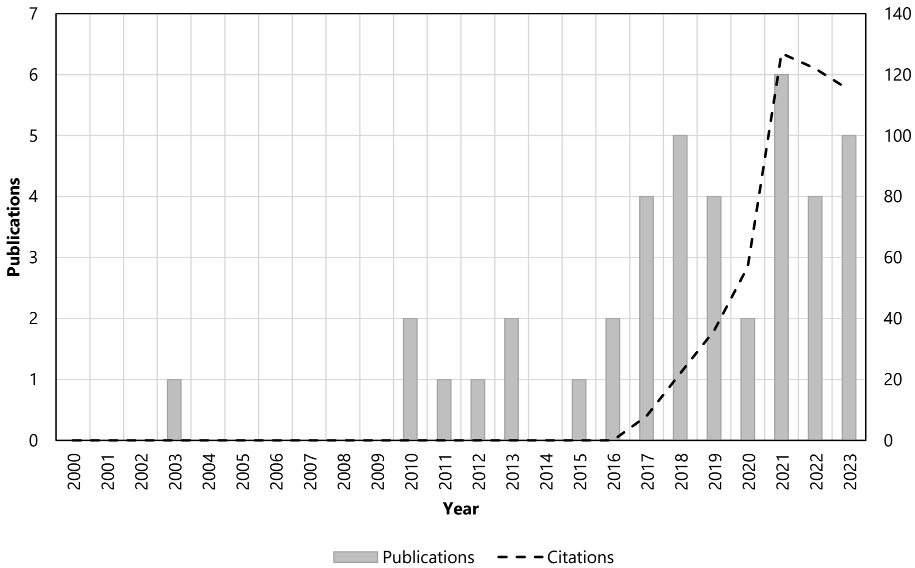

Figure 2. Publication and Citation Report on MSFRCs and temperature.

Strength, ductility and durability are important aspects of the MSFRC due to its fundamental incidence on the serviceability working conditions of the structures. It is essential to evaluate these properties to gain a fairly accurate knowledge of the behavior (short-term and long-term properties) of MSFRCs depending on the environmental conditions to make the most of their mechanical advantages, exploit the uses properly and to avoid problems and accidents in service and ultimate limit states.

There is a wide margin to make contributions at the scientific level with direct application at the industry level regarding MSFRCs. On the one hand, further tests are required to acquire a good understanding of the behavior of MSFRCs under extreme environmental conditions for the satisfactory design and performance of structures, especially under situations where the material can be working for a long time at the target temperatures (aging). On the other hand, one of the next important steps is its gradual inclusion in design guidelines. Nowadays, international design guidelines are based on the experience of steel fibers, excluding macro synthetic fibers. However, some actions have already been done in this sense and several countries have introduced national regulations covering MSFRC, such as in the case of Spain [13].

This context motivates the present Thesis, which focuses on the study of the mechanical behavior of Fiber Reinforced Concrete with steel (reference) and different macro synthetic fibers in extreme environmental conditions. The range of temperatures selected covers from -30 and 60 °C, and several exposition times (3, 90 and 180 days). Mechanical properties tested at different temperatures are analyzed, specifically, compressive, flexural and direct tensile strengths. In addition, the bond strength between fibers and concrete-matrix is analyzed indirectly from a meso-scale perspective and the behavior of the synthetic fibers at single-fiber level is also discussed in a wider range of temperatures (from -30 to 140 °C), to analyze different parameters in FRC effecting the overall performance. Most of experiments were developed in the Institute of Concrete Science and Technology (ICITECH) at Universitat Politècnica de València. Direct tensile strength tests were performed in collaboration with the research group of the Department of Civil, Chemical, Environmental, and Material Engineering (DICAM) at University of Bologna (Italy) during the period of research abroad.

This Thesis aims to provide practical knowledge on the use of MSFRCs under temperatures, including extensive experimental results and a database that can be used as a base for generating mathematic models to predict FRC behavior under several extreme environmental conditions, which can hopefully contribute to the construction sector.

1.2. Objectives

The general objective of this project is to experimentally study the influence of extreme environmental conditions (extreme service temperatures from -30 to 60 °C) on the mechanical behavior of Macrosynthetic Fiber Reinforced Concretes, comparing with Steel Fiber Reinforced Concrete, in particular their compressive, flexural and tensile strengths, after short- and long- term exposition (3, 90 and 180 days).

This general objective integrates several specific objectives:

- Expanding the information on this topic to be able to obtain a better understanding, given that the state of the art is not extensive.
- Carrying out experimental campaigns comprising an extensive number of specimens to assess the strengths and durability under temperatures of FRCs covering a wide range of variables and with several specimens per series to compensate the natural dispersion of FRCs residual strengths.
- Adopting a protocol to perform the experimental program at target temperatures, given that a standardized methodology does not exist.
- Analyzing the effect of other factors (time of exposition, type of fiber, condition of conservation, state) on the residual flexural strength at different temperatures, including a statistical study.
- Proposing simple numerical model to simulate the temperature effect over time on MSFRCs, which up to date is lacking in the literature.

The scope of this investigation does not cover the effect of the curing temperature, creep nor fire exposition. It intends to research the influence of the extreme environmental conditions on the mechanical behavior at short- and long-term of MSFRC to ensure its safe use in certain applications.

1.3. Structure of the Document

This Thesis is divided into seven Chapters which follow the structure described below. It is worthy to mention that at the end of the most of these Chapters have been included a critical summary where the main conclusions are generally addressed.

Chapter 1 presents the context and the interest to conduct this investigation. The general and specific objectives are also explained. Finally, a short description about the contents in each chapter is given.

Chapter 2 consists of a State of the Art. It starts by summarizing general concepts related to FRCs and then, it explains the literature studies done on the effect of temperature in: (i) the change of fiber properties over time where fibers can be exposed to possible aggressive environment, (ii) the alteration of the concrete and FRC properties by its exposure to harsh environment factor during prolonged periods of time, and (iii) degradation of the bond behavior between matrix and fiber over time.

In Chapter 3, the experimental program performed in this study is explained, including the outline of the research, variables, materials, equipment, specimens, and the developments in the methodology derived from this Thesis. The obtained results during the complementary characterization tests are also compiled.

Chapter 4 shows the behavior of FRCs when exposed to different extreme environmental conditions at short-term (3 days). To evaluate this, fiber's behavior and the performance of the composites itself (MSFRCs and SFRC) are studied experimentally, analyzed and discussed. Indirectly, the fiber-matrix bond is also evaluated from a meso-scale perspective.

In Chapter 5, the experimental campaign to assess the mechanical behavior of MSFRC and SFRC under extreme environmental conditions at long-term (90 days and 180 days of exposition) and the results derived from these campaigns are analyzed and discussed. Additionally, an analysis in terms of aging of the studied properties is done.

Chapter 6 presents the analysis of the results obtained in this Thesis from a statistical point of view with the objective of strengthening the final remarks derived from the previous experimental campaigns and proposing simple numerical equations, which may be the base for future numerical models.

Chapter 7 presents the conclusions of this study. This chapter also proposes improvements and possible future research works.

Finally, references are attached in order to clarify the sources of this Thesis.

Chapter 2

State of the Art

The purpose of Chapter 2 is to present the State of Art on the topic of this Thesis, which is, the study of influence of extreme environmental conditions on the behavior of MSFRCs.

A brief introduction about FRC is presented in Section 2.1. In Section 2.2, specific concepts regarding MSFRC are provided. Afterwards, Section 2.3 includes a review of the scientific literature on the durability of MSFRCs and their components, specifically durability against aging caused by extreme environmental conditions. This section is divided in three subsections: temperature effects on synthetic fibers, temperature effects on concrete and FRC and finally, temperature effects on the bond strength between fiber and concrete-matrix. Additionally, the methodologies used in the different experimental programs are compared at the end of these Subsections. In Section 2.4, MSFRC design specifications published in Codes and Standards are commented. Finally, a critical summary is conducted in Section 2.5, in which agreements and disagreements on the topic are identified. Figure 3 sums up the outline of this Chapter.

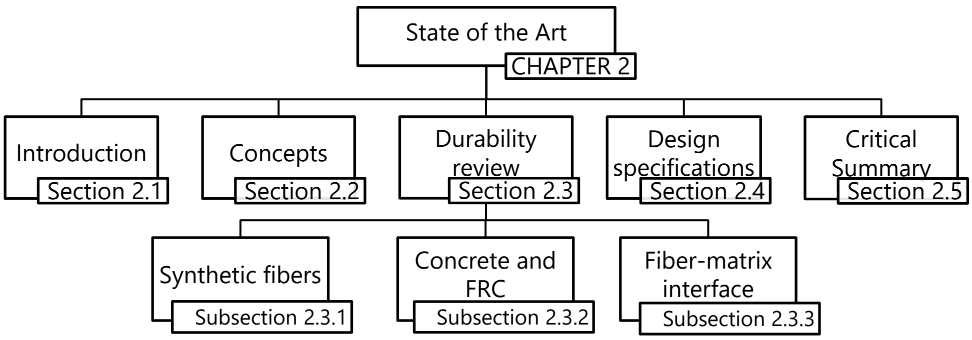

Figure 3. Outline of the Chapter 2.

2.1. Fiber Reinforced Concrete

Fiber Reinforced Concrete (FRC) is one of the most important advances in the special concretes' field and nowadays, this composite material is well stablished. Concrete has been generally referred as a fragile material, with a low tensile strength and deformability [14]. However, fibers allowed to partially overcome this drawback. The mechanical properties of the plain concrete are altered when fibers are introduced into the matrix, producing mixes with improved mechanical capacity, greater ductility, toughness, and durability [15].

2.1.1. Origin and Concept

Over the years, concrete has been conventionally reinforced with steel bar reinforcements placed in the tensile zone of structural members. The section forces may be equilibrated in structural members by utilizing the best performance of each material (steel in tension and concrete in compression). Depending on the exposure of the element, codes accept certain cracks of limited crack width (usually < 0.3 mm). The introduction of fibers acting as a continuous reinforcement, can support traditional reinforcements, obtaining a reduced crack width.

Even though the basic idea dates from centuries ago, its development emerged at the beginning of the 20th century when asbestos fibers were used to reinforce cement mortars [16]. This combination may be considered the first application of FRCs. From 1912 to 1927, there were various patents that included mixes reinforced with glass or steel fibers in France, Germany, and USA [17]. In the1960s, the concept of “disperse reinforcement” of concrete was proposed by adding steel fibers to the fresh mix. In this sense, notable works were done by Romualdi with Batson and Mandel in 1963 and 1964 [18,19]. These authors were the first to use Limit Elements Finite Method (LEFM) concepts to analyze the mechanics of the suppression of cracks in a cement-matrix by the fibers, which led to new research on the topic of FRC throughout the world.

With this idea in mind, fibers can replace traditional reinforcements in some cases, reducing the cost of the structure (material and labor costs). In general, the higher initial cost of 15-20 % of concrete that is compensated by the reduction of labor cost, and reduction of maintenance and rehabilitation operations [20,21]. Regarding production benefits, the handling of this type of fibers is safer and lighter and saves time in operations such as preparation and placing of the wire mesh [22].

Because of these benefits, plenty of regulations included definitions and recommendations for FRCs. The first definition was provided in 1988 by American Concrete Institute (ACI) Committee 544 [23], which defined FRC as a “*material made from hydraulic cements, containing fine and/or coarse aggregates, water, and discontinuous discrete fibers whose mission is to contribute to the improvement of certain characteristics of a concrete*”. Later, the publication of Model Code 2010 (MC 2010) [24] supported the use of FRC in structural purposes, and defined FRCs as composite materials that include fibers as structural reinforcement. In the last years, specifically in Spain, the Spanish Code on Structural Concrete [13], has described FRCs as concrete types that have short, discrete, and randomly distributed fibers in their mass. These definitions and the approaches adopted by these regulations caused a significant impact on the use of FRCs in the construction industry.

2.1.2. Types of FRCs

Different types of fibers have been fabricated to be added to the concrete-matrix as reinforcement, with different advantages and objectives. Fibers are produced with distinct constituent materials, shapes, surface textures and sizes which provide a tailored solution for different applications.

Steel Fiber Reinforced Concretes (SFRCs) are the most extensively FRC used, and steel fibers are the most commercialized fiber type [25]. Steel fibers can greatly improve the concrete-matrix properties. However, corrosion of steel fibers can be detrimental and lead to rapid deterioration of FRC structures [26]. In addition, steel fibers can also produce some problems in exterior projects if part of the fibers rise outside of the concrete section, negatively affecting aesthetics and/or safety, for example, in pavements for pneumatic wheels, or if users may be in contact with those fibers.

Synthetic Fiber Reinforced Concretes (SNFRCs) appeared more recently, but they are having a good acceptation into the market, especially, those reinforced with polypropylene (PP) fibers, since they present alkaline and corrosion resistance [27]. Synthetic fibers are extensively used in concrete structures nowadays [28,29], and they are significantly cheaper than steel reinforcements [2]. There are two types of synthetic fibers according to the size range, micro and macro fibers. Macro fibers are those typically used for a structural purpose. Macro Synthetic Fiber Reinforced Concrete (MSFRC), which are those concretes reinforced with macro synthetic fibers, and can be considered a good alternative to SFRCs, for certain applications.

Published research has shown that fracture behavior of MSFRC obtains higher structural capacities with lower fiber dosages than steel fibers in terms of weight of the fibers [30]. Consequently, this diminishes transport costs and the carbon footprint of the lifecycle of the material. Derived from the production methods, decreases of carbon emissions may also be found in [31,32].

Additionally, concrete might be also reinforced with fibers made of carbon, glass, or natural materials (*i.e.*, sisal, jute, etc.) [33–35], producing Carbon Fiber Reinforced Concretes (CFRCs), Glass Fiber Reinforced Concretes (GFRCs) and Natural Fiber Reinforced Concretes (NFRCs), respectively. Table 1 summarizes the most common fibers that have been used in the construction sector and their most important properties.

Table 1. Properties of the most common fibers, extracted from [23]**.**

Fiber type	Equivalent diameter [mm]	Specific gravity [kg/m³]	Tensile strength [MPa]	Elastic Modulus [GPa]	Ultimate elongation [%]
Steel	0.150-1	7840	345-3000	200	4-10
Synthetic	0.020-1	900-1400	200-860	1.5-8.3	3-13
Carbon	-	1400	4000	230-240	1.4-1.8
Glass	0.005-0.15	2500	1000-2600	70-80	1.5-3.5
Natural	0.025-0.40	1020-1500	65-700	0.9-40	1.2-25

The choice of the type of fiber and its dosage will depend on the application. Figure 4 shows the practical amount of fibers (% in volume) that is used in the case of steel, glass, synthetic and natural fibers. Although a minimum fiber content is not specified, when fibers are used with a structural purpose, it is not advisable to use dosages lower than 0.25 % by volume of concrete (equivalent to 20 kg/m³ of steel fibers or 2.5 kg/m³ of synthetic fibers). The upper limit of the fiber content (also known as critical volume) is usually set at 1.5 % by volume of concrete. For MSFRCs, a dosage of 0.4-1 % has been found to provide significant improvements on toughness after cracking and better crack control [36].

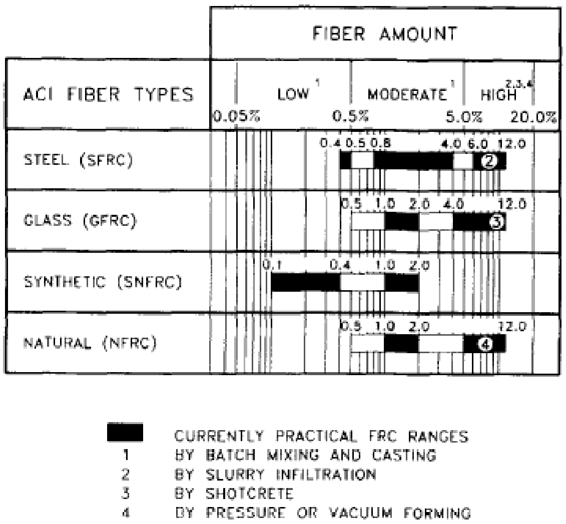

Figure 4. Regimes of fiber content in FRCs [23]**.**

Section 2.2 describes MSFRC in depth, their components, properties, and applications.

2.2. Macrosynthetic Fiber Reinforced Concrete (MSFRC)

Macrosynthetic Fiber Reinforced Concrete (MSFRC) is a composite material, combining a cement- matrix and a discontinuous reinforcement consisting of randomly distributed macro synthetic fibers. They attracted widespread attention to the scientific community in the last decades.

In 1995, the performance of different types of MSFRC based on PP, polyethylene (PE), polyacrylonitrile (PAN), polyvinyl alcohol (PVA), polyamides (PA), aramid, polyester (PES) and carbon reinforcements was revised by Zheng and Feldman [37]. Since then, the effect of the addition of synthetic fibers on concretes has been reviewed by other authors. In 2005, Portella [38] reviewed the effect of synthetic fibers in the fresh state concrete's properties. In 2010, Abtahi et al. [39] reviewed methods of sample preparation, and the history of fiber reinforcement in pavement engineering. It was also reviewed the effect of some synthetic fibers (PP, PES, asbestos, cellulose, carbon, glass, and nylon) on the properties of fiber-reinforced asphalt-concrete. They mainly discussed application of these different non-metallic fibers for producing asphalt concrete. In 2014, Bolat et al. [40] reviewed the influence of macro synthetic fiber reinforcement on physical and mechanical properties of concrete (PES, PP, and steel FRCs were compared with a plain concrete). Also in 2014, Mukhopadhyay and Khatana reviewed different types of non-metallic fibers including natural and polymer [41]. One year later, Shi Yin and collaborators [2] critically reviewed the use of MSFRC, presenting a detailed work based on the resulting properties of virgin and recycled macro fibers to reinforced concrete and degradation behavior of these fibers in concrete. In 2016, Thong et al. and Gu and Ozbakkaloglu [42,43] reviewed different aspect on MSFRC: the application of different forms of PVA in cement-base material and the application on commercial and recycled fibers in concrete, respectively. In the last five years, several reviews have been published in this topic, heightening the interest of the scientific community in macro synthetic fibers. In 2019, Pakravan et al. reviewed the use of PP, PE, and PVA fibers in cementitious composites [44]. In 2020, Chandrathilaka et al. [28] reviewed the material properties, fire behavior, durability, and structural performance of MSFRC with PP, PE and PVA. In this same year, Alberti and other authors [30] also reviewed the recent advances in structural FRC focused on macro synthetic fibers. Recently, in 2022, a review about mechanical properties of MSFRC at elevated temperatures (meta-analysis) was published by Clarke and collaborators [45].

These studies have contributed to the growing use of macro synthetic fibers worldwide. Actually, the Macro Synthetic Fiber Association (MSFA) have traced the development of the macro synthetic fibers. The market value in Europe is exceeding 100 € million nowadays and it is projected to be more than 200 € million by 2030 [46]. Australia has been very prone to the employment of macro synthetic fibers in reinforced shotcrete for ground stabilization in mines, with close to 100 % [47,48]. Their latest market report from September 2021 informs a growth of 10 % per year in macro synthetic fibers uptake globally over the last five years [46]. As consequence, numerous types of synthetic fibers have emerged and still are being developed at the synthetic industry.

2.2.1. Types of Synthetic Fibers

Many synthetic fiber reinforcements are available on the market, which have been formulated and produced specifically for mortars and concretes with different purposes. They can be classified depending on their length and on their material.

a) Micro vs macro fibers

Typically, fibers are available in two size ranges, micro and macro fibers. This classification depends on their length: up to 19 mm for micro and from 38 to 50 mm, for macro fibers, approximately.

The length of the fiber plays a more important role in the fracture behavior of concrete. On the one hand, micro fibers provide a good response to the formation of plastic shrinkage cracks [49], to improve cracking resistance, spalling protection, freeze-thaw durability and improve the homogeneity of concrete during the placement process [50–52]. However, they cannot provide any resistance to larger cracks caused by drying shrinkage and structural loads, as seen in Figure 5. On the other hand, macro fibers provide some structural capacity in either flexure [53] or shear [54] when adequately designed and enhance durability. The use of hybrid fiber reinforcement (both micro and macro fibers) is extended for ultra-high-performance fiber-reinforced concrete (UHPFRC), providing the enhancement of both types of reinforcement simultaneously [55].

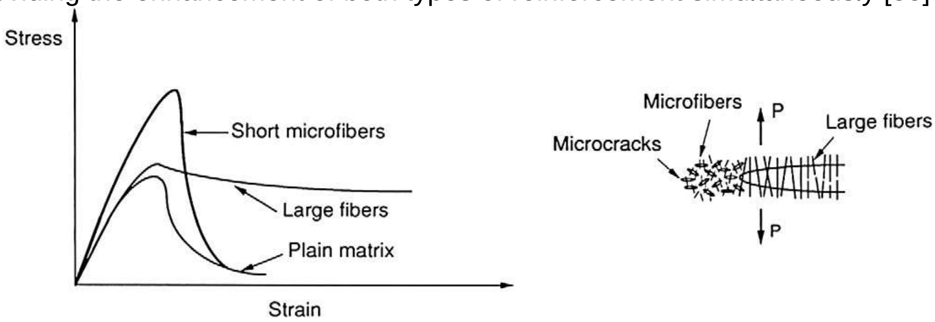

Figure 5. Different effect on plain concrete of micro and macro fibers [56]**.**

According to [57,58], longer fibers produce greater increase in concrete stiffness as compared to short fibers and the most ductile fibers (highest elongation and lowest strength) present the highest values of fracture energy. Other methods for the classification in micro and macro fibers is done according to their diameter: macro synthetic fibers are > 0.30 mm in diameter (or equivalent diameter), according to UNE-EN 14889-2 [59].

b) Material of the fiber

Synthetic fibers can be produced from a variety of formulations. Synthetic fibers can be made of acrylic [60], aramid [61], carbon [62], nylon, polyester, polyethylene, and polypropylene [63]. The properties of these synthetic fibers vary widely. Table 2 shows typical values for common fibers.

Table 2. Synthetic fiber reinforcement and their properties, adapted from [23]**.**

Fiber type	Equivalent diameter [mm]	Specific gravity [kg/m³]	Tensile strength [MPa]	Elastic Modulus [GPa]	Ultimate elongation [%]
Aramid	0.01	1440	2930	60	4.4
Aramid II	0.01	1440	2345	120	2.5
Carbon	0.01-0.013	1600-1700	485-795	25-35	2-2.4
Nylon	0.02	1140	965	6	20
PAN	0.015-0.10	1160-1180	270-1000	14-20	7.5-50.0
PE	0.025-1.016	920-960	75-585	5	3-80
PES	0.02	1340-1390	230-1100	15	12-150
PP	----	900-910	140-690	3.5-5	15
PVA	0.038	1300	880-1600	25-40	6-10

Among these synthetic fibers, PE, PP and PVA are the most popular because of their physical and mechanical advantages. From them, PP fibers are the most commonly used for the improvement of the physical and mechanical performance of FRCs since the mid-1980s. Since PP fibers are the synthetic fibers used in this Thesis, the next sections will focus only on PP fibers.

i) PP fibers

PP fibers are artificial synthetic fibers that resulted from developments produced in the petrochemical and textile industries. PP fibers are thermoplastics produced from propylene gas, which is obtained from the petroleum by products or cracking of natural gas feed stocks [64]. The raw material of polypropylene is derived from monomeric C_3H_6 which is purely a hydrocarbon [65]. Propylene polymerizes to produce long polymer chain under high temperature and pressure. However, PP fibers with controlled configurations of molecules can be made using special catalysts.

PP fibers were formerly 100 % homopolymer polypropylene graded monofilament fibers. They contained no reprocessed olefin materials. Today, PP fibers are made of high molecular weight isotactic polypropylene. Because of the sterically regular atomic arrangement of the macromolecule, it can be formed in crystalline structure, and then processed by stretching, spinning or extrusion process to achieve a high degree of orientation, which is necessary to obtain good fiber properties, in which the polypropylene resin is hot drawn through a die of circular cross section. A number of tows are produced and later, they are cut to the appropriate lengths.

PP fibers are made in different geometries. Figure 6 shows the most common used shapes in PP fibers for mortar- and concrete-matrixes. The type of shape (embossed, corrugate and twisted) and content affects the mechanical properties of MSFRC; for example, they affect the flexural strength and tensile strength. Comparing twisted and corrugated shapes, similar performances were obtained in FRC, with differences detected on the tail of the load-displacement curve.

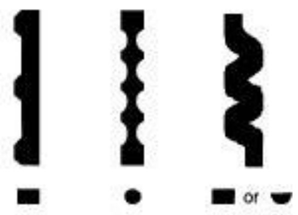

Figure 6. Typical shapes of PP fibers used as mortars and concretes reinforcement with different sections (from left to right): square embossed, circle corrugate and twisted [23]**.**

They can also present different diameters, ranging from about 50 μm to 0.5 mm and the specific surface area values, measured by adsorption techniques, in the range 80-600 mm^2/mm^3 [66]. Among their main properties, the modulus of elasticity of these fibers is in the range of 3.5–5 GPa, and the tensile strength is about 140–690 MPa (Table 2).

They are inert in an alkaline environment, acidic water, salt, chlorine, chemicals (due to its non-polar nature) and micro-organisms [40]. For example, Elastic Plastic Concrete company [67] did advanced alkalinity testing for their fibers. The fibers were subjected to an alkaline solution, which simulates a concrete environment. They reported that their fibers could last up to 100 years in an alkaline environment without any decrease of strength.

The chemical structure of the polypropylene makes it hydrophobic if compared with the cementitious matrix (PP fibers do not absorb water), leading to reduced bonding with the cement comparing to steel fibers and negatively affecting its dispersion in the matrix. Figure 7 compares the fiber-cement paste interface of steel and synthetic fiber. This is one of the major disadvantages associated with synthetic fibers, when compared with steel fibers [68]. For this reason, most of PP fibers developed for FRC undergo various proprietary surface treatments to improve the wetting of the fibers [69,70].

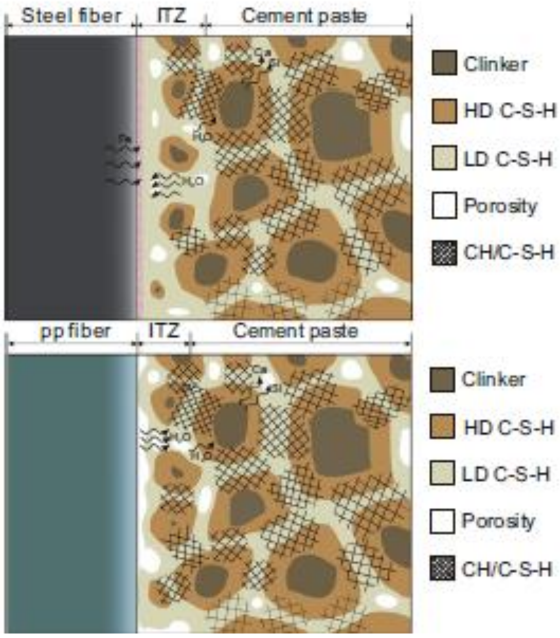

Figure 7. Diagram of two kinds of fiber-cement paste interface in FRC (steel fiber above and synthetic fiber below) [68]**.**

Other disadvantages of PP fibers are sensitivity to ultraviolet (UV) radiation (sunlight) and oxygen [71,72]. However, these disadvantages are not critical when they are embedded and protected inside the concrete-matrix [73].

To sum up, the main advantages of these fibers are their resistance to alkalis, the low price of the material and its production process. Their main disadvantages are their low modulus of elasticity and poor bond with the matrix. These disadvantages are not necessarily critical since they can be reduced [74]. PP fiber reinforcement for concretes is an outstanding alternative for certain structural applications (more information in Subsection 2.2.3).

2.2.2. Fresh and Hardened State Properties of MSFRC

The influence of PP fibers on the fresh and mechanical properties of FRC have been thoroughly studied by several researchers. This section summarizes the results from the literature.

a) Fresh state properties

PP fibers can affect concrete mix, placing and compacting [75]. Therefore, quality control, mixing and compaction procedures should be carefully considered when using PP fiber in FRC mixes [28].

PP fibers effect on the fresh properties of the mixtures depends on the content. The literature shows that most PP fibers mix well up to 1.0 % volumes with a relatively low effect on workability. At the 1.5 % volume of PP fibers, however, during the concrete mix, fibers can entangle and result in a non-uniform distribution in the concrete-matrix and balls of fibers. Although they do not absorb water, PP fibers, by adsorption, retain the water inside concrete-matrix, decreasing the amount of free water that will be exuded (which could promote cement hydration), but reduced the workability [76,77]. This challenge is usually tackled by adding more superplasticizer added to the mixes when increasing the content of fibers to maintain a suitable slump.

Other fresh state property that may be affected by the presence of PP fibers is air content, which can influence workability, strength and durability of concrete. However, very few studies are present in the literature on the possible influence of fibers on concrete air content and there is still disagreement within the research community. Macro synthetic fibers can lead to a slight increase in air content, and more adversely than steel fibers (about 15 % of increase as compared to steel fibers) [75].

b) Hardened state properties

The addition of PP fibers does not result in a clear effect in compressive strength in FRCs. Increasing the content of PP fibers may lead to a reduction in the compressive strength if using high volume fractions [78], but some studies have also reported that PP fibers may also increase compressive strength [79] for these volume fractions. Regarding to the modulus of elasticity of FRC, no significant improvement is observed in the literature with the addition of fibers, particularly for low dosages.

The most important hardened state properties of FRC are their flexural strength at limit of proportionality (LOP) and residual strengths since it is where major contribution of fibers can be seen. Under flexure, the low modulus of elasticity of PP fibers (compared to steel) is responsible for the load drop after reaching the peak load. Consequently, this should be considered when analyzing the width of the cracks at service limit state (SLS). In the case of ultimate limit state (ULS) the use of PP fibers, due to their contribution to residual stresses at high strain states, improves the robustness of the concrete element. Macro synthetic fibers, especially PP fibers, have been proven effective to provide post-cracking ductility, tensile strength, and toughness [80]. Moreover, adding fibers can also improve shear strength of concrete significantly [81].

i) Tests for the evaluation of flexural strengths in MSFRC

Most of the testing protocols for FRC have been developed for SFRCs (most common FRC) and they are commonly applied to MSFRCs. In the case of flexural strengths, three-point bending tests (3PBTs) such as the European (EN 14651 [82]), American (ASTM C1609 [83]) and Japanese (JSCE-G 552 [84]), are the most frequently used. Other tests were once proposed but they were discontinued [85]. Moreover, it deserves to mention other suitable tests to determine the mechanical properties of FRC. These standard tests are the four-point bending test (ASTM C1399 [86]), the panel tests (either round (ASTM C1550 [87]) or square (EN 14488 [88]), and DEWS test [89].

Among these methods, the most recommended is the three-point bending configuration described in EN 14651, as pointed out in [90]. The EN 14651 method indirectly evaluates the tensile behavior of FRC, considering the areas below the diagram of the applied force (F_L) versus the deformation. Although both midspan deflection and Crack Mouth Opening Displacement (CMOD) can be used as references for the diagram, the deformation is generally expressed in terms of CMOD measured at the bottom face of the notched specimen. Figure 8 shows the typical load-CMOD curve for FRCs obtained following the procedure described. It allows determining the flexural strengths at the LOP and the residual flexural tensile strengths at different CMOD values. The most relevant residual strengths, f_{R1} and f_{R3}, are obtained at 0.5 mm and 2.5 mm, respectively. These CMOD values are related to SLS and ULS, respectively.

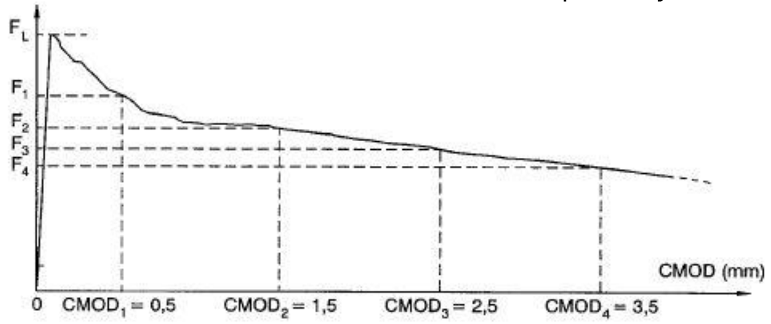

Figure 8. Typical stress-CMOD curve for FRC obtained by EN 14651 [82]**.**

As a result of all of these standards, MSFRC can be used widely with enough reliability. In fact, MSFRC are often successfully used in the construction field even beyond the typical requirements of the regulations.

2.2.3. MSFRC Applications

The development of PP fibers has spread the use of SNFRCs, especially in some fields, such as pavements and tunneling (segments and lining application), but the suitability of MSFRC is still controversial in structural field.

To date, micro-PP fibers are the most widespread PP fiber. They are used in low contents, usually less than 0.5 % by volume, and were intended to act as secondary reinforcement for crack control. They can prevent plastic shrinkage cracks in fresh concrete, due to the high elongation of PP fibers. These micro-PP fibers are also used in order to improve concrete performance against a fire event, since they melt and ignite around 160 °C, producing a pathway for water vapor, creating a network into the matrix. This gas escape results in reduction of pore pressure thus lessening the likelihood of explosive spalling [91,92], improving heat resistance [93].

In the last years, the interest on concretes reinforced with macro-PP fibers has increased. Compared to the SFRCs, MSFRCs offer advantages of high corrosion resistance. In addition, steel fibers are highly electrically conductive and alter magnetic fields, which limits their use in applications such as the runway of airports, high-speed railway systems, and nuclear power plants. Nevertheless, the use of steel fibers still predominates in elements with high structural responsibility. MSFRCs now have become increasingly popular in the construction of concrete pavements and footpaths [94], including narrow, winding, and steep roads, in which flexure and tension are significantly important, and they have shown to improve the flexural and tensile strength, leading to the increased durability, loading capacity, and structure lifetime. The use of macro-PP fibers in pavements can imply useful economical advantage as less use of shrinkage steel, reduction in thickness of slab by up to 30 % and ideal for joint free design [95].

They are also used in precast elements [96], as hydraulic precast tunnel segments [97,98] and underground water conduits. In these cases, macro-PP fibers significantly enhance both the bearing capacity and the ductility. MSFRC as a structural material is also considered in segmental lining applications [99,100], lining mine tunnels [101], and overlays in bridge decks. Herein, they also ensure compliance with the requirements for flexural, splitting, and minimum shear reinforcement, and also to static spalling reinforcement. Additionally, they are utilized in machine foundation and seismic and blast-resisting structures, where the composite is subjected to cyclically varying load during its lifetime [102].

Macro-PP fibers also play an important role in providing enhanced durability through resistance to corrosion, permeability, absorption, etc. MSFRC are applied in harsh environments, such as onshore atmosphere or sea defenses (seawater environment). These applications mentioned enable to fully exploit the advantages of macro-PP fibers in terms of corrosion resistance in presence of an aggressive environment, while the combination of fibers with conventional reinforcement leads to enhanced structural performance, which could be particularly effective in the presence of possible unfavorable conditions. Figure 9 shows examples of common applications of MSFRCs.

(a) (b)

(c) (d)

Figure 9. MSFRC applications: (a) General paving for Palo Verde Wastewater Reclamation Facility Expansion, in USA; (b) Shotcrete ground support for Brisbane Cross River Rail Shotcrete Lining, in Australia; (c) Concrete topping for Scheldt Bridge, in Belgium and (d) Segmental lining for Pista Nueva Malaga Rail Tunnel project, in Spain [103]**.**

However, some authors discourage their use in outdoor applications in cracked section [104] or applications where the maximum ambient temperature is limited to the range of 100 °C [105]. Thus, PP fibers are considered to have poor weatherability and should be avoided in certain applications requiring lightfastness and heat resistance.

To sum up, the decision of using MSFRCs, should consider the requirements of the application. At present, macro-PP fibers are used mainly for pavements and tunneling, and future use is expected to increase. Practical applications are currently limited by the insufficient development of relevant standards. Additionally, developments are not exactly in the foreseen directions. Extension of application of MSFRC with development of technology and guidelines in construction is ensured. Future applications include not only general tunnel support, but also underground structures that are located in harsh environments, such as near the coast or under the sea among others.

2.3. Durability based on the Influence of Extreme Environmental Conditions on the Behavior of MSFRCs

The ability of concrete to withstand the damaging effects of environmental factors, and to perform satisfactorily under service conditions, is referred to as 'durability' [106]. The design and maintenance of a durable, safe, and sustainable FRC structure depends on a better understanding of their properties when they are subjected to environmental variations and the material aging. 'Aging' is defined as a natural process that accelerates or intensifies the uncertain response of the structures to imposed extreme environmental conditions [107]. In this context, FRC aging may refer to (i) the change of fiber properties over time where fibers can be exposed to possible aggressive environment, (ii) the alteration of the concrete and FRC matrix by its exposure to harsh environment factor during prolonged periods of time, which may reduce the bearing capacity and (iii) degradation of the bond strength between matrix and fiber over time.

The extreme environmental conditions that impact structural concrete performance, and hence, they may affect FRCs, include RH, temperature, and wind velocity [108]. Additionally, PP fibers show thermally unstable behavior because of its low melting point (around 160 °C). Thus, it is expected that MSFRC with PP fiber may be susceptible for temperature-dependent variation for mechanical properties. However, the decrease in performance detected on fibers and concrete-matrix will not necessarily have an equivalent effect in a MSFRC concrete level, since concrete-matrix is known to be quite stable in moderate temperature variations and it provides a protective cover, which can minimize the susceptibility to temperature.

In this Thesis, RH and temperature are the environmental factor that are analyzed, focusing more on temperature. The word 'Extreme' refers to non-standardized values of this factor but which can be reached relatively easy in some weathers or in industrial applications (i.e., hardstands, bottling plants, tanks). The range of temperatures studied in this Thesis comprises values between −30 and 60 °C, however a wider range (from –70 to 100 °C) has been introduced in these Sections, in order to have more global vision of the components' behavior with temperature dependence. Studies related to curing temperatures [109,110] or thermal cycles [111,112] are outside of the scope of this work.

To examine the influence on durability and aging in MSFRCs, studies that deals the effect of extreme environmental conditions on the properties of both constituents (fiber and concrete-matrix) and their bond are recompiled in Subsections 2.3.1, 2.3.2 and 2.3.3, respectively.

2.3.1. Influence of Temperature on Synthetic Fibers

The thermal behavior of synthetic materials is influenced by wide differential temperature ranges. As seen in Subsection 2.2.1, there is an extensive variety of types and formulations of synthetic fibers on the market and each type has different thermal properties [113]. Figure 10 presents a diagram of the continuous operating temperatures for different types of plastic in the industry. The continuous operating temperature is defined in the ASTM D-794 [114] as "*the highest temperature at which a material can perform reliably in a long-term application*". This is based on an aging test with a minimum of 5000 hours of exposition. Failure is established when properties drop to 50 % of their initial value.

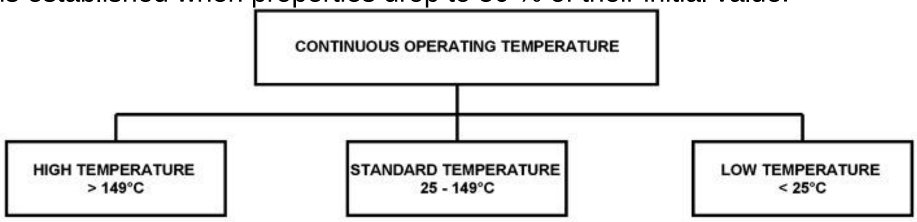

PLASTIC/POLYMER	°C
POLYIMIDES	260-427
SILICONES	204-316
FLUOROPLASTICS	149-288
POLYAMIDE-IMIDE	271-285
EPOXY	79-260
POLYPHENYLENE SULFIDE	260
ALLYLS	149-232
PHENOLICS	100-232
POLYETHERSULFONES	204
POLYSULFONES	171-204
MELAMINES	149-204
THERMOSET POLYESTER	66-204
UREAS	93-177
ACRYLATE RUBBER	204
FLUOROSILICONES	204
NYLONS	107-177
THERMOPLASTIC POLYESTER	154-160
POLYARYLETHER	121-160
POLYMETHYLPENTENE	121-160
POLYCARBONATE	82-154
ALKYDS	121-149
CHLORINATED POLYETHYLENE	149

PLASTIC/POLYMER	°C
PPO/PPE BASED	77-127
POLYPROPYLENE	96-121
POLYURETHANE	88-121
VINYLS	66-110
POLYBUTYLENE	107
ACETALS	91-104
ABS & SAN	71-104
POLYSTYRENE	52-96
ABS/POLYCARBONATE ALLOY	88-93
ACRYLICS	60-93
CELLULOSICS	49-93
POLYETHYLENE & COPOLYMER	49-82

PLASTIC/POLYMER	°C
CHLORINATED POLYETHYLENE	-51
POLYURETHANE	-65
FLUOROSILICONE	-68
SILICONE	-118
FLUOROPLASTICS	-184

Figure 10. Continuous operating temperature for plastics [115]**.**

In the case of PP, it loses more than 50 % of their properties from 96 to 121 °C, values much higher than those feasible in daily conditions, therefore, its use seems viable in a common range of temperatures even for long-term exposures. Nevertheless, some PP properties are thermal- dependent (named herein critical properties) and the behavior of the composite material FRC could be compromised (as well as by the durability of the PP).

a) Critical properties

PP is a semi-crystalline material (a thermoplastic polymer) that shows the two transition regions characterized by: (i) glass transition which usually occurs below the ambient temperature but affects the behavior up to 100 °C; and (ii) α -relaxation occurs during polymer crystalline phase due to rotation and translation of polymer chains, just below the melting point region, around 160 °C [116].

Glass transition temperature (T_g) is the temperature, below which the physical properties of plastics change to those of a crystalline state, and they can be dramatically different above and below its T_g. Above T_g, they behave like rubbery (viscoelastic) materials. Below T_g, PP molecules have relatively little mobility, they normally have an elastic but brittle behavior [117]. The value of the glass transition temperature depends on the strain rate and cooling or heating rate, so there cannot be an exact value for T_g. As a reference value, T_g of PP is usually considered to be around -20 °C (see Figure 11).

The melting point (T_m) is the temperature at which plastics melt (change from solid to liquid state). T_m occurs as a range, so a melting point is determined by finding the highest temperature of a differential scanning calorimetry chart. Perfect isotactic PP has a melting point of 171 °C but commercial PP presents a melting point that ranges from 160 - 166 °C (see Figure 11), depending on the crystallinity.

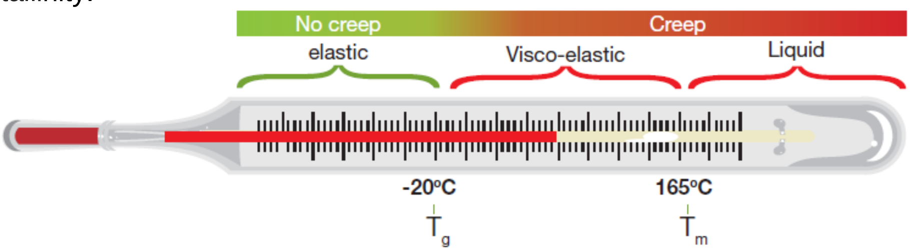

Figure 11. Temperature-dependence on PP fibers [118]**.**

Other important finding to consider while studying the performance of synthetic materials subjected at temperatures is the decrease of the critical properties, such as modulus of elasticity, tensile strength, environmental resistance, and the expected service life of the final product. Within the experimental range of temperature studied, the Young's Modulus was found to have an exponential relation with temperature, as defined by [119]. It has been described that Young's Modulus at -30 °C is three folds higher than at room temperature [120].

Additionally, dimensional changes of synthetic materials by the exposition to temperatures have been informed in the literature. These dimensional changes can generate misfit (δ) between different components of the composite material: volume changes, external stresses, Poisson effects and plastic deformation. For example, volume changes can be induced by daily and seasonal fluctuations in temperature (changes in temperature between day and night or concrete structures under daily cycles of loads) [1]. It is said that steel and concrete present similar thermal expansion coefficients at standard temperature, however, they can present certain incompatibilities due to thermal deformation at temperature (see Figure 12).

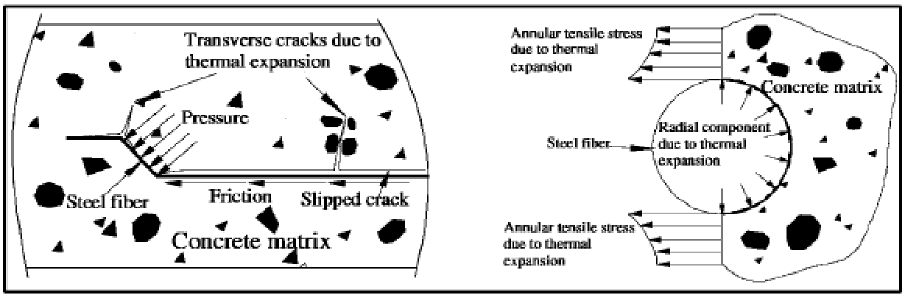

Figure 12. Cracking due to incompatibility of thermal deformation between steel fibers and concrete-matrix [121]**.**

In turn, thermoplastics tend to expand and contract anywhere from six to nine times more than metals [122]. This difference develops internal stresses in the composite material, and stress concentrations foster failure. Figure 13 shows the notable difference in thermal expansion coefficient (CTE) of steel, concrete and PP.

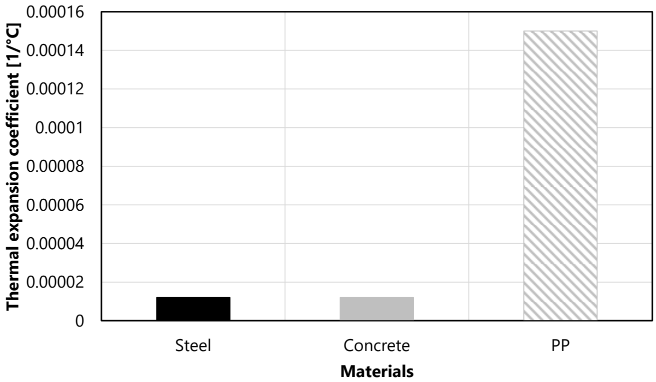

Figure 13. Thermal expansion coefficients of different materials at ambient temperature.

Additionally, according to [20], the existing variations in the Poisson's ratio values of the steel, concrete, and PP (see Figure 14) may also generate the aforementioned misfit δ (between different components of the composite material, by volume changes, external stresses, Poisson effects and plastic deformation).

This is worsened by temperature since Poisson effects are also dependent on the thermal expansion coefficients. Particularly, the higher Poisson's coefficient of PP fibers (0.40–0.45) compared to that steel fibers (0.27–0.30) results in significant lateral contraction of the fibers, facilitating debonding. It should be noted that the tensile strain of the fiber embedded into the matrix, next to the crack position, is much greater than that of the concrete-matrix. This may result locally in a Poisson contraction in the fiber greater than that of the concrete-matrix (regardless of whereas it is a steel or synthetic fiber). In this case, tensile normal stresses may be generated at the interface, and reduce or even eliminate the frictional resistance to slip.

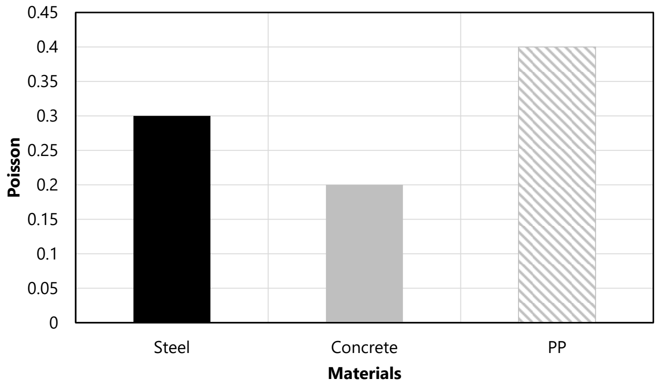

Figure 14. Comparison of the Poisson's ratio for different materials at standard temperature.

b) Durability of PP fibers

The primary concerns associated with this topic were the durability of fibers when are exposed to weathering conditions (either due to cracking or partial deterioration of the concrete), the ability of the components to retain its original properties, and the resistance to temperature (fire, frost, etc.) [123].

i) Chemical and aggressive agents

Polypropylene is fairly resistant to chemical and aggressive agents (salts, chlorides, sulphates, etc.) and it is not susceptible to corrosion. Nevertheless, polypropylene also presents a low resistance to thermo-oxidative and photooxidative degradation [124]. On the one hand, photo-oxidative degradation of PP fibers in cement matrices is not usually expected, except in a cracked cement matrix subjected to natural weathering. In this case, cracks may allow access of oxygen to the fiber (see Figure 15). Nowadays, this disadvantage may be treated with commercial chemical stabilizers. On the other hand, thermo-oxidative degradation should be considered, even at room temperature. This is because polymers are subjected to aging upon exposure to the environment, as a result of irreversible changes in the composition and structure of polymer molecules. The rate and extent of degradation depends on the composition, the temperature, and the time of exposure.

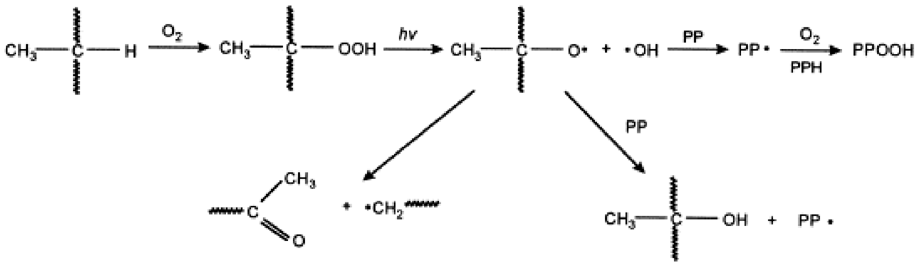

Figure 15. Polypropylene photo-oxidation (degradation) scheme [124]**.**

ii) *Creep*

Creep is a term used to define the tendency of a material to develop increasing strains through time when under a sustained load, this resulting in increasing deflection or elongation values (depending on the type of loading) with time in relation to the initial, instantaneous strain that the material experiences directly after the load is applied [125]. The creep behavior and creep failure law of PP have already been broadly investigated.

Figure 11 shows the creep behavior of synthetic fibers depending on temperature. Temperature plays an important role to affect normal response of a fiber under axial tensile loading rate and can change its behavior from elastic to viscoelastic. Fibers at normal conditions (room temperature and RH) show purely elastic behavior under tensile stress, but other temperatures can promote viscoelastic behavior since synthetic fibers subjected to time-dependent axial stress can experience the creep effect. While fibers should show a perfectly elastic behavior until peak capacity, once it moves from elastic to viscoelastic, it becomes impossible to return to its original state as there will be some permanent deformation [126].

Takaku [127] found that changes in temperature (from 40 to 130 °C, and from -30 to 70 °C respectively) had significant effects on the creep rate of PP fibers. In addition, experimental research [71] has studied the tensile creep behavior of PP to understand the long-term stability by using a multifunctional stress-aging tests under different aging environmental conditions (temperature, UV, and stress). The four types of analyzed PP displayed a critical failure strain (ε_{crit}). This value was independent of the tensile stress and UV irradiation, but it was depending only on the temperature and the nature of the PP. In the case of the same structure, the ε_{crit} of low-molecular weight PP was less than that of high molecular weight PP. In the case of similar molecular weights, the ε_{crit} of PP homopolymer was greater than that of propylene–ethylene copolymer. The ε_{crit} could not be observed for PP copolymer at low temperature. Increasing the tensile stress and irradiation with UV light accelerated the creep failure of PP, but did not change the creep failure law of PP. Among a few works on this phenomenon are those reported in [128].

iii) *Temperature*

Numerous investigations focused on the characterization of macro-PP fibers (individually, as a filament) to evaluate their response under temperatures. Nevertheless, there is little information on how the physical properties of synthetic fibers subjected at temperature change with time (aging).

At elevated temperatures, ADFIL Corporation [129] published a technical note about the durability of one type of their fibers subjected to accelerated aging tests, according to EN ISO 13438 [130], in which 30 monofilaments were stored in water at elevated temperature (80 °C) for 28, 56 and 112 days before testing (for simulating service lives up to 25, 50 and 100 years). Then, they tested their tensile strength and modulus over time. The product withstood the degradation process, but they detected a reduction of up to 32 % in tensile strength and up to 7 % in the modulus when compared to the initial values.

Hunger et al. [131] studied tensile stress and tensile creep behavior of the filaments at varying temperatures from −10 to 60 °C (see Figure 16). These authors indicated that the performance of synthetic fibers and especially, creep performance cannot be generalized since high-performing macro-PP fiber can sustain a load level of 40 % related to maximum strength in short-term tests even at a temperature of 40 °C, which would be enough for several applications.

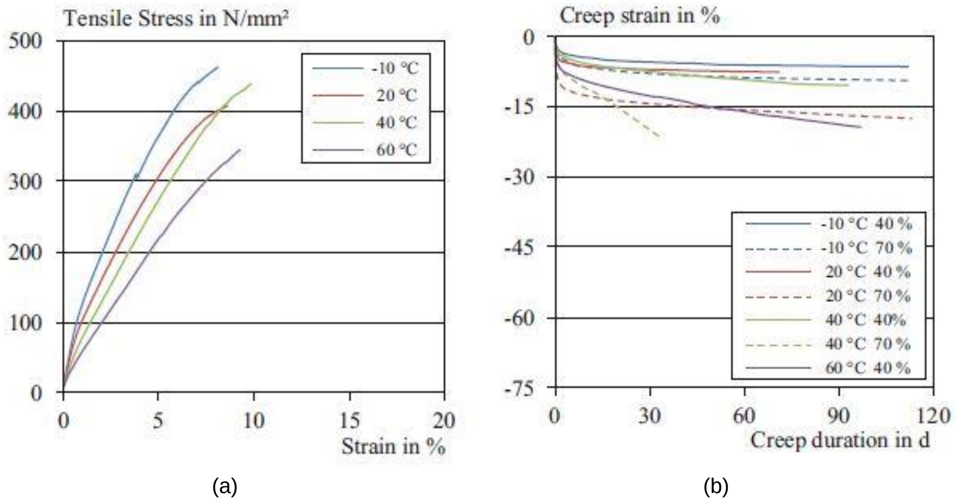

Figure 16. (a) Stress-strain curves and (b) Single fiber tensile creep behavior from -10 to 60 °C [131]**.**

In the low temperatures and sub-zero range, Hall [117] addressed various aspects of polymer materials. He stated that polypropylene tends to become brittle at these temperatures due to its nature, which is a serious drawback in certain applications when mechanical performance at such temperatures is required.

Regarding aging at standard temperatures, in 1981, Hannant carried out tests to determinate the effects of the environmental conditions over time on polypropylene [132]. PP fibers have been subjected to natural weathering, storage in laboratory air and storage under water (at 20 °C) for periods up to 18 years. The durability of the PP fibers in these conditions has been evaluated by tensile tests. It was found when samples were left to endure natural weathering, a reduction in strength occurred between five and ten years, however, the strength after eighteen-years was identical to the strength after ten-years. It was concluded that it was unlikely that the composite will ever become brittle due to excessive bonding and that the bond strength between cement and polypropylene as calculated from the test results was relatively unaffected by exposure conditions for time periods up to 18 years. Also, Brown et al. [133] studied long-term properties of virgin PP fibers in the concrete under a reactive environment. When PP fibers were exposed to an ionic environment of sodium and chloride ions created by saltwater at different temperatures, approximately from -7 to 70 °C for six months, the tensile properties of the PP fibers remained unchanged.

To conclude, the field of polymer mechanics has received significant attention and continues to evolve, facilitating a better understanding of synthetic materials. It has been proved that the behavior of synthetic fibers is thermal-dependent and showed that PP fibers can retain most of its toughness and strength over many years, giving increased confidence in the long-term stability (expected life) of polypropylene inside the concrete-matrix.

c) Comparison of methodologies

As reported in the previous Subsection, there is not a unique method to evaluate the aging and durability in terms of temperature of PP fibers. Different procedures (immersion in different solution at temperature, immersion in hot water, exposition to temperature, etc.), time (from a few hours up to approximately 18 years) and specimens are applied to simulate aging and exposure to different environments.

Most of these tests applied in synthetic materials are compiled in the Chapter ‘Thermal Properties of Polymeric Materials’ from [122], in order to determine their thermal properties, according to different ASTM regulations. In the case of synthetic fibers for concrete, most of these methods are from the plastic and textile industries. Recently, EN 14889-2 ‘Fibers for concrete — Part 2: Polymer fibers — Definition, specifications and conformity’ [59] have been published and this document have allowed to collect concepts and test that are necessary to define the performance of this type of reinforcement before commercializing (including factory production control specifications). The requested mechanical properties for polymer fibers in this regulation include geometrical dimensions, density, tensile strength, modulus of elasticity, among others. This standard is a technical advance from a regulation perspective, to support the use of synthetic fibers for structural or non-structural concretes, mortars and grouts, including sprayed concretes, flooring, precast, in-situ and repair concretes.

2.3.2. Influence of Temperature on Plain Concrete and on FRCs

Additional to the effects of temperature on synthetic fibers, concrete also show changes in its behavior due to this factor. In this Subsection, the review of the literature focuses on the effect of temperature on the principal mechanical properties (compressive, tensile and flexural strengths) of plain concrete and FRCs.

a) Compressive strength

The effect of temperature on compressive strength has been examined in depth in plain concrete [134] and more limited, in FRCs, since the fibers do not modify greatly the compressive strength of the matrix [135]. Firstly, studies are recompiled and discussed about the influence of elevated temperatures. Secondly, literature about the effect of low temperatures in compressive strength and lastly, the influence of humidity in this property.

i) Studies at elevated temperatures

Gardner et al. [136] evaluated the effect of temperature (temperatures of 20 (reference), 85 and 105 °C) on the strength and the permeability of plain normal and plain high-strength concrete mixes (40 and 100 MPa). Compression tests were carried out immediately after the conditioning period (where the temperature is still maintained). The results showed that, for both concrete mixes, similar compressive strength was obtained at 20, 85 and 105 °C.

In FRCs, Del Prete [137] observed that compressive strength decreased up to 20 % when the temperature increased to 100 °C. Navarro et al. [138] studied compression of FRC from -30 °C until 100 °C (see Figure 17). They detected that compressive strength decreased up to 15 % when the temperature increased from the temperature reference (22 °C) up to 100 °C.

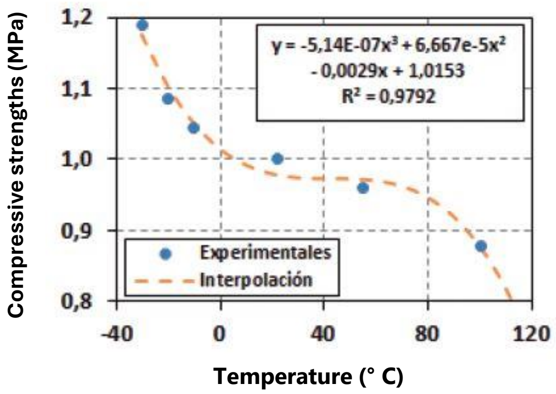

Figure 17. Compressive strength results in terms of temperature [138]**.**

At very elevated temperatures, Chang et al. [139] also reported that the residual compressive strength at 200 °C still retains 90 % of the original unheated value. Pachideh and Gholhaki [140] demonstrated that compressive strength of specimens containing steel and PP fibers are decreased with increase of temperature (from 20 up to 700 °C).

ii) Studies at low and sub-zero temperatures

Several authors indicated that decreasing the temperature of concrete below the standard temperate of 20 °C leads to enhancements in the compressive strengths of concrete [141]. However, exposing concrete to cold temperatures also increases brittleness [142]. Below zero degrees, a system formed by ice and concrete that exhibits surprising behavior and advantageous for some applications [143]. For example, for certain temperatures below zero, the compressive strength can be tripled, due to the great resistance of the ice and the micro restressing that water creates when it freezes [144]. Nonetheless, the rate of increase in the modulus of elasticity has been found to be smaller than that for the compressive strength.

Figure 18 shows experimental data adapted by [145], which highlights the increasing trend in compressive strength and modulus of elasticity (with decreasing temperatures). Shoukry et al. [146] also studied the effects of low and high temperatures (-25 to 55 °C) and humidity conditions on the modulus of elasticity and compressive strength. Their results indicate that concrete strength and modulus of elasticity are inversely related to temperature and moisture content. A linear relationship between the decrease in the modulus of elasticity and the increase of temperature of heating has been also established in [147].

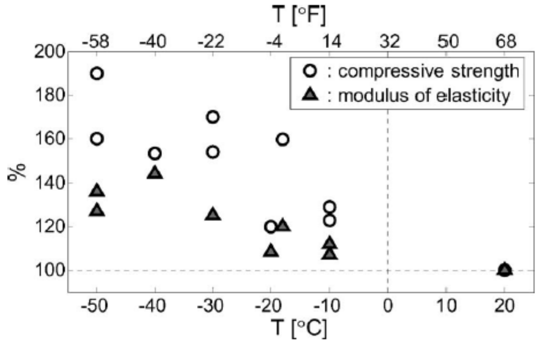

Figure 18. Experimental values of modulus of elasticity and compressive strength of plain concrete vs temperature—expressed as a percentage of the values measured at 20 °C [145]**.**

In more recent studies, Cai et al. [148] also studied the effect of low temperature (-35 °C) on the compressive strength of plain concrete with different strength grades. The results showed that all increased at the studied temperature of - 35 °C (see Figure 19). Xie and Yan [149] exposed reinforced concrete structures to low temperatures (ranging from 20 to -165 °C) in order to investigate their compressive strength after the exposure. Their results confirmed previous research, and the compressive strength increased by 11 %, 29 % and 23 %, at 0, -40 and -80 °C respectively.

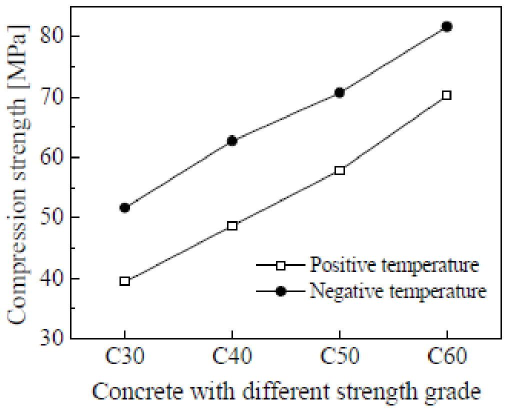

Figure 19. Relationship between compressive strength and the strength classes in plain concrete at positive and negative temperatures [148]**.**

In FRCs, Navarro et al. [138] studied compression of FRC from -30 °C until 100 °C (see Figure 17). They detected that compressive strength increased up to 20 % when the temperature decreased from the temperature reference (22 °C) up to -30 °C. At very low temperatures, approaching those of liquefied natural gas, Rostásy and Sprenger [150] found that the addition of steel fibers greatly reduced the loss of both compressive under repeated thermal cycles down to −170 °C. Reactive powder concretes were found to have excellent freeze–thaw resistance, even in the absence of air entrainment [151].

iii) Studies regarding to humidity content

Literature is fairly consensual on the fact that humid environments lead to better mechanical performance of plain concrete. As for mixes with synthetic fibers, it argues that humid environments optimize cement hydration, but drier ones promote the formation of a binding film between the polymers and the cementitious mix. Mixed regimes would seem to be the most appropriate to promote a better performance of concrete containing synthetic reinforcement or plastics in general. For instance, Madandoust et al. [152] assessed the effect of steel and PP fibers on concrete, which were exposed under six conditions: wet, 3-day wet, 14-day wet, air-dry controlled, air-dry uncontrolled, and 90 °C vapor. In compression results, mixes under wet conditions (3 and 14 days) were nearly the same. Under 90 °C vapor and wet conditions, the hydration process and chemical reactions increased. The difference between the results values under air-dry uncontrolled and controlled exposition was negligible. Humidity of concrete plays a decisive role in its behavior at low temperatures [145]. Actually, the water inside concrete-matrix can freeze that influences the mechanical properties of this material (see Figure 20).

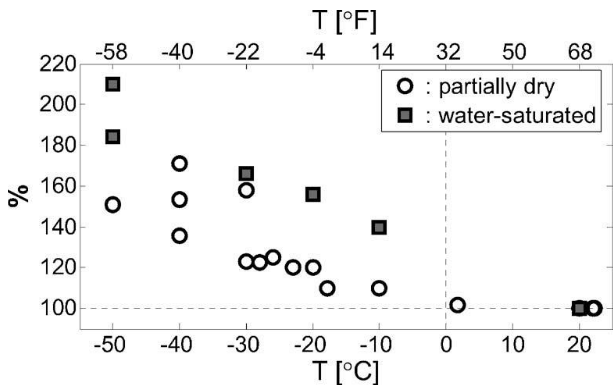

Figure 20. Measured values of compressive strength of water-saturated and partially dried concrete vs temperature— expressed as a percentage of the values measured at 20°C [145]**.**

iv) Summary on compressive strength under extreme environmental conditions

It can be summarized that compressive strength is affected by temperatures, even below 100 °C. When temperature drops, compressive strengths increase and vice versa. Humidity could be considered as important factor in some cases (especially, at low temperatures) but there is not a clear agreement in its effect on FRC compressive strengths.

b) Tensile and flexural strengths

In this Subsection, the effect of temperature on tensile and flexural strengths of concrete reinforced with steel and PP fibers are examined. Firstly, studies are recompiled and discussed about the influence of elevated temperatures at short-term. Secondly, studies in the low temperatures and sub-zero range on the tensile and flexural strengths at short-term are presented. Later, long-term studies are presented herein in the same topic. Finally, a comparison of employed methodologies is collected.

i) Studies at elevated temperatures

Kim et al. [153] reported the results on the splitting tensile strengths in plain concrete, after exposing the specimens to the moderate temperatures of 10, 23, 35 and 50 °C for 28 days. Lower splitting tensile strengths were observed when increasing the temperature, and the E-modulus followed the same trend. Mi et al. [154] investigated the fracture properties on plain concrete in dry environments at different temperatures (5, 20, 40, and 60 °C) and ages (3, 7, 14, 28, and 60 days). The results show that the concrete exposed at higher temperatures exhibited a temperature-age crossed effect. This effect can be seen in Figure 21.

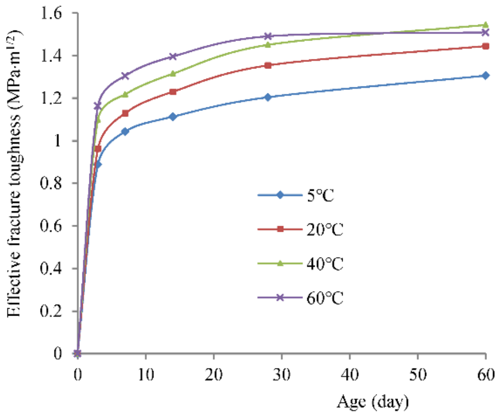

Figure 21. Effective fracture toughness for plain concrete exposed to dry environments under different temperatures [154]**.**

Richardson and Ovington examined the effect of temperature on MSFRCs (PP fibers) and SFRC under 60 °C [155]. All beams had decreased flexural strengths at 60 °C if compared to the results at room temperature. The MSFRC beams showed an average of 12 % reduction and the SFRC beams showed an average of 49 % reduction in CMOD1 (see Figure 22). This is backed up by Lau et al.

[156] who state that steel fibers are beneficial, despite the exposure to temperatures.

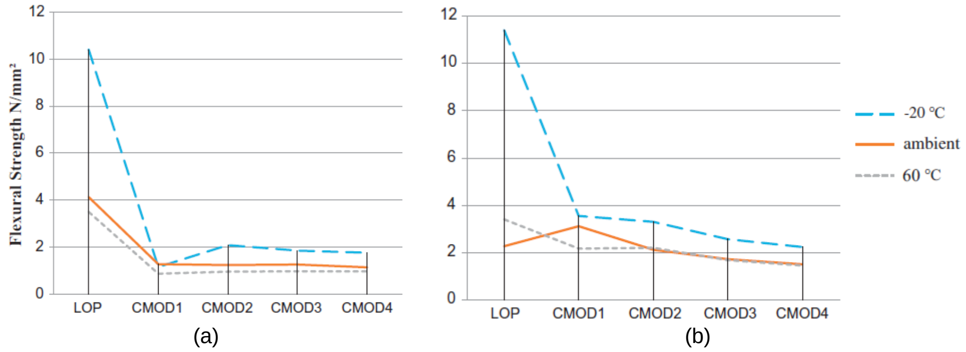

Figure 22. Comparison of (a) MSFRC (PP fibers), and (b) SFRC at varying temperatures, in terms of flexural strength at various CMOD [155]**.**

Navarro et al. [138] studied the flexural behavior of a MSFRC from -30 to 100 °C. As can be seen in Figure 23, a reduction at the peak load and at the residual flexural strengths up to 50 % when the temperature increased to 100 °C, was detected.

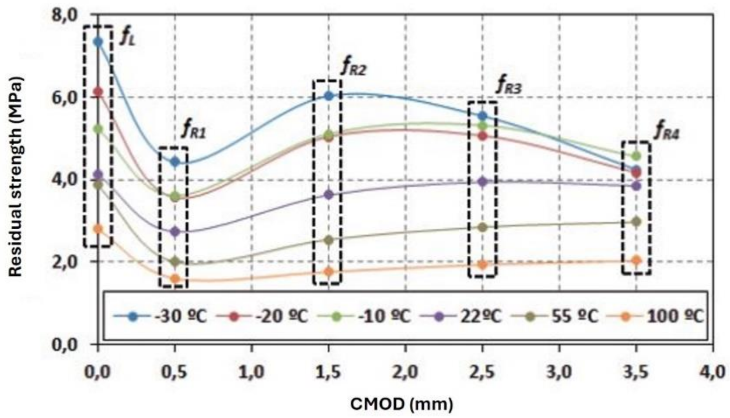

Figure 23. Flexural strength results in terms of temperature [138]**.**

ii) Studies at low and sub-zero temperatures

Several authors indicated that decreasing the temperature of plain concrete below the standard temperate of 20°C leads to enhancements in its tensile strengths, but also increases brittleness [157,158]. Lee et al [141] presented similar results for the splitting tensile strength. Rocco et al. [159] studied the fracture properties of ordinary concrete, under temperatures ranging from 20 to

-170 °C. Their results showed that as the temperature decreased, the tensile strength and the fracture energy increased, especially until -70 °C. Below this temperature, these properties tended to increase slowly or to remain constant (see Figure 24).

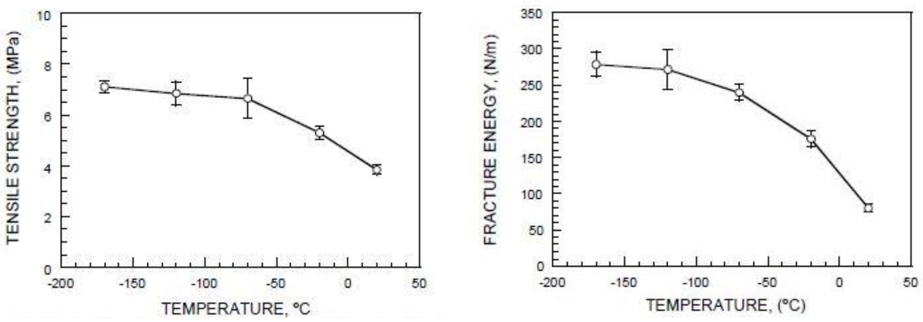

Figure 24. Effect of low temperatures on (a) tensile strength and (b) fracture energy of concrete [159]**.**

Furthermore, Montejo et al. [145] provided an extensive literary review focused on the low temperature effect on plain concrete and they presented that the tensile strength, assessed through splitting in cylinders, exhibits a more significant increase with decreasing temperature compared to the compressive strength. Mirzazadeh et al. [160] investigated the behavior of beams made of reinforced concrete at low temperatures (-25 °C) and they compared with those at room temperature (15 °C). Four large-scale beams were produced and tested. The beams tested at -25°C demonstrated an increase in strength (13 %) and ductility (34 %) compared to the beams tested at 15 °C.

In FRCs, Pigeon et al [161] reported the mechanical flexural strengths of SFRC at low temperatures, following ASTM C1018. The tests were performed at standard temperature (20 °C), at -10 °C and at -30 °C. The results show that, under flexural loading, the toughness of SFRC increases with a temperature decrease. This increase appears to be related to the increase in the strength of the matrix at low temperatures, which increases the energy required for fiber pull-out. In addition, Richardson and Ovington [155] examined the effect of temperature on SFRCs and MSFRCs at -20 °C (see Figure 22). All beams tested at -20 °C exhibited a significant increase in flexural strengths when compared to the same beam tested at room temperatures. The flexural strength at the LOP showed an average of 99 % increase in the plain beam, an average of 150 % increase in the MSFRC beam (PP fibers) and, an average of 79 % increase in the SFRC beam. A significant increase in the performance of concrete was observed at a temperature of -20 °C. Synthetic fibers provided the optimal performance based on the flexural strength percentage change when compared to the control and steel fiber samples.

Navarro et al. [138] also showed consistent results on their flexural and Barcelona tests with the previous one (see Figure 23). They also concluded that the fibers presented a more homogeneous behavior at 22 °C since the coefficients of variation (CoV) were smaller. Stanislav et al. [162] evaluated the flexural behavior of two MSFRCs (MSFRC-4 – with 4 kg/m³- and MSFRC-8 – with 8 kg/m³) at different temperatures (up to -30 °C) of notched prisms whereby 3PBTs according to EN 14651, once the temperature was reached in the core of the beams. The results proved that low temperatures (below 0 °C) led to rise the energy required to produce fiber pull-out, and therefore, post-cracking flexural behavior was improved: f_{R1} increased to 54 % and f_{R3} increased to 71 %. This large increase in flexural strength can be seen in Figure 25 and it is believed to be due to the formation of ice within the pores of the concrete and a grip effect, according to [163].

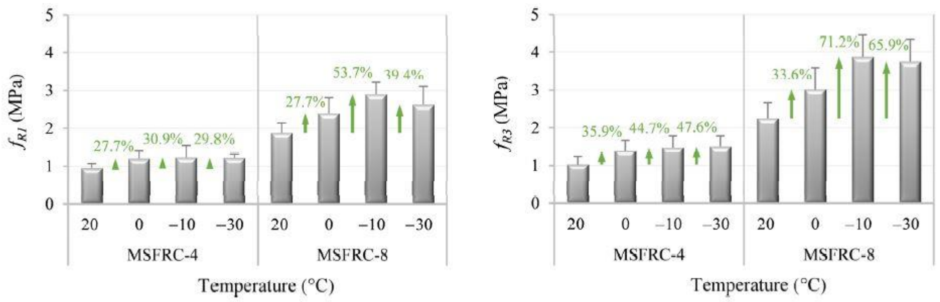

Figure 25. Mean values of f_{R1} and f_{R3} of the different MSFRCs under low temperatures [162]**.**

At very low temperatures, Rostásy and Sprenger [150] found that the addition of steel fibers greatly reduced the loss of tensile strengths under repeated thermal cycles down to −170 °C. Rocco et al. [159] assessed the fracture properties of a conventional concrete at temperature ranging from 20 to -170 °C by standard 3PBTs and cylinder splitting tests. The results show that very low temperatures improve the fracture properties of concrete. This increase of the strengths at very low temperatures can be explained by the freezing of water in the bulk of the concrete.

iii) Long-term studies at temperatures

All these previous works have been focused on the response of FRCs under elevated and low temperatures at short-term. To date, one of the most recurrent reasons for preferring steel fibers than macro synthetic fibers in certain applications in which both types of fibers could be considered feasible, is the uncertainty regarding the long-term performance of MSFRC.

The effects of elevated temperatures (up to 60 °C) on the long-term behavior have been studied by some researchers. Buratti et al. [164] presented the experimental results on cracked MSFRC (PP fibers) elements at different temperatures (20–50 °C). Long-term behavior was evaluated by four-point bending tests. Increasing the temperature had a significant effect on long-term deformations producing, in some cases, creep failure.

The characterization of the long-term deformations of MSFRC with polypropylene fibers depending on the temperature was also studied by Del Prete et al. [165]. Their creep curves showed a sudden increase in the slope when temperature increased, for all the type of tests considered. Thus, temperature also has a significant influence on the long-term behavior of FRC, particularly, in creep performance, with higher creep deformation at higher temperature. The flexural creep of MSFRC is a different controversial issue regarding its long-term behavior since long-term durability can be compromised by time-dependent phenomena. Information on long-term flexural behavior of FRC is also available in the technical literature [166].

Other authors also studied long-term behavior at temperatures. Caballero-Jorna et al [167] studied the effect of moderate temperatures (5, 20, 35 and 50 °C) on the flexural strengths of MSFRC (polypropylene) and SFRC in reduced-size specimens (100 × 100 × 500 mm) after two months of exposition. The tests were performed at the target moderate temperatures in non-pre-cracked and in pre-cracked specimens. The findings suggested that these temperatures did not deteriorate the behavior of the FRC tested to a great extent. At very elevated temperatures, Bayasi and Dhaheri [168] also found that prolonged exposure to temperatures in the range of 100–200 °C led to a decrease in flexural strength and post-peak load-bearing capacity of fibrillated polypropylene fiber concretes. However, there was no effect of exposure at temperatures below 100 °C.

These (and similar) results suggest that FRC will function properly at the high ambient temperatures that may be encountered in practice in hot climates (~40–50 °C).

iv) Comparison of methodologies

Researchers have used different methodologies and test set-ups to perform their experimental campaigns. In addition, the dimensions of the tested elements are diverse, and in most of the cases, the objective is to study the degradation of the fibers *per se* or how this degradation may affect. MSFRCs at very low (Liquid Natural Gas tanks) and high temperatures (fire situations), a range of temperatures outside of the scope of this Thesis.

In the literature, the different types of methodologies reported for testing concrete at temperatures can be divided in three groups (based on [169,170]):

- in stressed specimens (in steady state) which are prestressed to a certain fraction of their ultimate load and then are exposed to high temperature until failure, at a constant load (creep tests) [171].
- in specimens (in steady state) which are heated/cooled and then tested at target temperature [172].
- in specimens in residual conditions which are heated/cooled to a target temperature and then adjust to the environmental and tested at reference temperature (in transient state) [173].

These studies comprise a similar methodology: series of specimens are stored at different temperatures for various periods. The properties after the exposition are compared with the properties before the exposition or the properties after the exposition are contrast with those obtained at ambient temperature.

Most tests are in conducted in residual conditions (specimens are tested at standard temperature) due to the impossibility of manipulation of the samples at temperature, as pointed out by [174]. However, this Thesis focuses on the second type of test, which allows a more direct analysis of the temperature-induced effects on MSFRC properties. They followed a standardized test and modified some aspect to incorporate temperature during the test at short-term. Herein, the methods can be divided into two groups:

- methods that include modifications that allow insulate the specimen already at target temperature during the tests. In the first group, bubble wrap and gel sacks have been used to isolate the specimens during the test period when the specimens were removed from their storage areas [155,175].
- methods that incorporate temperature regulation during the tests. For example, tests are directly performed in-situ in environmental chambers with programming temperatures [176]. Additionally, external devices can be settled into the testing machine to regulate (increasing or reducing) temperature [148,177].

Figure 26 showed a comparison between some of the different methodologies used to evaluate temperature factor on mechanical properties of concrete while testing. In Figure 26-a and -b, it can be seen the specimens stored in an oven and a cooler respectively before testing (they are already tested after storing without any additional insulation system). In Figure 26-c, gel bags are used to maintain the temperature in the specimens previously exposed under the target temperature. Figure 26-d, Figure 26-e, and Figure 26-f show different scheme in which in test assembly have been incorporated the insulator blankets, furnace and the other complement to control temperature during the test.

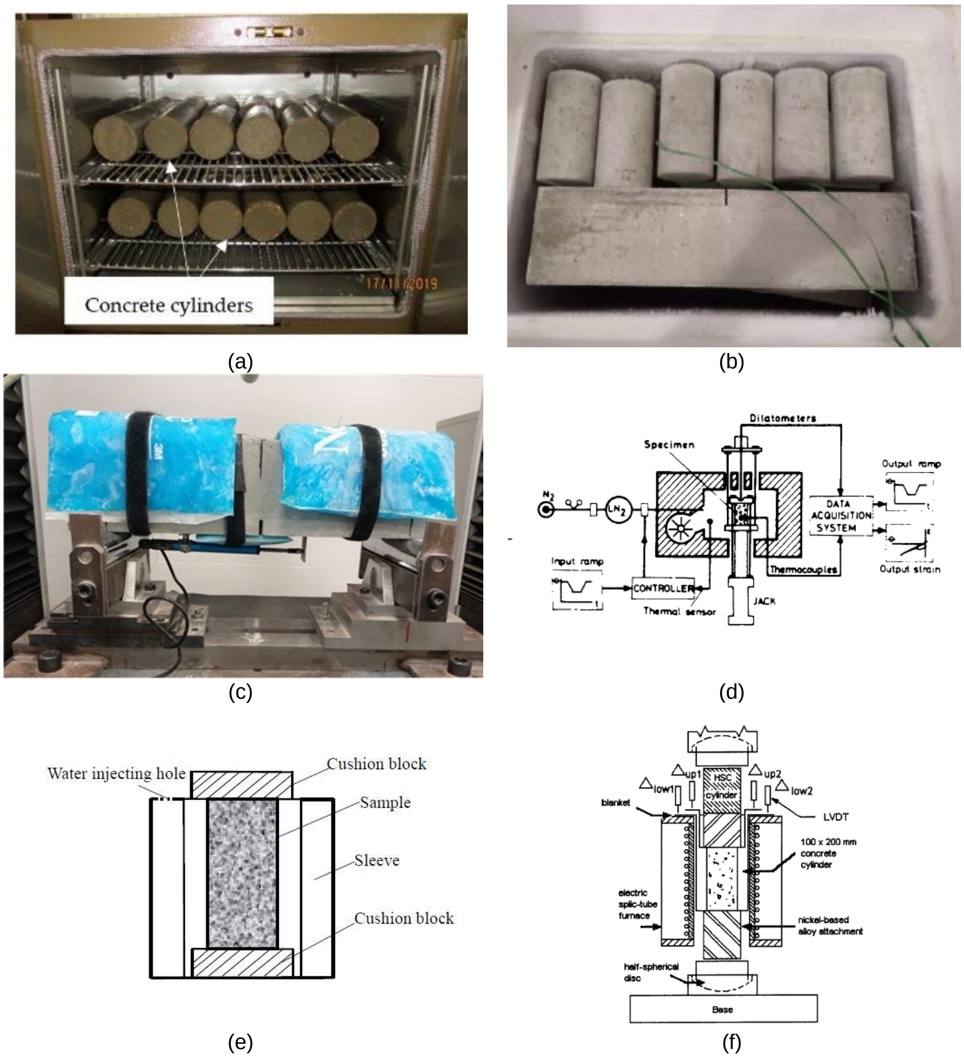

Figure 26. Different methodologies used to evaluate temperature factor: (a) [178]**; (b)** [162]**; (c)** [167]**; (d)** [177]**; (e)** [148]**; and (f)** [179]**.**

To evaluate the behavior at long-term, the most common process is accelerated testing in the laboratory, where the properties of the composites are determined before and after exposure to the accelerated aging conditions. In view of the variety of processes which may lead to aging, it is difficult to determine a universal test, and each method has limitations in the applicable temperature range and/or the test conditions. Most of studies are performed to evaluate creep and not only temperature effect over time.

To conclude, there are not standardized methods to evaluate temperature as a factor on main mechanical properties of FRCs. In order to evaluate effects produced at short- term, a modification is usually included in the standardized method to test at temperature or in most cases, the specimens are tested at reference temperature after a period of exposition. Regarding the effects produced after long-term exposure, mechanical properties of FRCs are studied mainly from a creep perspective, that includes the temperature factor [180].

v) Summary on tensile and flexural strength at temperatures

The changes in the environmental conditions (temperature and RH) alter tensile and flexural strengths of FRCs, but the quantification of these variations is not similar among the different investigations. In addition, the methods and range of temperatures studied differ. In general, it can be said that low temperatures tend to increase these mechanical properties of plain concrete and FRC and, high temperatures have the opposite effect. More investigations are needed to clarify the long-term performance of FRCs since most of the studies are focused on creep behavior, but not directly on temperature as a factor. The aforementioned differences between the methods described difficult obtaining a consensual knowledge about the influence of extreme environmental conditions on MSFRCs.

2.3.3. Influence of Temperature on the Fiber-matrix Interface

Similarly to the Interfacial Transition Zone (ITZ) between cement paste and aggregate in concrete [181], the region responsible for fiber and matrix bonding is known as fiber-matrix interface. In other words, it is the zone of gradual transition and highly heterogeneous between fiber and the concrete-matrix. The fiber-matrix interface plays an important role in FRC behavior since it drastically influences its toughness, flexural response, and long-term properties [182]. This is also effective for energy absorption, crack control and load transfer caused by fibers and to understand the stress distribution mechanism incorporated between fiber and concrete-matrix [183].

In order to understand the effect of temperature to fiber-matrix interface, which may affects one of the two mechanisms of the failure of fibers in FRC - the fiber-matrix debonding process, also known as fiber pull-out (the other mechanism, the fiber rupture, was indirectly seen in Section 2.3.1) -, nano-, micro- and meso- scale investigations of this region are necessary and to date, it is an ongoing topic. This subsection analyzes the mechanism of elements involved in this interface and examines the changing behavior under non-standard temperatures. For this purpose, fiber-matrix interface structure at nano- and micro-scale, is firstly presented. Later, fiber-matrix interface's information from a meso-scale is collected.

a) Fiber-matrix interface structure at nano- and micro- scale

At a nano- and micro- scale, the effectiveness of fibers as reinforcement depends on the structure and properties of the fiber-matrix interface. The structure is formed by two layers: (i) aggregate contact surface and (ii) porous transition zone also called as matrix contact layer. The composition of aggregate contact surface is made with CH crystals and C-H-S gel, while matrix contact layer is made with CH (more than in aggregate contact layer), C-H-S gel, and little ettringite ($Ca_6Al_2(SO_4)_3(OH)_{12}\cdot26H_2O$) [184]. These layers are weak in nature and hence, fiber-matrix interface itself. Figure 27 displayed the schematic representation of this region.

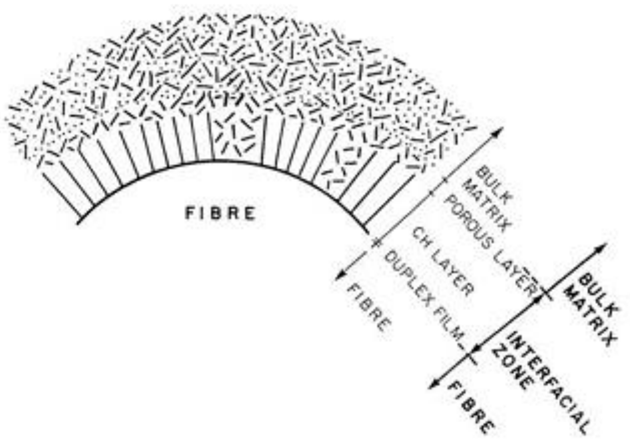

Figure 27. Schematic representation of the fiber-matrix interface of an FRC [185]**.**

Zhao and Sun [186] found that the mechanical properties of the hydration products do not vary as the surface of the fiber is approached, which indicates that there is no mechanical gradient for the hydration products across the interface and thus, it has an efficient and strong bond. Xu et al. [187] demonstrated that increasing w/c ratio led to a lower mechanical property given an increase in the volume fractions of porosity, and therefore, a weak fiber-matrix interface.

As a consequence of the previous idea, it can be expected that bond strength increases with temperature since temperature affects the rate of hydration at early-age, and this rate affects the porosity of the paste. However, some adverse effects can be involved simultaneously which counteract the expected improvement in bond strength with temperature, such an adverse effect may be the paste-aggregate interface cracking.

Other factor which affects fiber-matrix interface is the fiber type [187]. In terms of the formation mechanism, different properties of steel and PP fibers (hydrophilic vs. hydrophobic nature, and high elastic modulus and the tensile strength of steel fibers compared to PP fibers) are responsible for the difference of each fiber-matrix interface. For steel fibers, the presence of an iron oxide layer that is always formed, results in a higher w/c ratio in the vicinity of this fiber surface. However, for PP fibers, high porosity, repellent nature and no existing of this metal oxide led to a relatively weaker interface than steel fibers. Other authors have also reported a poor adhesion of the PP fiber to the surrounding cement matrix due to their chemical inertness [74].

Finally, the thickness of fiber-matrix interface has been also found to depend on the fiber type. The steel fiber-matrix interface is approximately 30 µm wide. PP fibers present a fiber-matrix interface's thickness nearly of 15 µm. This difference in thickness is governed by the fiber size, according to the wall effect [188].

b) Fiber-matrix interface properties in meso- scale

From a meso- scale point of view, the effectiveness of fibers as reinforcement depends on fiber-matrix interactions and matrix properties. On the one hand, the complete fiber pull-out has been described vastly in the literature. This generally takes place in two phases: first, fiber debonding occurs along the embedded length, (L_e), and then, a frictional behavior is observed. In this sense, various parameters are particularly important in the frictional behavior (stress-transfer mechanism): the friction resistance and the mechanical anchorage of the fiber. Regarding to the former, it appears the concept of normal stress (named also as clamping stress). This is one of the responsible of the friction resistance which is produced by a misfit (δ) between the fiber radius and the radius of the hole. A variation in the radius of the hole in the matrix or in the radius of the fiber or both for any reason would induce a different response (increasing or reducing the frictional resistance). If δ is negative, that occurs when the reduction in the radius of the hole in the matrix is greater than the reduction of the fiber radius, frictional resistance will be enhanced. Nevertheless, if δ is positive, the clamping stress will not develop, and the frictional resistance will be reduced. To date, some effects which can generate this misfit δ, have been informed in Subsection 2.3.1.

Regarding mechanical anchorage, with the purpose of improving bond strength of the fiber and the matrix, plenty of studies have been published about fiber's geometry. Some authors say that this factor influences more when micro-PP fibers and bundled fibers are used [189]. Different geometric shapes have been investigated since then, for both steel and synthetic fibers (e.g., crimps, hooks, deformed fibers). Concretely, in PP fibers, its bond strength can be enhanced by manufacturing the fibers with a twisted shape, wavy curl formation, or texturing the fiber surface [190,191]. This fiber surface or geometry may be affected by temperature. In PP fibers, no studies regarding superficial alteration by temperatures have been found. In other kind of synthetic fibers (PVA fibers), this topic has been addressed [192].

Furthermore, only few studies investigated the fiber-matrix interface properties, from a meso- scale perspective, within the selected temperature range of this Thesis. In MSFRCs, Richardson et al. [155] studied the influence of temperature on the bond strength between polypropylene (PP) fibers and the matrix through pull-out tests at a low temperature of -20 °C. Their results show that the frozen cube achieved a much greater concrete to polypropylene bond strength, with an 18 % increase in bond strength when compared to the cube at 20 ˚C. This would indicate that the bond strength was increased when the temperature is reduced.

Figure 28. Pull out – test rig [155]**.**

Stanislav et al. [162] analyzed the structural flexural response of the tested FRC beams at low temperatures and claimed its positive effect on the energy required to produce fiber pull-out, since the concrete-matrix that embeds the fibers shrinks with the decrease in temperature, provoking an increase in confinement pressure along the fibers and thus, enhancing the anchorage capacity of fibers.

Moreover, in SFRCs, the effect of temperatures (ranging to 100 up to 800 °C) was studied on the bond mechanisms associated with the pull-out behavior of two types of steel fibers [193]. A series of pull-out tests were performed on 4D and 5D hooked end steel fibers embedded in four different cementitious matrixes, namely normal strength concrete (NSC), medium strength concrete (MSC), high strength concrete (HSC) and ultra-high-performance mortar (UHPM). The comparisons between the two fiber types showed that the mechanical anchorage contribution provided by the 5D hooked fiber was significantly higher than that of the 4D hooked fiber, especially for HSC, in all the temperatures.

At long-term, bond strength between polypropylene and cement paste was relatively unaffected by exposure condition or time for periods up to 18 years [132]. Polypropylene has no physicochemical bonding with cement paste, but nevertheless excellent mechanical bond has been achieved. Photographic evidence support that the measured bond strengths may depend on the intermolecular shear strengths of the aligned polymer chains, which are naturally time stable and do not depend on the matrix microstructure.

However, in a more recent study conducted by Del Prete et al. [165], the long-term behavior of concrete reinforced with PP fibers was experimentally characterized using uniaxial tests, with a specific focus on the moderate temperature effect (from 20 up to 40 °C). Their results on notched pre-cracked cylinders allowed to observe the long-term bond behavior between the fibers and the matrix (bond or slippage). The progressive elongation of fibers with temperature and time, led to the reduction of their cross-section, which weakened the long-term bond capacity. In SFRCs, it has been mentioned that the impact of moderate to elevated temperatures primarily changes the long-term behavior of fiber–concrete bond [194].

To conclude, factors like the damage to the fiber-matrix interface, debonding, and pull-out of fibers, significantly impact the mechanical behavior of MSFRCs, especially under certain environmental conditions. Thus, some conditions of temperature and humidity may not be compatible with a good performance of certain fibers.

i) Comparison of methodologies

Various experimental set-ups are employed in the literature to assess the fiber-matrix interface, and in turn, bond strength between fibers and the matrix in FRC. Regarding the scale, most of them are focused on nano- and micro- scales, but it can be analyzed from a meso-scale perspective. A typical multiscale categorization is sketched in Figure 29, adapted from [187].

FRC is treated as a homogeneous continuum at macro- scale, of which the stress-strain relation runs the response of a structure (*e.g.* a dam). When scaling down to meso- scale, the composite consisting of fibers, aggregates and cement matrix becomes discernible. The development of tests (compression, flexure, etc.) contributes to define constitutive behavior of the FRC as material. Thereafter, at micro- scale, the fiber-matrix interface is revealed through Scanning Electron Microscopy (SEM), Transmission Electron Microscopy (TEM), Electron Backscattered Diffraction (EBSD), X-ray Diffraction, Energy Dispersive Spectrometer (EDS), etc. The development of fiber pull-out tests is motivated in some cases to obtain the bond-slip behavior as a first step at micro- scale. Further, at nano- scale, the crystalline nanostructure in the fiber-matrix interface is determined by other techniques, as nanoindentation.

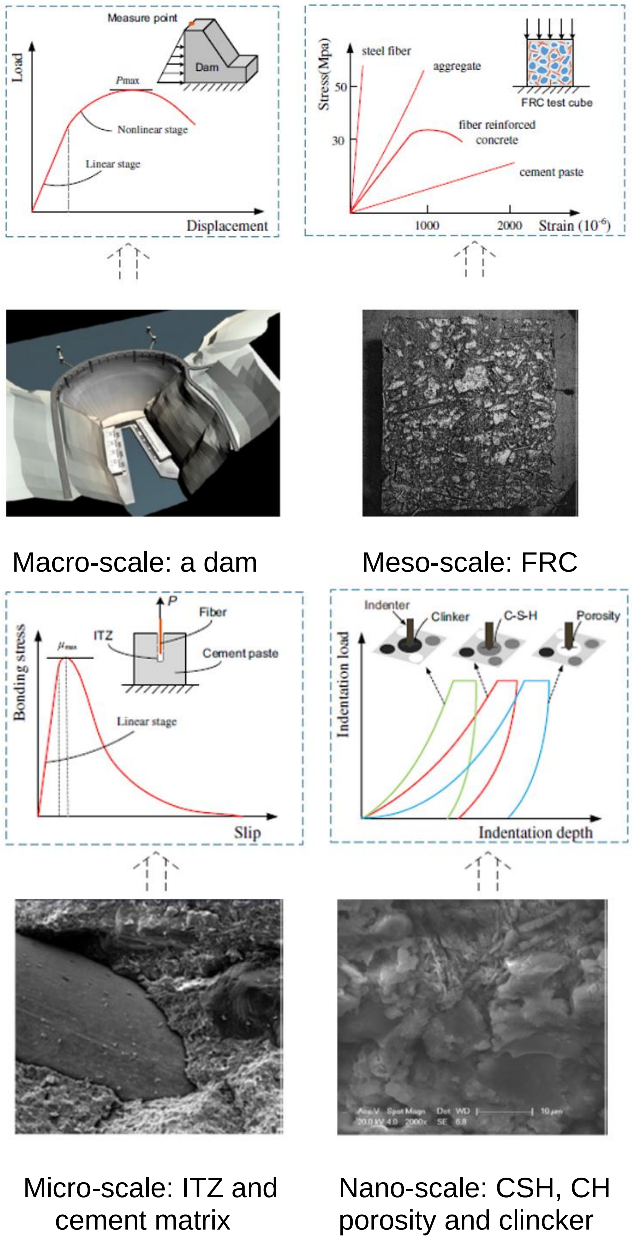

Figure 29. Representation of the multiscale structure of FRC and the typical test means [187]**.**

Regarding methods to determinate the bond strength from a meso-scale perspective, they can be divided in two categories: (i) direct and (ii) indirect tests.

- In the first category, one of the commonly used methods of characterizing the bond between fiber and concrete-matrix systems is the direct pull-out test, where a fiber which fully penetrates a cube or cylinder of concrete is pulled out by direct tension while applied load as well as displacement at the loaded and/ or free end of the fiber are recorded [195,196]. Pull-out tests are commonly utilized to investigate bridging mechanisms, according to UNE-EN-12504-3 [197].
- In the second category, indirect tests such as flexural and direct tensile tests are also performed and might offer insights at the meso-scale regarding fiber pull-out or debonding behavior within the cementitious matrix [198]. Since uniaxial tests are difficult to implement, flexural tests are normally used to characterize tensile strengths. Nevertheless, it should be noted that the response obtained under flexural and tensile loads may not be identical. In flexural conditions, there is a zone with compression stresses and the deformation and stress increase linearly, which contributes to a more stable crack propagation. The differences on the most used approaches can be seen in Figure 30, adapted from [199].

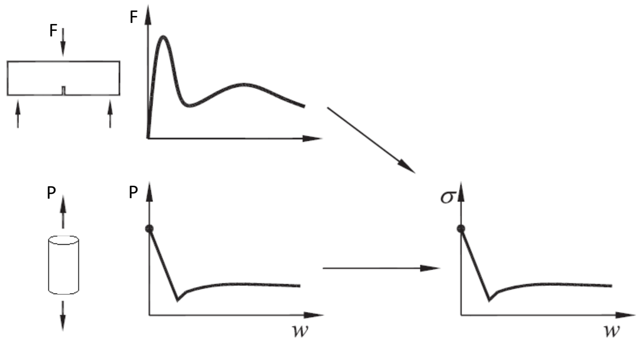

Figure 30. Differences between the approaches to determine the tensile properties of MSFRCs [199]**.**

Normally, these tests are performed at standard temperatures since there is not a regulation to perform at other temperatures. As described previously, scarce studies were done to study fiber-matrix interface at meso- scale, at temperatures.

To conclude, several methods and perspectives to study the fiber-matrix interface between fiber and concrete exist, however, none includes temperature factor as the main objective. More studies are necessary to understand the behavior of MSFRC in realistic conditions, particularly regarding fracture characteristics at low and moderate high temperatures.

2.4. Design Specifications of MSFRC

The dissemination of knowledge collected over recent decades regarding MSFRCs to the engineering community has been hindered by the absence of specifications and standards. Even though Macro synthetic fibers have been included in some national structural design guidelines of several countries (as Spain, Germany, Italy, etc.), most of international standards incorporate only SFRCs [200].

The publication of the MC 2010 [24] promoted the use of SFRC in structural applications and warned over the use of other types of FRCs. Similarly, the new Eurocode 2 [201] only incorporated steel fiber as reinforcement for FRC, excluding other types of fiber reinforcements. Currently, concrete designed with PP fibers relies heavily on manufacturer's recommendations currently in order to achieve the designer's requirements. Due to this, it is of interest to consider statements, codes and regulations that include other potential fiber reinforcements in order to make an appropriate choice for the fiber type. Considering the expansion in MSFRC applications, their recent inclusion in standards and codes was expected.

Subsection 2.4.1 summarizes notes about MSFRC and temperature effects considered in MC 2010, as well as the classification of FRC according to their contribution in the post-cracking behavior. Subsection 2.4.2 provides a global overview of the information regarding MSFRCs included in the standards.

2.4.1. Fib Model Code

MC 2010 states "*Fiber materials with a Young's modulus which is significantly affected by time and/or thermo-hygrometrical phenomena are not covered by this Model Code*". This warning points out clearly to synthetic, organic, and natural fibers. It also declares that using these type of reinforcement, post-cracking long term behavior can be affected by additional creep of the fibers themselves. Claims have been made by manufacturers that steel fibers do not suffer performance loss with temperature and age, but this has yet to be verified [202]. These arguments support MC 2010 statements, generating mistrust in the use of other kind of fibers.

However, macro synthetic fibers can be used in some specific applications where those concerns do not apply but giving coverage from a normative perspective, *e.g.*, in applications where a SLS is not important, as a minimum shear reinforcement or in structures where FRC creep does not influence ULS capacity [203]. Some authors [204] add that the use of synthetic fibers as reinforcement should not be disregarded as long as additional factors are considered during the design.

The content on FRC in MC 2010 derives predominantly from SFRC experiences but it could be extrapolated to other types of FRCs under the designers' responsibility. The minimum requirements for structural FRC are independent of fiber material; they are based on the post-cracking behavior through the residual strength at different cracking levels. Designers should consider these conditions as they can help determine the appropriate fiber type and fiber dosage to utilize. With this in mind, a minimum performance class ''1.0 a'' must be guaranteed if FRC aims to substitute (even part of) conventional reinforcement, according to the proposed classification. This means that the minimum value for $f_{R1\mathrm{k}}$ is 1.0 MPa and for f_{R3k} is 0.5 MPa. In addition, it is compulsory that Equation (1) and Equation (2) would be fulfilled:

$$f_{R1\mathrm{k}} \geq 0.4\, f_{\mathrm{LOPk}}$$ **Equation (1)**

$$f_{R3\mathrm{k}} \geq 0.5\, f_{\mathrm{R1k}}$$ **Equation (2)**

where:

$f_{R1\mathrm{k}}$ is the post-cracking strength (characteristic value) corresponding to a CMOD of 0.5 mm, according to EN 14651.

$f_{R3\mathrm{k}}$ is the post-cracking strength corresponding to a CMOD of 2.5 mm, according to EN 14651.

f_{LOPk} is the flexural strength at LOP, according to EN 14651.

Ductility must be also guaranteed at the structural level, accordingly, at least one of the two following structural requirements (see Equation (3) and Equation (4)):

$$\delta_u \geq 20\, \delta_{SLS}$$ **Equation (3)**

$$\delta_{peak} \geq 5\, \delta_{SLS}$$ **Equation (4)**

where:

δ_u is the ultimate displacement of the structure.

δ_{peak} is the displacement at peak load.

δ_{SLS} is the displacement expected under service conditions.

Regarding to temperature topic, MC 2010 considers temperature as an imposed deformation (indirect action). The information given (as in the most regulations) is only valid for a reference temperature independently of the material. The reference temperature considered is 20 °C, since early concrete tests were done at ambient conditions where the temperature was generally between 18 to 21 °C [14]. The common range of environmental condition does not involve concrete subjected to extreme temperatures, high (*e. g.,* nuclear reactors) or low (*e. g.*, Liquid Natural Gas tanks) or very dry climatic conditions (average relative humidity RH < 40 %). In some sections, it deals with some range of temperatures (*e.g.*, 0 °C < T < 80 °C for creep and shrinkage, seasonal variation, etc.). The same holds true for variations in RH, with most values are kept around the mean values given in the same tables.

2.4.2. International Recommendations, Codes and Standards

Regarding the European Standards, in 2006, EN 14889 [205] and EN 14845 [206] were approved to include in both of them fibers for concrete. Standard EN 14889-2 refers to synthetic fibers for concretes. It requires verifying the long-term behavior by testing the resistance to deterioration for moisture and alkalis present in cement paste, according to EN 14649 [207]. These tests were initially proposed for glass fibers as accelerated tests to provide material degradation into a specific tolerance and allow to evaluate if a fiber is ‘‘adequate or not for structural concrete’’, assuming that the possible effect in the mechanical performance at the end of the service life is negligible.

Currently, macro synthetic fibers are excluded from the new Eurocode 2. In Spain, the Spanish Code on Structural Concrete considers three typologies of fibers: steel, synthetic and glass. The American Concrete Institute adds a fourth group of natural fibers.

In summary, although several international recommendations, codes and standards contemplate the use of MSFRCs, their presence is still limited due to the unsolved concerns regarding their performance at temperatures and at long-term.

2.5. Critical Summary

This Chapter 2 has provided a global overview about the influence of extreme environmental conditions on MSFRCs, focusing mainly on temperatures.

In general, fibers are added to improve plain concrete properties and durability. The FRC performance depends on three elements: (i) the fibers, (ii) the concrete-matrix, and (iii) the bond between fiber and matrix. Subsequently, failure of FRC elements is the result of a failure of, at least, one of these elements.

As previously mentioned, PP fibers are employed in the reinforcement of concrete as they present some advantages including improved performance and durability. The current manufacturing processes used in the plastic industry makes it possible to obtain fibers with different geometrical and mechanical properties. Nevertheless, one of the main drawbacks of synthetic fibers is that their properties are influenced by hygrothermal phenomena [208]. Temperature changes affect their chemical, physical and mechanical properties, which can lead to dramatic degradations and loss of bearing capacities. Additionally, it has also been demonstrated that the nature of concrete-matrix is affected by temperature. These results produce mistrust in using synthetic fibers in several applications due to these results could compromise the mechanical behavior of MSFRC. However, the decrease in performance detected in synthetic fibers and plain concrete will not necessarily have an equivalent effect in a FRC level. Currently, there is not sufficient information about the performance of FRCs exposed to changes in temperatures and RH, and furthermore, there is not an agreement about the influence of temperature on MSFRCs behavior at short- and long-term. To date, this topic is a point of on-going discussion at the technical and scientific level, as well as the influence of temperature on interface between fiber and matrix (bond strength).

On the one hand, some authors [165,176] affirm that the variation induced by the temperature range selected in this Thesis, affects in a great manner the properties of MSFRC, provoking a deterioration that reduces the bearing capacity of the structural elements and bond strength, especially, at long-term, where creep or aging can also take part.

On the other hand, other authors [167] claim that the variation induced by the selected temperature range are within an acceptable range of use on MSFRC (similar to those of SFRC, providing toughness and ductility) in applications with structural responsibility. At long-term, the use of PP fibers has been shown to give excellent properties retention (toughness and strength) in FRCs over many years, thus giving increased confidence in the long-term stability of polypropylene in a cementitious environment [132].

Additionally, there is not a standardized method to evaluate the influence of temperatures in mechanical properties. In this Chapter, most common used methodologies have been described. There is a great variety of dimensions of specimens, range of temperature, concepts in order to test (steady or transient, residual or in-situ) that complicate the joint analysis.

Therefore, the scarce information, the lack of consensus, together the methodologies used to evaluate this justifies the need for developing this Thesis, in order to evaluate MSFRC behavior in extreme environmental conditions. The significance of this research is that it provides, for the first time, a complete study on the mechanical behavior of MSFRCs exposed to temperatures after different exposure times and considering the presence of an existing previous crack. This research will allow to determine whether FRC should be designed with temperature induced mechanical degradation in mind. This could help structural designers in using MSFRC in a safer way and promote their inclusion in regulations and codes.

Chapter 3

Experimental Program and Methodology

This chapter describes the experimental program and the selection of methodologies that were performed in this Thesis to achieve the goals defined in Section 1.2 (Chapter 1).

This experimental program investigates the short- (3 days) and long-term (90 and 180 days) behavior of FRCs under extreme environmental conditions. To do this, three types of MSFRC with PF1, PF2 and PF3 (PP) fibers and one SFRC with SF fibers are selected. The short-term study focuses on understanding FRC's response to temperature variations through experimental campaigns examining fiber and material level. At fiber level, only the PF1 fiber is selected to perform direct tensile tests from -30 to 140 °C (considering other factors, as rate). At material level, mechanical properties are evaluated through direct tensile tests, compressive and flexural strength tests at temperatures ranging from -30 to 60 °C, in pre-cracked and non-pre-cracked specimens. The long-term study assesses FRC's behavior after 90 and 180 days of exposure under consistent temperatures. All these tests were performed in specimens at service conditions, that is, tested at the target temperatures, making a total of 210 fibers, 434 beams, 186 cubes and 30 cylinders.

Key variables, combination planned in the Thesis, materials used, methodologies, and specimen production are presented. Part of this experimental program is developed in collaborative research with the University of Bologna. The experimental program is summed up in Table 3.

Table 3. Experimental program implemented in this Thesis.

Period of exposure	Level	Performed tests	Temperature [°C]	Fiber type used
Short-term (3 days)	Fiber level	Direct tensile strength	-30 to 140	PF1
	Material level	Compressive strength	-15 to 60	PF1, PF2, PF3, SF
		Flexural tensile strength	-15 to 60	PF1, PF2, PF3, SF
		Direct tensile strength	-30 to 40	PF1
Long-term (90 and 180 days)	Material level	Compressive strength	-15 to 60	PF1, PF2, PF3, SF
		Flexural tensile strength	-15 to 60	PF1, PF2, PF3, SF

3.1. Outline of the Research Activity

This experimental program is divided into two study: the first study aims to investigate the behavior of MSFRCs at short-term when they are exposed to extreme environmental conditions, and the second study is focused on studying the long-term behavior of MSFRCs under extreme environmental conditions. In turn, the first study (short-term exposure) is subdivided into two parts which correspond to different levels: at the fiber and at the material level. Both studies are performed to increase understanding on the mechanical MSFRCs behavior under extreme environmental conditions since the response of the single fiber and the FRC matrix (including its interaction) may be different. The second study (long-term exposure) is focused on the material level.

3.1.1. First Study: Short-term Exposure

The first study of this experimental program is divided in two studies at short-term: (i) at fiber level and (ii) at material level. In total, it compiles four experimental campaigns, according to the performed tests: (i) direct tensile strength at fiber level, and (ii) compressive, (iii) flexure and (iv) direct tensile strength at material level.

The first experimental campaign is an experimental study of the fiber's viscoelastic behavior carried out at a fiber level[1]. One type of a commercial polypropylene fiber (named PF1) is chosen to evaluate, through direct tensile tests according to EN 14889-2, their mechanical properties (ultimate tensile strength and E-modulus), measured at temperatures from -30 to 140 °C.

[1] This study was developed in collaboration with the research group of the Department of Civil, Chemical, Environmental, and Material Engineering (DICAM) at University of Bologna (Italy) during the period of research abroad.

The second experimental campaign compiles the study of compressive strengths of FRCs subjected at temperatures (-15 up to 60 °C), after a short-term of period of exposure. It is carried out at material level. To do this, only a type of concrete was selected (C30/37). Moreover, the matrix was reinforced with three types of PP fibers (PF1, PF2 and PF3) and with one type of steel fibers (named SF) to compare their behavior. The fiber contents were 7 kg/m³ and 21 kg/m³, respectively. Compression tests were carried out on cubes according to UNE-EN 12390-3, incorporating a modification to consider temperature as factor during the test.

The third experimental campaign studies the same matrix, fibers and temperatures from the second campaign and it is also carried out at the material level. 3PBTs were performed at the target temperatures, following a testing methodology based on the standard UNE-EN 14651. The adopted configuration had a modification in order to include and to assess the influence of temperatures on flexural strengths. Notched prisms of MSFRCs and SFRC were tested after 3 days of conservation in diverse conditions, corresponding to the target temperatures. Additionally, some of these prisms were pre-cracked at 28 days, at standard temperature, until CMOD = 0.5 mm, before final testing, to compare pre-cracked and non-pre-cracked states.

The fourth experimental campaign analyzes experimentally the tensile behavior of MSFRC, at the material level[2]. Additionally, it indirectly evaluates the fiber-matrix interface from a meso-scale perspective (material level). PF1 was used to reinforce (8 kg/m³) a C45/55 matrix concrete. Direct tensile tests on MSFRC notched cylinders in fixed end boundary conditions were carried out using a special chamber to maintain the temperatures during the tests. The specimens were subjected to temperatures ranges from -30 up to 40 °C and after 3 days, they were tested.

3.1.2. Second Study: Long-term Exposure

The second study of this experimental program is divided in two campaigns measuring (i) compressive and (ii) flexural tensile strengths, both at material level, at long-term. They are focused on evaluating aging produced by temperature on these mechanical properties of FRCs. The first campaign of this second study analyzes the influence of extreme environmental conditions (-15 up to 60 °C) on compressive strengths of the same MSFRCs and SFRC after long-term periods of exposure. As long- term, a minimum of 5.000 hours of thermal aging is necessary according to [122], thus is, 180 days. To obtain additional conclusions and try to identify any trends between these ages, the age of 90 days was also studied. In turn, the second campaign examines, after long-term of exposure, the influence of the same environmental conditions on flexural

[2] This study was also developed in collaboration with DICAM research group at University of Bologna (Italy).

strengths. The selected matrix, type of fibers and pre-cracking condition are the same to the defined for these tests at short-term exposure to be able to compare the obtained results at different ages. For 90 days of exposure, the number of variables studied were reduced.

3.2. Experimental Program

In this Section, the experimental program is described in detail for both parts (short- and long-term exposure), explaining the planned combination of tests and specimens used to carry out the program, resulting in a total of 210 tested fibers, 186 cubes, 434 beams and 30 cylinders.

3.2.1. First Study: Short-term Exposure

The extent experimental campaigns implemented at short-term are collected in Table 4.

Table 4. Summary of the number and specimen type, their dimensions and the type of test performed at short-term.

Level	Type of test	Specimens type	Nº of specimens	Dimensions [mm]
Fiber	Direct tensile strength	Single fiber	210	*See Table 16
Material	Compressive strength	Cube	78	150 × 150 × 150
	Flexural tensile strength	Notched beam	182	150 × 150 × 600
	Uniaxial direct tensile strength	Notched cored cylinder	30	Ø125 × 200

a) First experimental campaign: single fiber tensile strength

Regarding to the fiber level, the study of the viscoelastic fiber's behavior was carried out. An experimental program was defined to determine the ultimate tensile strength (UTS) and E-modulus of the fiber at certain temperature for short-term exposure. To perform this testing program, only a type of fiber named PF1 was selected (more information about this fiber is provided in Table 16). Ten levels of temperature were selected to analyze its influence: -30, -20, -10, 0, 20, 40, 60, 80, 120 and 140 °C. The simulation of these environmental conditions is explained in Subsection 3.4.1. Per each temperature, 5 fibers were tested under tensile load. In addition, different load rates were also assessed: 1, 2, 9, 20 and 40 MPa/s. These rates were calculated from EN 14889-1 (see Table 5), taking the boundaries indicated for materials with a modulus of elasticity (E) lower than 150 GPa, the half and the double of these boundaries respectively, and the estimated velocity that the fibers had when they were tested inside the concrete-matrix under direct uniaxial load. These combinations resulted in more than 200 tests.

Table 5. Stress Rate according to [205]**.**

E-modulus of the material (E) [MPa]	Stress rate [MPa/s]	
	Min	Max
< 150000	2	20
≥ 150000	6	60

The objective was to research whereas the velocity of the test affects the properties obtained through the experimental tests, simultaneously with the temperature, increasing or decreasing its effect. Table 6 sums up this experimental campaign.

Table 6. Experimental study at single fiber level on tensile strength of fibers at short-term, including Nº of specimens performed.

Temperature [°C]	Rate [MPa/s]					Nº specimens (*)
-30	1	2	9	20	40	25
-20	1	2	9	20	40	25
-10	1	2	9	20	40	25
0	1	2	9	20	40	25
20	1	2	9	20	40	25
40	1	2	9	20	40	25
60	1	2	9	20	40	25
80	1	2	9	20	40	25
120			9			5
140			9			5

(*) 5 specimens per rate

b) Second experimental campaign: FRC compressive strength

In relation with the study at material level, at short-term (after 3 days of exposure), compressive strength was studied in MSFRCs and SFRC. Only a concrete-matrix was selected, in which different types of fibers (macro synthetic – PF1, PF2 and PF3 – and steel – SF –) were added. Table 7 sums up the exposure conditions to store the specimens during the exposure period, whose simulation is described in Subsection 3.4.1. The assigned codes (M15, 05, 20, 20S, 40 and 60S) will be kept for all the document and each one corresponds with one of the exposure conditions.

Table 7. Exposure conditions used and their codes.

Exposure conditions	**Air condition**				**Submerged condition**	
Temperature [°C]	-15	5	20	40	20	60
RH [%]	65	75	95	50	100	100
Code	M15	5	20	40	20S	60S

Compressive strength was examined through compression tests at on FRC specimens, after being exposed to different environmental conditions (exposure at different temperatures and conditions – air/submerged –). The methodology used to evaluate temperature as a factor during compression testing is explained in Subsection 3.4.3. Table 8 sums up the proposed combinations in this experimental campaign. As can be seen, six conditions were simulated. Per each combination (exposure condition and type of studied FRCs), 3 or 6 cubes of 150 mm side were tested, making a total of 78 specimens.

Table 8. Number of cubes at FRC level on compressive strength on FRCs at 3 days of exposure.

Code	**M15**	**05**	**20**	**40**	**20S**	**60S**
PF1	6	6	6	6	6	6
PF2	3		3			3
PF3	3		3			3
SF	6		6		6	6

c) Third experimental campaign: FRC flexural tensile strength

Table 9 summarizes the studied combinations in this work under flexural strengths (at material level) at short-term. The combinations include type of fibers (macro synthetic or steel fibers aforementioned), exposure condition (see Table 7) and pre-cracking conditions (P for pre-cracked specimens until a CMOD = 0.5 mm, at 28 days, at an ambient temperature of 20 °C; N for non-pre-cracked specimens). The RH was measured in all the conditions (it could be considered constant) during the time of exposure. In all, 26 combinations of study have been performed to analyze the behavior at temperatures at short-term of MSFRCs and SFRC. Per combination, seven standard notched beams (150 × 150 × 600 mm) were tested for each test series to compensate the variability of the measures. 126 beams of MSFRCs and 56 beams of SFRC were tested, in total,182 beams have been performed in this study.

Table 9. Number of beams tested at the FRC level on flexural tensile strengths on FRCs at 3 days of exposure.

Code		M15	05	20	40	20S	60S
PF1	P	7	7	7	7	7	7
	N	7	7	7	7	7	7
PF2	P						
	N	7		7			7
PF3	P						
	N	7		7			7
SF	P	7		7		7	7
	N	7		7		7	7

d) Fourth experimental campaign: FRC direct tensile strength

Direct tensile strengths were also evaluated by means of uniaxial direct tensile tests, at a material level, at short-term. This experimental campaign allowed to study indirectly the bond between fiber and matrix at different temperatures on MSFRC. In this case, PF1 was the only fiber selected to reinforce the matrix. Table 10 summarizes the planned combinations and number of specimens tested in this experimental campaign.

Table 10. Experimental campaign on direct tensile strength on MSFRC-PF1 at 3 days of exposure, including Nº of specimens performed.

Temperature [°C]	Nº specimens
-30	5
-20	5
-10	5
0	5
20	5
40	5

As can be seen, six different conditions were selected to conditionate and test the specimens, each of which ones corresponds with a level of temperature: - 30, -20, -10, 0, 20, and 40 °C. Per each combination, 5 cylinders were tested (150 mm and Ø 125 mm), making a total of 30 specimens. The methodology used to evaluate this property is explained in Subsection 3.4.3.

3.2.2. Second Study: Long-term Exposure

The experimental campaign implemented at long- term is collected in Table 11.

Table 11. Outline of the number and specimen type, their dimensions and the type of test performed at long-term.

Type of test	Specimens type	Nº of specimens	Dimensions [mm]
Compressive strength	Cube	108	150 × 150 × 150
Flexural tensile strength	Notched beam	252	150 × 150 × 600

a) First experimental campaign: FRC compressive strength

In relation with the study (at material level) at long-term, compressive strength was studied after 90 and 180 days of exposure. Table 12 and Table 13 sum up the experimental studies on compressive strengths at these ages, respectively. Compressive strength was examined through compression tests at temperatures on FRCs. The methodology used to evaluate temperature as a factor during compression testing was the same that those used at short-term. Per each temperature (six levels were selected), 3 or 6 cubes of 150 mm side were tested per each type of studied FRC. The same concrete-matrix used at short-term was produce herein to perform these tests. In total, 108 cubes were tested in compression at long-term, of which 30 were tested at 90 days and the rest (78) at 180 days.

Table 12. Number of cubes at FRC level on compressive strength on FRCs at 90 days of exposure.

Code	M15	5	20	40	20S	60S
PF1	6		3			6
SF	6		3			6

Table 13. Number of cubes at FRC level on compressive strength on FRCs at 180 days of exposure.

Code	M15	5	20	40	20S	60S
PF1	6	3	6	3	6	6
PF2	3		3	3		3
PF3	3		3	3		3
SF	6		6		6	6

b) Second experimental campaign: FRC flexural tensile strengths

Flexural tensile strengths were evaluated by means of three-point bending tests at long-term, at material level. This property was examined at 90 and 180 days. The methodology used to evaluate temperature as a factor during flexural testing is explained in Subsection 3.4.3 and it is the same that used at short-term. Table 14 and Table 15 summarize the studied combinations in this work under flexural strengths at long-term at 90 and 180 days, respectively, considering type of fiber used, conditions and state. In total, 10 combinations were performed at 90 days and 26 combinations were performed at 180 days. The combinations studied after 180 days of exposure are similar to those studied after 3 days of exposure, to guarantee comparability. The dosage of FRC to carry out these tests was the same as that used for the second campaign at short-term and the compression tests at long-term.

Table 14. Number of beams at FRC level on flexural strength on FRCs at 90 days of exposure.

Code		M15	05	20	40	20S	60S
PF1	P	7					7
	N	7		7			7
SF	P	7					7
	N	7		7			7

Table 15. Number of beams at FRC level on flexural strength on FRCs at 180 days of exposure.

Code		M15	05	20	40	20S	60S
PF1	P	7		7		7	7
	N	7	7	7	7	7	7
PF2	P						
	N	7		7	7		7
PF3	P						
	N	7		7	7		7
SF	P	7		7		7	7
	N	7		7		7	7

3.3. Materials

3.3.1. Fibers used

The macro synthetic fibers used in this Thesis were MasterFiber 254 (PF1), MasterFiber 249 (PF2) and MasterFiber 255 SPA (PF3) from Master Builders Solutions, and the steel fiber used (SF) was DRAMIX 65/35, from Bekaert.

Table 16 collects the main properties of these fibers. The content of fiber depends on the campaign, so it is specified in the following sections. Additionally, Figure 31 shows the fibers used in this work.

Table 16. Properties of fibers used in this work.

PROPERTIES	**Code**			
	PF1	**PF2**	**PF3**	**SF**
Raw material	Polypropylene	Polypropylene (Polyolefin 100 %) (*)	Polypropylene (**)	Steel
Design	Embossed (colorless)	Monofilament (colorless)	Embossed (white)	Hooked-end 3D
Equivalent diameter [mm]	0.81	0.85 (cross-section: 0.55 mm²)	0.70	0.55
Length [mm]	54	48	40	35
Aspect ratio	67	56.5	79	65
Cross section shape	Irregular	Elliptical	Irregular	Circular
Tensile strength [MPa]	552	400 (>400) (according to ASTM-D638)	500	1345
E-Modulus [GPa]	7	4.7(>6) (according to ASTM-D790A)	7	210
Secant modulus [GPa]	6	---	6	---
Water absorption	----	Nil	---	---
Density [kg/m³]	910	910	910	---
Alkaline/Acid resistance	High	High	High	---
Melting point [°C]	150 - 170	160 (according to ASTM-D648)	150 - 170	---
Ignition point [°C]	350	350 (according to ASTM-D648)	350	---
Combustion gases in fire conditions	---	Carbon monoxide, carbon dioxide and other gases or fumes may be evolved	---	---
Recommended dosage [kg/m³]	2.5-10	2.5-8 (3-10)	2.5-10	Minimum 15

(*) It is extruded from a natural polypropylene homo polymer and formed into a crimped profile to anchor it in a cementitious matrix.
(**) Chemical base polymer of modified polypropylene.

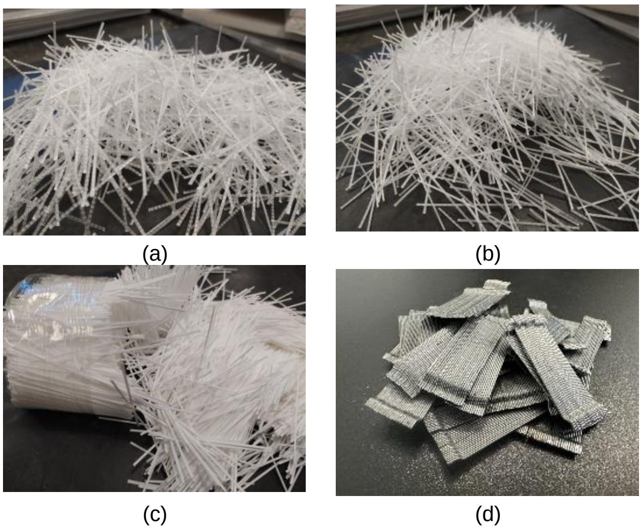

Figure 31. Fibers used: (a) PF1; (b) PF2; (c); PF3 and (d) SF.

3.3.2. Concrete Mix Design used

a) Experimental campaigns on compressive and flexural tensile strengths

To perform the experimental studies at short- and long- term on compressive and flexural strengths, only one matrix was selected. The mixture proportions (see Table 17) were decided to have a standard and a good quality concrete, with a compression class C30/37, a maximum aggregate size (MAS) of 20 mm and a slump of around 190 mm. The cement used was Cement I 42.5 R SR5 from Lafarge. The aggregates used were calcareous crushed coarse (4 – 8 mm, 8 – 16 mm and 16 – 20 mm) and mixed siliceous-calcareous fine aggregate (0 – 2 mm and 0 – 6 mm). The water/cement ratio was 0.55.

PF1, PF2, PF3 and SF were used to reinforce this matrix. The fiber content was fixed in 7 kg/m³ (volume = 0.75 %) for macro synthetic fibers and for steel fibers, it was of 21 kg/m³ (volume = 0.25 %), resulting in equivalent flexural strengths. The superplasticizer used was Sika Viscocrete© 5980, whose dosage was adjusted to reach the required slump, with contents between 1.4 and 0.7 % by cement weight, depending on the fiber type (synthetic and steel, respectively). An air-reducing additive (MC Bauchemie©) was added in all the mixes in a percentage of 0.4 % by cement weight.

Table 17. Dosage of FRC used in compression and flexural tests.

Materials	[kg/m³]
Cement I 42.5R SR5	280
Gravel (4-8 mm)	146
Gravel (8-16 mm)	402
Gravel (16-20 mm)	183
Sand (0-2 mm)	211
Sand (0-6 mm)	897
Water	154

Based on this designed dosage, cubes (150 mm side) and beams (150 × 150 × 600 mm) were cast. The mixing was performed in a P375T08 planetary concrete mixer with a capacity of 500 liters (l) (see Figure 32-a). 37 batches were cast in total, and each batch had a volume of approximately 270 l. The total mixing time was 10 minutes. The following steps were conducted to mix the described concrete materials and produced the mixes in the same sequence to ensure the reproducibility of the results:

- Dried mixing of aggregates and cement for four minutes.
- Tap water, air-reduced admixture and more than half of the required superplasticizer were poured into the mixer and mixed for one minute (see Figure 32-b).
- Then, the gradual addition of the fibers was carried out to avoid the balling effect when fibers are included and after, the rest of the superplasticizer was added.
- Finally, fresh concrete with fibers was mixed for five minutes.

Once the mixes were manufactured, concrete was poured into the moulds (see Figure 32-c and -d) and compacted with a tapping bar to produce the specimens. 24 hours after casting, the specimens were demolded and moved to be cured during 28 days in a humidity chamber (20 °C and 95 % RH).

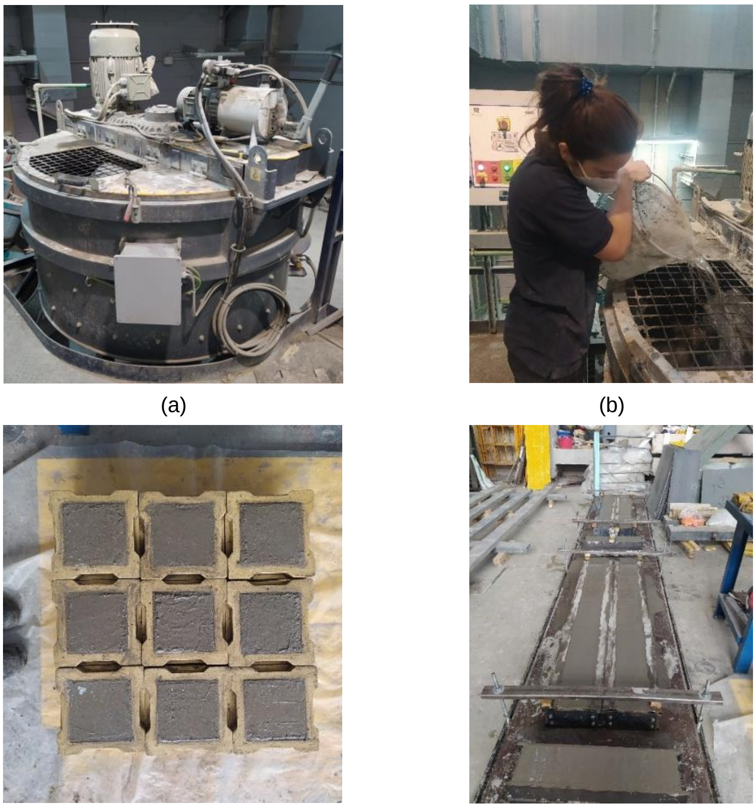

(a) (b) (c) (d)

Figure 32. (a) P375T08 planetary concrete mixer used; (b) adding water to the mixing; (c) FRC cubes after pouring and compacting and (d) FRC beams after pouring and compacting.

i) Characterization tests

To characterize these concrete mixes, several properties were tested. Consistency (EN 12350-2 [209]), air content (EN 12350-7 [210] and fresh density (EN 12350-6 [211]) were evaluated in the fresh state. The results showed that the consistency class was S4 for all the mixes, the density in a fresh state was around 2350 kg/m³, and the air content was always under 2 %. In hardened state, compressive strength was assessed at 28 days after curing in standard conditions (EN 12390-3 [212]), in three specimens per batch. The result of the average of the compressive strength was 37 MPa. It is important to point out that some variations between some few batches in terms of compression strengths were detected during the characterization. This is explained by the change of the consignment of the materials throughout the extensive campaigns. It will be considered in future chapters. Figure 33 shows the characterization test performed.

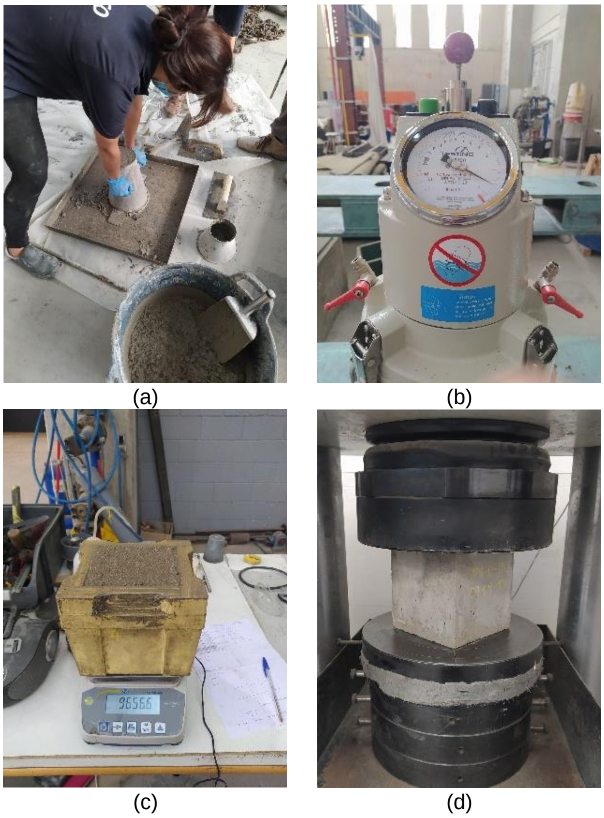

Figure 33. Photos of some of the characterization tests performed: (a) slump; (b) air content; (c) fresh density, and (d) compressive tests.

b) Experimental campaign on direct tensile strength

To accomplish these tests, concrete mix designed according to EN 14845-1 and indicated in Table 18, was selected. A typical concrete from the precast sector, a C45/55, with a MAS of 15 mm and a slump around 60 mm, was selected. The materials used to produce it were cement CEM I 52.5R, two types of sands (0 – 1 mm and 0 – 5 mm), coarse aggregate (5 – 15 mm) water and superplasticizer (around 0.7 % by cement weight). The water/cement ratio was 0.46. The fiber used to reinforce the matrix was PF1, described in Table 16, in the content of 8 kg/m³.

Table 18. Dosage of FRC used in direct tensile tests.

Materials	(kg/m^3)
CEM I 52.5 R	400.00
Gravel (5-15 mm)	836.80
Sand (0-1 mm)	171.74
Sand (0-5 mm)	729.48
Water	184.00

From this dosage, cubes (150 × 150 mm) and beams (150 × 150 × 600 mm) were cast. From these beams, cylinders samples are extracted to perform the test (the procedure is explained in Subsection 3.4.3). The mixing was performed in a 360 planetary concrete mixer from IMER Group with a capacity of 360 l. Three batches were cast and each batch had a volume of approximately 70 l. The total mixing time was 15 minutes approximately. The following steps were conducted to mix the described concrete materials and produced the mixes in the same sequence to ensure the reproducibility of the results:

- Firstly, dried mixing of aggregates and cement were carried out.
- Tap water and the required superplasticizer were poured into the mixer, and all the components were mixed together.
- Then, when the mix was homogeneous, the fibers were added gradually to avoid the balling effect and the rest of the superplasticizer was added.

Once manufactured the mixes, concrete was poured into the moulds and compacted (see Figure 34). After 24 hours, the specimens were demolded and moved to be cured in standard conditions in a humidity chamber, until they were moved to their corresponding environmental conditions of exposure.

(a) (b)

Figure 34. (a) Vibrating the concrete poured into the moulds and (b) FRC specimens after pouring and compacting.

i) Characterization tests

To characterize these concrete mixes, consistency (EN 12350-2) and compression (EN 12390-3) were verified. The results showed that the consistency class was S2, and the compressive strengths class achieved was C45/55 in all the mixes. Two specimens were tested in compression to characterize each batch. Figure 35 shows the characterization test performed.

(a) (b)

Figure 35. Example of some of the characterization tests performed: (a) slump, and (b) compression tests.

3.4. Methodology

3.4.1. Simulation of Extreme Environmental Conditions

One of the most important steps in this Thesis was to select and to define the extreme environmental conditions to simulate and perform the tests. To analyze the aging and performance of FRC exposed to extreme environmental conditions, different levels of temperatures were selected, mainly depending on the material's properties. The temperatures selected were different for each of the two levels under investigation (namely fiber and material level).

a) Fiber level

To define the potential temperature that can affect the single-fiber's behavior, at a fiber level, a review of the aging data of the thermoplastic control material to estimate the appropriate conditioning temperatures for the candidate material was done. Manufacturers provide the technical information for the chosen fiber, according with EN 14889-2, such as melting point.

Based on the interest temperature range explained in Chapter 2, the following levels of temperature were defined: -30, -20, -10, 0, 20, 40, 60, and 80 °C. Two additional temperatures were chosen, 120 and 140 °C, near to its melting point (around 160 °C), to complete the study, despite being outside of the main scope of this work. To simulate these environments, fibers were exposed before testing at the target temperatures inside an MTS 651 environmental chamber, which was at the defined temperature (Figure 36) for the target period of exposure. This environmental chamber was used to acclimate the fibers and it was also settled into the testing machine to perform the mechanical tests, enabling to perform a wide array of conditions that closely replicate the temperatures that materials may experience in their actual operating environments.

Figure 36. MTS 651 Environmental Chamber.

b) Material level

From a material level, MSFRCs are expected to behave differently to SFRC under environmental conditions. In this work, several environmental exposures have been studied in order to determine the effect of humidity and temperature. Here, six different extreme environmental conditions are investigated: -15, 5, 20, 40 and 60 °C, within different conservation conditions. Each condition has been designed with the objective of simulating real conditions to provide confidence in the operating range of a material (extreme environmental condition) and they are summarized in the following table (see Table 19). To evaluate the overall long-term mechanical behavior of MSFRC and SFRC elements, the conditions collected in Table 19 were also applied.

Table 19. Programed Extreme Environmental Conditions in this study.

M15	**05**	**20**	**20S**	**40**	**60S**
-15 °C and RH 65 %	5 °C and RH 75 %	20 °C and RH 95 %	20 °C and submerged in water	40 °C and RH 50 %	60 °C and submerged in water
					

Two former conditions simulate winter seasons since temperatures of -15 °C are easily reliable to happen in cold regions with prolonged freezing seasons or 5 °C may occur in moderately cool weather. The following two of them recreate standard conditions. The rest of conditions reproduce Mediterranean's summer conditions. It must be realized that in hot environments, temperatures exceeding 60 °C do not occur or are hard to reach even under severe climatic conditions, but this temperature can be reached in some industrial applications (i.e., concrete heaters, industrial containers, etc.). The effect of temperature and humidity was programmed to be analyzed when the concrete was under work conditions and the whole concrete mass was at these temperatures. Additionally, the suffix -S indicates that the specimens are submerged in water during the period of conservation. The temperature of the water allowed to reach the target temperature while maintain the specimens under immersion.

In order to simulate these scenarios, different spaces to storage were used. These spaces were at the target temperature when the specimens were placed in. An industrial fridge was utilized to cool the specimens and represents the moderately cool weather and winter seasons. The model selected was a CH 402 T A+ horizontal freezer with automatic temperature control. In addition, using a controlled temperature room to represent warm and relative hot humid weather, specimens were subjected under 20 and 40 °C. The humidity chamber also allows the control of the RH during the time of conservation. For the specimens which are in immersion, at 20 and 60 °C, thermal baths of water at target temperature were put in service, to represent situations where concrete is saturated and simultaneously, exposed to temperatures. This was one of the reasons why the maximum selected temperature was 60 °C; this is sufficiently high to accelerate the aging processes involved and relatively easy to achieve and maintain. In fact, temperatures in the range of 50 – 60 °C are usually accepted for this purpose [1].

Regarding to direct tensile strength, different conditions (temperatures) were defined: 30, -20, -10, 0, 20 and 40 °C. In this study, temperatures below 0, 0 and 20 °C, were simulated in a climatic chamber (see Figure 37-a). Temperature of 40 °C is acquired by means of an oven (see Figure 37-b).

(a) (b)

Figure 37. Simulation of conditions during the experimental interface study.

3.4.2. Selection of the Time of Exposure

As was identified in the introduction of Chapter 3, a clear division was defined in term of exposure time in order to distinguish short- from long- term mechanical behavior of FRC when are exposed to extreme environmental conditions. Having reached this point, it is necessary to justify which periods were selected as short-term and long-term. It is also important to point out that all the tests planned were performed in time (with a maximum deviation of one day).

As short-term, at fiber level, 10 minutes of exposure was fixed for the fibers, given that this time was sufficient to acclimate the specimens due to the size of the fiber (it was checked in previous tests). At a material level (compressive, flexural tensile and direct tensile strengths), a period of three days was set. To define this period, a preliminary test was carried out to check the necessary time that the whole mass of concrete specimens needed to reach the target temperature in the interior of the specimen. A beam was equipped with a thermocouple type-K in the geometrical center (core), as shown in Figure 38. This concrete beam was stored in different thermal conditions and the internal temperature was registered during all the process. It was shown that three days is a long enough time to obtain the target temperature in whole concrete mass.

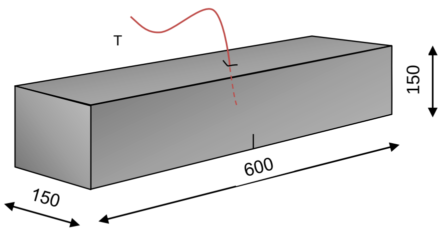

Figure 38. Location of the thermocouple (T) in concrete beams in the core (all dimensions in mm).

Additionally, to ensure that a period of 3 days of conditioning was enough to achieve the target temperature in the core of the notched cylinders in direct tensile test, an extra cylinder without notch was drilled in 3 different sections at equal radial distance of 120 °C (2, 4 and 6 cm in depth, respectively), and in which one, a thermocouple type-K was installed (see Figure 39) . The specimen with the thermocouples was subjected under the same cycle as a specimen that would be tested later. It was demonstrated that three days is an adequate period of exposure since the specimens are able to reach the target temperature in the core.

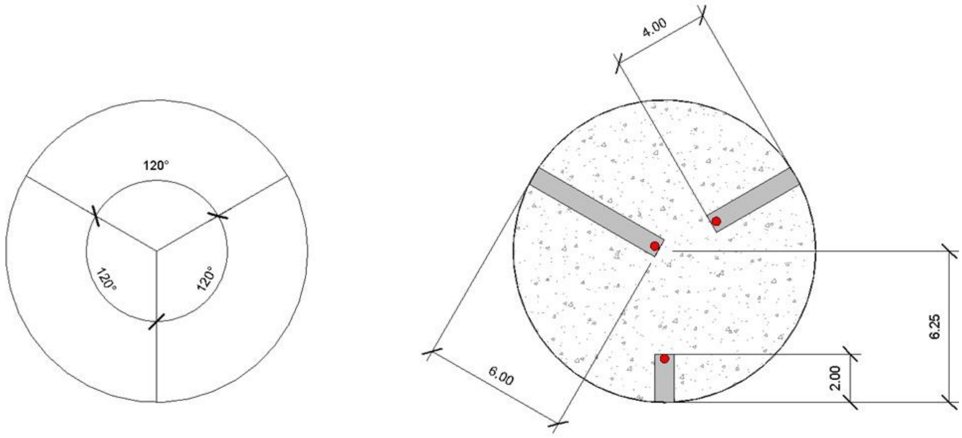

Figure 39. Location of the thermocouple in concrete cylinders in the core (all dimensions in cm).

3.4.3. Testing Properties at Temperatures

The effect of temperatures has not been thoroughly researched on FRCs up today, since there are no standardized methods that allow to evaluate and compare properly the obtained outcomes in this topic. The methodologies explained in this Subsection are developments derived from this Thesis.

As explained in Chapter 2, the methods to evaluate temperature as a factor can be divided in three groups: (i) methods performed in specimens in steady state which are prestressed to a certain percentage of their ultimate load and then are exposed to temperature until failure; (ii) methods performed in specimens in steady state which are heated/cooled and then tested at target temperature; and finally, (iii) in specimens in residual conditions in transient state. In this Thesis, the whole experimental campaign is developed following the concept of the second group. The experimental set-ups and the procedures adopted for fiber and material level are described item by item in this Subsection.

a) Fiber level

At fiber level, an MTS landmark 500 machine was used to perform direct tensile strength tests on individual fiber. The procedures were done according to EN 14889-2, for Class II fibers, with some modifications. The tensile strength was determined only in 5 individual filaments per conditions. To test individual fiber, the extremes of the fiber were mechanically clamped in between aluminum plates with inner rough surface (to provide friction and prevent fiber slip), connected with bolts and nuts. To create inner rough surface of aluminum plates, sandpaper of grade P120 was glued to inner surface of each plate. A system comprised of lower plate, fiber and superior plate was created (see Figure 40).

(a) (b) (c)

Figure 40. Photos of fiber tensile test procedure: (a) Aluminum plates used to hold fiber during the test; and (b), (c) Tightening of plates to prevent fiber slip.

The upper plate was connected to grip of machine actuator. The test was performed with actuator movement controlled by machine control system. Also, the whole test set-up was covered inside the MTS 651 environmental chamber for testing of fibers at temperature. A complementary system of nitrogen liquid incorporated to the chamber to perform tests at low temperatures (see Figure 41).

Figure 41. Set-up for direct tensile test on fibers at low temperatures. Nitrogen liquid incorporated to the MTS 651 environmental chamber.

Before testing (at different rates), the fiber specimen was conditioned at the target temperature for 10 minutes, as explained in Subsection 3.4.2. Figure 42 shows the test set-up used in laboratory for direct tensile test on individual fibers at temperature.

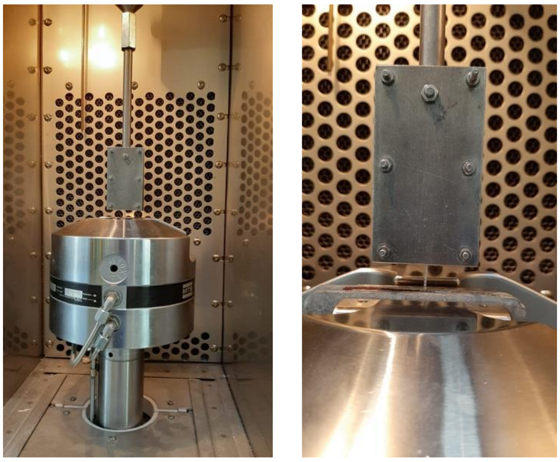

(a) (b)

Figure 42. (a) Fiber test set-up inside temperature chamber; (b) Zoomed view of fiber and plates in position before testing.

The requirements of load rate and temperature were registered in the software-controlled system, and force vs displacement graph was plotted by the system based on actuator movement and force measured. During the test, after the pre-load was applied, free length of each fiber was measured using a vernier caliper. According to EN 14889-2, the distance between the clamping points was around 25 mm since fibers were gripped 15 mm in both extremes.

All the results were included in the calculation for the average and standard deviation, excepted the slipped fibers (that were discarded). The tensile strength is calculated from the failure force divided by the cross-sectional area (provided in Table 16). The elastic modulus is evaluated as the slope of the secant line form the 10 % to the 30 % of the tensile strength. For the elastic secant modulus (10-30), the maximum strength calculated was divided by the strain computed from the elongation measured during the test dividing by the fiber's initial length.

b) Material level: compressive, flexural and direct tensile strengths

i) Compressive strengths

After curing and after being exposed to their corresponding programed environmental condition for the defined period of exposure, compression tests were performed at the target temperatures. Compressive strengths were determined following the standard EN 12390-3. To evaluate the effect of temperature after a short- or long-term of exposure (3, 90 or 180 days) of the FRCs under investigation, a modification was introduced in the mentioned method.

The modification consisted of a special cell. It is important to notice that target temperatures were maintained in the inside of the specimens during the evolution of the tests. This cell, developed in previous work [213] and improved herein, can be placed in the loading frame, and allows to maintain the temperature constant during the test. The system has not a temperature control system. The advantages of the set-up proposed in this work are that this method uses a simple system that isolates the specimen, and it is easy to implement in a laboratory work. The cell is fabricated in a detachable format with 8-mm extruded polystyrene panels (see Figure 43). After testing, this cell is removed, and the external temperature is measured with the IR thermometer.

Figure 43. Insulation system used during compression test.

ii) Flexural tensile strengths

Flexural residual tests (three-point bending test set-up) were carried out a determined temperature. They were performed following the standard EN 14651 with some modifications. These modifications include: the deformation of CMOD was monitored in real-time by a LVDT mounted at the mouth of the notch. The tests were controlled by the velocity in the force application. Also, a system similar to the used one in compression tests, was implemented herein (see Figure 44). The system also included gel as a cooling/heating agent.

Figure 44. Insulation system used during 3PBTs.

To start the test after the specimen was exposed during the defined period and being at the desired temperature, it was preloaded with approximately 10 kN. Subsequently, the INSTRON 3389 testing machine applied the load at a vertical displacement criterion of 0.5 mm/min, and it stops the loading when the load reaches 80 % of the expected peak load. Afterwards, the loading rate was decreased to 0.05 mm/min until 0.2 - 0.3 mm (in the post-peak range) and finally, it was modified to 0.2 mm/min until the end of the test. During the test, the information on load and CMOD was collected at a frequency of 2 Hz.

After testing, the insulation system is removed and the external temperature is measured, as explained before. The number of fibers at the fracture surface was registered per each specimen tested. For this purpose, beams were divided into two halves (Figure 45-a). Each face of the fracture surface, in turn, was divided into three horizontal equal layers (Figure 45-b). Fibers were counted manually, obtaining the number of fibers in each third ($N_{1/3}$) and the total number of fibers (N).

(a) (b)

Figure 45. (a) Dividing the specimens into two halves after testing to produce fracture surfaces (b) Examples of fracture surfaces for specimens reinforced with macro synthetic (above) and steel fibers (with the thirds marked).

iii) Influence of an existing pre-crack

This work also analyzes the relation between temperature and precracking condition. Some specimens were first pre-cracked (before storing in the defined environmental conditions) at standard temperature (at 20 °C, without the insulation system) at 28 days at a pre-defined crack-opening (CMOD = 0.5 mm) for which the residual strength f_{R1} is determined. The complete testing procedure consisted of three main stages (Figure 46). In the first stage, specimens were pre-cracked using a 3PBT configuration as proposed in EN 14651 up to the desired CMOD = 0.5 mm (point B in Figure 46-a) and then unloaded (point C in Figure 46-a). After this point, prims remained for 10 minutes in the frame to allow potential crack opening recovery (point D in Figure 46-a). In the second stage, the cracked specimens are placed into their specific extreme environmental conditions during the predefined time. Afterwards, in the third stage, the specimens were removed from their conditions, and tested until failure using a 3PBT configuration following the general guidelines of EN 14651 standard (Figure 46-b), but in this phase, the specimens kept the temperature due to the designed system (Figure 44). After testing, the number of fibers at the fracture surface was also counted in each specimen tested.

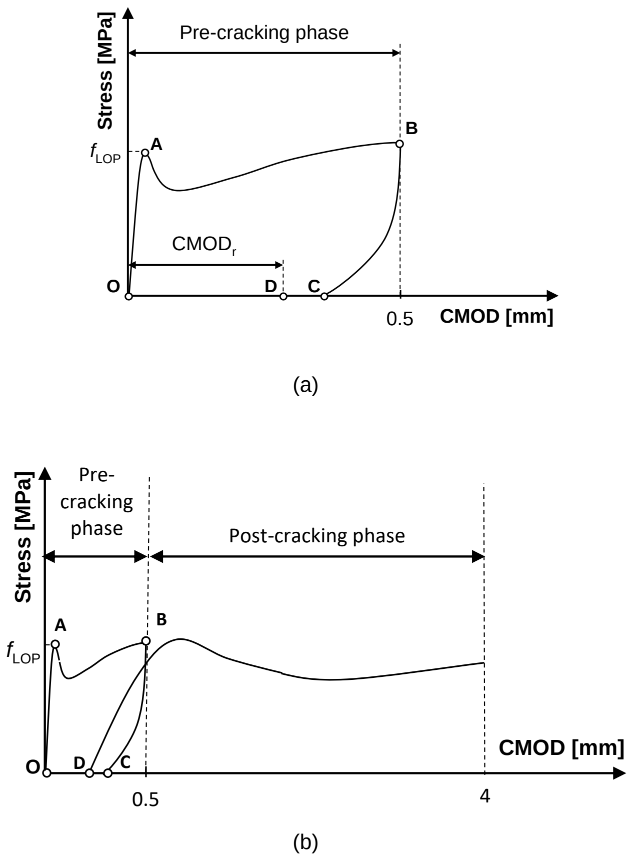

Figure 46. CMOD-Stress diagram: (a) first stage at standard temperature and (b) complete procedure.

iv) *Direct tensile strength*

Direct tensile tests were performed to investigate through tensile strength on notched MSFRC cylinders to determinate this property at specific temperatures, as well as to indirectly determine the bond between the fibers and the matrix. These cylinders were not cast directly; they were cored from MSFRC beams. Each beam of 150 × 150 × 600 mm³ was sawed into three equal parts and one cylinder was extracted from a resulting prism (the direction of coring was considered along the original beam length). Figure 47 shows the phases of this process.

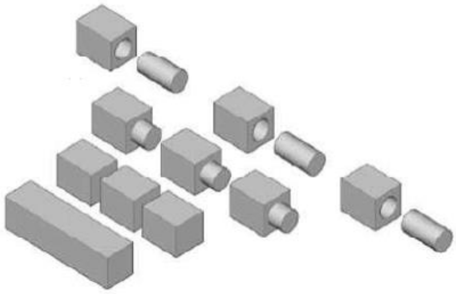

Figure 47. Phases of the cylinder coring.

Then, the obtained cylinder with a height of 200 mm and Ø 125 mm were cut in both extremes in order to straighten the ends’ surfaces, obtained a cylinder with a total height of 150 mm (Figure 48-a).

For the test, each cylinder was equipped with circular steel plates on both ends (with a diameter of 125 mm and a thickness of 40 mm, as can be seen in Figure 48-b) and was connected to the upper and lower grip system of the machine trough articulated joins allowing the rotations so that during the application of the vertical displacement, no additional stress could be induced. These steel plates were glued with one type of adhesive, called Geolite Gel, for temperatures range from -30 up to 40 °C. Finally, the cylinders were notched at 75 mm of height with a depth of 10 mm.

(a) (b)

Figure 48. (a) Scheme of the process of coring; (b) Preparation of the cylinders.

After curing and before doing the direct tensile tests at temperatures, the cylinders were moved to their corresponding conditions for 3 days before testing. The direct tension test was performed using the same machine used for the fiber tests (MTS Landmark servo hydraulic machine, with a capacity of 100 kN, Model 307.10) but adjusting the set-up to the specimen size. The displacements were measured by means of three Clip-on Displacement sensors placed at equal radial distance of 120 °C. During the test, the three different signals were recorded to control the measurements until a final Crack Opening Displacement (COD) of 4 mm.

This methodology is not very common since it presents some difficulties in the execution of the tests. These difficulties consist of the no symmetrical crack opening displacements. This was controlled during the test by the rate COD/mean COD and a pre-defined stop parameter (a mean value of COD had to be achieved in all the crack during each loading step to continue with the development of the test). With the procedure followed, this risk was minimized, and all specimens had a controlled symmetrical crack opening. Figure 49 shows the set-up used for tensile direct test at temperature.

(a) (b)

Figure 49. (a) Set-up for tensile direct tests on cylinders at temperature; (b) Cylinder after testing under tensile direct.

Finally, considering the significance of fiber concentration in the cross-section, fibers were counted after cylinder were divided in two halves. After, fibers were also classified as slipped or broken to study their failure model in function of temperature (Figure 50).

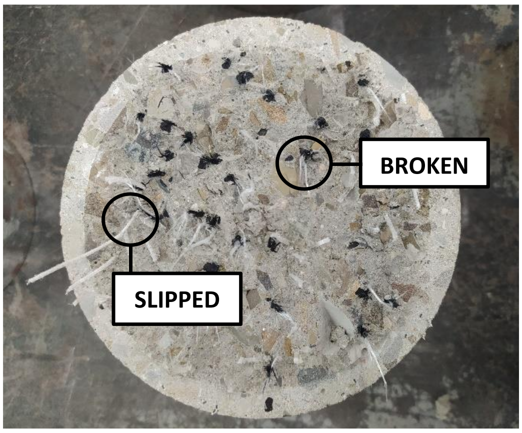

Figure 50. Difference between slipped and broken fibers in a cross-section tested.

3.4.4. Temperature Control During the Tests

To guarantee that temperature was maintained and kept constant during the tests, different temperature methods were used. On the one hand, MTS 651 environmental chamber allows control the temperature because it has a temperature regulator system. Thus, direct tensile tests on fiber and FRC was performed easily in this sense. On other hand, for flexural tensile test, a prism per each combination was instrumented with a type-K thermocouple in the core (similar to the instrumentation performed in Figure 38). Next, Figure 51 displays the results obtained from the thermocouples installed in the core of the beams.

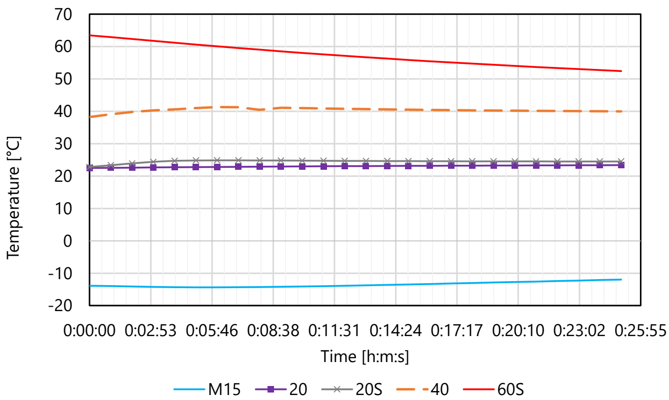

Figure 51. Results obtained from the thermocouple installed in the core of the beams for each temperature during the performance of the flexural test.

The thermocouple was introduced during the production of the specimens, and it continuously recorded the internal temperature via an Automatic Data Acquisition System. The maximum variation of the internal temperatures registered during the tests was 10 °C, for the group tested at the target temperature of 60 ºC, and the difference registered is lower than 5 ºC in the other groups. For 5 °C, the thermocouple did not record (since M15 group had very low internal temperature variation, it was not repeated).

Furthermore, the external temperature and the temperature after testing over the cross-sections were also checked using a Fluke 64 Max infrared (IR) thermometer, which confirmed a uniform temperature distribution. Since compression tests last less time than 3PBTs (< 2 minutes vs around 30 minutes, respectively), the internal temperature was not monitored by thermocouples on cubes, only the IR thermometer, was employed to measure the temperature on the surface. Figure 52 shows how temperature was checked with the IR thermometer after the different tests performed.

(a) (b)

Figure 52. Checking surface temperature after testing and removing the insulation system on: (a) a warmed beam (at 40 °C) and (b) a cooled cube (at -15 °C).

Chapter 4

Behavior of MSFRCs under Different Environmental Conditions at Short-term Exposure

This chapter displays the results derived from the experimental campaign concerning the short-term behavior of MSFRCs under different environmental conditions by using the materials and methodologies defined in previous chapter. This chapter is divided in the introduction and five sections. Section 4.1 describes the results obtained from the fiber level study, analyzing in detail the effects of temperature in UTS and E-modulus. Section 4.2 shows the results obtained in compressive strengths at short-term and Section 4.3, the flexural strengths results at short-term (considering the analysis of the pre-cracked state and the number of fibers on the cross-sections). Section 4.4 addresses the analysis of the direct tensile strengths results and indirectly, the fiber-matrix interface from a meso- scale perspective. These last three sections constitute the study at material level. At last, the general results of these experimental programs are summarized and discussed in Section 4.5 and also, they are compared to the conclusions of studies of several authors. Figure 53 displays the outline of these sections of the chapter.

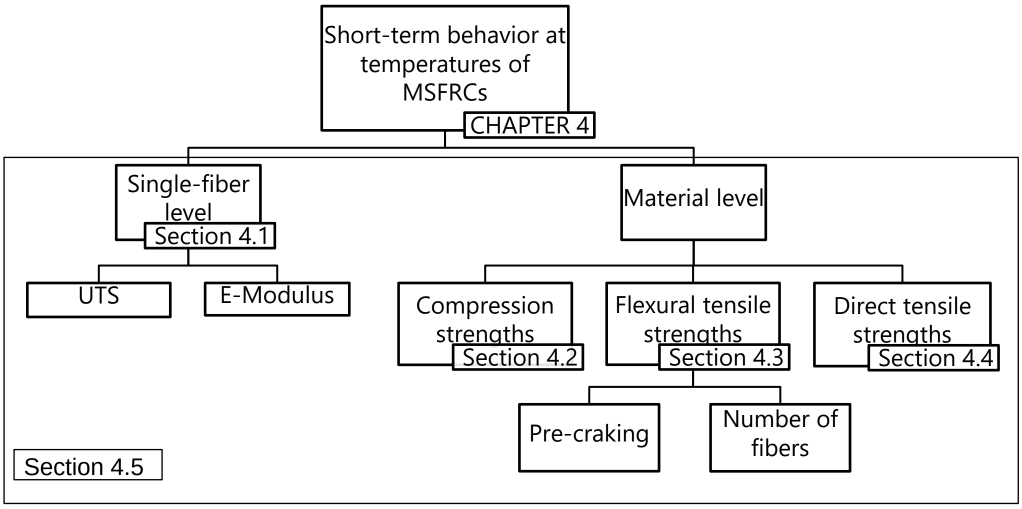

Figure 53. Outline of the Chapter 4.

4.1. Influence of Environmental Conditions on Fiber's Behavior

In this Section, the results of the fiber's viscoelastic behavior, at a fiber scale, is described. Fiber material, in particular, PP shows drastic variations on mechanical properties with temperature, specifically for the studied temperature range (- 30 to 140 °C).

Ultimate tensile strength (UTS) and E-modulus for PF1 fibers were measured performing direct tensile tests on five individual fibers at -30, -20, -10, 0, 20 (reference), 40, 60 and 80 °C. Tests were carried out until the failure of the fiber, rejecting those tests in which the fiber slipped. An additional factor, stress-rate, was also studied to research whereas it influences, simultaneously with the temperature, the properties obtained on fibers at single-fiber level. The selected loading (stress) rates were: 1, 2, 9, 20 and 40 MPa/s. Additional tests were performed for temperatures of 120 and 140 °C at 9 MPa/s, also testing five fibers per temperatures.

UTS of the fibers was calculated as the maximum force obtained from direct tensile tests divided by the cross-sectional area of the fiber (provided by the manufacturers). For the E-modulus (10-30) which is the elastic modulus evaluated as the slope of the secant line from the 10 % to the 30 % of the tensile strength, the value was calculated by the strength at these points divided by the strain (computed from the elongation measured during the direct tensile test dividing by the fiber's initial length).

The mean results for these mechanical properties are collected in Table 20 and Table 21, for low temperatures and Table 22 and Table 23, for moderate high temperatures. In general, the obtained data present a small scatter at low and moderate high temperatures, both for UTS and E-modulus. The mean coefficient of variation (CoV) calculated for UTS is around 7 % and for E-modulus is just about 10 %. As can be seen from Table 20 to Table 23, the results at low temperatures have a higher variation compared to the results at temperatures ≥ 20 °C.

Table 20. The average UTS results for low temperatures (below and up to 0°C).

T [°C]	**-30**		**-20**		**-10**		**0**	
Stress rate [MPa/s]	**Mean UTS [MPa]**	**CoV [%]**	**Mean UTS [MPa]**	**CoV [%]**	**Mean UTS [MPa]**	**CoV [%]**	**Mean UTS [MPa]**	**CoV [%]**
1	500.1	6.1	578.8	10.8	476.5	14.6	521.8	2.7
2	500.7	10.6	594.5	10.3	477.8	10.6	533.4	6.6
9	547.6	5.8	544.5	5.1	465.6	5.3	528.4	7.2
20	524.8	7.6	524.8	4.7	532.2	7.9	496.5	6.5
40	502.2	9.1	477.5	5.4	501.6	3.4	485.6	6.0

Table 21. The average E-modulus results for low temperatures (below and up to 0°C).

T [°C]	**-30**		**-20**		**-10**		**0**	
Stress rate [MPa/s]	**Mean E [MPa]**	**CoV [%]**	**Mean E [MPa]**	**CoV [%]**	**Mean E [MPa]**	**CoV [%]**	**Mean E [MPa]**	**CoV [%]**
1	6891.8	4.5	6367.0	8.6	6534.0	11.1	5954.0	9.4
2	6874.2	16.5	6355.0	16.8	6045.4	9.4	5701.0	7.1
9	6617.6	5.6	6764.8	6.0	6327.4	7.6	5929.8	10.1
20	6661.0	7.9	6421.8	6.7	7129.4	14.1	6220.8	13.7
40	6840.0	15.0	7350.2	15.4	5996.2	18.2	6188.6	7.7

Table 22. The average UTS results for moderate high temperatures (between 20 - 80 °C).

T [°C]	**20**		**40**		**60**		**80**	
Stress rate [MPa/s]	**Mean UTS [MPa]**	**CoV [%]**	**Mean UTS [MPa]**	**CoV [%]**	**Mean UTS [MPa]**	**CoV [%]**	**Mean UTS [MPa]**	**CoV [%]**
1	443.8	2.5	431.4	1.4	362.0	7.1	357.5	6.9
2	420.0	9.3	424.1	6.2	415.5	7.5	349.5	7.7
9	447.0	7.4	436.0	7.8	395.9	9.3	372.7	7.0
20	440.8	6.4	472.9	4.4	426.6	7.4	373.1	6.0
40	472.0	1.0	455.1	5.1	4166	4.3	362.3	8.3

Table 23. The average E-modulus results for moderate high temperatures (between 20 – 80 °C).

T [°C]	**20**		**40**		**60**		**80**	
Stress rate [MPa/s]	**Mean E [MPa]**	**CoV [%]**	**Mean E [MPa]**	**CoV [%]**	**Mean E [MPa]**	**CoV [%]**	**Mean E [MPa]**	**CoV [%]**
1	4717.4	7.8	6339.8	6.3	3148.8	11.2	2325.6	9.6
2	4332.2	10.0	3359.0	11.4	3324.8	15.0	2376.2	4.7
9	5406.0	4.1	4072.2	11.6	3863.4	10.5	2504.6	4.6
20	4996.8	7.7	4708.6	7.3	3668.0	6.2	2809.2	5.6
40	5633.8	5.0	5150.0	5.5	3652.4	6.9	2929.0	14

The data of UTS at low and high temperatures have been depicted in Figure 54 for each stress rate (1, 2, 9, 20 and 40 MPa/s) through dots. For each temperature, a representative color was defined: tones of blue represent -30, -20 and-10 °C, grey for 0 °C; purple for 20 °C; tones of orange, 40 °C and 60 °C and red, 80 °C. Dashed lines represent the tendency that follows UTS values depending on the stress rate.

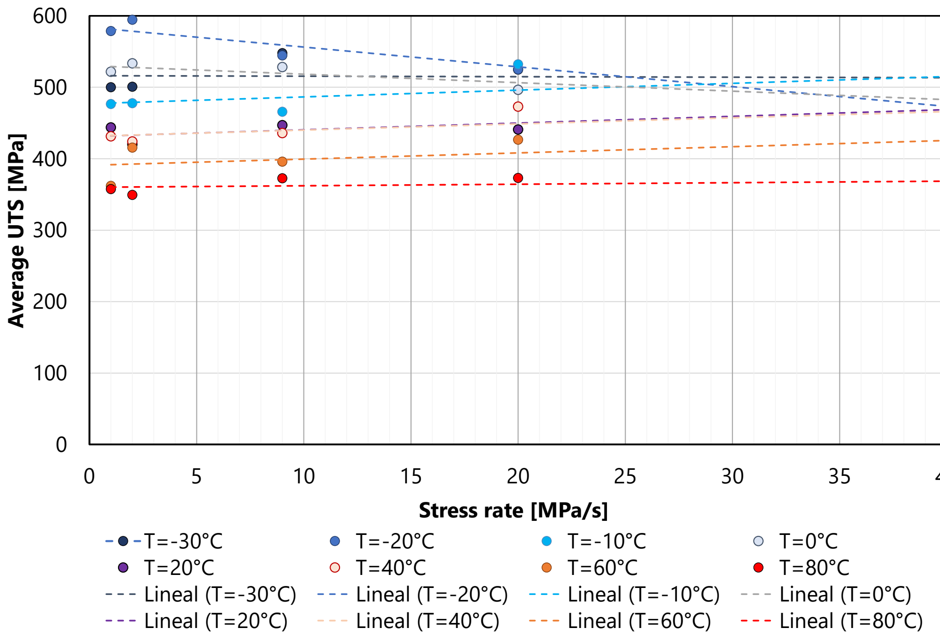

Figure 54. Average UTS vs. Stress rate at different temperatures.

As can be seen, temperature influences the UTS of the single fiber given that a decrease of a 10 % and a 20 % are seen at 60 and 80 °C respectively. At 40 °C, UTS of the fiber does not present any significant change in relation with the results obtained at 20 °C. At low temperature, an increase is noted on UTS. This increase is around a 10-20 %, depending on temperature (from 0 to -20 °C); however, at -30 °C, it is not possible to find any variation compared with the reference at 20 °C. This could be explained by the properties of polypropylene fiber. As commented in Chapter 2, PP is a semi-crystalline material (– a thermoplastic polymer –) which, according with the literature, shows the T_g within the study temperature range. In this work, the fiber's UTS was different after -20 °C; thus, the T_g may be around -20 °C, indicating a change in fiber behavior. Generally, below the glass transition temperature, the molecular movement is frozen with fewer changes in properties, but when the glass transition temperature is exceeded, brisk molecular movement takes place, resulting in a decrease in elastic modulus and volume expansion [122]. This property is not considered in the specifications for fiber for concretes in the standard EN 14889-2, nevertheless, it is an important property when considering polymers for a particular end-use at low temperatures, as structural for concrete. One of the difficulties for including the glass transition temperature variable is that it is not an intrinsic property, it depends on the cooling or heating rate, and therefore, there cannot be an exact value for T_g for a particular material.

On the contrary, the stress rate is not an influential factor in these cases since no effects are detected when the selected stress rates are modified. However, it can affect the results to some extent at low temperatures, given than the obtained trends are not so constant as the results at moderate high temperature. Contrary to the obtained results, some studies indicate that single fibers tested under direct tensile tests showed to be rate sensitive with fiber tensile strength, obtaining higher value when increasing the loading rate at standard temperatures [191].

Figure 55 shows the obtained mean results of E-modulus for each temperature and stress rate. The color code was maintained. As can be seen, temperature affects the E-modulus of the single fiber, in a great extent, being the effect more pronounced than in the UTS of the fiber. For moderate high temperatures (from 40 to 80 °C), a decrease of a 20, 35, and 55 % are seen at 40, 60 and 80 °C, compared with the results obtained at 20 °C. At low temperature, an increase is noted on E-modulus. This increase is around a 10-30 %, reaching its maximum at -20 °C. After this temperature, the E-modulus is reduced. This can be explained by the T_g, previously commented.

The stress rate seems to have more influence in E-modulus than in UTS. An ascending trend (dashed lines) is detected, which indicates that for higher stress rates, the mean values obtained are also higher, which was expected according to the literature [208].

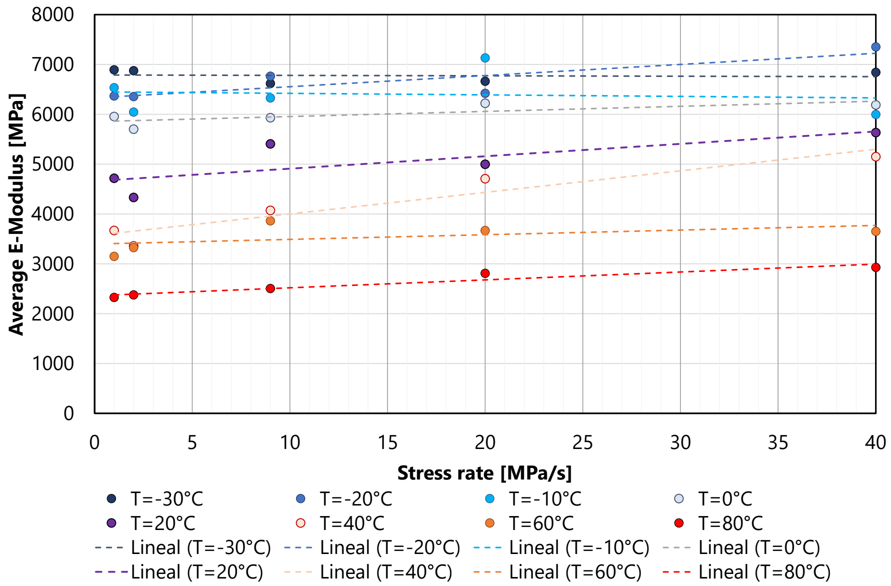

Figure 55. Average E-Modulus vs. Stress rate at different temperatures.

The increases of UTS and E-modulus registered at low temperature have a drawback. At low temperatures, all thermoplastics tend to become rigid and brittle, mainly because the mobility of polymer chains is greatly reduced. Brittleness temperature is defined as the temperature at which plastics exhibit brittle failure under specified impact conditions [122]. In this case, this fact was verified by a study focused on the failure of the fiber (see Subsection 4.4.2) and it is in agreement with [214], who have been reported previously that temperature may influence the type of breakage of the fibers embedded inside the matrix. So, it can be affirmed that PP fibers present brittle failure by applying tensile load under low temperatures (below zero to -30 °C).

Moreover, uniaxial tests were performed on fibers at 120 and 140 °C at one stress rate, 9 MPa/s. At these temperatures and for this stress rate, the average results of UTS were 325.2 MPa (CoV of 6.2 %) and 253.9 MPa (CoV of 3.2 %), respectively. For the E-modulus, the average values obtained were 1873.0 MPa (CoV of 9.4 %) at 120 °C and 1111.0 MPa (CoV of 16.9 %) at 140 °C. These results are in line with [215] and follow the trend previously analyzed. To compare all the results of the direct tensile tests on fiber, including those at 120 and 140 °C, the mean stress-strain curves of 5 filaments are depicted in Figure 56. For each temperature, the color code is maintained (results at 120 and 140 °C are in darker tones of red). The curves start with an initial stress value of 10 MPa, which is the initial stress given to the fibers to put them in tension.

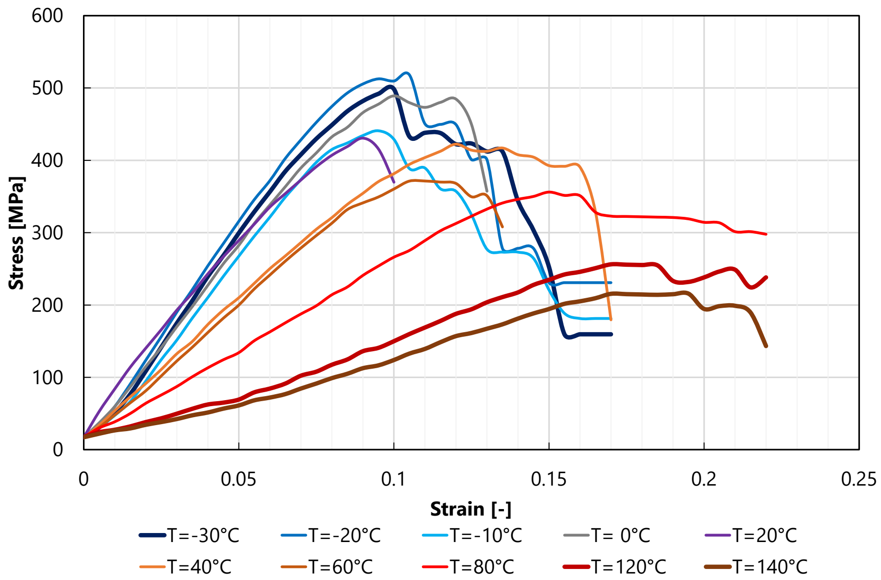

Figure 56. Comparison of the mean stress-strain curves of the target fiber at temperatures at 9 MPa/s.

At a temperature of -30 °C, the variation of UTS and elastic modulus compared to 20 °C is an increase of 22.5 % in both properties, whereas UTS and elastic modulus at 140 °C were reduced in almost a 50 % and 80 % respectively, compared to 20 °C. The obtained results agree with the published results from other authors [216]. For a constant stress rate, the UTS and elastic modulus increase by 55 % with decreasing temperature (from 140 °C to -30 °C). Similarly, the E-modulus shows a linear trend for moderate temperatures, that is, it reduces when temperature increases. This trend is reversed at low temperatures but in the range from -10 to -30 °C, the variation is smaller than in the UTS. These results are consistent with the model for the modulus of elasticity depending on the temperature proposed by Bai et al. [217], which divides the response into two temperature ranges: -20 °C to 40 °C and 40 °C to 140 °C.

To sum up, this type of polypropylene fiber showed thermally unstable behavior in the temperature range of -30 to 140 °C because of its low melting point (around 160 °C) and T_g (around -20 °C). It can be said that this PP fiber for FRC is susceptible to temperatures, but it is reliable up to 60 °C. UTS and the elastic modulus decrease as temperature increases. Overall, it can be said that high temperatures have a negative impact on ultimate tensile strength and stiffness, which becomes especially notable beyond 60 °C. These results were expected since similar conclusions were obtained by other authors [131]. Also, it can be concluded that the load rate on tensile tests on these fibers at the temperatures tested does not have a significant effect. Nevertheless, these results only explain the behavior of this type of fiber (critical temperatures at which relevant changes occur seems to be fiber specific), and at the fiber level.

4.2. Influence of Environmental Conditions on Compressive Strengths

Compressive strengths are evaluated in this work under the exposition to extreme environmental conditions (-15 - 60 °C). They were calculated by dividing the maximum force by the area of the cubes for each specimen. Compressive strengths were not expected to vary for moderate high temperatures since water contained inside concrete (free and combined) does not start to evaporate until 100 °C. This could be a reason why most of studies in compressive strengths have focused on temperatures over 100 °C, not studying lower temperatures. For temperatures below zero, the variations due to the drop of temperature were also checked in this work.

Table 24 collects the compressive strength values (average of three specimens and CoV) of the cubes reinforced with the different selected types of fibers (PF1, PF2, PF3 and SF) and tested at the simulated environmental conditions (see Chapter 3). These simulations include temperatures range from -15 to 60 °C and different RH (considering that the suffix -S indicates that specimens were submerged). The variability between the groups is < 10 % in most of the cases. It is also shown the percentage of variation of compressive strengths from 20 °C to the rest of temperatures.

For temperatures below zero, both FRC exhibited an increase of 25-30 % in the compressive strength after 3 days of exposition. For temperatures above zero degrees, in the range between 5-40 °C, no effects are detected, since all the results range between 34.5 MPa and 37 MPa. This indicates that, for these temperatures, the compressive strength does not depend on the temperature and SFRC and MSFRC have the same response. For 60 °C, a minor decrease of around 10-15 % was experimented in SFRC and MSFRCs.

Table 24. Compressive strengths for the studied FRC at short-term under the extreme environmental conditions.

Code		Compressive strengths at temperatures		
		Average [MPa]	CoV [%]	% Variation from 20 °C
PF1	M15	47.5	7	27
	05	37.0	5	-1
	20	37.5	3	-
	20S	33.5	4	-11
	40	35.5	1	-5
	60S	31.5	6	-16
PF2	M15	44.5	12	33
	20	33.5	4	-
	60	28.0	14	-16
PF3	M15	43.0	2	26
	20	34.0	5	-
	60	30.5	4	-11
SF	M15	51.5	2	52
	20	34.0	5	-
	20S	36.0	2	6
	60S	29.0	5	-15

In order to determine if the effects of these environmental conditions in the compressive strength were produced by the change on the matrix, a control mix without fibers was cast and tested under the same conditions. The results indicate that the effects of these temperatures in the SFRC and MSFRC tested are as noticeable as in concrete without fibers (Table 25), results that are supported by others studies [178] and therefore, they can be attributed to effects of temperature on the concrete-matrix. As can be seen, the variation (in %) from 20 °C for this plain concrete-matrix was similar (even more pronounced) to the variation for FRCs (in %).

Table 25. Compressive strengths for the studied plain concrete at the extreme defined conditions.

Code		Compressive strengths at temperatures		
		Average [MPa]	CoV [%]	% Variation from 20 °C
Plain concrete	M15	51.50	8	34
	20	38.50	2	-
	60S	30.50	11	-21

Compressive curves obtained from the tests were analyzed for each type of FRC and temperature (see Figure 57). These curves are illustrative of the compressive behavior since the specimens used were cubes and they were not set out. For temperatures below 0 °C, the slope of the curve increased, indicating an increase in the stiffness of concrete and a more brittle behavior, especially for SFRC. On the contrary, for high temperatures, a slight decrease in the slope of the curve was detected.

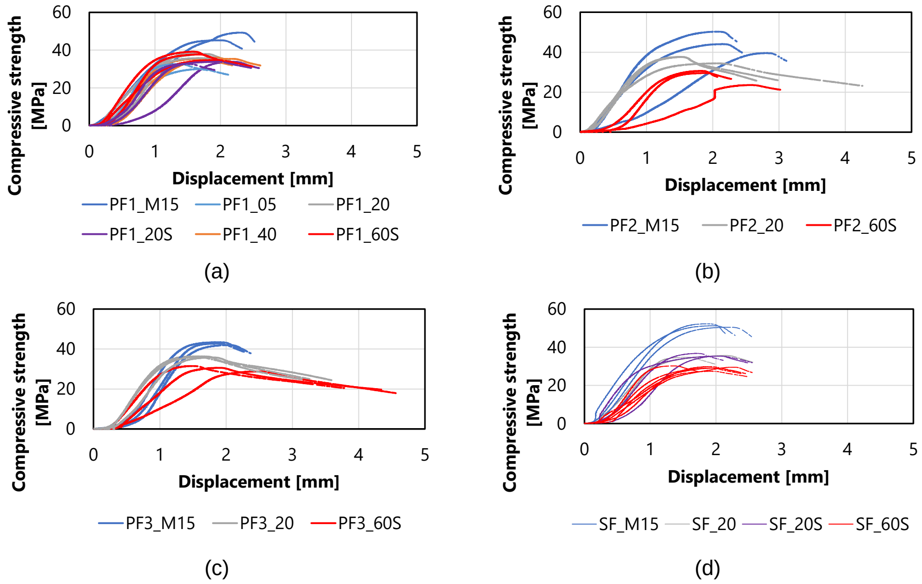

Figure 57. Curves obtained in compression tests at temperatures at short-term for: (a) PF1 cubes; (b) PF2 cubes; (c) PF3 cubes and (d) SF cubes.

Additionally, Figure 58 was depicted to compare these results. It represents a comparison between the average obtained for the different FRCs studied, after having been exposed at different environmental conditions for 3 days, and their CoVs. It can be clearly seen the descending tendency with temperature that compressive strength present (axis Y), independently of the fiber type (axis X).

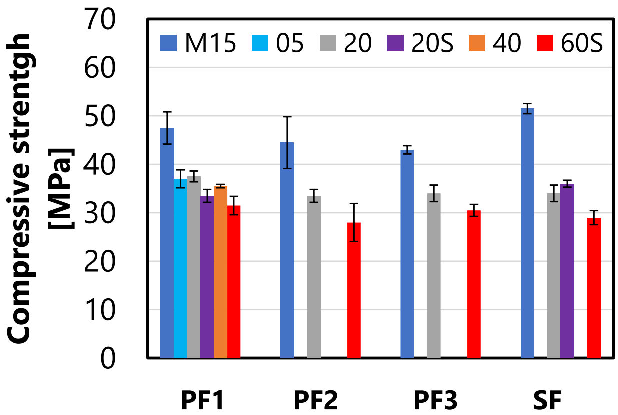

Figure 58. Compressive strengths after 3 days of conservation at different temperatures for the studied FRCs.

For sub-zero temperatures, the compressive strength increases as the temperature decreases. Most of studies in literature exhibited similar tendencies on compressive strengths with temperature [138]. The improved performance at sub-zero temperatures of FRC could be explained by the hypothesis of the formation of ice inside the pores of the concrete [145,149] but, as was previously commented, only scarce information has been published related to compressive strength in the range of 20–60 °C. The reduction experimented could be explained through the difference between the CTE of cement paste and aggregates [153,218], that may provoke debonding. In the current study, only one specimen showed debonding of the paste aggregate in MSFRC with PF2 tested at 60 °C (see Figure 59).

Figure 59. Debonded paste aggregate at 60 °C.

Humidity is also considered as an important environmental factor that can affect concrete behavior [146,219]. However, saturation does not affect to a great extent the results obtained (comparing 20 and 20S specimens), which is in line with the results of some previous works [220].

To sum up, the environmental conditions studied affect the compressive strength of plain concrete and FRCs (MFRCs and SFRC) in a similar manner. Compressive strength is reduced when the temperature increases from 20 °C in a 15-20 % and is increased when the temperature decreases from 20 °C up to - 15 °C in a 25-30 %. The stiffness of the FRCs is also modified by the temperature variations. However, saturation is not a significant factor for compressive strengths in the FRCs studied.

4.3. Influence of Environmental Conditions on Flexural Strengths

To investigate the flexural behavior of FRCs when they are subjected to realistic situations, three-point bending tests at different extreme environmental conditions were performed and the results are collected in this Section. According to the procedure already described in Chapter 3, the flexural strength at the limit of proportionality (f_{LOP}) and the residual flexural strengths at CMOD = 0.5, 1.5, 2.5 and 3.5 mm (f_{R1}, f_{R2}, f_{R3} and f_{R4}, respectively) are presented and analyzed depending on the defined conditions at temperatures. They were calculated using the following Equations (5) and (6):

$$f_{LOP} = \frac{3}{2} \cdot \frac{F_L l}{b {h_{sp}}^2} \quad \textbf{Equation (5)}$$

$$f_{Rj} = \frac{3}{2} \cdot \frac{\mathrm{F}_j \mathrm{l}}{b {h_{sp}}^2} \quad \textbf{Equation (6)}$$

where F_L and F_j are the axial load recorded during the test, respectively; l, the distance between supports (500 mm); b, the width of the sample cross-section (150 mm) and h_{sp}, the distance between the top of the notch and top of the cross-section (125 mm).

The average of the outcomes of the seven prims for non-pre-cracked specimens were tabulated in Table 26 as well as their CoV.

Table 26. Results of the f_{LOP} and the residual flexural strengths obtained at defined extreme conditions for non-pre-cracked specimens.

Code		f_{LOP} [MPa]	CoV [%]	f_{R1} [MPa]	CoV [%]	f_{R2} [MPa]	CoV [%]	f_{R3} [MPa]	CoV [%]	f_{R4} [MPa]	CoV [%]
PF1-N	M15	6.76	4	2.11	31	2.92	24	3.02	22	2.66	22
	05	4.03	4	1.80	30	2.22	30	2.28	28	2.07	28
	20	3.27	8	1.45	18	1.85	17	1.99	15	1.99	14
	20S	3.55	6	1.15	15	1.38	22	1.45	26	1.46	28
	40	2.72	18	1.63	10	2.00	9	2.18	11	2.27	13
	60S	2.49	6	1.26	19	1.46	20	1.57	22	1.58	21
PF2-N	M15	6.11	7	1.31	36	1.65	35	1.73	33	1.61	34
	20	3.03	4	1.18	16	1.37	22	1.38	24	1.28	26
	60S	2.37	6	0.75	11	0.85	14	0.89	16	0.90	16
PF3-N	M15	5.11	6	1.66	14	2.34	21	2.50	23	2.22	23
	20	2.76	8	1.37	20	1.88	23	2.17	26	2.19	28
	60S	2.59	7	1.01	21	1.35	21	1.55	18	1.65	19
SF-N	M15	5.99	6	1.01	47	1.35	24	1.25	22	1.14	22
	20	2.58	3	1.29	20	1.30	21	1.26	22	1.10	19
	20S	3.54	13	1.60	21	1.57	20	1.44	19	1.31	17
	60S	2.80	6	0.98	26	1.09	18	1.02	16	0.91	17

The results obtained from 3PBT of the non-pre-cracked FRC show a dispersion of around 20–30 % for in most of the cases, which is a typical value for this type of test [221]. For the results of f_{LOP}, the obtained CoVs were around 10 % for many of the cases, as expected since this property is mainly dependent on the matrix.

The results show that when decreasing the temperature below 0 °C, f_{LOP} increased up to twice its value (compared with f_{LOP} at 20 °C), due to the freezing process of the water inside the concrete-matrix, after 3 days of exposure. When increasing the temperature, f_{LOP} decreased by 10–20 %, as previously was observed in compression results (see Subsection 4.2). The results show similar values in f_{LOP} for all the mixes independently of the fiber type, and this is logical since f_{LOP} is a property that depends on the matrix. For f_{R1}, f_{R2}, $f_{R3}$and f_{R4} values, the range of temperatures tested (-15 to 60 °C) do not affect the post-cracking behavior of the FRCs to a great extent (see Table 26).

Additionally, these results were plotted through the stress-CMOD curves obtained by 3PBT for non-pre-cracked beams, for each studied type of fiber and temperature from Figure 60 to Figure 63. The mean values of seven specimens for each series are presented with a line, and the envelope (shaded areas) represents the scatter (maximum and minimum values of the tests) in the results. As can be seen, the dispersion of this test is high *per se*. The reasons for this variability include the number of fibers in the cross-section and the distribution and orientation of the fibers, among others. Also, there are some differences in the shape of the post-cracking average curves. The curves suggest the presence of a secondary flatter peak stress (after cracking) at cold temperatures (at 5 °C and −15 °C) for both types of FRCs while at standard and moderate high temperatures the curve is flat or continuously increasing for the CMODs studied.

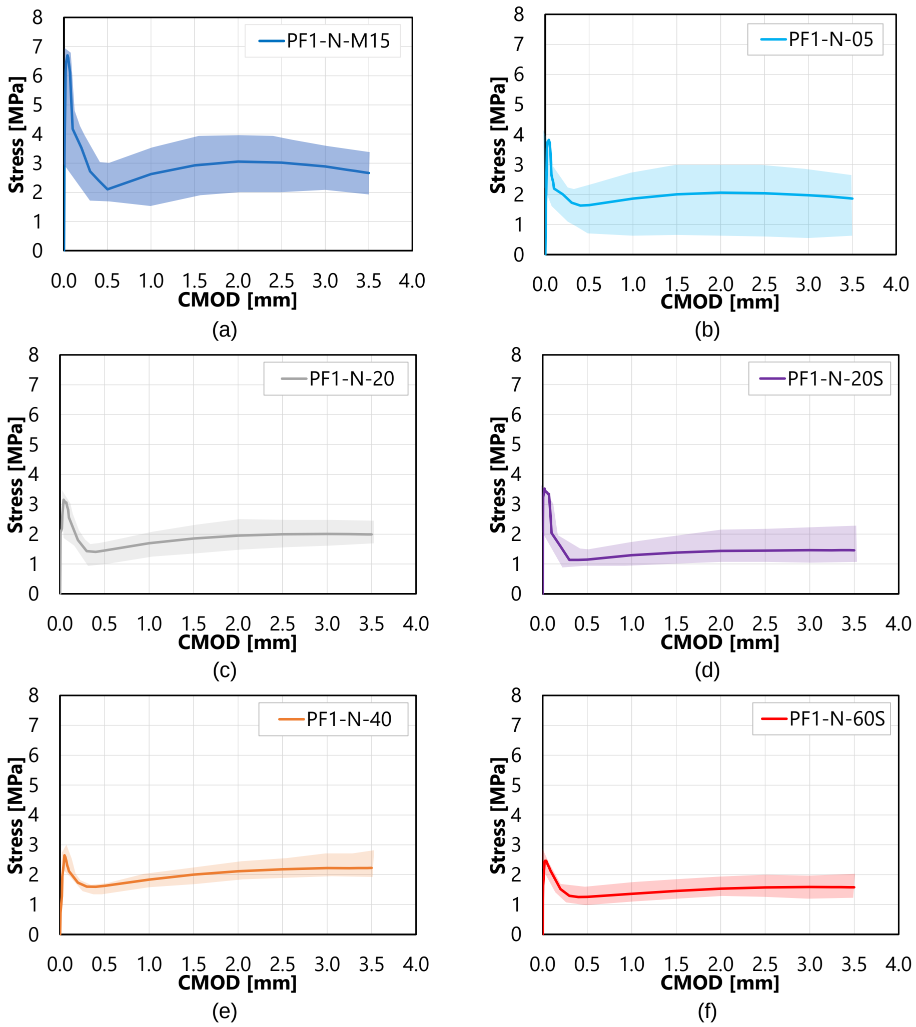

Figure 60. Flexural behavior of MSFRC-PF1 at non-pre-cracked state: (a) at -15 °C; (b) at 5 °C; (c) at 20 °C; (d) at 20 °C, in water immersion; (e) at 40 °C, and (f) at 60 °C, in water immersion.

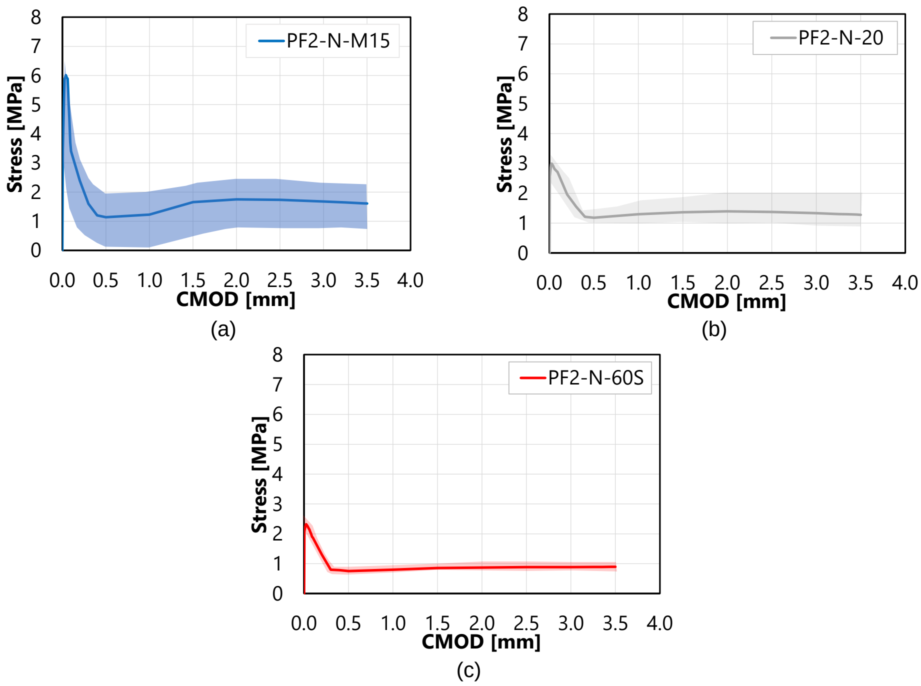

Figure 61. Flexural behavior of MSFRC-PF2 at non-pre-cracked state: (a) at -15 °C; (b) at 20 °C; and (c) at 60 °C, in water immersion.

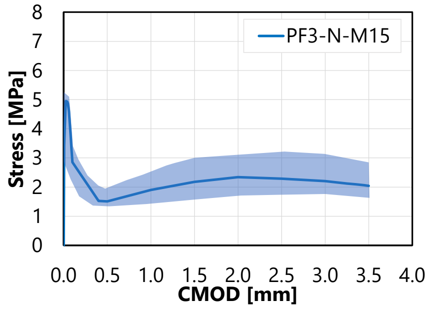

(a)

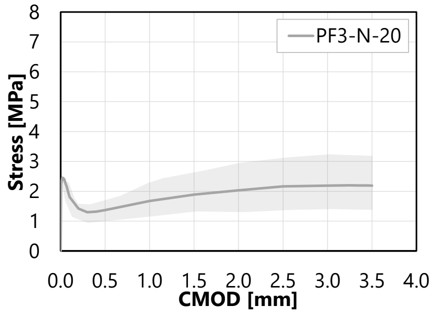

(b)

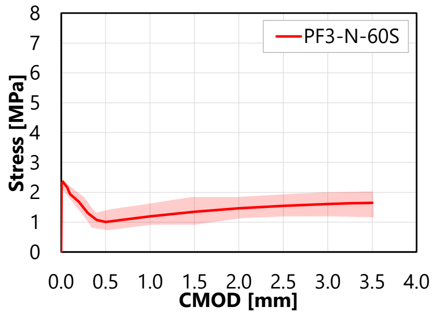

(c)

Figure 62. Flexural behavior of MSFRC-PF3 at non-pre-cracked state: (a) at -15 °C; (b) at 20 °C; and (c) at 60 °C, in water immersion.

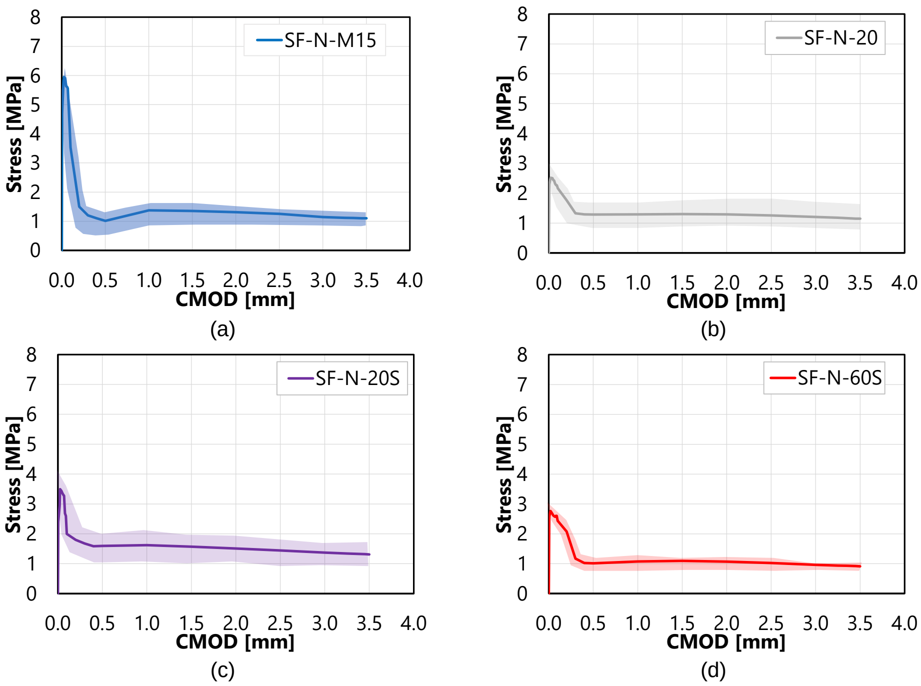

Figure 63. Flexural behavior of SFRC at non-pre-cracked state: (a) at -15 °C; (b) at 20 °C; (c) at 20 °C, in water immersion; and (d) at 60 °C, in water immersion.

4.3.1. Combined Effect of Pre-cracking and Temperature on Flexural Tensile Strengths

Cracking is a common situation that can put a structure out of service, not due to collapse, nor due to lack of stability, but for functional reasons of comfort, appearance, or durability. In FRC, fibers influence the transmission of tensile stresses across cracks with a bridging effect. This well-known effect contributes to controlling crack width and improving the post-cracking behaviour of concrete. Once an FRC element is cracked, fibres are exposed to environmental conditions, which may alter their performance. This alteration will potentially depend on the fibers' material (*e.g.*, steel, polypropylene, glass, etc.). Thus, to clarify this, the combined effect of pre-cracking and temperature was studied in the MSFRCs with fiber type PF1 and in SFRC, exposed to the pre-defined extreme environmental conditions. For these pre-cracked specimens, the results of the residual flexural strength corresponding with the limit of proportionality (LOP) and CMOD = $CMOD_j$ (j = 1, 2, 3, 4) were tabulated in Table 27 with their corresponding CoVs. In this case, the results of the three-point bending tests show a scatter of around 15–30 % for residual flexural strengths in most of the cases and around 10 % for the strengths at LOP, for many of the cases, being like those obtained for non-pre-cracked specimens. It is also important to remark that for these specimens, f_{LOP} and f_{R1} were obtained at ambient temperature at 28 days.

Table 27. Results of f_{LOP} the and the residual flexural strengths for pre-cracked specimens.

Code		Tested at 20 °C at 28 days				f_{R2} [MPa]	CoV [%]	f_{R3} [MPa]	CoV [%]	f_{R4} [MPa]	CoV [%]
		f_{LOP} [MPa]	CoV [%]	f_{R1} [MPa]	CoV [%]						
PF1-P	M15	3.42	5	1.69	18	3.01	20	3.20	21	3.02	22
	05	3.49	6	1.42	28	2.15	17	2.28	19	2.17	19
	20	3.47	19	1.66	18	2.16	23	2.36	24	2.39	25
	20S	2.78	9	1.22	16	1.52	19	1.59	22	1.52	22
	40	2.47	7	1.72	16	1.84	15	2.05	15	2.12	16
	60S	3.17	6	1.41	16	1.24	18	1.38	18	1.42	18
SF-P	M15	3.25	5	1.59	27	1.74	29	1.58	29	1.41	28
	20	2.97	3	1.02	25	1.08	25	1.05	24	0.98	23
	20S	3.12	11	1.65	22	1.69	21	1.57	22	1.46	20
	60S	3.35	6	1.13	14	1.10	25	1.03	26	0.93	27

Additionally, Figure 64 represents these results tabled above through the stress-CMOD curves obtained by 3PBT for pre-cracked beams. The mean values of seven specimens for each series are presented with a line, and the envelope (shaded areas) represents the scatter (maximum and minimum values of the tests) in the results.

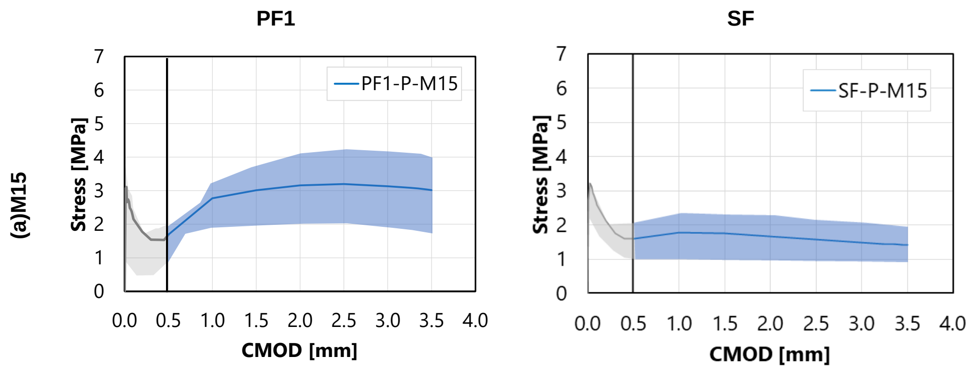

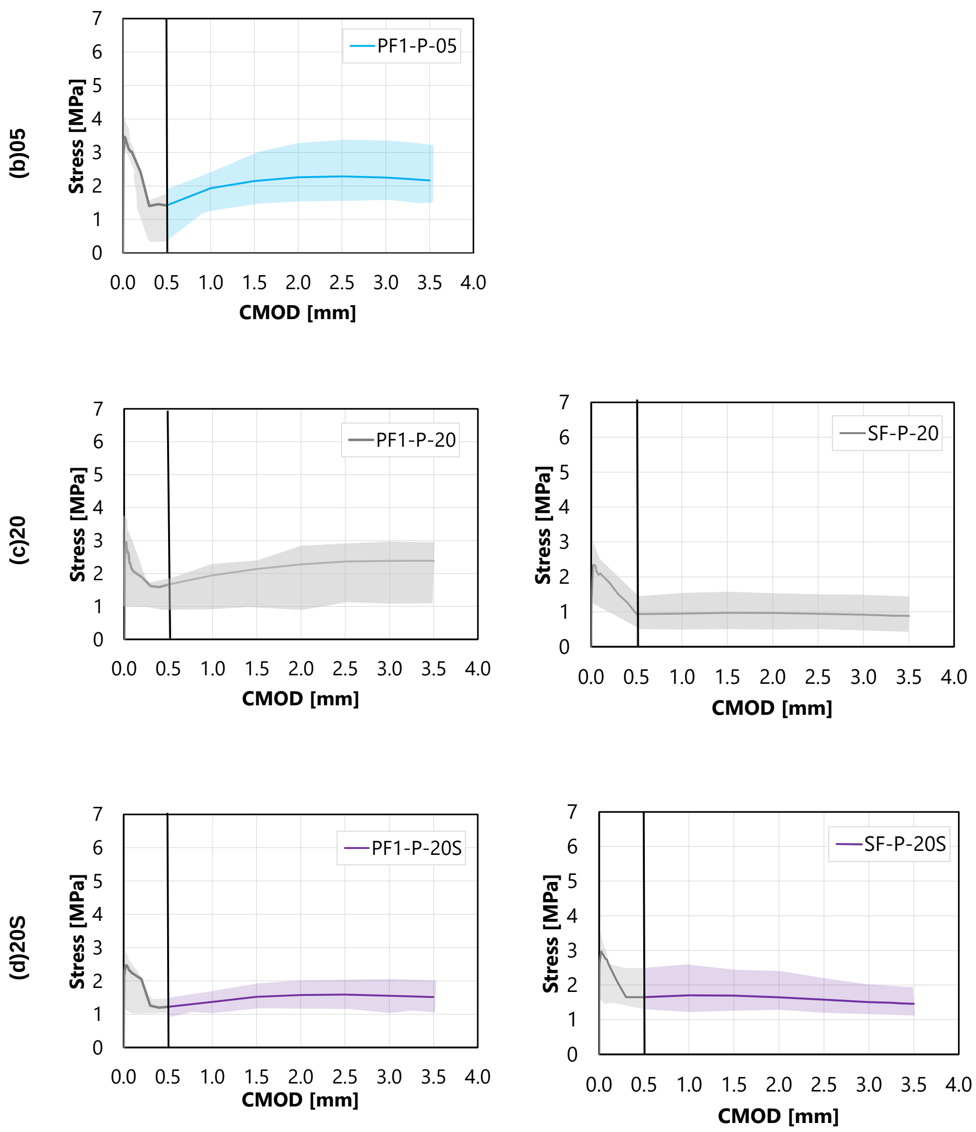
(b)05
PF1-P-05
(c)20
PF1-P-20
SF-P-20
(d)20S
PF1-P-20S
SF-P-20S
Stress [MPa]
CMOD [mm]
0.0 0.5 1.0 1.5 2.0 2.5 3.0 3.5 4.0
0 1 2 3 4 5 6 7

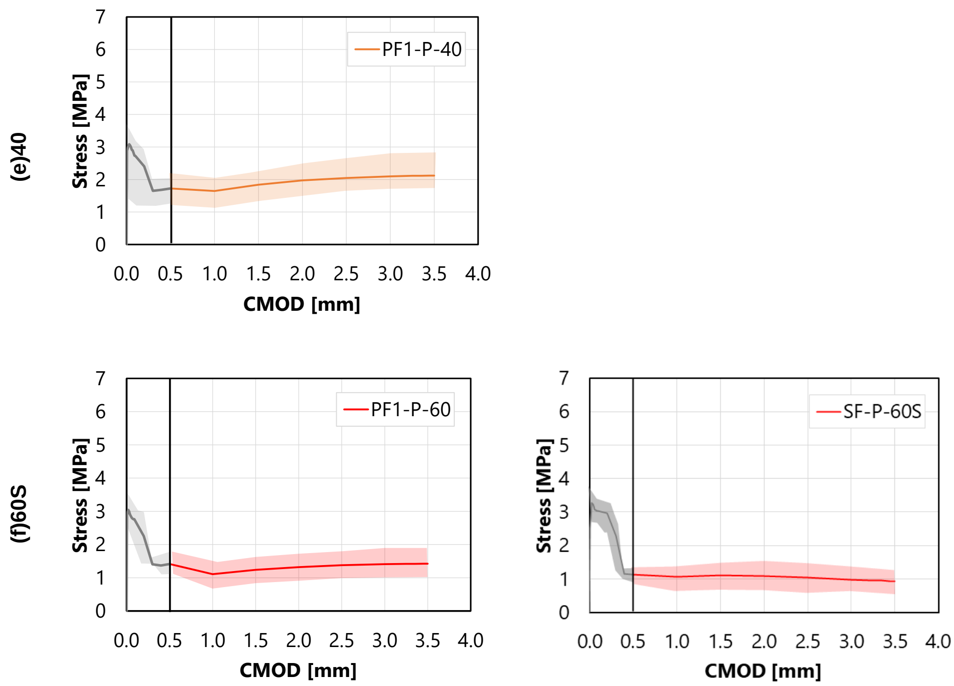

Figure 64. Flexural behavior of MSFRC (with PF1 fibers) and SFRC in pre-cracked specimens: (a) at -15 °C; (b) at 5 °C; (c) at 20 °C; (d) at 20 °C, in water immersion; (e) at 40 °C, and (f) at 60 °C, in water immersion.

Furthermore, to compare directly non-pre-cracked and pre-cracked elements, Figure 65 shows the mean stress-CMOD curves obtained from 7 prims for both groups from by means of the three-point bending tests at different temperatures. The phase of pre-cracking up to 0.5 mm was carried out at 20 °C and is therefore depicted with grey lines.

The effect of the temperature (after cracking) on the residual tensile strengths (f_{R2}, f_{R3} and f_{R4}) was studied for both groups. Similar trends can be observed in this comparison.

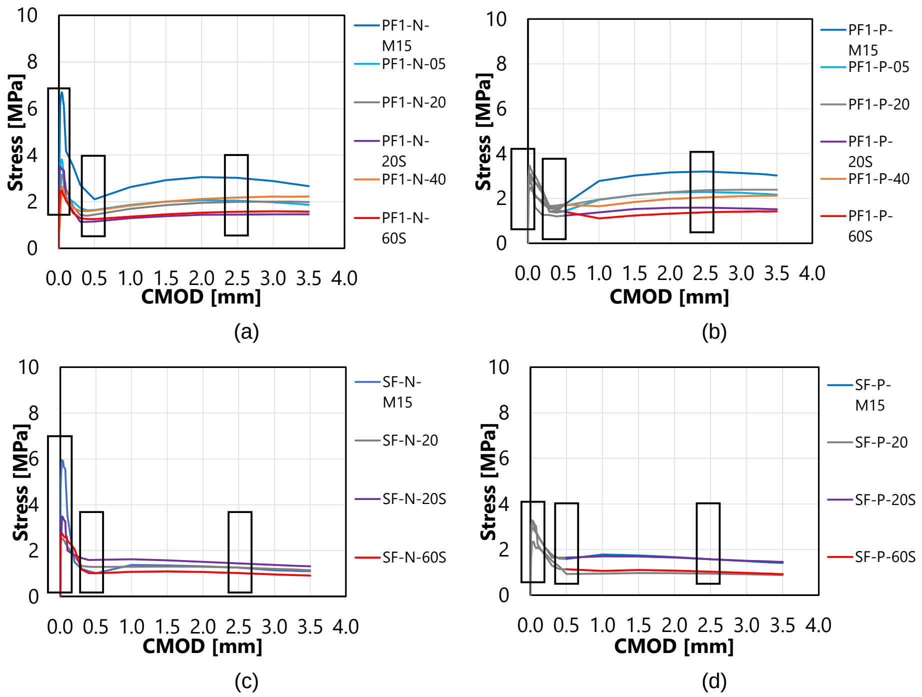

Figure 65. Average stress-CMOD curves of pre-cracked and non-pre-cracked specimens: (a) PF1-N; (b) PF1-P; (c) SF-N and (d) SF-P.

To conclude, the results show that no significant differences can be detected in residual flexural strengths between pre-cracked and non-pre-cracked specimens reinforced with PF1 nor with SF fibers.

4.3.2. Effect of Number of Fibers on Flexural Tensile Strengths

In this Subsection, an additional parameter is studied, which is said to influence the variability of the values of residual strengths [90], and this parameter is the number of fibers present in the cross-section generated during the test.

It was considered necessary to carry out a deeper analysis considering the effect of the number of fibers, since it may lead to misleading conclusions on the effect of temperature on tested FRC specimens in their flexural bending behavior [137].

a) Study of the number of fibers present in the cross-section

As was explained in Chapter 3, the specimens were broken in two halves after failure and the fibers broken or slipped in the formed cross-section were counted. Table 28 and Table 29 collect the mean values and their CoV per series obtained for non-pre-cracked and pre-cracked specimens, respectively.

Table 28. Total number of fibers (N) and number of fibers in lower third ($N_{1/3}$) in the cross-section per series for non-pre-cracked specimens.

Code		N	CoV [%]	$N_{1/3}$	CoV [%]
PF1-N	**M15**	95	13	32	18
	5	79	22	25	36
	20	80	7	28	13
	20S	70	16	23	24
	40	97	7	29	25
	60S	87	10	25	13
PF2-N	**M15**	75	15	22	25
	20	73	14	24	20
	60S	66	7	18	21
PF3-N	**M15**	104	16	31	14
	20	104	19	34	20
	60S	110	13	35	11
SF-N	**M15**	43	16	14	17
	20	51	16	17	34
	20S	52	13	18	19
	60S	48	18	13	22

Table 29. Total number of fibers (N) and number of fibers in lower third ($N_{1/3}$) in the cross-section per series for pre-cracked specimens.

Code		N	CoV [%]	$N_{1/3}$	CoV [%]
PF1-P	**M15**	100	12	30	16
	5	85	6	24	22
	20	92	16	33	20
	20S	78	16	25	20
	40	96	11	32	23
	60S	78	8	22	18
SF-P	**M15**	60	16	20	26
	20	46	22	20	20
	20S	54	16	19	23
	60S	47	17	18	19

The results show that the number of fibers present in the cross-section of MSFRC specimens (between 70 and 110 fibers in average) was higher than that of SFRC specimens (around 50 fibers in average). The quantity of macro synthetic fibers was one-third of the weight of the steel fibers, and this quantity is enough for reaching similar residual strengths. However, the amount of macro synthetic fibers represents more volume than the correspondent amount of steel fibers (0.75 % vol. vs 0.25 % vol). This explained the obtained results. Despite this, the distribution of fibers for non-pre-cracked and pre-cracked specimens was similar and followed a normal distribution independently of the fiber type (see Figure 66).

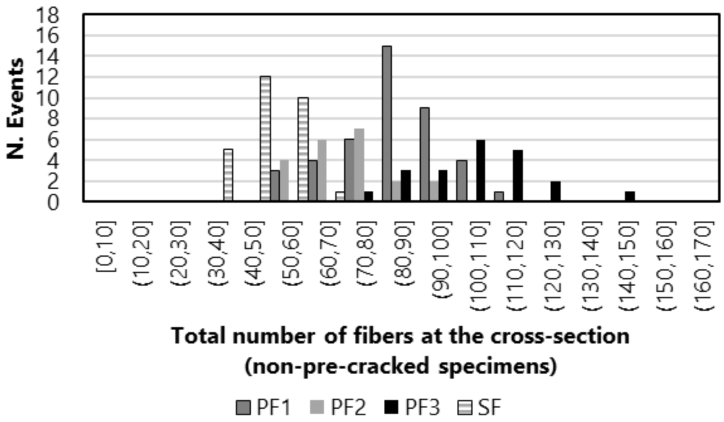

(a)

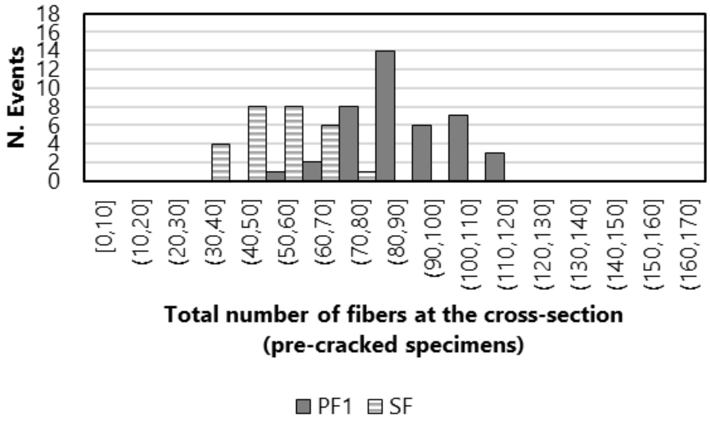

(b)

Figure 66. The total number of fibers at the cross-section for each type of fiber according to the number of events (N. Events): (a) non-pre-cracked and (b) pre-cracked specimens.

First advances in literature [30] showed that not all the fibers influence the residual strengths for the initial CMOD commonly used for SLS design (f_{R1}). It also describes that good linear correlation may be obtained when comparing the number of fibers in the lower third of the fracture surface with f_{R1}. In addition, for the case of f_{R3} (related with ULS design), it has a good linear correlation with the total number of fibers.

In this work, a good linear correlation was found when the total number of fibers is related to f_{R1} (better than if only the number of fibers on the lower third is used) and f_{R3}. For example, in Figure 67, it is possible to compare the residual flexural strengths f_{R1} vs. the number of fibers presented at the cross-section (in the lower third or total) obtained from the series MSFRC-PF1 in pre-cracked specimens. The graphs show that the values for the number of fibers in the lower third are more disperse than the total number of fibers, and the coefficient R^2 are higher in all the cases except one (group 20S). Furthermore, the highest values of the coefficient in the regression are obtained at low temperatures, and they decrease with the increase of temperature. This result indicates that FRC increases its brittleness at low temperatures.

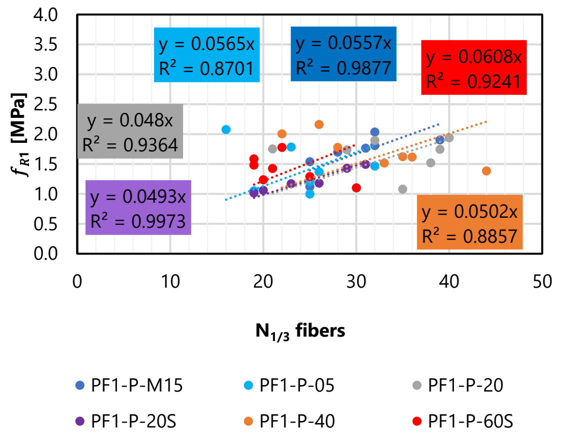

(a)

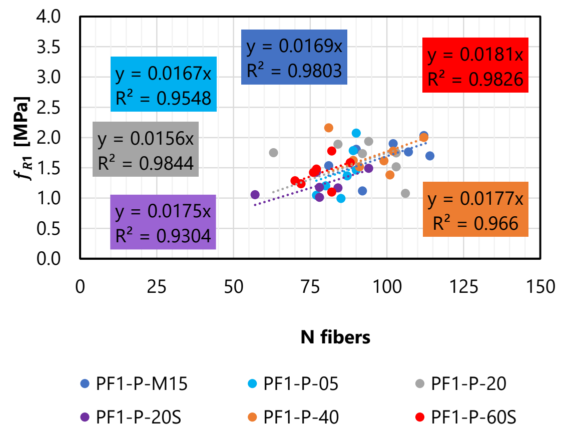

(b)

Figure 67. Linear regressions trend of residual flexural strength f_{R1} as a function of the number of fibers and temperatures for MSFRC-PF1 in pre-cracked specimens: (a) fibers in the lower third and (b) total number of fibers.

Figure 68 shows the residual flexural strengths f_{R3} vs. the total number of fibers presented at the cross-section obtained from the series MSFRC-PF1 in pre-cracked specimens, showing a good linear correlation. The same effect can be appreciated herein regarding brittleness.

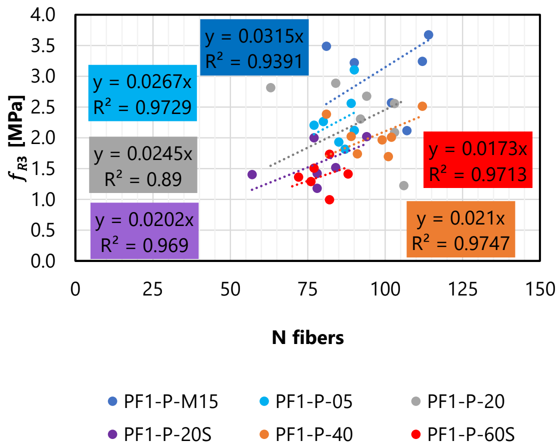

Figure 68. Linear regressions trend of residual flexural strength f_{R3} as a function of the number of fibers and temperatures for MSFRC-PF1 in pre-cracked specimens.

b) Effect of number of fibers on flexural strengths at temperature

With the previous analysis, the ratios f_{R1}/N and f_{R3}/N were calculated for all the temperatures for non-pre-cracked specimens, with N being the total number of fibers. For pre-cracked elements, only f_{R3}/N were calculated since f_{R1} values are obtained at standard temperatures. These results were plotted in Figure 69 and Figure 70. The normalized values of f_{R1}/N and f_{R3}/N indicate an increasing trend for low temperatures when compared to the standard temperature of 20 °C and a decreasing trend for moderate temperatures comparing to the ambient temperature, in both, steel and macro synthetic fibers, as happened without considering the number of fibers but much less pronounced. The effect of low temperature (particularly, below 0 °C) is more predominant than the effects at elevated temperatures. Furthermore, the effect of temperature is more influential for large CMOD than for small CMOD, as also occurred if the number of fibers is not contemplated but in a minor extent.

The results also show that no significant differences can be detected between pre-cracked and non-pre-cracked if N is taking into account.

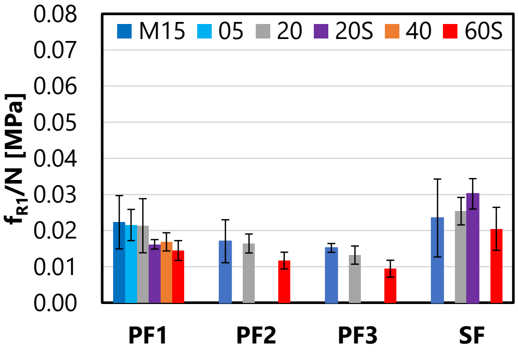

(a)

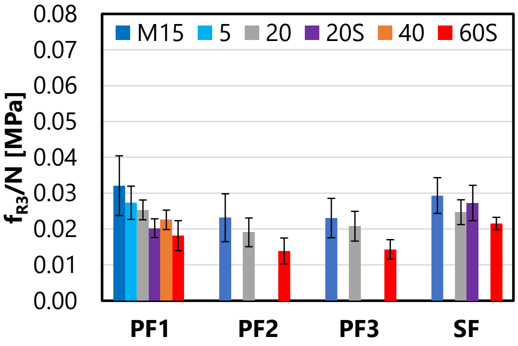

(b)

Figure 69. Normalized residual flexural strength f_{R1} and f_{R3} after short-term exposure at the target environmental conditions: (a) f_{R1}/N for non-pre-cracked specimens; and (b) f_{R3}/N for non-pre-cracked specimens.

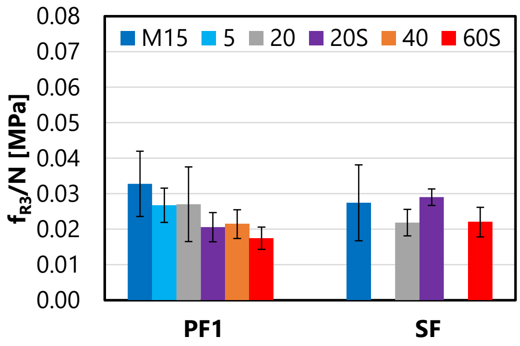

Figure 70. Normalized residual flexural strength f_{R3}/N after short-term exposure at the target environmental conditions for pre-cracked specimens.

To sum up, the influence of the temperature on the flexural behavior of FRC is maintained even considering the effect of the number of fibers, however, a great part of the results is conditioned by the number of fibers, that is, this variation means that part of the detected differences is an effect of the distribution of fibers and not an effect of temperature itself.

4.4. Influence of Environmental Conditions on Direct Tensile Strengths

Direct tensile tests were performed to identify the effect of temperature on tensile strengths of FRCs. As it was seen in Chapter 2, plastics expand and contract at considerably different rates if they are compared to steel and concrete-matrix. The CTE is an important factor in any application involving two different materials subjected to temperatures. In this context, the influence of environmental conditions on the interaction between concrete and fibers was also analyzed indirectly from a meso- scale perspective by the direct tensile strengths.

The nominal stress from direct tensile test was computed by dividing the maximum force by the area of the notched section for each specimen. The uniaxial tests on the cylinders are summarized by means of the tensile strength at limit of proportionality (LOP), named f^*_{LOP}, and four residual strength values, indicated as f^*_{R1}, f^*_{R2}, f^*_{R3}, f^*_{R4}, associated to COD values of 0.42 mm, 1.25 mm, 2.08 mm, and 2.92 mm. In this study, these COD values are proposed in analogy of CMOD values given by EN 14651.

Table 30 collects the mean results of f^*_{LOP}, f^*_{R1}, f^*_{R2}, f^*_{R3} and f^*_{R4} for 5 specimens and their corresponding CoVs. It is interesting to note that tensile strength

f^*_{LOP} is more sensitive to the addition of fibers as compared with compressive strength or f_{LOP}.

Table 30. Results for direct tensile tests on MSFRC cylinders at temperatures from -30 to 40 °C.

T [°C]	f^*_{LOP} [MPa]	CoV [%]	f^*_{R1} [MPa]	CoV [%]	f^*_{R2} [MPa]	CoV [%]	f^*_{R3} [MPa]	CoV [%]	f^*_{R4} [MPa]	CoV [%]
-30	3.71	18	1.04	39	1.51	40	1.38	37	1.05	30
-20	3.56	6	0.78	29	1.12	29	1.10	28	0.82	26
-10	3.33	9	0.95	22	1.31	25	1.29	26	1.00	33
0	3.26	8	0.88	32	1.24	32	1.28	33	1.00	29
20	3.21	16	0.79	17	1.15	15	1.24	13	1.13	14
40	2.56	15	0.48	31	0.72	29	0.79	28	0.74	26

The variability of these results is within the range of 20-35 %, that is the common due to the fiber distribution. At -30 °C, the outcomes obtained are especially more disperse than the rest of them. It could be explained by the higher fragility or by the T_g of PP fibers. From Table 30, it may be also concluded that the increase of temperature produces a decrease in the peak load and in all the residual tension strengths and on the contrary, for temperatures below zero, the trend is the inverse.

To analyze the results for direct tensile tests on MSFRC cylinders at temperatures from -30 to 40 °C, the mean stress-COD curves (mean of five specimens per temperature) have been depicted in Figure 71. The color code is maintained: tones of blue represent -30, -20 and-10 °C, grey for 0 °C; purple for 20 °C and orange, 40 °C. In this figure, the peak load (f^*_{LOP}) and the residual tensile strengths (f^*_{R1}, f^*_{R2}, f^*_{R3} and f^*_{R4}) can be seen.

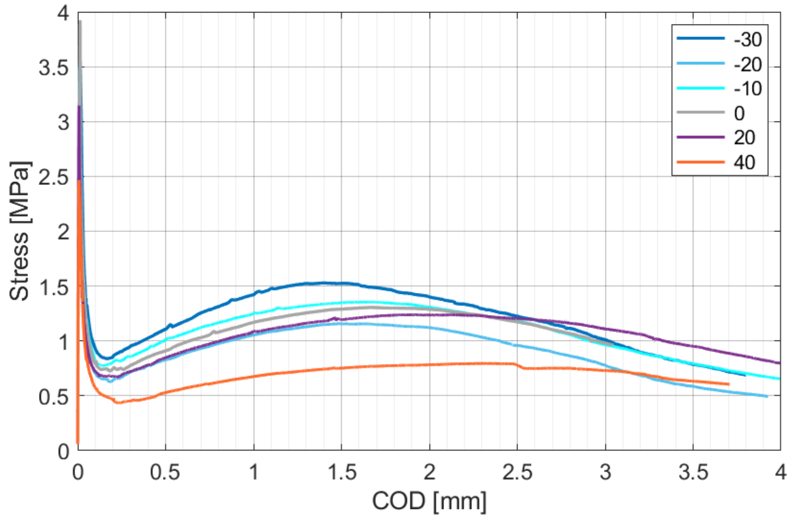

Figure 71. Comparison of the mean stress-COD curves of cylinders at temperatures.

The peak load (f^*_{LOP}) decreases by 30 % when increasing the temperature from -30 °C to 40 °C. The trend obtained from the data agrees with previous research [145]. There is an increment with the diminution of temperature and vice versa, as a reflection of the matrix, that support the results of the previous sections. The improved performance at sub-zero temperatures of FRC could be explained by the hypothesis of the formation of ice inside the pores of the concrete. At moderate temperatures, the degradation of the matrix by the temperature due to, among other factors, the loss of cohesion, changes in the microstructure, etc. produces a reduction of f^*_{LOP}.

In addition, the residual strengths f^*_{R1}, f^*_{R2}, f^*_{R3} and f^*_{R4} are also influenced by the temperature (ranging from -30 °C to 40 °C), decreased by 55 %, 50 %, 40 % and 30 %, respectively. The effect of low and high temperature on the residual strengths is similar, considering the variability of these tests and the number of fibers. At low temperatures, the behavior at below zero temperatures from -30 to -10 °C are similar, but not at -20 °C. Thus, it is probably that this effect would be principally caused by a change at the molecular level of the material constituting the fibers, due to the transition from the state rubbery to glassy once the T_g is reached. At moderate high temperature (40 °C), a decrease is noted compared to the reference temperature in all the residual tensile strengths. It could be due to the degradation on the matrix due to the temperature plus the fiber behavior, or by dehydration of the cement paste, and hence, the weakening of the area fiber–matrix interface [222].

Moreover, for large COD (f^*_{R3} and f^*_{R4}), a lower reduction is noted (if compared to f^*_{R1} and f^*_{R2}). This response could be explained by the fragility of the fibers when they freeze, which could potentially be noticeable when cracks are larger. Some authors justify this fact by a confinement effect caused by the contraction of the matrix at low temperature [155,162,223]. This can be seen in Figure 71 (the curves suggest the presence of a secondary flatter peak stress (after cracking) similar to what happened in 3PBTs at cold temperatures.

The stress and COD values where this secondary peak occurred were analyzed for these series. At low temperatures, the material tends to stiffen and this increase in stiffness is indicated by the shift of the second peak of the stress – COD curves, displaced to the left part of the graph as the temperature decreases. Figure 72-a represents these maximum stress values after the peak load (second peak) at the defined temperatures. Figure 72-b shows the COD values corresponding to the second peak at each target temperature.

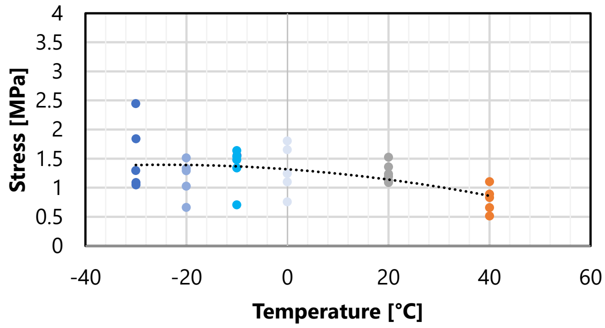

(a)

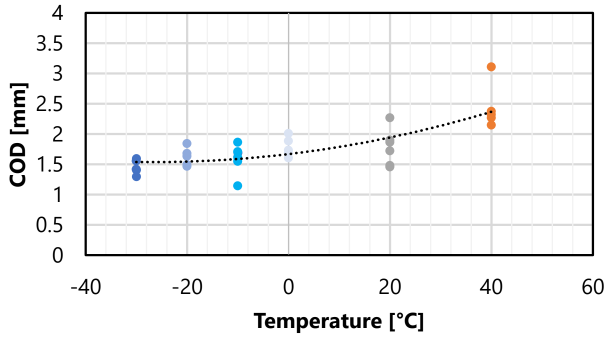

(b)

Figure 72. (a): Maximum stress values after the first peak (second peak) versus target temperatures, and (b): COD values corresponding to the second peak versus target temperatures.

To conclude, at low temperatures, an increase in the peak load and residual strengths is noted, together with the fiber and matrix embrittlement and the shape of the nominal stress – COD curve is modified by temperature. At high temperature, a decrease in the peak load and residual strengths is presented, probably as a consequence of viscous slippage at the interface.

4.4.1. Effect of the Number of Fibers present in the Cross-section on Direct Tensile Strengths at Temperatures

An in-depth analysis is also done, similar to that done on flexural tensile strengths, considering number and distribution of fibers present in the cross-section on tensile strengths. Figure 73 shows the values of residual strengths (axis Y) vs. the total number of fibers in the fracture surface (axis X): (a) f^*_{R1}; (b) f^*_{R2}; (c) f^*_{R3} and (d) f^*_{R4}. The color code is maintained for each temperature. Additionally, an equation (linear regression) is proposed in the corresponding-colored square.

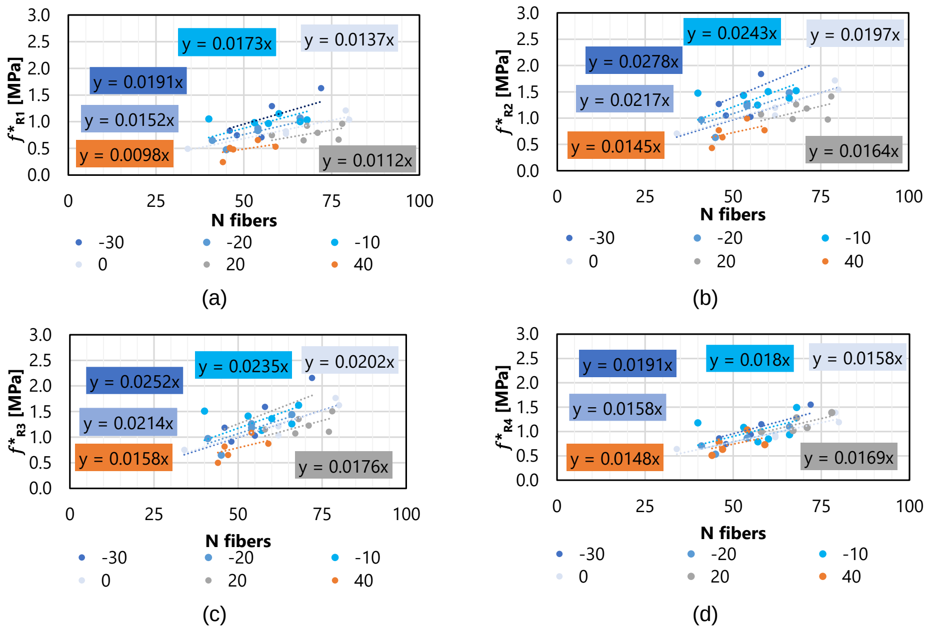

Figure 73. Linear regression trend of residual strengths as a function of the total number of fibers: (a) f^*_{R1};(b) f^*_{R2};(c) f^*_{R3} and (d) f^*_{R4}.

The graphs in Figure 73 show the residual strengths have a linear dependence on the number of fibers, it increases with the increase of the number of fibers present in the fracture surface. Furthermore, the highest value is recorded at the coldest temperature, -30 °C, and decreases with the increase of temperature.

This result indicates that FRC increases its brittleness at low temperatures, as happened in 3PBTs. It is important to highlight that in practice, the results may be affected by several factors, *e.g.*, the alignment of the metal plates that are connected to the testing machine, or the distribution of the fibers present in the cross-section, as shown in Figure 74, which was a non-homogeneous distribution.

Figure 74. Example of a cylinder with a non-homogeneous distribution of fiber on its fracture surface.

When aforementioned results (f^*_{R1}, f^*_{R2}, f^*_{R3} and f^*_{R4}) are normalized by the total number of fibers, the residual strengths maintain the same trend, but less pronounced. Figure 75 shows the mean stress-COD curves (mean of five specimens per temperature) with the results normalized by N (total number of fibers) at temperatures from -30 to 40 °C.

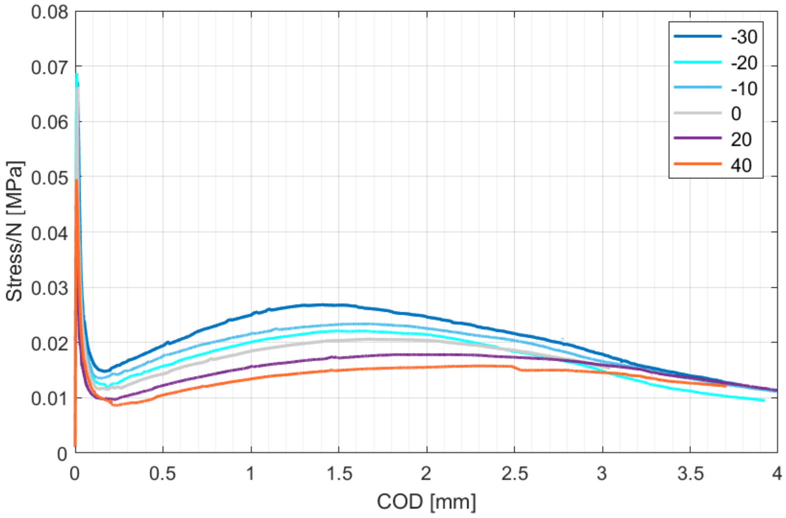

Figure 75. Comparison of the mean stress-COD curves, considering N, of cylinders at temperatures.

The results indicate a slight decreasing trend with increasing temperature (going from 20 °C to 40 °C). Moreover, at cold temperatures an increase is detected for f_{R1}^{*} and f_{R2}^{*} values (even the second peak is more prominent). However, at large CMOD (from 2.5mm), the behavior at low temperatures is not clear and, the residual strengths f_{R3}^{*} and f_{R4}^{*} decrease. This behavior at low temperatures is also found in the results at fiber level (see Subsection 4.1), that indicates that it could reflect the behavior of single fibers.

4.4.2. Study on the Fiber Breakage (inside concrete-matrix) at Temperatures

In this Subsection, the influence the type of breakage of the fibers embedded inside the matrix was evaluated. This phenomenon is analyzed after the failure of the tested cylinders by counting the number of broken fibers and number of slipped fibers and using the ratio of the number of broken fibers (N_{broken}) divided by the total number of fibers (N). The results indicate that at low temperatures this ratio is greater, which indicates a more fragile behavior of the fiber inside concrete-matrix (see Figure 76).

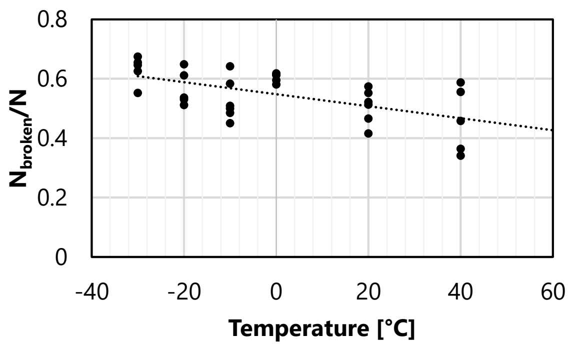

Figure 76. Correlation between the ratio number of broken fibers (N_{broken}) divided by the total number of fibers (N), depending on the temperature.

4.5. General Discussion

In this Chapter 4, the behavior of MSFRCs and SFRC under the defined environmental conditions at short-term exposure have been comprehensively examined in terms of (i) fiber level and (ii) material level, including compressive, flexural and tensile direct strengths. This section includes a general discussion for the different levels of study.

4.5.1. Single-fiber Level: Discussion

The results obtained from uniaxial tests on the fibers at different temperatures showed a dependence of their elastic modulus on temperature while the effect on UTS is more limited, in the range of -30 to 140 °C. It is worthy to mention that the effect of temperature on PF1 fiber becomes especially noticeable beyond 60 °C with a reduction in strength and stiffness.

In this regard, numerous investigations focused on the study of macro synthetic fibers' behavior to evaluate their response at high temperatures. For instance, Takaku [127] found that polypropylene fibers are highly dependent on temperature from 40 to 130 °C. More recently, Liu et al [224] studied combined effects of temperature (between -30 to 70 °C), tensile stress (different loads: 500-2400 N) and UV light. As for the effects chosen in this study, temperature had the most significant effects on polypropylene fibers since temperature increased the free volume of PP and provoked the subsequent weakening of intermolecular forces.

Moreover, ADFIL Corporation [129] showed the behavior (UTS and E-modulus) of one type of their fibers after storing in water at 80 °C for 28, 56 and 112 days. Fibers withstood the degradation process, but they detected a reduction of up to 32 % in tensile strength and up to 7 % in the modulus when compared to the initial values. On the contrary, it was found in this work that temperature influences the UTS of the single fiber with a decrease of 20 % at 80 °C and a decrease of 55 % for E-modulus at 80 °C, compared with the results obtained at 20 °C. Despite of the range of magnitude of the variation is similar for UTS, better results were reported in terms of E-modulus by [215]. In line with this, Hunger et al [131] indicated that the performance of synthetic fibers cannot be generalized since the properties of the fibers vary thoroughly from one to another and the results are specific for each type and application. At temperatures below 0 °C, Hall [117] stated that polypropylene tends to become brittle due to its nature (it is caused by the mobility of polymer chains that is greatly reduced). The results of this Thesis are coherent with those observed in the literature regarding the basic properties of the PP (as UTS and E-modulus) at temperatures.

Despite these results at the single-fiber level, it should be mentioned that plain concrete behavior below 0 °C also becomes more brittle and its strength is reduced at high temperatures, therefore, the final effect in FRCs needs to be quantified at the material level.

4.5.2. Material Level: Discussion

The results are discussed in the following Subsections in function on the property examined: compressive, flexural and direct tensile strengths.

a) Compression behavior

The environmental conditions studied affect the compressive strengths of the plain concrete (without fibers) in a similar manner to FRCs (MFRCs and SFRC). The obtained results of compression tests tested at temperatures in this Thesis are similar to those published by several authors [137,138].

For sub-zero temperatures, the compressive strength increases. This could be explained by the changes on the microstructure were though given that the water changes the state (liquid to solid) – ice formation. Other explanation could be the Van der Waals force, that increased because of the decrease of the distance between them (interatomic distance). These hypotheses were supported in several works [148,149]. Some authors have shown that compressive strength at low temperatures (up to −170 °C) can increase up to 400 % when compared to 20 °C [159]. However, such an increase is not detected in other studies performed at temperatures closer to those defined in this work. The results obtained in this work are within the order of magnitude of compressive strengths at sub-zero temperatures (considering the strength class) obtained in [148].

For moderate high temperatures, compressive strength is reduced when the temperature increases from 20 to 60 °C, in a 15-20 %. This could be explained by the stiffness of the system between cement paste and aggregates that gradually decreases with increasing temperature, which causes the weakness of the interface between paste and aggregates and a modification on the pore structure, and hence, a diminution on the compressive strengths [225,226]. Another hypothesis is the increase of the debonding between concrete components since the CTE of cement paste is different from the CTE of typical aggregates. Depending on its moisture content, the CTE of cement paste is around 11–20 $\times 10^{-6}$ per °C, while the CTE of the aggregates is normally lower, in most cases, 5–13 $\times 10^{-6}$ per °C [40].

In general, scarce information has been published related to compressive strength in concrete for the range of 20–60 °C. In one study [178], concrete lost 10–20 % of its initial compressive strength when heated to 100 °C but this extent of decrease was already reached at 60 °C in the current study. The results obtained herein are in line with [224], which showed that the compressive strength of concrete can decrease around 10–50 % (depending on the strength class) with the growth of temperature (from 10 up to 30 °C) with a strong linear relationship.

Regarding to humidity, this factor does not affect to a great extent the compression results obtained in the Thesis (comparing 20 and 20S specimens), which is contrary to the results of previous works [158,177]. The difference with other studies can be produced by the size of the specimens and also by the initial moisture content.

b) Flexural behavior

Limited information is available about the flexural strengths of FRC, as a composite material, at different temperatures.

Regarding the strength at LOP, f_{LOP} was expected to have a similar behavior than compressive strength, since these properties depend mainly on the matrix (the contribution of fibers is mainly noted in the post-cracking behavior). For low temperatures, a significant increase in terms of strengths at LOP was observed, that agrees with the results collected in [138], in 3PBTs. This improved performance at sub-zero temperatures of FRC could be explained by the hypothesis of the formation of ice inside the pores of the concrete. This increase in the strength at LOP was also associated with the embrittlement of a concrete-matrix [117]. For moderate high temperatures, in this work, f_{LOP} decreases for all FRCs studied, similarly to the decrease obtained in compressive strengths (around 20 %). The degradation of the matrix by the temperature could be explained by, among other factors, the debonded paste-aggregate, changes in the microstructure, etc.

In addition, the post-cracking behavior on FRC is normally characterized by means of 3PBT on notched prisms [90]. In this work, the 3PBT results show that the values of residual flexural strengths obtained (f_{Ri}) do not vary relevantly with temperature, especially for small CMODs. Despite the reduced modulus of elasticity of the macro synthetic fibers compared to steel fibers (typically <10 GPa for polymeric versus 210 GPa of steel fibers), the load drops after reaching the peak load were equivalent for all the cases, which could be explained by the fiber content. For f_{R1} values, an increase of a 30 % in average is shown at −15 °C for both FRCs and a decrease of a 20 % in average at 60 °C. f_{R3} values were also quite similar for the analyzed FRCs, but the temperature effect was greater than for f_{R1} values in all the cases. In this case, f_{R3} was a 35 % higher in average at low temperatures and a 25 % lower in average at moderate temperatures.

If the normalized flexural strength values are considered (dividing by N), the temperature effect on f_{R1} and f_{R3} is attenuated. The variations detected are an increase of a 5 % and 20 % in average for f_{R1} and f_{R3} values at low temperatures (M15 group) for both types of FRC and a decrease of a 15 % and 20 % in average for f_{R1} and f_{R3} values at moderate-high temperatures (60S) for the studied MSFRCs and SFRC. It should be highlighted that the decrease in f_{R1} and f_{R3} happened in both FRCs, even though synthetic fibers have a lower T_m compared with steel fibers. Thus, for both SFRC and MSFRCs, the residual flexural strengths were not degraded to great extent after 3 days at the tested conditions. The results on f_{R1} and f_{R3} are in line with those obtained by [162] for below zero temperatures, but the effect was lower since they showed an increase of their residual flexural strengths once temperatures dropped below 0 °C up to 71 % while the increased obtained in this experimental campaign was up to 20 %.

Besides, in this Thesis, residual strengths seem to decrease for the temperature range from 5 to 60 °C for 3 days but keeping enough residual flexural strength for both small and large values of CMOD in terms of mechanical performance, which makes them still suitable for some structural applications, on contrarily to what was stated in [155]. Focusing on f_{R1} and f_{R3}, given that these are the values to be considered in the structural design of any concrete element performed with FRC, it can be said that the studied SFRC could be classified as 1.0-1.5 (c or d) and MSFRCs as 1.0-1.5 (c, d or e) depending on the temperature, according to the fib Model Code 2010 [24] (see Table 31 and Table 32). Furthermore, it states that FRC can be used to substitute reinforcement when f_{R3}/f_{R1}> 0.5 and f_{R1}/f_{LOP} > 0.4. These requirements were verified for each type of FRC and for the extreme temperature of the selected range (-15, 20 (reference) and 60 °C) for non-pre-cracked and pre-cracked specimens respectively.

Table 31. Verification of compliance with the structural requirements for the studied FRCs in non-pre-cracked state after 3 days of exposure.

Requirements		T [°C]	PF1-N	PF2-N	PF3-N	SF-N
f_{R3}/f_{R1}	>0.5	-15	1.4	1.5	1.6	1.2
f_{R1}/f_{LOP}	>0.4		0.3	0.2	0.3	0.2
f_{R3}/f_{R1}	>0.5	20	1.4	1.2	1.6	1.0
f_{R1}/f_{LOP}	>0.4		0.6	0.4	0.5	0.5
f_{R3}/f_{R1}	>0.5	60S	1.3	1.2	1.5	1.0
f_{R1}/f_{LOP}	>0.4		0.5	0.3	0.4	0.4

Table 32. Verification of compliance with the structural requirements for the studied FRCs in pre-cracked state after 3 days of exposure.

Requirements		T [°C]	PF1-P	SF-P
f_{R3}/f_{R1}	>0.5	-15	1.9	1.0
f_{R1}/f_{LOP}	>0.4		0.5	0.3
f_{R3}/f_{R1}	>0.5	20	1.4	1.0
f_{R1}/f_{LOP}	>0.4		0.5	0.5
f_{R3}/f_{R1}	>0.5	60S	1.3	0.9
f_{R1}/f_{LOP}	>0.4		0.4	0.3

As can be seen, the first condition is satisfied for all the groups tested, in all the studied conditions, but the second is not (values in red do not accomplish the requirements). For non-pre-cracked elements, the ratio f_{R1}/f_{LOP} at -15 °C is not fulfilled for any FRC studied. Furthermore, for PF2 mixes, f_{R1}/f_{LOP} is also not fulfilled for 20 (reference) and 60 °C and or SF mixes, it is not fulfilled besides at 60 °C. For pre-cracked specimens, the requirement f_{R1}/f_{LOP} > 0.4 is not satisfied in SFRC (despite being f_{R1} and f_{LOP} tested at 20 °C). This can be explained because of fiber content that produces a fewer number of steel fibers in the cross-section (explained previously). To overcome this, higher fiber contents should be used to achieve to fulfil the structural requirements.

In general, it can be said that special attention should be paid when FRCs are designed in regions with temperatures below 0 °C, since at - 15 °C, FRCs become more brittle; although f_{LOP} values are higher at low temperatures compare with at ambient temperature (which delay the initiation of flexural cracks at service state), when the first crack is produced (especially in SFRCs), specimens collapsed almost suddenly, with very small deformation and no prior warning.

This fact provoked the ratio f_{R1}/f_{LOP} required in MC 2010 is hardly reached. This also could be solved with higher fiber contents (to increase f_{R1}, compensating the effect of temperature on the limit of proportionality and to provide sufficient ductility). Additional criteria to compensate the low ductility by an increase in strength in LOP as happened in these cases should be considered in new standards and codes of practice [227].

Lastly, regarding to the interaction temperature and pre-cracking state, Del Prete et al. [137] concluded that pre-cracking had not an important effect for short-term exposure. Their study involved pre-cracking at standard temperature up to a CMOD of 0.15 mm, then unloading and storing at 20 or 40 °C and 55 % RH for two days, and finally three-point bending test to failure. In fact, their results corresponding to pre-cracked specimens at two different temperatures (20 and 40 °C) are similar to the results for non-pre-cracked specimens. Their results are confirmed with those obtained in the present work, and it can be said that the pre-cracking process did not influence the behavior of FRCs at the studied non-standard temperatures for short-term exposures. In fact, the obtained results fulfill, in most cases, the ratios indicated to be categorized as structural FRCs for pre-cracked specimens (see Table 33).

c) Tensile behavior

The tested FRCs in this Thesis did not have exactly the same response in tensile and flexural behavior but similar trends were identified.

Regarding the strength at LOP, f_{LOP}^{*} was expected to have a similar behavior than compressive strength, since these properties depend mainly on the matrix. According to [145], this effect is even more pronounced in f_{LOP}^{*} than in compressive strengths. Several authors mentioned a decrease in the splitting tensile and direct tensile strengths with the increase of temperatures. At low temperatures, the effect inverse is detected, and this is in line with the literature [148].

The post-cracking behavior on FRC was also tested by means of uniaxial tests on notched cylinders, in order to additionally evaluate the fiber-matrix interface at a meso- scale perspective. The residual strengths f_{R1}^{*}, f_{R2}^{*}, f_{R3}^{*} and f_{R4}^{*} were influenced by the temperature (ranging from -30 °C to 40 °C). The effect of low and high temperature on the residual strengths was within a normal range of variation, considering the variability of these tests and the number of fibers. It is true that certain trend can be noted depending on temperature. At low temperatures, the behavior at below zero temperatures from -30 to -10 °C were similar and in general, the results for residual strengths increase when temperature decreases. Since authors justify this fact by a confinement effect caused by the contraction at low temperature of the matrix, which could produce increased frictional grip [163]. This affirmation is also supported by [155] who claimed that a greater fiber-matrix bond (18 %) was achieved at low temperature. For large COD (f_{R3}^{*} and f_{R4}^{*}), a lower reduction is noted (if compared to f_{R1}^{*} and f_{R2}^{*}). This response could be explained by the fragility of the fibers when they freeze. At moderate high temperature (40 °C), a small decrease is noted compared to the reference temperature in all the residual tensile strengths. This result could be due to the degradation on the matrix due to the temperature plus the fiber behavior.

4.5.3. Comparison between the Study Levels

From a general point of view, Figure 77 compares the differences in the behavior at temperature of a single-fiber filament and the behavior of the composite material MSFRC (in uniaxial and flexural bending tests). This figure represents the mean values for UTS of the fibers from -30 to 40 °C (left vertical axis, values represented with squares and trendline with a continuous line), for the residual strengths of MSFRC specimens obtained from 3PBT from -15 to 40 °C (right vertical axis, values plotted with circles and trendlines with dotted lines) and uniaxial tests, within the temperatures ranging from -30 to 40 °C (right vertical axis, values represented with triangles and trendlines with dashed lines).

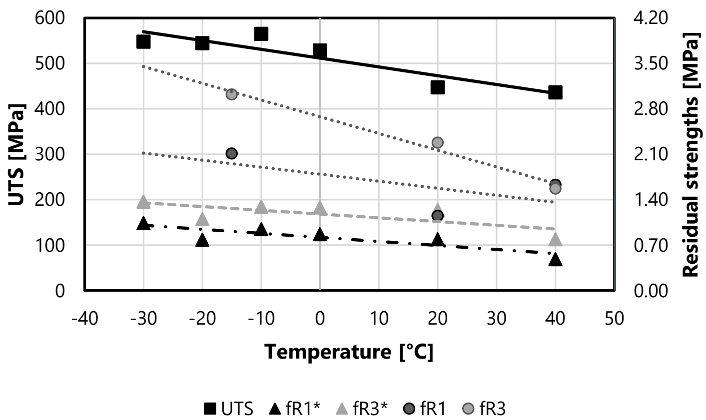

Figure 77. Comparison of the obtained results for all the levels of study (fiber and material) in this work at different temperatures (-30 to 40 °C).

The trend followed by all the properties is similar, showing a negative correlation between temperature and strengths. It is worthily remarkable that the effect of temperature on the fiber is less influential than in the residual strengths on the MSFRC specimens. A total of 20 % of variation is obtained comparing the values in fibers UTS at -30 and 40°C, while a 40-50 % of variation is obtained in MSFRC residual strengths, both in uniaxial and flexural behavior. However, it is also important to considerer that the variation of 3PBT and uniaxial tests performed on MSFRC usually has high variability (since it depends on several factors, concrete, number of fibers in the cross-section, etc.). This result was not expected since previous works had demonstrated that PP has a thermal dependent behavior that is decreased when embedded into concrete. This result suggests that the temperature affects the fiber-matrix bond of MSFRC for large CMODs (f_{R3}).

4.5.4. Summary of the Results

To sum up, despite the fibers' behavior is being affected negatively by temperatures, when macro synthetic fibers are embedded inside the matrix and work together, they did not negatively influence their behavior in tension and in flexure of FRC in a significant manner. At low temperatures, an increase in the peak load and in residual strengths are noted, together with the fiber and matrix embrittlement and the shape of the nominal stress – COD or CMOD curve is modified showing a secondary flatter peak. At high temperatures, a decrease in the peak load and in residual strengths is obtained in all the tests, that is a product of viscous slippage at the interface. Special caution should be taken when engineers design FRC in cold regions since this material also becomes more brittle. For temperatures above 0 °C up to 60 °C, a decrease with the temperature was detected, similar to the decrease in compressive strengths since this property is mainly affected by the matrix.

Despite some existing concerns, it is possible to obtain a satisfactory result with MSFRCs in terms of compressive, tension, and flexural behavior when exposed to moderate temperatures during short-term periods of time (~3 days).

Chapter 5

Behavior of MSFRCs after Long-term Exposure under Different Environmental Conditions

Chapter 5 presents the results obtained from the experimental campaign exposing specimens to long-term conditions and its analysis. Specifically, it includes the analysis of the material's ability to retain mechanical properties (compressive and flexural strengths) when exposed to temperatures for extended periods of time (90 and 180 days). This chapter is divided in the introduction and three sections. Section 5.1 explains the results obtained in compressive strengths after 90 and 180 days. Section 5.2 shows the results obtained in flexural strengths, regarding the material analysis at 90 and 180 days and also, the influence of other factors (as pre-cracking state or fiber type). Additionally, a detailed analysis on residual flexural strengths considering the number of fibers in the cross-section is also done in this Section. Lastly, Section 5.3 gives a general discussion about the behavior of MSFRCs under different environmental conditions after being exposed for 3 and 6 months, comparing with the results at three days and the results from other authors in the literature. The database generated by the previous and the present chapter, will be open access published with the aim of representing a reference in the field of FRCs and it lets to develop numerical model to predict properly the FRC behavior. Figure 78 displays the outline of these sections of the chapter.

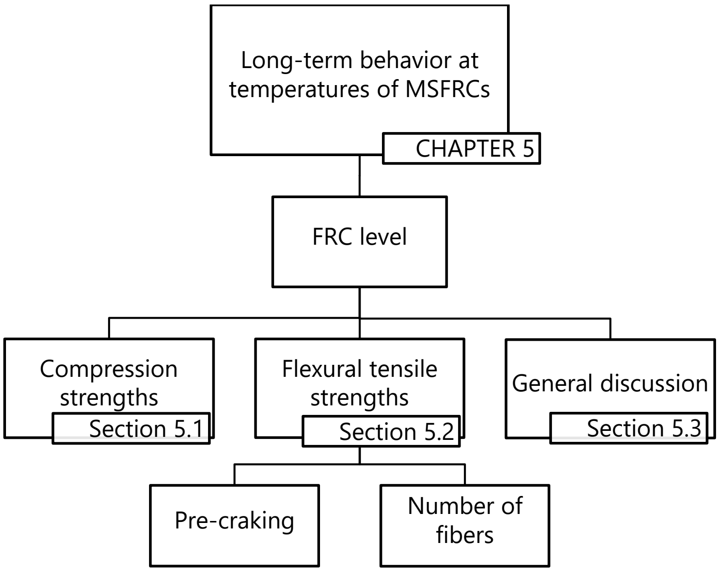

Figure 78. Outline of the Chapter 5.

5.1. Influence of Environmental Conditions on Compressive Strengths

Compressive strengths have resulted to be dependent on temperature at short-term (after 3 days of exposition), but to an acceptable extent. In this Section, the influence of long-term exposure to extreme environmental conditions is studied and analyzed on compressive strengths. Two experimental campaigns were carried out: one of them is performed after 90 days and the other one is performed after 180 days. The results are presented in the following Subsections.

5.1.1. Compressive Strength's Results after 90 days of exposure

The results from compression tests at 90 days at the predefined temperature for each type of FRC are collected in Table 33, with their corresponding CoVs in percentage. In this case, only PF1 and SF fibers are used to reinforce the matrix, and the extreme temperature of the selected range are examined (to discern the evolution of compression in function on temperature and time of exposition). Compressive strength was calculated as previously explained in the Section 4.2. The results of both kind of FRCs (MSFRC and SFRC) present similar trends. An increase of 10-20 % is noted at -15 °C and a decrease of 20-25 % is detected at 60 °C after 90 days of exposure. A linear relation between compressive strengths and temperature is detected. The variations observed are similar to those obtained after short-term exposure (see Chapter 4). At 90 days, this factor (saturation) was not evaluated.

Table 33. Results of compression tests after 90 days of exposure at temperature for MSFRC and SFRC.

Code		Compressive strengths at temperature		
		Average [MPa]	CoV [%]	% Variation from 20 °C
PF1	M15	52.5	3.5	+13
	20	46.5	3.7	-
	60S	34.5	11	-25
SF	M15	51.0	1.1	+21
	20	42.0	2.4	-
	60S	33.5	4.5	-20

The increase registered at the temperature below zero are in line with the results obtained by several authors [145]. The process that is hypothesized to produce this effect is the process of freezing free water trapped into the pores of concrete, which fills the pores in and increases the strength of the material. In the case of moderate temperatures (20-60 °C), several authors [138] have shown similar decrease. These results suggest that the decrease produced is a matrix issue and not a result of long-term degradation (see Chapter 4).

Figure 79 plotted the compression curves obtained from the tests, which were analyzed for each type of FRC and temperature. In this case, the slope of the curve is practically modified in a minor extent than at 3 days by low or high temperatures, but the maximum compressive strengths varied with temperature in the similar percentage of variation. It can be said that the exposition to the different target conditions altered the mode of failure of the tested specimens in this case, less than they altered the mode of failure at 3 days, although the same trend was maintained.

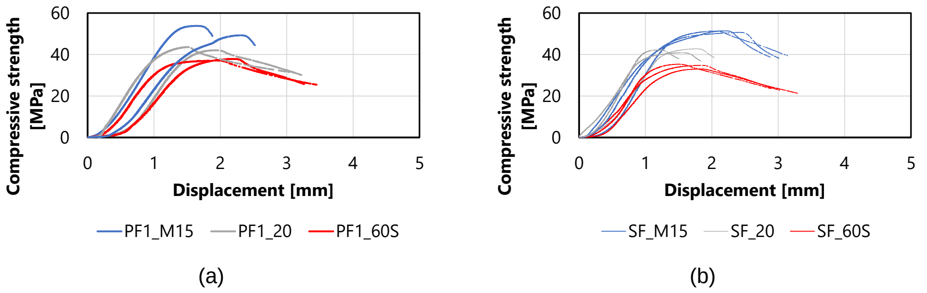

Figure 79. Curves obtained in compression tests at temperatures for: (a) PF1 cubes; and (b) SF cubes, after 90 days subjected to -15 and 60 °C in immersion.

To summarize, the results of compressive strengths at 90 days follow the same trend than those at short-term (3 days). At low temperatures (at -15 °C), an increase of a 15 % in average is detected. This could be explained by the ice formation of pore water, gel water, and chemical-bounded water in concrete enhance the compressive strengths of FRC, as was pointed out in [143]. At high temperature, a decrease of a 25 % in average compared to 20 °C is detected. This reduction may be attributed by the differential thermal volume changes of the materials involved [228,229].

5.1.2. Compressive Strength's Results after 180 days of exposure

The results of compressive strengths after 180 days of exposition under different studied conditions are tabulated in Table 34. The average compressive strength of three specimens and their CoVs for each group are given there. This table also included the variation (in %) to compared to the result at the reference temperature.

For all tested PF mixtures, decreasing the temperature of concrete samples below 20 °C improve compressive strengths. The variation that experimented the compressive strengths at low temperatures in percentage, respected to 20 °C, is within the range of 15-30 % for mixes reinforce with PF1 and PF2 fibers. For mixes reinforced with PF3 and SF, the values obtained are similar to the values obtained at 20 °C. The inverse effect is noted from 40 to 60 °C, with a decrease in compressive strengths with the increase of temperature. In this case, the variation in % respect standard temperature ranges from 15 to 30 % for PF3 and SF mixes. For PF1 and PF2 mixes, the effect is not so notable at high temperatures. Additionally, the effect of humidity in this study seems not to be influential (comparing 20 and 20S values, independently of fiber type), that is in line with the results pointed in Chapter 4.

Table 34. Results of compression tests after 180 days of exposure at temperature for MSFRCs and SFRC.

Code		Compressive strengths at temperature		
		Average [MPa]	**CoV [%]**	**% Variation from 20 °C**
PF1	**M15**	56.5	5	31
	05	45.0	2	5
	20	43.0	2	-
	20S	48.0	5	12
	40	38.0	3	-12
	60S	42.0	2	-2
PF2	**M15**	47.0	5	15
	20	41.0	1	-
	40	37.0	5	-10
	60	44.0	1	7
PF3	**M15**	49.0	1	5
	20	46.5	4	-
	40	41.0	3	-12
	60	38.0	1	-18
SF	**M15**	48.5	5	-5
	20	51.0	1	-
	20S	49.0	3	-4
	60S	37.0	4	-27

Figure 80 represents the curves obtained in the compression tests, which are illustrative of the compression behavior which are modified depending on the temperature. The graphs show the increase of compressive strength and the stiffening of the matrix at low temperature. At hot temperatures, the contrary effect is observed. Therefore, the elastic modulus is also changed by temperature, independently of the fiber type.

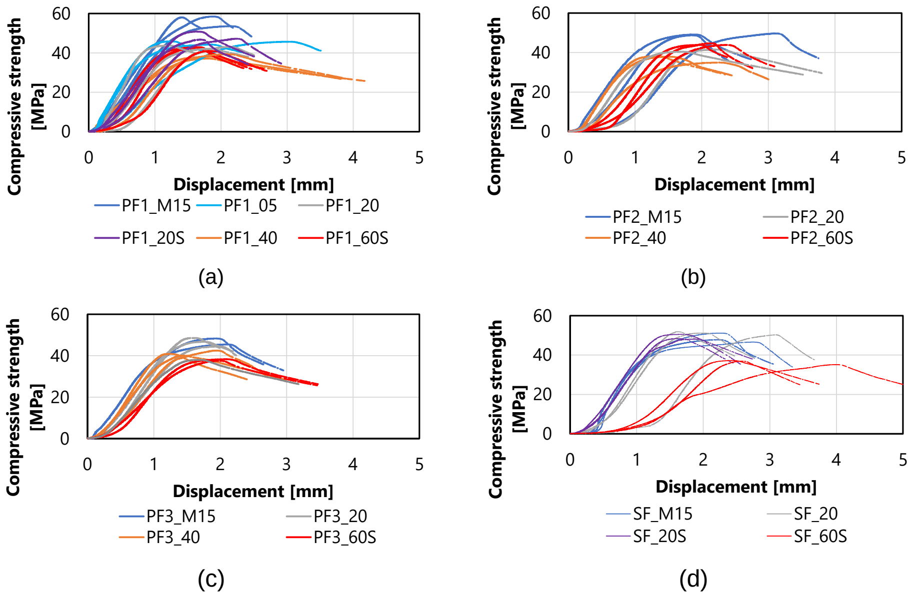

Figure 80. Curves obtained in compression tests at temperatures for: (a) PF1 cubes; (b) PF2 cubes; (c) PF3 cubes and (d) SF cubes, after 180 days of exposure.

To sum up, the results of compressive strengths at 180 days follow the same trend than the rest of the tests performed. At low temperatures (M15), an increase of a 15 % in average is noted. At high temperature (60S), a decrease of a 25 % in average is found. The same hypothesis given in the previous Subsection to explain this behavior can be applied herein. Moreover, it is also important to point out that the humidity is not relevant since the values obtained in the environmental conditions 20 and 20S, are very similar (their percentage of variation is over ± 10 %), at 180 days, similar to those at 3 days.

5.1.3. Analysis of Aging: Comparison between 3, 90 vs 180 Days' Compression Results under Temperatures

The analysis of aging regarding to compressive strengths was carried out assessing the material's capacity to sustain their compressive strengths after being subjected to the defined extreme environmental conditions (from -15 to 60 °C) for prolonged periods of time (90 and 180 days). For this purpose, the results at long-term of this study are compared with the compression results for these FRCs obtained at short-term (3 days), in Chapter 4.

The results are collected in Table 35 for the different temperatures tested and ages, and also, the percentage of variation that the series undergone by aging. Values of CoV are not included to facilitate the comparison.

It can be seen that compressive strengths experience an increase due to the time of exposure (for the same level of temperature). This variation is in the range of 0-25 % for compressive strengths at 90 days and more pronounced at 180 days, considering the results after 3 days of exposition as the reference, and is due to the maturation and normal acquisition of strength. On the contrary, temperature affects the concrete-matrix (comparing the value of compressive strength at target temperature with the value at standard temperature) in an equal percentage of variation, independently on fiber type used and for each time of exposure (see previous Subsections 5.1.1 and 5.1.2). The increase of temperature up to 60 °C implies a negative influence on compressive strengths of a 20-35 %, and a decrease of temperature below zero up to -15 °C, implies an 10-25 % of increase on compressive strengths.

Considering this, to analyze in detail the capacity to maintain their compressive strengths after being subjected to the defined extreme environmental conditions (from -15 to 60 °C) for prolonged periods of time, only 3 and 180 days were selected. The following procedure was followed: firstly, the percentage of strength retention after 3 days of exposure was calculated at each objective temperature, by comparing the value obtained of compressive strength at the target temperature to those obtained at 20 or 20S for each type of fiber. If compressive strength under the defined temperature after the period of time is higher than the reference at this age, the strength retention is blocked on 100 %. Afterwards, the percentage of strength retention after 180 days at each target temperature for each type of fiber, was calculated. Comparing both percentages, it can be seen if the difference on strength retention for compressive strengths at temperature is higher at long-term than at short-term. In most cases, the difference of strength retention is ± 20 %. There is not a clear trend, but it can be said that a good retention of compressive strengths is proven for the environmental conditions and time of exposure selected, since the percentage of the difference between the strength retention with age is not so noticeable.

Thus, for moderate high temperatures, the improvement in compressive strength with age is counteracted with the temperature effect resulting in no significant variation on the specimens studied in general terms, and for low temperatures, the experimented variation is more noteworthy than at moderate-high temperatures following the same reasoning.

Table 35. Comparison of compression results of FRC at 3, 90 and 180 days at different temperatures.

CODE		Compressive strengths [MPa]			Strength retention due to temperature		Difference of strength retention
		3 days	90 days	180 days	3 days	180 days	
PF1	M15	47.5	52.5	56.5	100 %	100 %	-
	5	37.0	-	45.0	99 %	100 %	1 %
	20	37.5	46.5	43.0	-	-	-
	20S	33.5	-	48.0	89 %	100 %	11 %
	40	35.5	-	38.0	95 %	88 %	-7 %
	60S	31.5	34.5	42.0	94 %	98 %	4 %
PF2	M15	44.5	-	47.0	100 %	100 %	-
	20	33.5	-	41.0	-	-	-
	40	-	-	37.0	-	-	-
	60S	28.0	-	44.0	84 %	100 %	16 %
PF3	M15	43.0	-	49.0	100 %	100 %	-
	20	34.0	-	46.5	-	-	-
	40	-	-	41.0	-	-	-
	60S	30.5	-	38.0	90 %	82 %	-8 %
SF	M15	51.5	51.0	48.5	100 %	95 %	-5 %
	20	34.0	42.0	51.0	-	-	-
	20S	36.0	-	49.0	100 %	96 %	-4 %
	60S	29.0	33.5	37.0	85 %	73 %	-12 %

Additionally, Figure 81 shows the trends for each type of FRCs, taking into account environmental conditions and times of exposure (3, 90 and 180 days). It is possible to see the effect of the age though the evolution of the strengths (increasing with time) and also, the variation that experimented with temperature (decreasing with temperature). The color code is the same of the previous sections and the CoV is not included in the figure to avoid making it unintelligible. It is worthy to mention that, for a matrix with a class of compressive strengths C30/37, the minimum obtained value was 28 MPa, for high temperature (60 °C) at short-term and the maximum obtained value was 56.5 MPa, for low temperature (-15 °C) at long-term (180 days).

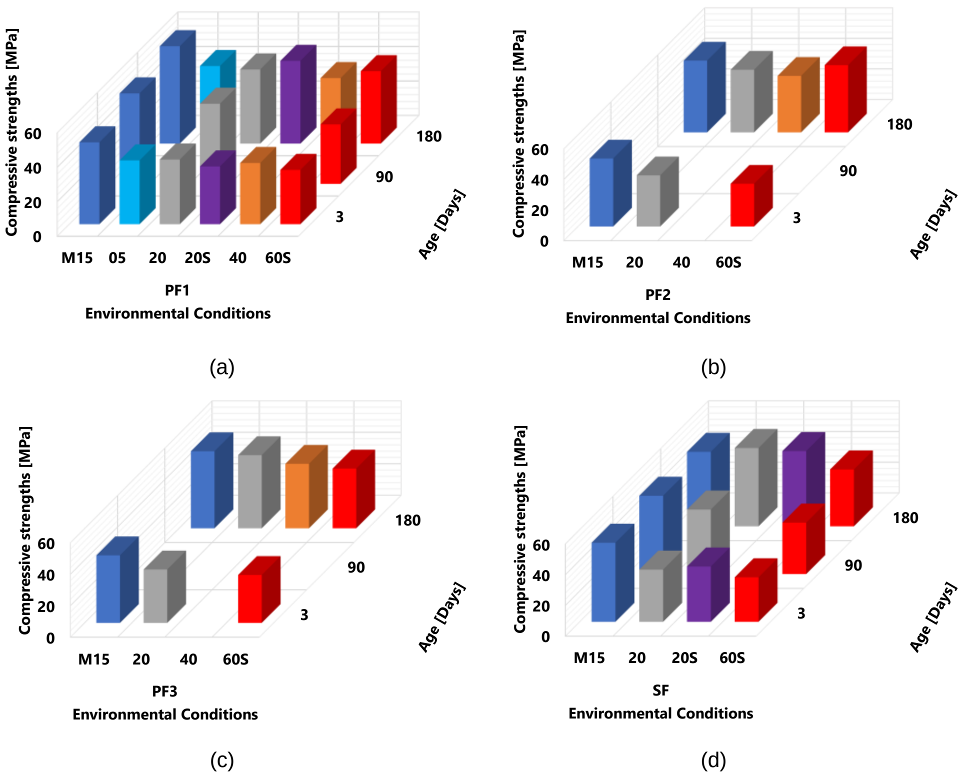

Figure 81. Comparison between 3, 90 vs 180 days' compression results under temperatures for: (a) PF1, (b) PF2, (c) PF3 and (d) SF.

To sum up, no degradation is detected by the combined effect of age and temperature after 90 and 180 days compared with the results at 3 days, maintaining the selected class of concrete (or being this affected in a minor extent). Humidity seems not affect the results at long-term, following the trend experienced at short-term.

5.2. Influence of Environmental Conditions on Flexural Strengths

Long-term flexural behavior of FRCs in realistic environmental conditions are examined by means of 3PBTs at temperature. At three days, although some variations were detected, satisfactory results with MSFRCs and SFRC in terms flexural behavior were obtained. After 90 and 180 days, it is necessary to confirm that the degradation in these composite materials is not substantial, in order to exploit their utility. To do this, the flexural strength at the limit of proportionality (f_{LOP}) and the residual flexural strengths at CMOD = 0.5, 1.5, 2.5 and 3.5 mm

(f_{R1}, f_{R2}, f_{R3} and f_{R4}, respectively) are presented and also analyzed in function of time of exposures (aging). They were calculated using Equations (5) and (6) given in Subsection 4.3. Additionally, other parameters, as the defined conditions (non-pre-cracked and pre-cracked) and the number of fibers, are also considered and studied.

5.2.1. Effect of Temperature on Flexural Tensile Strengths in Non-Pre-Cracked State at long-term

In this Subsection, the results of flexural strengths in non-pre-cracked state are divided into two groups, those obtained after 90 days of exposure and those obtained after 180 days of exposure.

a) Flexural strength's results after 90 days of exposure

The results at 90 days for non-pre-cracked specimens and their CoVs, are displayed in Table 36. In this case, only PF1 and SF fibers were used to reinforce the matrix. As occurred at 3 days, the CoVs for f_{LOP} were lower than those for the rest of the residual flexural strengths and all these coefficients are included in the common range of variation for these types of tests.

Table 36. Results of the f_{LOP} and the residual flexural strengths obtained at defined extreme conditions for non-pre-cracked specimens after 90 days of exposure.

Code		f_{LOP} [MPa]	CoV [%]	f_{R1} [MPa]	CoV [%]	f_{R2} [MPa]	CoV [%]	f_{R3} [MPa]	CoV [%]	f_{R4} [MPa]	CoV [%]
PF1-N	**M15**	5.12	5	1.99	35	2.41	29	1.81	26	1.50	23
	20	3.84	10	3.21	26	4.59	27	5.05	26	5.00	27
	60S	4.48	4	2.20	6	2.77	4	2.93	6	2.81	7
SF-N	**M15**	4.42	5	2.35	16	2.23	19	1.91	16	1.63	17
	20	3.65	8	1.42	13	1.35	18	1.24	19	1.13	24
	60S	3.30	3	1.56	33	1.47	36	1.34	33	1.18	33

The results of residual strengths of PF1-N specimens at 20 °C were higher than expected. This is explained by the variation detected in compression and the average of the number of fibers in the cross-section. Thus, herein, it is indispensable to consider the analysis done in Subsection 5.2.3; if not considered, it may be led to misunderstanding in the conclusions about the effect of temperature on residuals flexural strengths. However, the results at LOP can already be commented since this property is conditioned mainly by the matrix. In general terms, the results at LOP, for SF mixes, were foreseeable. An increase of a 15 % was detected at - 15 °C compared with 20 °C and a decrease of a 10 % was noted at 60 °C compared with 20 °C. For PF1 mixes, an increase is noted at high temperatures as well as at low temperatures (around 20 %). This variation could be attributed to the production process scatter since the high temperature tends to reduce the response of the matrix.

Additionally, Figure 82 and Figure 83 show the mean flexural behavior of seven specimens of MSFRC with PF1 fibers and SFRC in non-pre-cracked state at the different temperatures. Additionally, the shaded areas represent the scatter (maximum and minimum values of the tests) in the results. MSFRC displays a hardening behavior under bending loads in this case and, on the contrary, SFRC presents a softening behavior. As it was commented previously, results at 20 °C for MSFRC are higher than expected in terms of post-cracking residual flexural strengths. Similar to the results obtained at 3 days at -15 °C for both types of FRCs, particularly for macro synthetic fibers, the curves suggest the existence of a secondary flatter peak stress. This phenomenon was also examined in the uniaxial tests on FRC cylinders and in the flexural tests at short-term (3 days). On the contrary, no significant effects are detected in residuals flexural strengths for both type of FRCs in non-pre-cracked state at 60 °C.

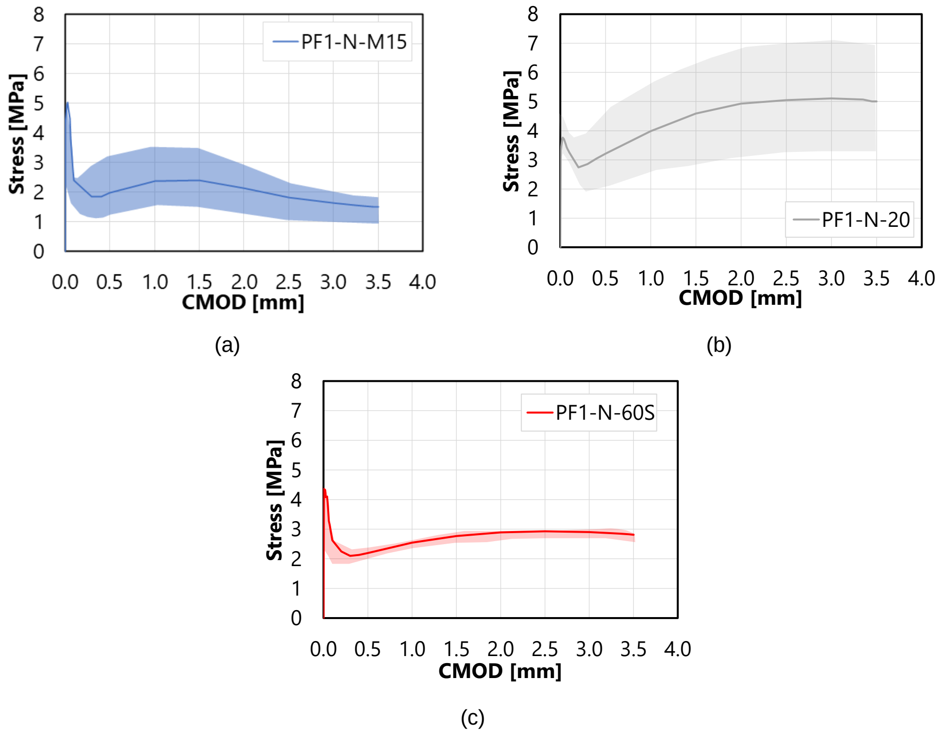

Figure 82. Flexural behavior of MSFRC-PF1 at non-pre-cracked state after 90 days: (a) at -15 °C; (b) at 20 °C, and (c) at 60 °C, in water immersion.

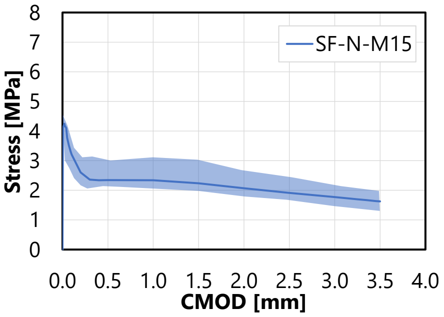

(a)

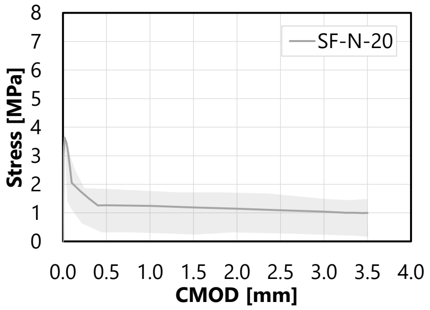

(b)

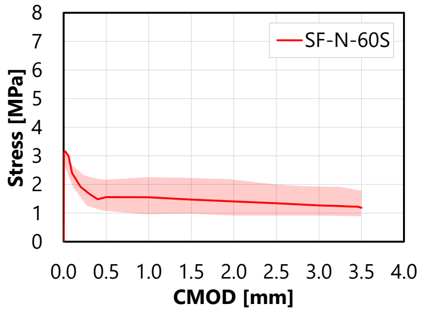

(c)

Figure 83. Flexural behavior of SFRC at non-pre-cracked state after 90 days: (a) at -15 °C; (b) at 20 °C, and (c) at 60 °C, in water immersion.

To summarize, MSFRC and SFRC exhibited similar trends regarding temperature after 90 days exposure to those after 3 days of exposure: a small reduction at moderate-high temperatures. At low temperatures, SFRC also presents the expected increase. It is important to consider the number of fibers in the cross-section generated, which is done in Section 5.2.3.

b) Flexural strength's results after 180 days of exposure

Regarding results after 180 days of exposure for non-pre-cracked specimens, the mean values of seven beams and their CoVs, are displayed in Table 37. In this case, matrix was reinforced with PF1, PF2, PF3 and SF fibers. As occurred at 3 and 90 days, the CoVs for f_{LOP} were lower than those for the rest of the residual flexural strengths and all these coefficients are within the common range of variation for these types of tests.

Table 37. Results of the f_{LOP} and the residual flexural strengths obtained at defined extreme conditions for non-pre-cracked specimens after 180 days of exposure.

Code		f_{LOP} [MPa]	CoV [%]	f_{R1} [MPa]	CoV [%]	f_{R2} [MPa]	CoV [%]	f_{R3} [MPa]	CoV [%]	f_{R4} [MPa]	CoV [%]
PF1-N	M15	4.61	11	2.30	21	3.13	19	3.18	19	2.63	19
	05	4.59	12	2.25	16	2.32	14	3.45	12	3.25	11
	20	4.55	6	2.12	35	2.67	35	2.76	40	2.72	40
	20S	4.52	4	2.04	24	2.69	27	2.88	28	2.81	29
	40	4.25	9	2.16	20	2.56	29	2.76	29	2.82	27
	60S	4.05	4	2.17	27	2.72	26	2.80	25	2.65	20
PF2-N	M15	5.21	9	1.47	26	1.92	26	2.04	27	1.96	28
	20	4.45	5	1.61	17	1.78	28	1.97	22	1.88	20
	40	4.16	6	1.56	23	1.56	24	1.55	22	1.48	22
	60S	4.23	3	1.39	20	1.74	20	1.77	20	1.65	20
PF3-N	M15	5.49	6	2.17	17	3.15	12	3.23	14	2.67	16
	20	4.92	3	1.71	19	2.32	21	2.62	20	2.50	19
	40	4.62	12	1.77	30	1.93	30	2.14	27	2.14	25
	60S	3.68	14	1.58	21	2.03	25	2.24	24	2.18	24
SF-N	M15	6.00	15	1.77	40	1.92	20	1.70	18	1.48	20
	20	3.80	8	1.58	26	1.44	27	1.27	28	1.17	28
	20S	4.43	4	1.93	27	1.88	29	1.65	31	1.54	21
	60S	4.54	4	2.03	19	2.02	18	1.78	18	1.51	19

After a period of 180 days, the trend for f_{LOP} values are maintained for macro synthetic and steel fibers if comparing with the trend at short-term. At -15 °C, increments of 12, 17 and 57 % are detected for PF3, PF2 and SF mixes. The variation for PF1 mixes was minor. Additionally, low temperatures above zero degrees do not have an equivalent impact on f_{LOP}. For high temperatures, at 40 °C, all the MSFRCs experienced a reduction in f_{LOP} of a 7 %, and at 60 °C, a wider fluctuation was noted, and for MSFRCs, a decrease between 5 and 20 % was found. For SFRC, an increase was produced but it was not significant.

Therefore, the effect of temperature on the residual strengths is not noticeable in a first view. The average values of f_{R1} varies from 1.39 to 2.30 MPa; for f_{R2}, these values range from 1.44 to 3.15 MPa; for f_{R3} results, the values are between 1.27 and 3.45 and lastly, f_{R4} values are within the range of 1.17-3.25 MPa. This indicates that the stresses obtained at small CMODs (f_{R1} and f_{R2})

experienced a lower effect of temperature than those at large CMOD (f_{R3} and f_{R4}), but the extent of this temperature effect is not important.

The shape of the mean curve stress-CMOD for non-pre-cracked specimens after 180 days of exposure to the defined extreme conditions are depicted from Figure 84 to Figure 87.

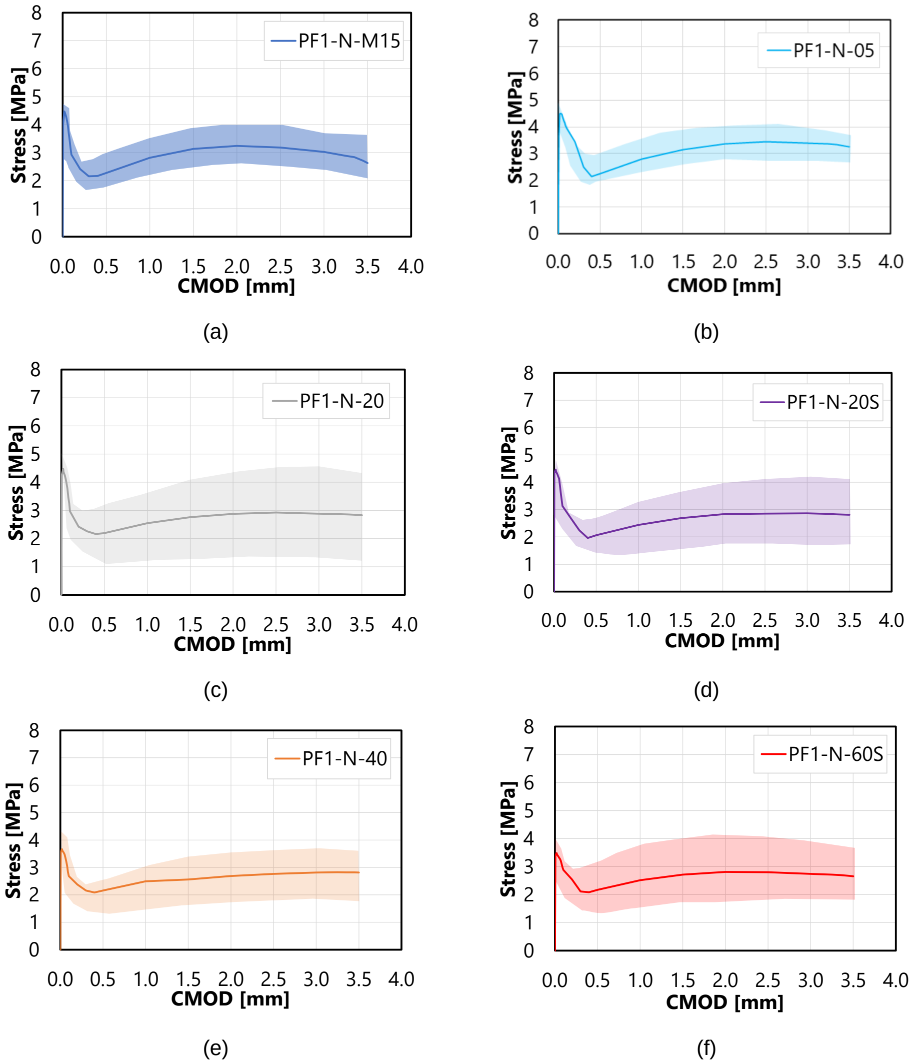

Figure 84. Flexural behavior of MSFRC-PF1 at non-pre-cracked state after 180 days: (a) at -15 °C; (b) at 5 °C; (c) at 20 °C; (d) at 20 °C, in water immersion; (e) at 40 °C, and (c) at 60 °C, in water immersion.

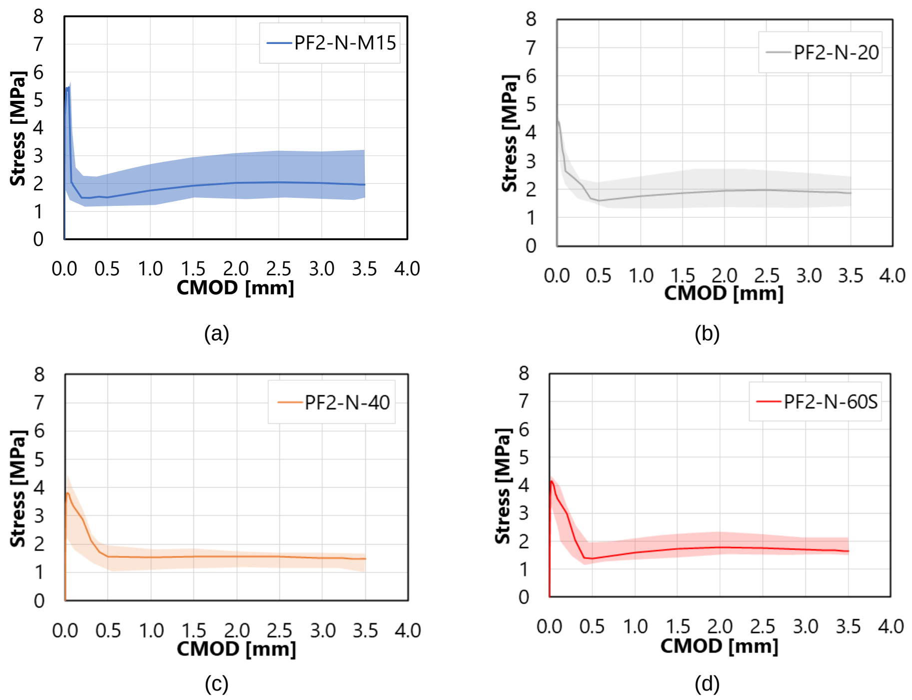

Figure 85. Flexural behavior of MSFRC-PF2 at non-pre-cracked state after 180 days: (a) at -15 °C; (b) at 20 °C; (c) at 40 °C, and (d) at 60 °C, in water immersion.

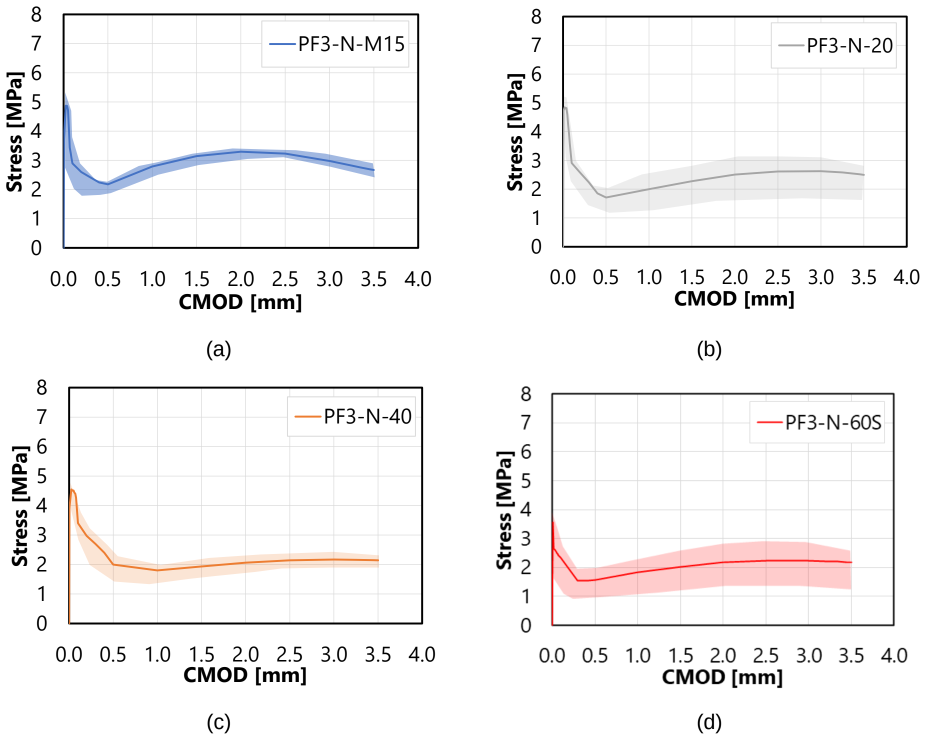

Figure 86. Flexural behavior of MSFRC-PF3 at non-pre-cracked state after 180 days: (a) at -15 °C; (b) at 20 °C; (c) at 40 °C, and (d) at 60 °C, in water immersion.

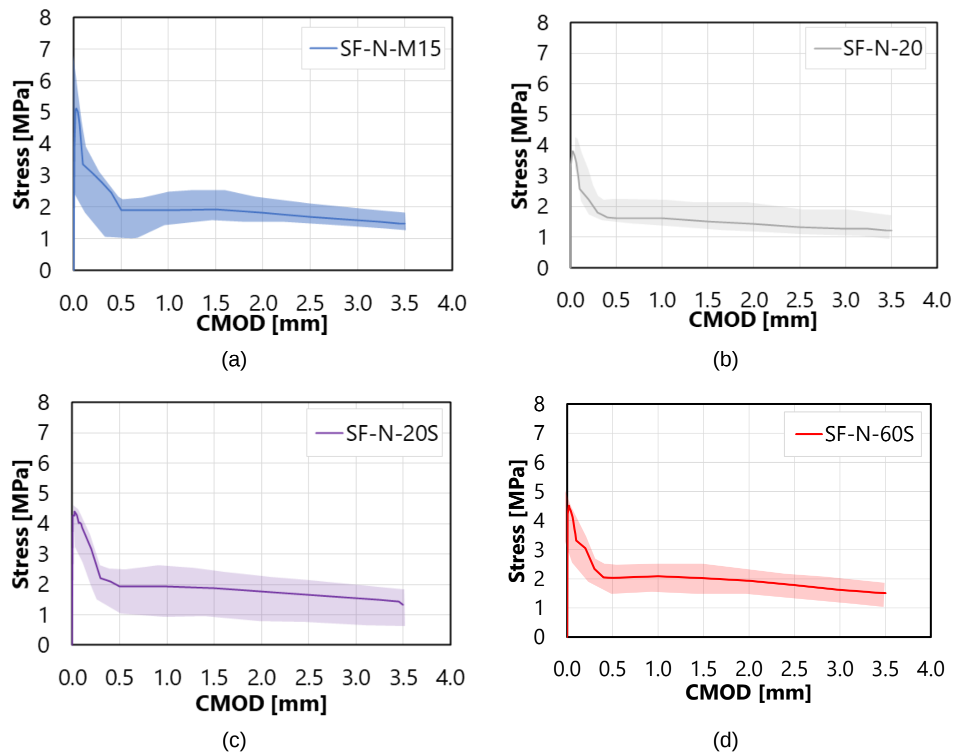

Figure 87. Flexural behavior of SFRC at non-pre-cracked state after 180 days: (a) at -15 °C; (b) at 20 °C; (c) at 20 °C, in water immersion, and (d) at 60 °C, in water immersion.

Regarding humidity variations, comparing 20 and 20S values, no difference was found, indicating that this factor is not determinate for residuals strengths in this study.

To summarize, MSFRCs and SFRC exhibited similar trends in flexure by 3PBTs after 180 days exposure. In general, at −15 °C, both FRCs experienced an increase in f_{LOP} and the residual flexural strengths of for non-pre-cracked specimens. On the contrary, no significant high temperature effects are detected in residuals flexural strengths for both type of FRCs in non-pre-cracked state. Humidity is not a determinate factor.

c) Analysis of aging: comparison between short- and long-term bending results under extreme environmental conditions

In this Subsection, it is possible to study through the results obtained previously, the aging of the flexural strengths with temperature and time in non-pre-cracked state. This analysis was carried out on f_{LOP}, f_{R1} and f_{R3} to assess the material's capacity to sustain these strengths after being subjected to low (- 15 °C) and high (60 °C, submerged) temperatures, comparing with the reference (20 °C). For this purpose, the results at 180 days are compared with the results for these FRCs obtained at short-term (3 days), in Chapter 4.

From Table 38 to Table 41, the results for f_{LOP}, f_{R1} and f_{R3} at -15, 20 and 60 °C after 3, 90 and 180 days of exposure, are collected for each type of fiber: PF1, PF2, PF3 and SF respectively. Values of CoV are not included herein to facilitate the comparison. To analyze in detail the capacity to sustain their flexural strengths after being subjected to the defined extreme environmental conditions for prolonged periods of time, the percentage of strength retention after 3 days of exposure was calculated at each objective temperature (comparing the value obtained of flexural strength at the target temperature to those obtained at 20 °C) for each type of fiber. Afterwards, the percentage of strength retention after 180 days at each target temperature for each type of fiber, was calculated. The two percentages of strength retention (after 3 days and after 180 days) can be compared, resulting in a difference in the strength retention positive or negative (additional degradation with age). It is important to clarify that when the strength under the defined temperature after the period of time is higher than the reference at this age, the strength retention is blocked on 100 %.

Table 38. Evaluation of degradation by temperature of the flexural strengths results of MSFRC-PF1 between 3 and 180 days.

CODE		PF1			Strength retention due to temperature		Difference
		3 Days	90 Days	180 Days	3 Days	180 Days	
f_{LOP}	**M15**	6.76	5.12	4.61	100 %	100 %	-
	20	3.27	3.84	4.55	-	-	-
	60S	2.49	4.49	4.05	67 %	89 %	22 %
f_{R1}	**M15**	2.11	1.99	2.30	100 %	100 %	-
	20	1.45	-	2.12	-	-	-
	60S	1.26	2.19	2.17	87 %	100 %	13 %
f_{R3}	**M15**	3.02	1.81	3.13	100 %	100 %	-
	20	1.99	-	2.76	-	-	
	60S	1.57	2.93	2.80	79 %	100 %	21 %

Table 39. Evaluation of degradation by temperature of the flexural strengths results of MSFRC-PF2 between 3 and 180 days.

CODE		PF2		Strength retention due to temperature		Difference
		3 Days	180 Days	3 Days	180 Days	
f_{LOP}	M15	6.11	5.21	100 %	100 %	-
	20	3.03	4.45	-	-	-
	60S	2.37	4.23	78 %	95 %	17 %
f_{R1}	M15	1.31	1.47	100 %	91 %	-9 %
	20	1.18	1.61	-	-	-
	60S	0.75	1.39	64 %	86 %	22%
f_{R3}	M15	1.73	2.04	100 %	100 %	-
	20	1.38	1.97	-	-	-
	60S	0.88	1.77	64 %	89 %	25 %

Table 40. Evaluation of degradation by temperature of the flexural strengths results of MSFRC-PF3 between 3 and 180 days.

CODE		PF3		Strength retention due to temperature		Difference
		3 Days	180 Days	3 Days	180 Days	
f_{LOP}	M15	5.11	5.49	100 %	100 %	-
	20	2.76	4.93	-	-	-
	60S	2.58	3.68	93 %	75 %	-18 %
f_{R1}	M15	1.66	2.17	100 %	100 %	-
	20	1.37	1.71	-	-	-
	60S	1.01	1.58	74 %	92 %	18 %
f_{R3}	M15	2.50	3.23	100 %	100 %	-
	20	2.17	2.61	-	-	-
	60S	1.55	2.24	71 %	86 %	15 %

Table 41. Evaluation of degradation by temperature of the flexural strengths results of SFRC-SF between 3 and 180 days.

CODE		SF			Strength retention due to temperature		Difference
		3 Days	90 Days	180 Days	3 Days	180 Days	
f_{LOP}	M15	5.99	4.43	5.99	100 %	100 %	-
	20	2.91	3.65	3.81	-	-	-
	60S	2.80	3.31	4.54	96 %	100 %	4 %
f_{R1}	M15	1.02	2.35	1.77	79 %	100 %	21 %
	20	1.29	1.42	1.58	-	-	-
	60S	0.98	1.56	2.03	76 %	100 %	24 %
f_{R3}	M15	1.25	1.91	1.70	99 %	100 %	1 %
	20	1.26	1.24	1.27	-	-	-
	60S	1.02	1.34	1.78	81 %	100 %	19 %

As can be seen, the results at 180 days are higher than those at 3 days. This is product of the evolution of strengths with age. In terms of time- and thermal-dependent behavior, all the types of tested FRCs behave in the same manner. It can be said also that their aging evaluated by the loss of flexural capability after 180 days was excellent, finding a good post-cracking performance (even strengthening it in most of the situations), which gives increased confidence in the long-term behavior of FRCs exposed to temperatures.

5.2.2. Combined Effect of Pre-cracking and Temperature on Flexural Tensile Strengths at long-term

The combined effect of pre-cracking and temperature on flexural tensile strengths was examined at short-term in Chapter 4. The present Section analyzes the existence of a synergy between these factors and long periods of exposition. To achieve this aim, MSFRC with PF1 fiber and SFRC, exposed to the pre-defined extreme environmental conditions, were studied at the two selected ages (90 and 180 days) after being pre-cracked at ambient temperature at 28 days up to 0.5 mm. Thus, f_{LOP} and f_{R1} results for these pre-cracked specimens were obtained at 20 °C at 28 days and the rest of the residual flexural strengths (f_{R2}, f_{R3} and f_{R4}) were obtained at temperatures at 90 or 180 days.

a) Flexural strength's results after 90 days of exposure

For the pre-cracked specimens at 90 days, the results of the residual flexural strength corresponding with the limit of proportionality (LOP) and CMOD = $CMOD_j$ (j = 1, 2, 3, 4) were tabulated in Table 42 with their corresponding CoVs.

In this case, the results of 3PBTs show in most of the cases less than a 10 % variation for the strengths al LOP and a variation of around 15–35 % for residual flexural strengths. Regarding f_{LOP}, all the values are in the range between 3.35 and 3.83 MPa, which is logical since the specimens (independently of the fiber type) are all tested at 20 °C at 28 days.

Table 42. Results of the f_{LOP} and the residual flexural strengths obtained at defined extreme conditions for pre-cracked specimens after 90 days of exposure.

Code		Tested at 20 °C at 28 days				f_{R2} [MPa]	CoV [%]	f_{R3} [MPa]	CoV [%]	f_{R4} [MPa]	CoV [%]
		f_{LOP} [MPa]	CoV [%]	f_{R1} MPa]	CoV [%]						
PF1-P	M15	3.82	5	1.63	29	2.56	33	2.57	30	2.18	26
	60S	3.72	7	2.13	28	2.74	30	2.86	32	2.79	31
SF-P	M15	3.83	6	1.88	15	2.11	34	1.80	34	1.53	30
	60S	3.35	6	1.23	13	1.40	19	1.33	21	1.21	19

Additionally, Figure 88 shows these results at 90 days for pre-cracked specimens through the stress-CMOD curves obtained by 3PBTs. The mean values of seven specimens for each series are presented with a line, and the envelope (shaded areas) represents the scatter (maximum and minimum values of the tests) in the results. As happened in non-pre-cracked specimens at 90 days, MSFRC presents a hardening behavior under bending loads independent of the tested temperatures and SFRC presents a softening behavior in both conditions (at -15 and 60 °C). The shapes of stress-CMOD curves in these cases are very similar to those obtained in non-pre-cracked beams.

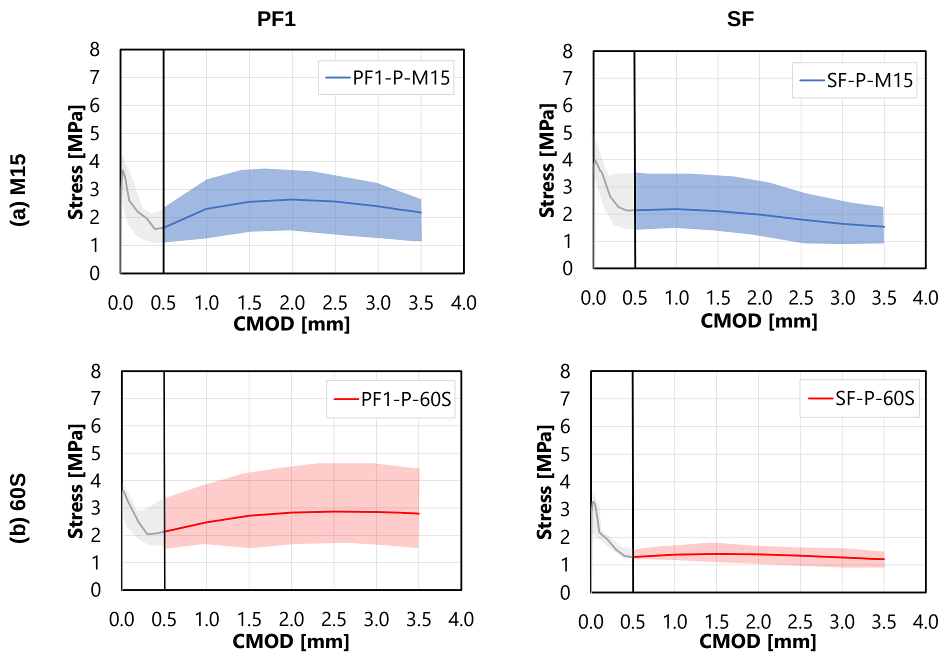

Figure 88. Flexural behavior of MSFRC (with PF1 fibers) and SFRC in pre-cracked specimens after 90 days: (a) at -15 °C and (b) at 60 °C, in water immersion.

To summarize, pre-cracked specimens of MSFRC and SFRC present similar trends in flexure by 3PBTs after 90 days exposure than those non-pre-cracked specimens. In general, at −15 °C, both FRCs experienced an increase in f_{LOP} and the residual flexural strengths of for non-pre-cracked specimens. On the contrary, no significant effects are detected in residuals flexural strengths for both type of FRCs in pre-cracked state. Regarding to the shape of the curve stress-CMOD, MSFRC displays a hardening behavior under bending loads and SFRC presents a softening behavior, as occurs in non-pre-cracked specimens.

b) Flexural strength's results after 180 days of exposure

To see the evolution of the f_{LOP} and the residual flexural strengths with time, all the data for pre-cracked specimens obtained by 3PBTs at 180 days are recompiled in Table 43. f_{LOP} and f_{R1} results for these pre-cracked specimens were obtained at 20 °C at 28 days, equal than in the rest of the studied ages for pre-cracked specimens, so any effects could be detected in these parameters. As it can be seen, the scatter is within the same range than the previously presented results.

Table 43. Results of the f_{LOP} and the residual flexural strengths obtained at defined extreme conditions for pre-cracked specimens after 180 days of exposure.

Code		Tested at 20 °C at 28 days				f_{R2} [MPa]	CoV [%]	f_{R3} [MPa]	CoV [%]	f_{R4} [MPa]	CoV [%]
		f_{LOP} [MPa]	CoV [%]	f_{R1} [MPa]	CoV [%]						
PF1-P	M15	3.75	14	2.07	21	2.89	18	3.17	17	2.80	13
	20	3.19	6	1.95	21	2.62	22	2.80	22	2.93	22
	20S	3.55	6	1.72	23	2.49	23	2.71	23	2.62	23
	60S	3.22	5	1.59	13	1.99	19	2.17	17	2.21	16
SF-P	M15	2.85	4	1.30	23	1.66	25	1.48	25	1.33	26
	20	3.73	4	1.61	23	2.10	24	1.93	23	1.64	25
	20S	3.31	6	1.70	18	1.99	15	1.77	17	1.54	21
	60S	3.49	5	1.67	13	1.85	15	1.60	16	1.39	17

As f_{LOP} values were obtained at 20 °C at 28 days, equivalent results were expected regardless of the fiber type. When these FRCs were design, only a matrix was chosen and the quantity of fibers were selected, keeping in mind the type, to achieve similar strengths in terms of post-cracking behavior. Thus, f_{R1} values may be also considered similar given that the inter-groups variations are insignificant (all the values were obtained at 20 °C at 28 days).

For large CMODs, the obtained residual strengths continue aligned with the results at early ages. Furthermore, these results are displayed by means of the average stress-CMOD curves (based on seven tested specimens for each case) in Figure 89, whereas result scatter (envelope) is represented by a shaded area. At -15 °C, it is possible to distinguish the second flatter peak for both types of FRC that was seen formerly from Figure 82 to Figure 88. In general, MSFRC presents a hardening behavior after the crack and SFRC has a softening behavior but in this case, these trends are less pronounced that those at 90 days nor those in non-pre-cracked specimens.

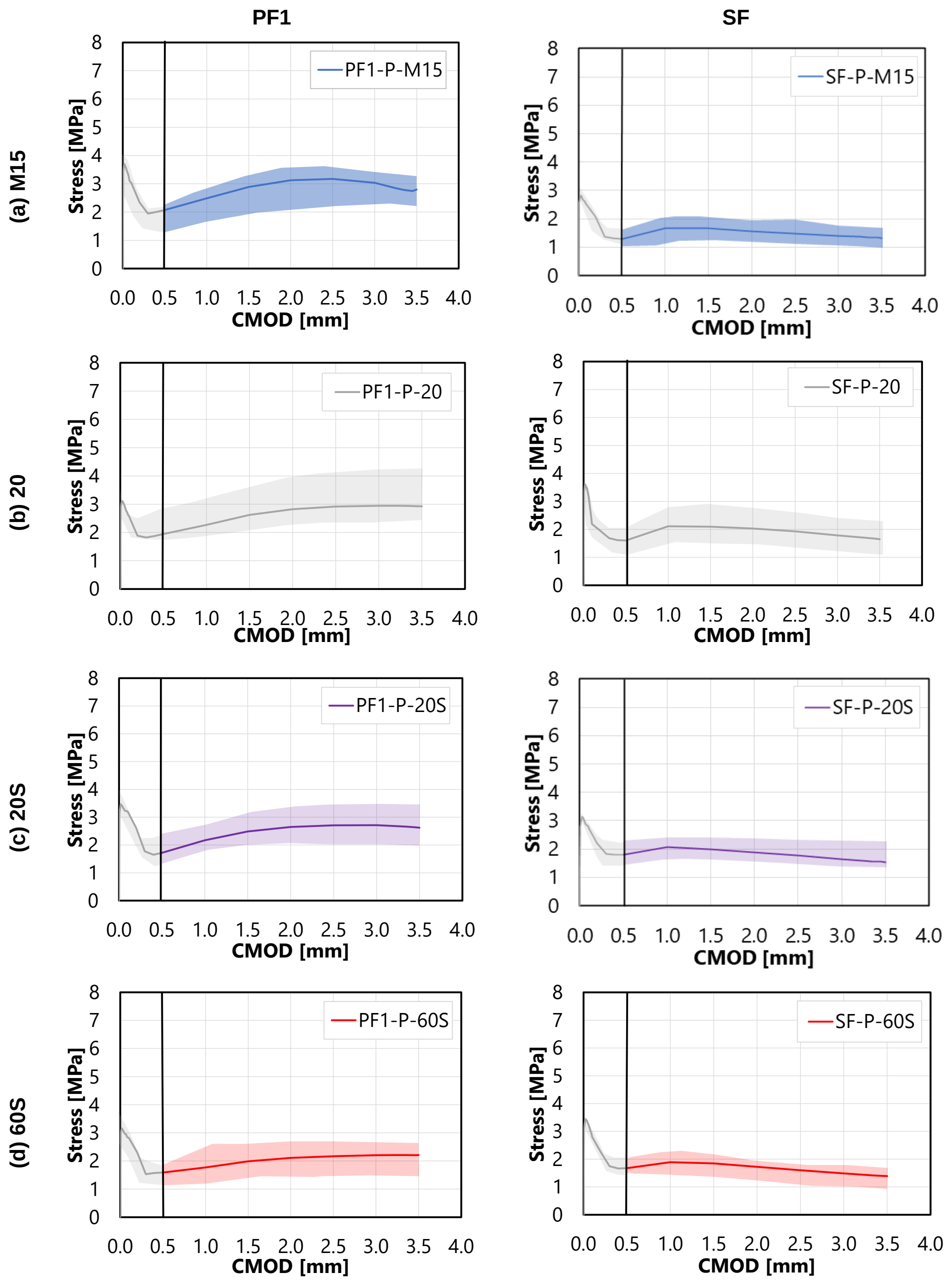

Figure 89. Flexural behavior of MSFRC (with PF1 fibers) and SFRC in pre-cracked specimens after 180 days: (a) at -15 °C; (b) at 20 °C; (c) at 20 °C, in water immersion and (d) at 60 °C, in water immersion.

To summarize, pre-cracked specimens of MSFRC and SFRC present similar trends in flexure by 3PBTs after 180 days exposure than those non-pre-cracked specimens. In general, no significant effects by temperature are detected in residuals flexural strengths for both type of FRCs in pre-cracked state. Regarding to the shape of the curve stress-CMOD, MSFRC displays a hardening behavior under bending loads and SFRC presents a softening behavior, as occurs in non-pre-cracked specimens.

c) Comparison between non-pre-cracked and pre-cracked state bending results under extreme environmental conditions

In this Subsection, a comparative analysis of flexural results under different temperatures to evaluate the impact of pre-cracking state (non-pre-cracked and pre-cracked) at two different time of exposures (90 and 180 days) is conducted. Furthermore, these findings are compared to those obtained after 3 days (as discussed in Chapter 4) to examine the combined effects of temperature and crack conditions over time, particularly focusing on f_{R3}.

Firstly, Figure 90 is presented to contrast the results of non-pre-cracked and pre-cracked beams after 90 days of exposure. It displays the mean stress-CMOD curves obtained from 7 prims for both groups from the 3PBTs performed at the different studied temperatures. Figure 90-a and -b compare the behavior for MSFRC-PF1, and Figure 90-c and -d compare the behavior for SFRC. The left figures show the behavior of non-pre-cracked specimens and the right figures the behavior of pre-cracked specimens. In the latter, the phase of pre-cracking up to 0.5 mm was carried out at 20 °C and is therefore depicted with grey lines. The results indicate that no significant differences can be appreciated between non-pre-cracked and pre-cracked specimens reinforced with PF1 and with SF fibers. The only difference between both states that can be appreciated is the modification of f_{LOP} due to the exposition of temperature. For MSFRC-PF1-N, the values at 20 °C were not considered (to avoid leading to disperse conclusions) since the number of fibers in the section were not contemplated.

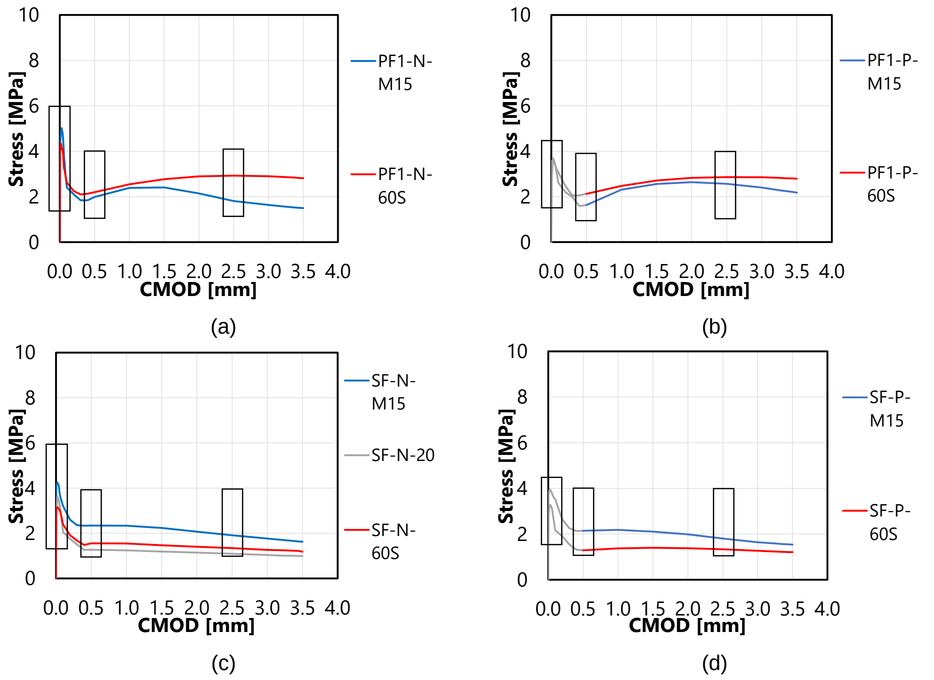

Figure 90. Average stress-CMOD curves of non-pre-cracked and pre-cracked specimens: (a) PF1-N; (b) PF1-P; (c) SF-N and (d) SF-P, after 90 days of exposition at different temperatures.

Secondly, to compare the results of non-pre-cracked and pre-cracked beams after 180 days of exposure, Figure 91 is displayed. Figure 91-a and -b compares the mean stress-CMOD curves for non-pre-cracked and pre-cracked specimens, reinforced with PF1 fibers and Figure 91-c and -d compares the mean stress-CMOD curves for non-pre-cracked and pre-cracked specimens, reinforced with SF fibers, after 180 days of exposure. Both groups show very similar curves. It can be said that temperature effect is less noticeable in SFRC than MSFRC given that the values are less disperse and there is less variation between the curves for each temperature. It can be also affirmed that temperature affects more the results at large crack openings (f_{R3} and f_{R4}) than the results at small crack openings (f_{R2}) in both states equally and have inverse relationship with residual strengths.

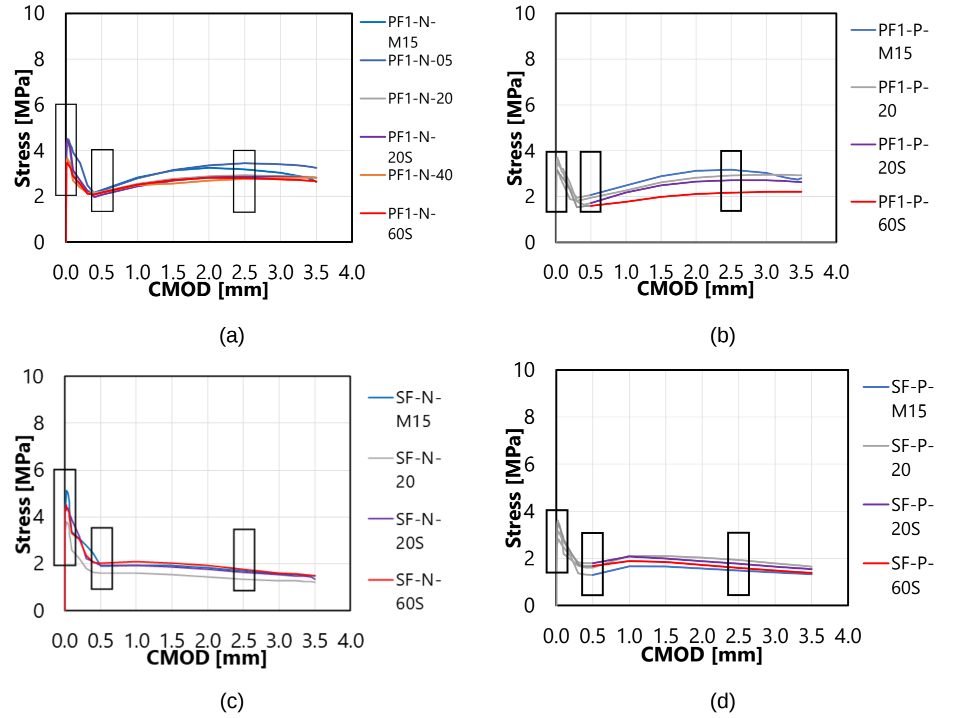

Figure 91. Average stress-CMOD curves of non-pre-cracked and pre-cracked specimens: (a) PF1-N; (b) PF1-P; (c) SF-N and (d) SF-P, after 180 days of exposition at different temperatures.

To conclude, no effects are detected between non-pre-cracked and pre-cracked specimens independently on fiber type and the time of exposure at the defined environmental conditions.

5.2.3. Effect of Number of Fibers on Flexural Tensile Strengths at Extreme Environmental Conditions

The effect of the number of fibers present in the cross-section is also studied in this Subsection. In Chapter 4, the results obtained after short-term exposure to temperatures were affected by the number of fibers in the section, affecting the variability of the values of residual strengths, and showing with more clarity the temperature effect. In this Section, the study of the number of fibers in the cross-section is done to determine how it affects the flexural strengths after long-term of exposure to temperatures. As was explained in Chapter 3, the cross-section was divided in three thirds and the number of fibers at each part was counted manually after the failure of the specimen. The total number of fibers at the cross-section (N) was obtained by adding these partial counts, and in order to take it into account in this analysis, the average value of N was calculated per series.

a) Study of the number of fibers present in the fracture surface

Table 44 and Table 45 collect the mean values of N and their CoVs per series obtained at different ages (90 and 180 days), for non-pre-cracked and pre-cracked specimens, respectively. Additionally, the number of fibers in the lower third, designated as $N_{1/3}$, was also considered to compare both results.

Table 44. Total number of fibers (N) and number of fibers in lower third ($N_{1/3}$) in the fracture surface per series for non-pre-cracked specimens.

Code		**90 Days**				**180 Days**			
		N	**CoV [%]**	**$N_{1/3}$**	**CoV [%]**	**N**	**CoV [%]**	**$N_{1/3}$**	**CoV [%]**
PF1-N	**-15**	91	8	29	14	88	8	27	14
	5					93	5	30	12
	20	140	15	44	28	97	24	33	30
	20S					93	20	29	22
	40					92	15	29	22
	60S	81	9	29	10	88	16	28	28
PF2-N	**-15**					73	15	24	24
	20					83	13	26	27
						79	10	25	15
	60S					72	16	22	21
PF3-N	**-15**					111	8	40	16
	20					119	17	43	15
						109	8	33	13
	60S					106	15	31	25
SF-N	**-15**	48	15	15	27	52	10	14	24
	20	44	22	13	32	50	7	17	34
	20S					47	24	16	32
	60S	50	15	13	32	48	17	18	23

Table 45. Total number of fibers (N) and number of fibers in lower third ($N_{1/3}$) in the fracture surface per series for pre-cracked specimens.

Code		90 Days				180 Days			
		N	CoV [%]	$N_{1/3}$	CoV [%]	N	CoV [%]	$N_{1/3}$	CoV [%]
PF1-P	-15	88	14	27	23	88	8	27	14
	20					96	11	32	13
	20S					83	12	31	8
	60S	90	17	30	33	87	12	23	19
SF-P	-15	47	11	16	18	48	16	14	31
	20					48	18	16	21
	20S					48	10	17	7
	60S	48	16	15	14	42	19	14	30

From these tables, it can be extracted that the mean experimental distribution of fibers in 504 fracture surfaces (including the specimens tested at 90 and 180 days), with dimensions of 150 × 125 mm², is 95 of MSFRC (with PF1, PF2 and PF3) and 48 of SFRC (with SF), produced with 7 kg/m³ and 21 kg /m³ respectively. The number of fibers obtained at 90 and 180 days is similar, and they are also in the line with the number of fibers obtained at short-term (3 days). In general, the number of fibers at the fracture surface is notably different between steel and PP fibers. It is also important to note that there is a great difference between the number of fibers among the different macro synthetic fibers, since this factor does not depend only on the raw material of the fiber (regarding to the % vol.), but on many factors, as aspect ratio, shape, etc. Additionally, as was commented in the Subsection 5.2.1, the values of residual strengths for PF1-N specimens at 20 °C (PF1-N-20) at 90 days could be explained by a much higher value of N (140) than the average (see Table 44).

Furthermore, Figure 92 depicts the total number of fibers at the generated cross-sections within an interval (including both sides, without distinguishing between broken or slippage) versus the number of events, that is the number of times that a beam has a specific total number of fibers in that interval. The distribution for PF1 fibers at 90 days resulted in a non-normal dispersion of the fibers into the matrix, specifically in non-pre-cracked specimens that justifies the obtained results at 20 °C in residual flexural strengths (see Table 36).

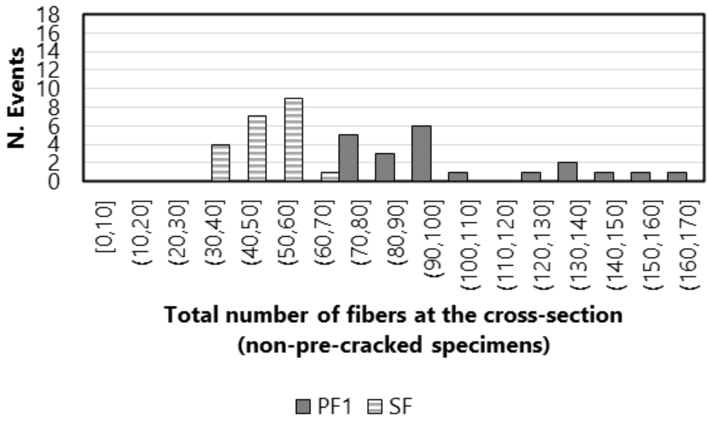

(a)

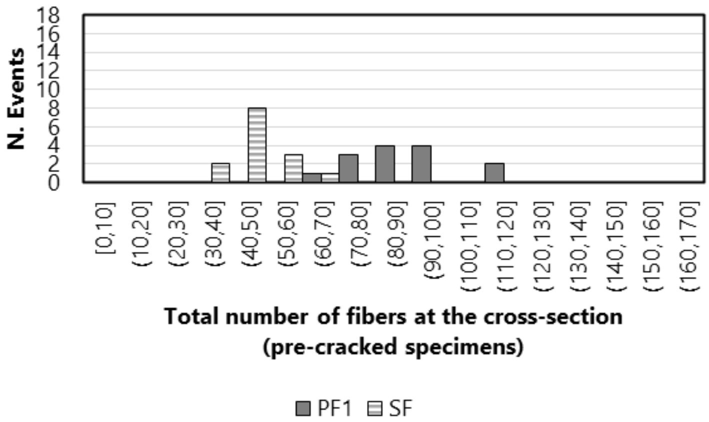

(b)

Figure 92. The total number of fibers at the cross-section for each type of fiber according to the number of events (N. Events) for (a) non-pre cracked specimens and (b) for pre-cracked specimens at 90 days.

Figure 93 represents the results of the fiber analysis at 180 days following the same methodology. In Figure 93-a, for non-pre-cracked specimens and in Figure 93-b, for pre-cracked specimens. Again, the results show that the number of fibers present in the cross-section of MSFRC specimens was higher than that of SFRC specimens, and differences were also detected between the different types of macro synthetic fibers selected. These results were similar to those obtained at short-term and the distribution of fibers in both states was similar and followed a normal distribution (with some skewness in some series).

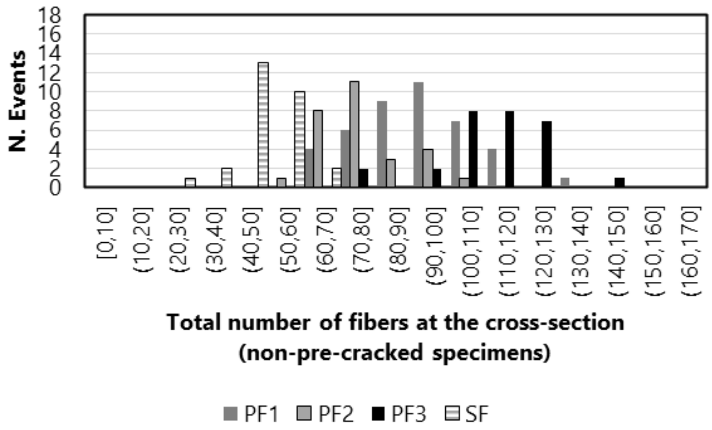

(a)

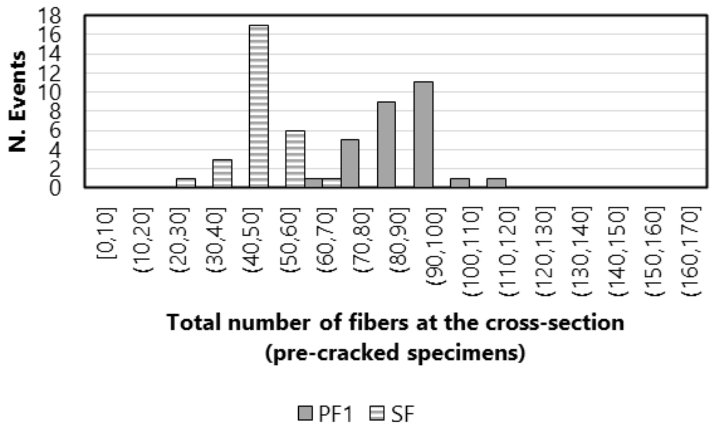

(b)

Figure 93. The total number of fibers at the cross-section for each type of fiber according to the number of events (N. Events) for (a) non-pre cracked specimens and (b) pre-cracked specimens at 180 days.

As was explained in Chapter 4, a better correlation was found between the total number of fibers (N) with f_{R1} and f_{R3} instead of $N_{1/3}$. Thus, N was selected as parameter to normalize the results of residual flexural strengths at long-term (at 90 days as well as 180 days).

b) Flexural strength's results considering N after 90 days of exposure

After that, the ratios f_{R1}/N and f_{R3}/N were calculated for the 90 days' results. The results obtained are depicted in Figure 94. Figure 94-a represents f_{R1}/N of non-pre-cracked beams. Results of f_{R1}/N of non-pre-cracked beams at 20 °C were not included in this Subsection because they were considered to not be reliable, for the reasons given previously (non-homogeneous distribution of fibers, the number of fibers, etc.). Figure 94-b shows f_{R3}/N of non-pre-cracked beams at temperature and Figure 95 represents f_{R3}/N of pre-cracked beams at temperature. f_{R1}/N of pre-cracked beams was not represented because pre-cracking was performed at 20 °C at 28 days, thus the influence of temperature cannot be detected.

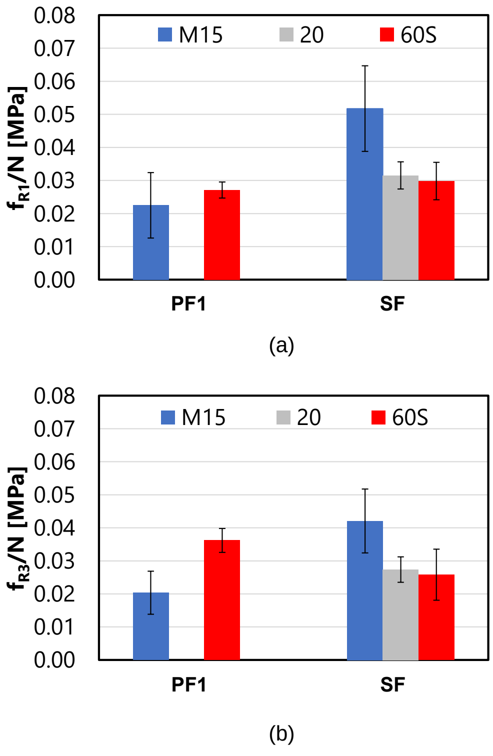

Figure 94. Normalized residual flexural strength f_{R1} and f_{R3} after long-term exposure (90 days) at the target environmental conditions: (a) f_{R1} /N for non-pre-cracked specimens; and (b) f_{R3}/N for non-pre-cracked specimens.

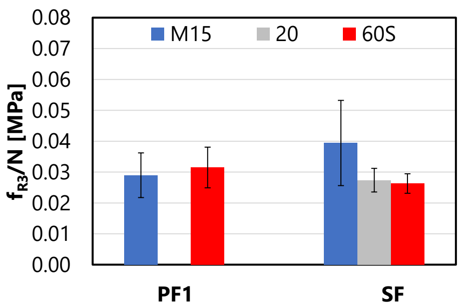

Figure 95. Normalized residual flexural strength f_{R3}/N for pre-cracked specimens.

The results for small CMOD (0.5 mm) follow different trends for MSFRC-PF1 and SFRC-SF. Temperature did not affect f_{R1}/N for MSFRC since the obtained results are constant for all the temperatures. However, SFRC experienced an increase when exposed to -15 °C (almost the double), coupled with an increased brittleness (sudden cracking during 3PBT). The results for large CMOD (2.5 mm), f_{R3}/N, present similar behavior to f_{R1}/N in non-pre-cracked and pre-cracked specimens reinforced with PF1 and SF respectively, after 90 days of temperature exposure. Furthermore, the interaction between temperature and pre-cracking was studied for CMOD = 2.5 mm.

The results of non-pre-cracked and pre-cracked SF specimens show an increase due to low temperatures, which is consistent with previous results and the literature. However, beams reinforced with PP fibers show comparable values in f_{R3} for low temperatures to those obtained at 60 °C or even a slight reduction for non-pre-cracked elements. At 60 °C, no significant variations are detected for both types of FRCs and both conditions (NP and P). These results were not expected for MSFRC since high temperatures are reported to affect the PP fiber's behavior. The pre-cracking state seems not to affect the behavior of the different types of FRCs studied.

Considering N in the analysis of these results, the tendency of the effect of temperature is seen less prominent in the range from 20 to 60 °C for both types of FRCs. For low temperature, the positive effect detected at short-term is maintained also herein for SFRC and it is not so prominent for MSFRC.

c) Flexural strength's results considering N after 180 days of exposure

In turn, the ratios f_{R1}/N and f_{R3}/N were calculated for the 180 days' results. The results obtained are depicted in Figure 96 and Figure 97. This figure shows the average results and the variation of f_{R1}/N and f_{R3}/N, for non-pre-cracked and pre-cracked beams with PP and SF fibers, tested at the temperatures of –15, 5, 20, 40 and 60 °C. Figure 96-a represents f_{R1}/N of non-pre-cracked beams. Figure 96-b shows f_{R3}/N of non-pre-cracked beams and Figure 97 represents f_{R3}/N of pre-cracked beams. The color code is maintained for each temperature tested.

For f_{R1}/N values, for MSFRCs, the results are stable independently of temperature and type of macro synthetic fiber used (PF1, PF2 or PF3). However, a slightly negative trend is detected with temperature in f_{R3}/N. This trend is more noticeable in larger CMOD residual flexural strengths for non-pre-cracked specimens. This variation could be explained by the changes in the bond fiber-matrix, and the variability of the tests.

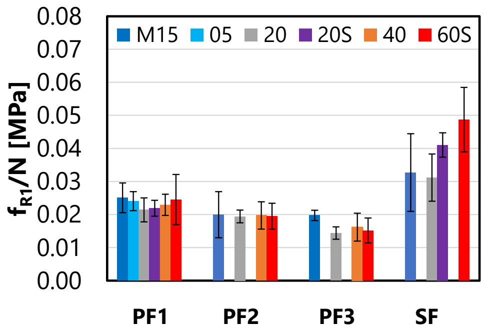

(a)

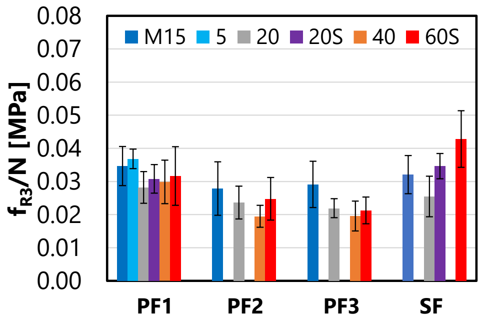

(b)

Figure 96. Normalized residual flexural strength f_{R1} and f_{R3} after long-term exposure (180 days) at the target environmental conditions: (a) f_{R1} /N for non-pre-cracked specimens; and (b) f_{R3}/N for non-pre-cracked specimens.

For f_{R1}/N values, for SFRC, the results are in the same range of variation for all the tested temperatures with a positive trend with temperature. This result could be explained by the high scatter for these parameters. The two parameters,

f_{R1} /N and f_{R3}/N, present similar enhancements in the range between 20 and 60 °C for non-pre-cracked specimens. However, this increment is not evidenced in pre-cracked specimens.

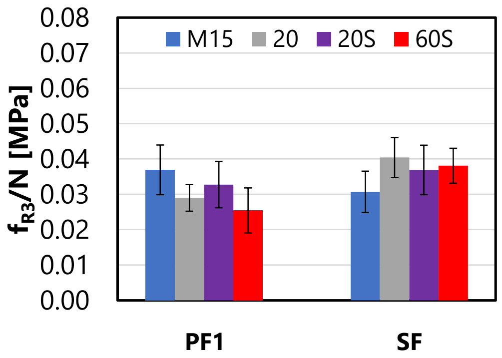

Figure 97. Normalized residual flexural strength f_{R3}/N for pre-cracked specimens.

Moreover, Figure 96-b and Figure 97 allow to compare the flexural behavior at large CMOD (2.5 mm) for non-pre-cracked and pre-cracked specimens. As can be seen, the effect of the interaction between temperature and state is not detrimental for the mechanical performance of these FRCs, as was seen in Subsection 5.2.2.c. For MSFRC, the slight negative trend is maintained with temperature, independently on the state, and for SFRC, the values present a slightly positive trend for P than for NP specimens, but for both states, but there is not a significant difference.

In conclusion, for residual strengths normalized by N and the variations detected the tested MSFRCs can reach similar structural reliability level compared to SFRC elements under these environmental conditions after being exposed during these range of time. In this case, temperature effect is less noticeable if N is considered but it can be seen, in general terms, that at low temperatures, a positive effect of temperature on residual flexural strengths is detected, together with a more brittleness behavior. Contrarily, the effect of moderate-high temperature is not as influential as expected. Lastly, the effect of pre-cracking does not affect the behavior of FRC exposed to temperatures at long-term.

d) Analysis of aging: comparison between short- and long-term residual flexural results (considering N) under extreme environmental conditions

In this Subsection, a study of the evolution of residual strength over time is done per temperature and fiber type, as well as an analysis of aging, similar to that done in Subsection 5.2.1.c. Both studies are carried out for residual flexural strengths normalized by N.

Firstly, the results of f_{R1}/N and f_{R3}/N at long-term (after 90 and 180 days of exposure) are compared with the results obtained at short-term (after 3 days of exposure) to see their evolution through time, for a level of temperature. From Table 46 to Table 49, the results for these parameters at -15 °C are collected for each type of fiber: PF1, PF2, PF3 and SF respectively. Results shaded in grey were obtained at 20 °C at 28 days, according to the methodology used. Some values of CoV are in red since they are higher than expected (this could be explained by the variability of the test itself). This occurred more frequently in f_{R1} values because of the brittleness that experienced some specimens.

As can be seen, all the data are in the range between 0.02 and 0.05 MPa and there is not a great difference between the results for non-pre-cracked (NP) and pre-cracked (P) specimens. In terms of time- and thermal-dependent behavior, all the types of tested FRCs behave in the same manner. The effect of temperature is more notable for large CMODs. Regarding to aging by temperature, the results at 180 days are higher than those at 3 days. This could be product of the evolution of strengths with age. It can be said the evolution is excellent since a good post-cracking performance is found over time (the results were strengthened in all the situations after 180 days). In spite of these results at long-term, it is important to keep in mind the more brittle behavior of FRCs at low temperatures (-15 °C).

Table 46. Comparison of the average residual strengths results of MSFRC-PF1 at 3, 90 and 180 days at -15 °C.

Code	PF1											
	3 Days				90 Days				180 Days			
	P		NP		P		NP		P		NP	
	MPa	CoV [%]	MPa	CoV [%]	MPa	CoV [%]	MPa	CoV [%]	MPa	CoV [%]	MPa	CoV [%]
f_{R1}/N	0.02	16	0.02	33	0.02	24	0.02	44	0.02	22	0.03	18
f_{R3}/N	0.03	28	0.03	26	0.03	25	0.02	32	0.04	19	0.04	17

Table 47. Comparison of the average of the residual strengths results of MSFRC-PF2 at 3 and 180 days at -15 °C.

Code	PF2							
	3 Days				180 Days			
	P		NP		P		NP	
	MPa	CoV [%]	MPa	CoV [%]	MPa	CoV [%]	MPa	CoV [%]
f_{R1}/N	---	---	0.02	35	---	---	0.02	18
f_{R3}/N	---	---	0.02	29	---	---	0.03	23

Table 48. Comparison of the average of the residual strengths results of MSFRC-PF3 at 3 and 180 days at -15 °C.

Code	PF3							
	3 Days				180 Days			
	P		NP		P		NP	
	MPa	CoV [%]	MPa	CoV [%]	MPa	CoV [%]	MPa	CoV [%]
f_{R1}/N	---	---	0.02	8	---	---	0.02	20
f_{R3}/N	---	---	0.02	24	---	---	0.03	15

Table 49. Comparison of the average of the residual strengths results of SFRC-SF at 3, 90 and 180 days at -15 °C.

Code	SF											
	3 Days				90 Days				180 Days			
	P		NP		P		NP		P		NP	
	MPa	CoV [%]	MPa	CoV [%]	MPa	CoV [%]	MPa	CoV [%]	MPa	CoV [%]	MPa	CoV [%]
f_{R1}/N	0.03	35	0.02	46	0.04	11	0.05	25	0.03	25	0.03	36
f_{R3}/N	0.03	39	0.03	17	0.04	35	0.04	23	0.03	19	0.03	18

Furthermore, Figure 98 shows graphically the evolution of f_{R1}/N and f_{R3}/N of the different FRCs and state over time, at -15 °C. In this case, to see the tendency, only the results at 3 and 180 days were represented. No degradation is noted in these properties with the age and temperature. Additionally, it is not possible to detect any effect of the state (pre-cracking) on the behavior of MSFRC and SFRC.

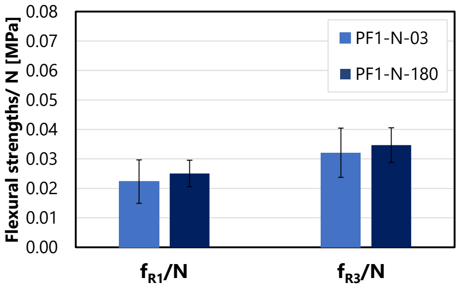

(a)

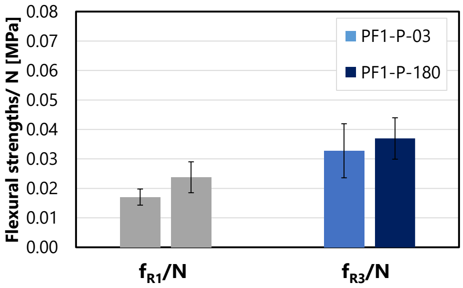

(b)

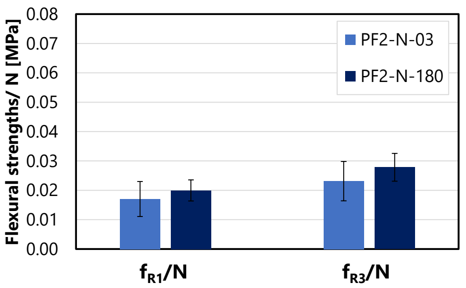

(c)

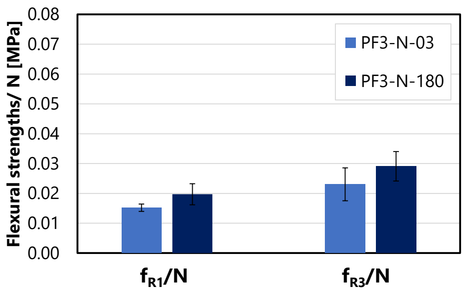

(d)

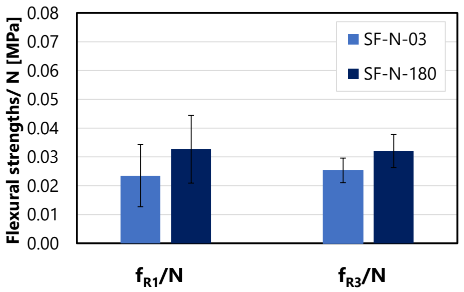

(e)

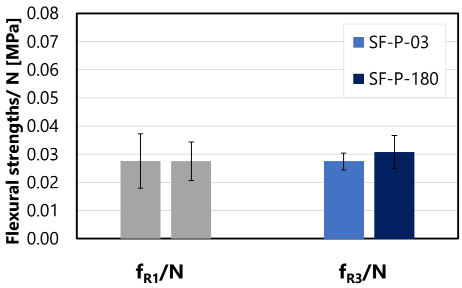

(f)

Figure 98. Evolution of residual strengths of the different types of FRCs studied at -15 °C: (a) MSFRC-PF1 in non-pre-cracked specimens; (b) MSFRC-PF1 in pre-cracked specimens; (c) MSFRC-PF2 in non-pre-cracked specimens; (d) MSFRC-PF3 in non-pre-cracked specimens; (e) SFRC-SF in non-pre-cracked specimens and (f) SFRC-SF in pre-cracked specimens.

Additionally, the average results of the residual flexural strengths divided by N at short- and long-term for each type of FRCs at the standard temperature, for both states, are tabled from Table 50 to Table 53. The results marked in grey were obtained at 28 days in the pre-cracking phase, after curing. All the obtained data are included into the range of 0.02 and 0.04 MPa. The results presented less dispersion than those at -15 °C.

Table 50. Comparison of the average of the residual strengths results of MSFRC-PF1 at 3, 90 and 180 days at 20 °C.

Code	PF1											
	3 Days				90 Days				180 Days			
	P		NP		P		NP		P		NP	
	MPa	CoV [%]	MPa	CoV [%]	MPa	CoV [%]	MPa	CoV [%]	MPa	CoV [%]	MPa	CoV [%]
f_{R1}/N	0.02	30	0.02	35	---	---	0.02	15	0.02	17	0.02	17
f_{R3}/N	0.03	39	0.03	11	---	---	0.03	14	0.03	13	0.03	17

Table 51. Comparison of the average of the residual strengths results of MSFRC-PF2 at 3 and 180 days at 20 °C.

Code	PF2							
	3 Days				180 Days			
	P		NP		P		NP	
	MPa	CoV [%]	MPa	CoV [%]	MPa	CoV [%]	MPa	CoV [%]
f_{R1}/N	---	---	0.02	16	---	---	0.02	13
f_{R3}/N	---	---	0.02	21	---	---	0.02	21

Table 52. Comparison of the average of the residual strengths results of MSFRC-PF3 at 3 and 180 days at 20 °C.

Code	PF3							
	3 Days				180 Days			
	P		NP		P		NP	
	MPa	CoV [%]	MPa	CoV [%]	MPa	CoV [%]	MPa	CoV [%]
f_{R1}/N	---	---	0.01	19	---	---	0.01	10
f_{R3}/N	---	---	0.02	20	---	---	0.02	12

Table 53. Comparison of the average of the residual strengths results of SFRC-SF at 3, 90 and 180 days at 20 °C.

Code	SF											
	3 Days				90 Days				180 Days			
	P		NP		P		NP		P		NP	
	MPa	CoV [%]	MPa	CoV [%]	MPa	CoV [%]	MPa	CoV [%]	MPa	CoV [%]	MPa	CoV [%]
f_{R1}/N	0.02	15	0.03	3	---	---	0.03	13	0.03	19	0.03	23
f_{R3}/N	0.02	17	0.03	14	---	---	0.03	14	0.04	14	0.03	24

Figure 99 represents these results. The only effect evaluated on the residual flexural strengths is the time of exposure, since all the data were obtained at the standard temperature of 20 °C.

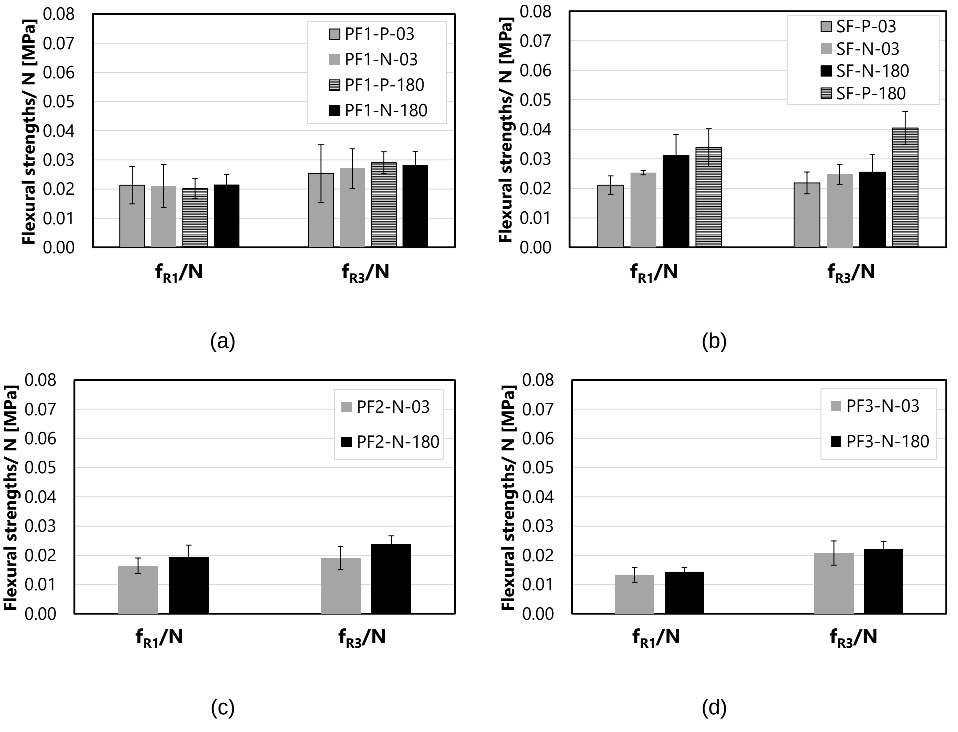

Figure 99. Evolution of residual strengths of the different types of FRCs studied at 20 °C: (a) MSFRC-PF1 specimens; (b) SFRC-SF specimens; (c) MSFRC-PF2 in non-pre-cracked specimens, and (d) MSFRC-PF3 in non-pre-cracked specimens.

The strengthening observed is given typically by the maturation of concrete-matrix over time. The notable increase for SF-P at 180 days is like to be product of a scatter in the casting procedure plus the internal variability in these experimental tests.

The average results of f_{R1}/N and f_{R3}/N after 3, 90 and 180 days at 60 °C in immersion, for each type of FRCs, are collected from Table 54 to Table 57. In this case, the CoVs of all the cases are more stable than for the rest of temperatures. All the results range from 0.01 to 0.04 MPa. Evaluating the aging by temperature, it can be said that specimens exposed to moderate high permanent temperature (60 °C, submerged) over the time (3 or 6 months) do not present a detrimental effect on their behavior. Furthermore, the state (non-pre-cracked or pre-cracked) had no detectable influence on the mechanical properties and overall performance of the studied FRCs.

Table 54. Comparison of the average of the residual strengths results of MSFRC-PF1 at 3, 90 and 180 days at 60 °C, in immersion.

Code	PF1											
	3 Days				90 Days				180 Days			
	P		NP		P		NP		P		NP	
	MPa	CoV [%]	MPa	CoV [%]	MPa	CoV [%]	MPa	CoV [%]	MPa	CoV [%]	MPa	CoV [%]
f_{R1}/N	0.02	15	0.01	19	0.02	18	0.03	9	0.02	21	0.03	15
f_{R3}/N	0.02	18	0.02	23	0.03	21	0.04	10	0.03	25	0.03	11

Table 55. Comparison of the average of the residual strengths results of MSFRC-PF2 at 3 and 180 days at 60 °C, in immersion.

Code	PF2							
	3 Days				180 Days			
	P		NP		P		NP	
	MPa	CoV [%]	MPa	CoV [%]	MPa	CoV [%]	MPa	CoV [%]
f_{R1}/N	---	---	0.01	20	---	---	0.02	17
f_{R3}/N	---	---	0.01	26	---	---	0.03	17

Table 56. Comparison of the average of the residual strengths results of MSFRC-PF3 at 3 and 180 days at 60 °C, in immersion.

Code	PF3							
	3 Days				180 Days			
	P		NP		P		NP	
	MPa	CoV [%]	MPa	CoV [%]	MPa	CoV [%]	MPa	CoV [%]
f_{R1}/N	---	---	0.01	25	---	---	0.02	24
f_{R3}/N	---	---	0.01	19	---	---	0.02	20

Table 57. Comparison of the average of the residual strengths results of SFRC-SF at 3, 90 and 180 days at 60 °C, in immersion.

Code	SF											
	3 Days				90 Days				180 Days			
	P		NP		P		NP		P		NP	
	MPa	CoV [%]	MPa	CoV [%]	MPa	CoV [%]	MPa	CoV [%]	MPa	CoV [%]	MPa	CoV [%]
f_{R1}/N	0.03	17	0.02	29	0.03	16	0.03	25	0.04	16	0.05	20
f_{R3}/N	0.02	19	0.02	8	0.03	12	0.03	27	0.04	13	0.04	20

Figure 100-a and Figure 100-b represent the mean results of f_{R1}/N and f_{R3}/N for MSFRC-PF1 in non-pre-cracked and pre-cracked state, respectively. At long-term, all the strengths presented similar enhancements compared to the strengths at short-term. This incremented could be experienced by the combined effect of time and high temperature. The same trends are observed for all the FRCs, in all the states (see Figure 100-c, Figure 100-d, Figure 100-e and Figure 100-f). The increase for SF-P at 180 days is product of a scatter in the casting procedure plus the internal variability in these experimental tests.

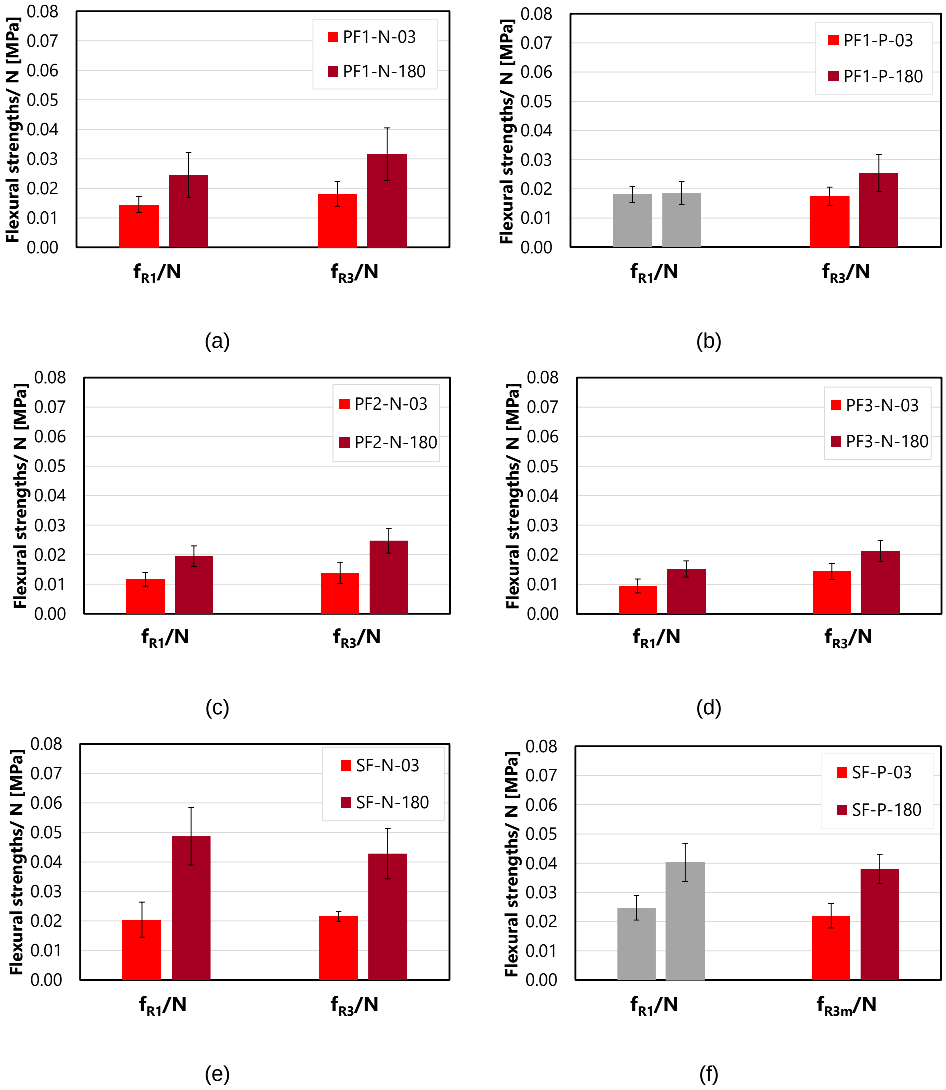

Figure 100. Evolution of residual strengths of the different types of FRCs studied at 60 °C, in immersion: (a) MSFRC-PF1 in non-pre-cracked specimens; (b) MSFRC-PF1 in pre-cracked specimens; (c) MSFRC-PF2 in non-pre-cracked specimens; (d) MSFRC-PF3 in non-pre-cracked specimens; (e) SFRC-SF in non-pre-cracked specimens and (f) SFRC-SF in pre-cracked specimens.

Secondly, the evaluation of the material's capacity to retain f_{R1}/N and f_{R3}/N after being subjected to -15 and 60 °C, comparing with 20 °C, and through time (from 3 to 180 days of exposure) is performed. From Table 58 to Table 63, these results are collected for each type of fiber. Values of CoV are not included to simplify the comparison. To analyze in detail the capacity to sustain their strengths, the percentage of flexural strength retention, explained previously, were calculated for 3 and 180 days. Comparing both percentages (difference), it is possible to discern the effect of temperature with aging. It is important to point out that when the strength under the defined temperature after the period of time is higher than the reference at this age, the strength retention is blocked on 100 %. For all the cases, the results improve with time, except for SF-P (as explained previously).

Table 58. Evaluation of degradation by temperature of the normalized residual strengths results of MSFRC-PF1 between 3 and 180 days in non-pre-cracked state.

Code		PF1			Strength retention due to temperature		Difference
		3 Days	90 Days	180 Days	3 Days	180 Days	
f_{R1} /N	M15	0.022	0.022	0.025	100 %	100 %	-
	20	0.021	0.023	0.021	-	-	-
	60S	0.014	0.027	0.025	67 %	100 %	33 %
f_{R3} /N	M15	0.032	0.020	0.035	100 %	100 %	-
	20	0.025	0.032	0.028	-	-	-
	60S	0.018	0.036	0.032	72 %	100 %	28 %

Table 59. Evaluation of degradation by temperature of the normalized residual strengths results of MSFRC-PF1 between 3 and 180 days in pre-cracked.

Code		PF1			Strength retention due to temperature		Difference
		3 Days	90 Days	180 Days	3 Days	180 Days	
f_{R3} /N	M15	0.033	0.029	0.037	100 %	100 %	-
	20	0.030	-	0.029	-	-	-
	60S	0.017	0.031	0.025	57 %	86 %	30 %

Table 60. Evaluation of degradation by temperature of the normalized residual strengths results of MSFRC-PF2 between 3 and 180 days in non-pre-cracked state.

Code		PF2		Strength retention due to temperature		Difference
		3 Days	180 Days	3 Days	180 Days	
f_{R1} /N	M15	0.017	0.020	100 %	100 %	-
	20	0.016	0.019	-	-	-
	60S	0.012	0.019	75 %	100 %	25 %
f_{R3} /N	M15	0.023	0.028	100 %	100 %	-
	20	0.019	0.024	-	-	-
	60S	0.014	0.025	74 %	100 %	26 %

Table 61. Evaluation of degradation by temperature of the normalized residual strengths results of MSFRC-PF3 between 3 and 180 days in non-pre-cracked state.

Code		PF3		Strength retention due to temperature		Difference
		3 Days	180 Days	3 Days	180 Days	
f_{R1} /N	M15	0.015	0.020	100 %	100 %	-
	20	0.013	0.014	-	-	-
	60S	0.009	0.015	69 %	100 %	31 %
f_{R3} /N	M15	0.023	0.029	100 %	100 %	-
	20	0.021	0.022	-	-	-
	60S	0.014	0.021	67 %	95 %	29 %

Table 62. Evaluation of degradation by temperature of the normalized residual strengths results of SFRC-SF between 3 and 180 days in non-pre-cracked state.

Code		SF			Strength retention due to temperature		Difference
		3 Days	90 Days	180 Days	3 Days	180 Days	
f_{R1} /N	M15	0.023	0.052	0.033	92 %	100 %	8 %
	20	0.025	0.032	0.031	-	-	-
	60S	0.014	0.027	0.025	56 %	81 %	25 %
f_{R3} /N	M15	0.029	0.042	0.032	100 %	100 %	-
	20	0.025	0.027	0.025	-	-	-
	60S	0.018	0.036	0.032	100 %	95 %	-5 %

Table 63. Evaluation of degradation by temperature of the normalized residual strengths results of SFRC-SF between 3 and 180 days in pre-cracked state.

Code		SF			Strength retention due to temperature		Difference
		3 Days	**90 Days**	**180 Days**	**3 Days**	**180 Days**	
f_{R3} /N	**M15**	0.027	0.039	0.031	100 %	78 %	-22 %
	20	0.020	-	0.040	-	-	-
	60S	0.022	0.026	0.038	100 %	95 %	-5 %

To sum up, the described outcomes reveal the enhanced performance of the given FRCs in terms of post-cracking flexural strengths over time—therefore, it can be said that the aging was excellent, presenting a good overall performance.

5.3. General Discussion

In this Chapter 5, the behavior of MSFRCs and SFRC under the defined environmental conditions at long-term exposure have been comprehensively examined and discussed in terms of material level, including compressive strengths and flexural strengths. An evaluation regarding to the aging is also done.

5.3.1. Compressive Behavior

Long-term exposure to temperatures affects this mechanical property of FRCs, as a consequence of a matrix effect. At temperatures below zero, it led to a significant enhancement in both SFRC and MSFRC, but also more brittleness. At moderate high temperatures, a decrease is detected compared to 20 °C. The results are in line with the obtained by Mi et al. [154], who found similar compressive strengths after 28 days for different temperatures (20, 50 and 80 °C). Also, the results side with other studies carried out at temperatures below 0 by [148]. In general, the effect of high temperatures is less notable than the effect at low temperature for all the FRC types and ages.

The results on compression tests at long-term (at 90 and at 180 days) were also evaluated and, compared with results for these FRCs obtained at short-term (after 3 days of exposition, see Chapter 4). It can be seen that there is an increment of a ~ 10 MPa on compressive strengths regarding the age (from 3 to 180 days of exposure). It seems to indicate that the variation is due to the maturation and normal acquisition of strengths (around 20 % in average). According to several authors [181], this improvement is due to a strengthening of the interfacial transition zone (ITZ) which is related to the exposition condition and age, given that more new hydration products are accumulated as the age was prolonged.

However, it was observed herein that the increase of temperature (up to 60 °C) implies a negative influence on compression which counteracts the expected improvement in strength with age, resulting in no significant variation with time and temperature. For low temperature (until -15 °C), the synergy of age and temperature implies a enhance on compressive strengths. It can be also seen that the trend is similar for all the FRC studied and it can be concluded that a good retention of compressive strength is reached for the studied environmental conditions over the estimated time.

Additionally, it is also important to point out that the humidity is not relevant at long-term since the values obtained under 20 and 20S environmental conditions, are very similar. This result is in line with those obtained at short-term. The evidence about the effect of humidity in literature is not clear.

5.3.2. Flexural Behavior

Flexural behavior for all the specimens is analyzed and discussed in this Subsection.

Regarding the flexural strengths at peak-load, the effect of temperature on the matrix is prevalent. f_{LOP} decreases with increasing temperature, and vice versa, as happened at short-term. In view of the preceding discussion about the results of compression at different temperatures, the values of f_{LOP} were expected and follow the same trend, due to this property depends on the matrix and hence, compressive strengths. This effect was also identified in [201]. Additionally, if comparing the results for air and immersion conditions, the effect of temperature does not seem to be further aggravated by humidity in the strength at LOP. This was not in line with the results obtained by [180].

A similar relationship is observed and may be established for the residual strengths (f_{R1} and f_{R3}) affected by the environmental conditions but in a minor extent than values at LOP. At low temperatures (below 0°C), the strengths increase. Some authors attributed the positive effect of low temperature due to the better bond achieved by the concrete contraction (i.e., the cavities embedding the fibers shrink and frictional bond increases due to confinement effects) as well as due to the increase of both Young's modulus and tenacity of the fibers [162]. As Bazant and Prat [230] suggested, the fracture toughness of brittle materials, as concrete, is known to decrease when temperature increases. In the temperature range from 0 to 20 °C, same values for residual strengths are observed. For temperatures over 20°C, the strengths decrease in a smaller variation than they experimented when are exposed at low temperatures. This can be explained, according with [222], by the thermal expansion of the matrix around the fiber which leading to a reduction of fiber-matrix bond, together with decrease of the mechanical properties of the surrounding matrix. Furthermore, the mechanical and physical properties of concrete measured under saturation conditions are larger than that of concrete under realistic circumstances [1]. However, these results are in line with the results obtained for these concrete and conditions after 3 days.

Based on the literature, there is scarce information of the flexural behavior of FRCs, especially MSFRCs, under long-term extreme environmental conditions and they are not in agreement. For instance, Caballero-Jorna et al. [167] investigated the effect of temperatures from 5 up to 50 °C on the flexural strengths of MSFRC and SFRC in reduced-size beams (100 × 100 × 500 mm) after 60 days of exposition. The tests were performed at the target moderate temperatures in non-pre-cracked and in pre-cracked specimens. The findings suggested that these temperatures did not affect in a great extent the performance of the FRC tested. However, Buratti et al. [176] presented the experimental results of long-term behavior on cracked MSFRC (with polypropylene fibers) elements at different temperatures. Long-term behavior was evaluated by four-point bending tests at increasing temperatures (20–50 °C). The increase of temperature had a significant effect on long-term deformations, producing in some cases, creep failure.

This lack of consensus generates, in part, mistrust in their use, limiting their application in structural design. Current structural design of FRC elements is based on f_{R1} and f_{R3}, as was described previously. Focusing on these values, an analysis of the flexural results obtained in this Thesis has been conducted to assess the performance of FRCs under investigation at both 90 and 180 days. It can be said that the studied SFRC could be classified as 1.0-2.5 (a or b) and MSFRCs as 2.0-3.5 (a or b) in function of temperature, according to the fib Model Code 2010 [24] (see Table 64 and Table 65). Regarding the requirements to FRC be considered as structural, all the cases fulfilled both conditions after 90 days of exposure.

Table 64. Verification of compliance with the structural requirements for the studied FRCs after 90 days of exposure.

Requirements		T [°C]	PF1-N	SF-N
f_{R3}/f_{R1}	>0.5	-15	0.9	0.8
f_{R1}/f_{LOP}	>0.4		0.4	0.5
f_{R3}/f_{R1}	>0.5	20	1.6	0.9
f_{R1}/f_{LOP}	>0.4		0.8	0.4
f_{R3}/f_{R1}	>0.5	60S	1.3	0.9
f_{R1}/f_{LOP}	>0.4		0.5	0.5

Additionally, the verification of compliance with the structural requirements for the studied FRCs after 180 days of exposure is also analyzed.

Table 65. Verification of compliance with the structural requirements for the studied FRCs after 180 days of exposure.

Requirements		T [°C]	PF1-N	PF2-N	PF3-N	SF-N
f_{R3}/f_{R1}	>0.5	-15	1.4	1.4	1.5	1.0
f_{R1}/f_{LOP}	>0.4		0.5	0.3	0.4	0.3
f_{R3}/f_{R1}	>0.5	20	1.3	1.2	1.5	0.8
f_{R1}/f_{LOP}	>0.4		0.5	0.4	0.3	0.4
f_{R3}/f_{R1}	>0.5	60S	1.3	1.3	1.4	0.9
f_{R1}/f_{LOP}	>0.4		0.5	0.3	0.4	0.4

As the results at 90 and 180 days, the former condition (f_{R3}/f_{R1} > 0.5) is satisfied for the extreme temperatures for all the FRCs tested. On the contrary, only PF1 mixes fulfil the second requirement (f_{R1}/f_{LOP} > 0.4) for all the temperatures tested. PF2 mixes have demonstrated that the selected content of this fiber type is not enough to achieve the structural requirements. Regarding PF3 at 20 °C, this result seems anomalous since at low and high temperatures, the condition is achieved. SF mixes presented some limitations to be consider structural at low temperature for the fiber dosage used in this work. Thus, the warning which was done at short-term is now reasserted: at temperatures below 0 °C, it is important to keep in mind the increase of f_{LOP} and the higher brittleness of the matrix, in order to reach the ratio f_{R1}/f_{LOP}.

Finally, the structural requirements for FRC (f_{R3}/f_{R1} > 0.5 and f_{R1}/f_{LOP} > 0.4) are verified at -15, 20 and 60 °C for the beams reinforced with PF1 and SF fibers in the pre-cracked state, at 90 and 180 days respectively. Table 66 and Table 67 show the calculation of these ratios and all they accomplish both, independent on the temperature and fiber type.

Table 66. Verification of compliance with the structural requirements for the studied FRCs in pre-cracked state after 90 days of exposure.

Requirements		T [°C]	PF1-P	SF-P
f_{R3}/f_{R1}	>0.5	-15	1.6	1.0
f_{R1}/f_{LOP}	>0.4		0.4	0.6
f_{R3}/f_{R1}	>0.5	60S	1.3	1.1
f_{R1}/f_{LOP}	>0.4		0.5	0.4

Table 67. Verification of compliance with the structural requirements for the studied FRCs in pre-cracked state after 180 days of exposure.

Requirements		T [°C]	PF1-P	SF-P
f_{R3}/f_{R1}	>0.5	-15	1.5	1.1
f_{R1}/f_{LOP}	>0.4		0.6	0.4
f_{R3}/f_{R1}	>0.5	20	1.4	1.2
f_{R1}/f_{LOP}	>0.4		0.6	0.5
f_{R3}/f_{R1}	>0.5	60S	1.4	1.0
f_{R1}/f_{LOP}	>0.4		0.5	0.5

In view of the results obtained and their verification of compliance with the structural requirements, it can be said that MSFRCs and SFRC may be a feasible alternative for some engineering applications at low temperatures (−15 °C) and at high temperatures (60 °C), considering the variation of properties detected at long-term and adjusting the fiber content according to the environment where they will be exposed.

5.3.3. Aging

The American Concrete Institute has clarified in its Frequently Asked Technical Questions the concept of aging in concrete as follows [231]: *"Aging, if one means merely the effect caused by the passage of time, has no effect on concrete. Of course, concrete sets, hardens, gains strength, and exhibits reduced permeability with the passage of time, but it is not the passage of time alone that causes these things to happen. If the concrete is kept very cold, none of this will happen. If all moisture is removed, none of this will happen. Many or even most concretes are confronted with potential deteriorative service conditions. If the concrete has not been provided with immunity against these influences, it may well slowly deteriorate as time passes, but not simply because time passes."*

Compressive and flexural FRC behavior under extreme environmental conditions have been examined over time in Chapters 4 and 5. Regarding to compression, no degradation is distinguished by the effect of temperature after 90 and 180 days if compared with the results at 3 days, maintaining the selected class of concrete (or being affected only in a minor extent). Regarding to flexural strengths, the loss of flexural capability after 180 days exposed to extreme environmental conditions is not clear.

As happened in the literature on flexural behavior under extreme environmental conditions at long-term, the aging by temperature on MSFRCs has not been extensively studied. Only a parameter is usually studied (as state, passage of time *per se*, etc.) and there is not considerable related works with aging by temperature at long-term. In addition, aging could be investigated from different perspectives, which make difficult the comparison of results. Some of these studies have been compared to the results observed in the present Thesis.

Hannant [132] showed the experimental results of Portland cement-based composites containing two types of PP fibers, which were subjected to different environmental conditions (natural weathering, storage in laboratory air, and storage in water immersion) for 18 years. The durability of the PP fibers in these conditions were evaluated by tensile tests at material level. Excellent strength retention was found, which gave increased confidence in the long-term behavior of FRC. The results presented by Hannant are in line with the results obtained in this Thesis, but the time of exposure tested in this work is shorter than that tested by Hannant. Bernard investigated long-term changes (in a period up to 10 years) on post-crack performance of Fiber Reinforced Shotcrete (FRS) round panels with either steel or macro synthetic fibers [202,232], but environmental conditions were not included. The results proved that some types of steel FRS exhibited a substantial decrease in the post-peak strength at increasing crack widths due to a progressive embrittlement with age, leading to fiber rupture and macro synthetic FRS shown a slight increase in the post-peak strength without any change in the fiber pull-out mechanism. In this Thesis, both FRCs behave in a similar manner over the time and no detrimental effect by long-term are noted in a great extent. Teixeira et al. in [233] discussed about the effect of aging (retention of strengths) on SFRC after 10 years. They focused on the change in mechanical properties (post-cracking tensile strengths) obtained by three- and four- point bending tests at the ages of 1 year and 10 years. They concluded that aging affects the serviceability post-cracking residual strength, increasing fiber interfacial bond strength. Comparing with the results obtained in this Thesis, it can be said that the aging is not so notable since the results are quite constant in the range.

More recently, RILEM TC 261-CFF [234] organized a Round-Robin Test (RRT) in creep FRC in the cracked state which included the aging effect assessment. To this purpose, in parallel to the creep test, tests were carried out at different ages (0, 180 and 360 days of creep test) to evaluate any variations in the residual performance. These tests revealed no significant differences at high deformations for the two types of concrete reinforced with steel and synthetic fibers, respectively, but a substantial increase in terms of LOP was reported. These results are in line with the results examined for the results on f_{LOP}. Additionally, the characterization of the long-term deformations of MSFRC with PP fibers depending on the temperature was also studied by Del Prete et al. [165], focusing on creep. They carried out tests on fibers that were introduced in MSFRC, that were also tested by long-term uniaxial test at temperature. Their creep curves showed a sudden increase in the slope when temperature increased, for all the type of tests considered.

From these results, it can be said that MSFRC could be a potential alternative, but it is necessary to guarantee the behavior from a structural perspective. To this purpose, the verification of the relationships given by the fib MC 2010 for structural FRCs: f_{R3}/f_{R1} > 0.5 and f_{R1}/f_{LOP} > 0.4, are studied for the flexural strengths obtained, considering the passage of time.

From Subsection 4.5.2-b and 5.3.2, it can be concluded that the ratio f_{R3}/f_{R1} are achieved for each situation and type of FRC, independently of the time of exposure. However, this does not happen for the ratio f_{R1}/f_{LOP}. To analyze more in depth and contrast these results visually, these results were depicted from Figure 101 to Figure 104. Formerly, f_{R1} and f_{R3} were normalized with respect to the parameter N. Now, they are normalized by N and by f_{LOP} (at target temperature or at ambient temperature, depending on the state). Figure 101 compares the aging through these ratios as a function of age (3 and 180 days) and state (non-pre-cracked and pre-cracked) for MSFRC-PF1. Figure 101-a and Figure 101-c represent results at 3 days and Figure 101-b and Figure 101-d represent results at 180 days. As can be seen, the results are less dispersed by the temperature effect at long-term than at short-term. The trend is maintained, and no significant degradation is noted with the passage of time. Focusing on CMOD = 0.5 mm, which corresponds with the ratio f_{R1}/f_{LOP}, it can be seen that this ratio is at the threshold in most of the cases.

On the other hand, when comparing Figure 101-a and Figure 101-b (non-pre-cracked elements, to Figure 101-c and Figure 101-d, that match with pre-cracked elements), it can be appreciated that there is no significant effect caused by the interaction between state and temperature. For pre-cracked specimens, the trend is reversed because the value f_{LOP} is obtained at standard temperature. In any case, the effect of pre-cracking is not influential for their behavior.

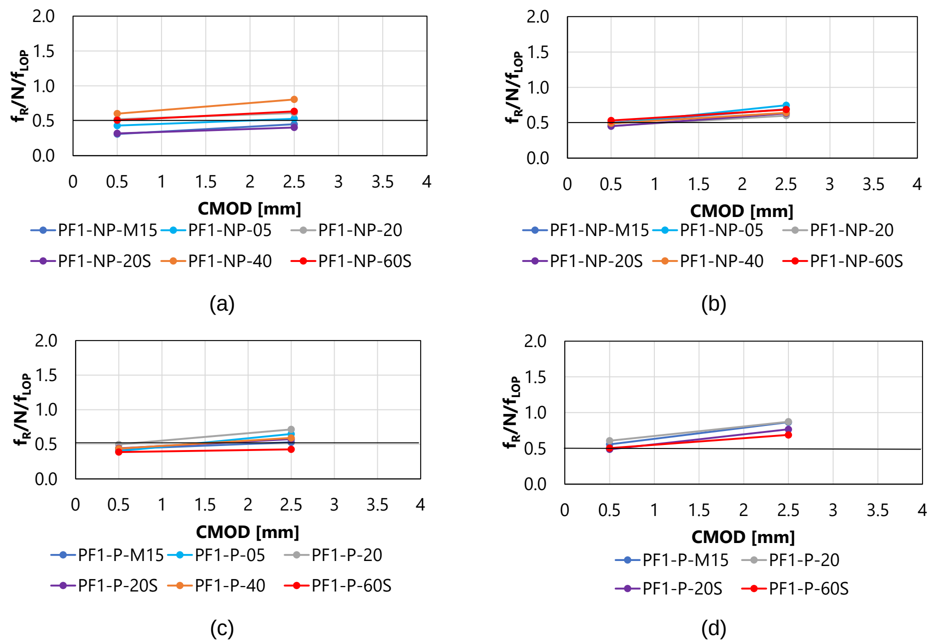

Figure 101. Comparison of the results from 3PBT for MSFRC reinforced with PF1: (a) at 3 days in non-pre-cracked state; (b) at 180 days in non-pre-cracked state; (c) at 3 days in pre-cracked state and (d) at 180 days in pre-cracked state.

The previous analysis is also done for the rest of the MSFRC. Figure 102 and Figure 103 show the results for MSFRC reinforced with PF2 and PF3, respectively. In this case, only non-pre-cracked specimens were studied. The mechanical performance at temperature depends on the fiber type. For MSFRC, in general, the ratio $f_R/N/f_{LOP}$ decreases with decreasing temperature for non-pre-cracked elements, independently of the exposure time. This could be explained by the increase of brittleness of the matrix which complicates reaching the structural requirements of $f_{R1}/f_{LOP} > 0.4$. However, the obtained ratios are in the boundary, close to the value of 0.4. This problem can be overcome increasing the fiber content.

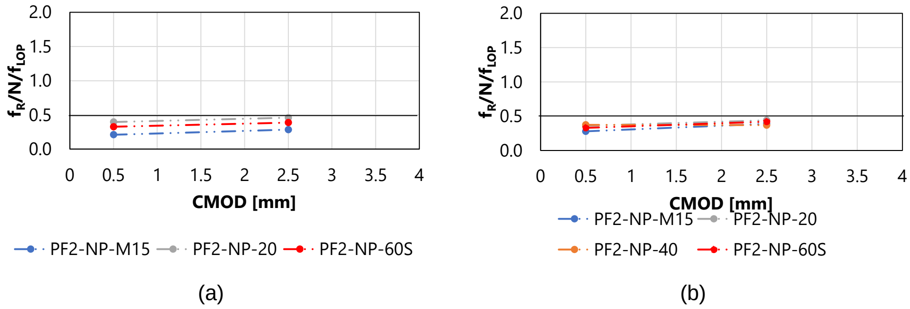

Figure 102. Comparison of the results from 3PBT for MSFRC reinforced with PF2: (a) at 3 days in non-pre-cracked state, and (b) at 180 days in non-pre-cracked state.

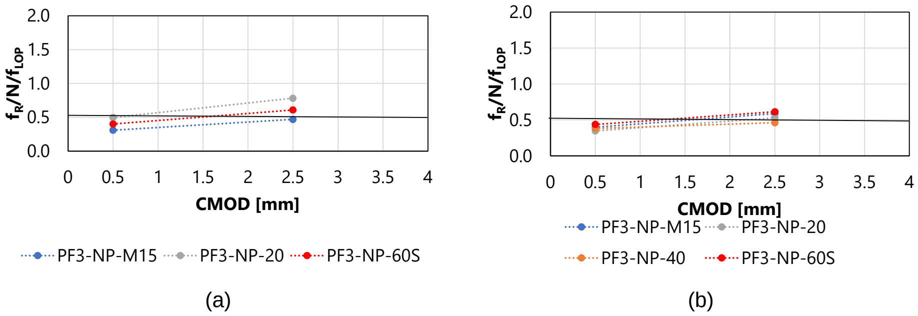

Figure 103. Comparison of the results from 3PBT for MSFRC reinforced with PF3: (a) at 3 days in non-pre-cracked state, and (b) at 180 days in non-pre-cracked state.

Figure 104 shows a comparison of the results from 3PBT for SFRC reinforced with SF: (a) at 3 days in non-pre-cracked state; (b) at 180 days in non-pre-cracked state; (c) at 3 days in pre-cracked state and (d) at 180 days in pre-cracked state. As occurs for PF2 and PF3 fibers (see Figure 102 and Figure 103), the ratio $f_R/N/f_{LOP}$ decreases with decreasing temperature for non-pre-cracked elements, independently of the exposure time. This could be compensated with a higher fiber content. For the rest of temperature, the values obtained are around the threshold value. In fact, at 60 °C, the requirement is fulfilled in some cases.

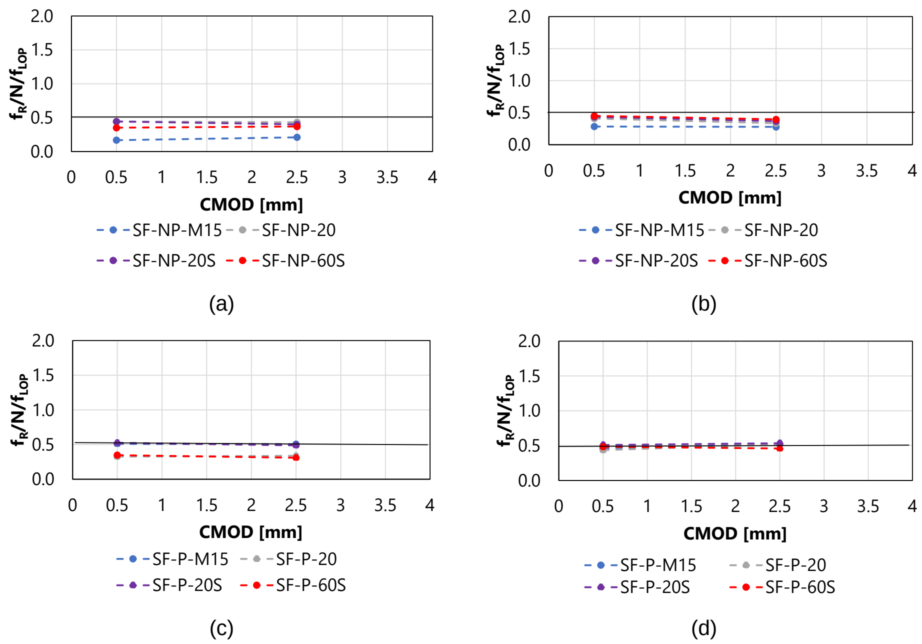

Figure 104. Comparison of the results from 3PBT for SFRC reinforced with SF: (a) at 3 days in non-pre-cracked state; (b) at 180 days in non-pre-cracked state; (c) at 3 days in pre-cracked state and (d) at 180 days in pre-cracked state.

To summarize, similar mechanical behavior was experimented by the different FRC studied under extreme environmental conditions. No notable degradation is distinguished by the effect of temperature at long-term if compared with the results at short-term. Regarding to flexural strengths, FRC have also demonstrated to sustain, inside an acceptable range, the flexural strengths after 180 days exposed to extreme environmental conditions. Therefore, FRCs' durability in terms of aging is enough for a wide range of operational temperatures and applications (considering the considerations derived from this Thesis after the verification of compliance of structural requirements).

5.3.4. General Summary

Long-term results follow the trend that presented short-term results, in compression as well as in flexure under the studied environmental conditions (from -15 to 60 °C). Regarding to compressive behavior, the variation detected reflects the effect of temperature on the matrix (an increase with a decrease of temperature and vice versa). This phenomenon is also observed for f_{LOP} at 90 and 180 days, for MSFRCs and SFRC (similar to that at 3 days). For residual flexural strengths, temperature affects in a limited extent. Additionally, the state factor is not an influential in the degradation of the performance of the studied FRC, independently of the time of exposure. It can be also concluded that aging under the conditions studied is excellent. The results are within the same order of magnitude for the selected class of concrete, fiber type, time, environmental conditions and state.

Chapter 6

Statistical Analysis of the Results of the FRC Flexural Behavior under extreme environmental conditions over time

Chapter 6 presents the analysis of the experimental results (434 prisms) obtained in previous Chapters from a statistical point of view. From the 434 prisms tested in total, 413 cases were valid to be included in the statistical study. The results are analyzed using an analysis of variances (ANOVA). Section 6.1 introduces the Exploratory Data Analysis (EDA) performed. These analyses performed are explained from Section 6.2 to Section 6.6, and in Section 6.7, they are discussed jointly. These analyses have allowed to propose relationships between dependent variables and the factors studied (per each fiber type), which are temperature, time of exposure at these temperatures and state (pre-cracking conditions). In Section 6.8, simple equations representing the behavior of FRCs at temperatures are presented, which may be used in future numerical models of FRC design codes and guidelines.

6.1. Introduction to the Exploratory Data Analysis performed

Once the experimental campaigns have been carried out and the results obtained, it was considered important to analyze the variability in the values through an EDA. This was done to identify significant influences and detect patterns between the experimental results and the studied factors. To do this, ANOVA multifactorial analyses are performed using the software Statgraphics Centurion 19 [235].

Regarding the variability detected in each dependent variable, it can be produced by: (i) the variation of the factors, (ii) the variation of those not considered, and (iii) the experimental noise (inherent error in any experiment). The variability of the dependent variable can be evaluated through the Square Sum (SS) parameter. Accordingly, the influence of a factor on the variability of the dependent variable is more significant when the factor has a greater SS. However, this statement must be contextualized, since a factor with more levels of variation is expected to produce greater variability in the dependent variable than a factor with fewer levels (*e.g.* a factor with four levels will have more variability than a factor with two levels). Thus, to normalize the influence of each factor on the variability of the dependent variable (regardless of the number of levels considered), that is, the normalization of SS according to the number of levels of a factor, the concept of degrees of freedom (DF) for both the experiments and the factors, is considered. If an experiment consists of a total of N number of experiments, then it is said that the experiment has N-1 total DF. A factor F_i for which N_{fi} levels are considered, will have N_{fi}-1 DF. The difference between the total DF and the sum of the DF of all factors is equal to residual DF. In this case, the residual is considered as an additional factor, grouping the entire variation not explained by the other factors. Additionally, the analysis will consider the concept of Mean Square, which is the quotient between SS and DF of the factor.

To conduct the ANOVA analysis, the data were entered in the program and the statistical tests were initiated. The **dependent variables** included flexural strength at peak-load and residual flexural strengths, as well as residual strengths normalized[3] by N (f_{LOP}, f_{R1}, f_{R3}, f_{R1}/N and f_{R3}/N). The **factors** chosen are: time of exposure, fiber type (named fiber), temperature, state, and fc. Regarding to their **levels**, time of exposure is the time at which the test is performed after curing period, and it has four levels: 0, 3, 90 and 180 days. Fiber type is a qualitative factor (not continuous), that represents the type of fiber, therefore, it has four levels (one per each type of fiber): PF1, PF2, PF3 and SF. Temperature presents six levels: -15, 5, 20, 20S, 40 and 60S. State is also a not continuous factor with two levels: non-pre-cracked and pre-cracked states. Lastly, compressive strengths at 28 days at standard temperature, fc, were included as a factor since some variations were detected between batches (inter-group variability) during the production of concrete mixes (see Chapter 3).

After initiating the analysis of variance, the software performed hypothesis contrasts, with the null hypothesis positing that the dependent variables under different conditions are equal to each other. Subsequently, **ANOVA tables** were generated. On the one hand, each column of the tables collects all the former concepts (SS, DF, Mean Square), F-ratios and P-Values. Since the Type III sum of squares has been chosen, the contribution of each factor was measured by deleting the effects of other factors. These computed P-Values represent the probability for a given statistical model that, when the null hypothesis is true, the

[3] As demonstrated in previous chapters, the parameter N should be considered. f_{LOP} was not divided by N (the total number of fibers in the cross-section) since it is mainly dependent on the matrix.

statistical summary (such as the sample mean difference between two compared groups) would be the same or of greater magnitude than the actual observed results [236]. Typically, the null hypothesis is rejected when the P-Value is equal to or less than a predetermined significance level, often set at 0.05, corresponding to a confidence level of 95 %. In this Chapter, factors with a P-Value equal to or less than 0.05 are considered statistically significant. Factors with P-Values greater than 0.05 are deemed not significant, and thus, they are eliminated from the analysis to gain degrees of freedom for the residual. This aids in further clarifying the significance of the effects of the remaining factors. On the other hand, each row of the table corresponds to one of the factors considered. The DF column indicates the degrees of freedom of the factors and those remaining for the residual. In general, it is recommended that the residual's DF ≥ 4 to ensure robustness of the ANOVA and its derived conclusions [237]. All the analyses performed in this chapter have DF much higher than 4 so the conclusions derived can be considered as robust. Table 68 outlines the analyses performed and the related subsection.

Table 68. Outline of the ANOVA tests carried out in this Thesis.

# of Analysis	Dependent variable	Factors	Specimens with fiber type	# of cases	Related subsection
1	f_{R3}; f_{R3}/N	▪ Time ▪ Fiber ▪ State ▪ Temperature ▪ fc	All (PF1, PF2, PF3 and SF)	413	6.2
2	f_{LOP}, f_{R1}, f_{R1}/N, f_{R3} and f_{R3}/N	▪ Time ▪ Temperature ▪ fc	PF1	182-188	6.3
3	f_{LOP}, f_{R1}, f_{R1}/N, f_{R3} and f_{R3}/N	▪ Time ▪ Temperature ▪ fc	PF2	48-49	6.4
4	f_{LOP}, f_{R1}, f_{R1}/N, f_{R3} and f_{R3}/N	▪ Time ▪ Temperature ▪ fc	PF3	46-48	6.5
5	f_{LOP}, f_{R1}, f_{R1}/N, f_{R3} and f_{R3}/N	▪ Time ▪ Temperature ▪ fc	SF	134-139	6.6

In total, five different analyses of variance are carried out to check the significance of the results obtained.

Analysis #1 examines the significance of the factor "State" across all data. This analysis is only performed in f_{R3} and f_{R3}/N, as these are the dependent variables that include specimens in both pre-cracked (P) and non-pre-cracked (NP) states, considering fiber type, time and temperature (complete cases).

Analysis #2 is carried out only for the results from elements reinforced with PF1 fibers on f_{LOP}, f_{R1}, f_{R1}/N, f_{R3} and f_{R3}/N. The objective is to determine the significant factors affecting these variables, with emphasis on temperature. Similarly, Analyses #3, 4 and 5 are performed in results obtained from elements reinforced with PF2, PF3 and SF fibers respectively.

After the ANOVA analyses have been performed, a multiple comparison procedure was applied to determine which means are significantly different from others. The method used to discriminate between the means is Duncan's multiple comparison at a 99.0 % confidence level. With this method, there is a 1.0 % risk of erroneously concluding significant differences when the true difference is zero. Subsequent Subsections provide a detailed discussion of the outcomes of each analysis, including ANOVA tests and their implications.

6.2. Statistical Study of the Influence of "State" factor on Flexural Strengths of FRCs at Extreme Environmental Conditions

This Section collects the results obtained from a multi-factor analysis of variance conducted on f_{R3} and f_{R3}/N values to determine which factors have a statistically significant effect (Analysis #1). The focus of these analyses lies on the "State" factor. Prior to running the ANOVA analysis, normality and homoscedasticity assumptions were verified. These verifications were done in each analysis.

6.2.1. f_{R3}

Table 69 presents the results of the ANOVA test on f_{R3}. The F-tests in this table allows to identify the significant factors, decomposing the variability of f_{R3} into contributions attributable to these factors.

Four P-values are less than 0.05, therefore, these factors have an effect statistically significant on f_{R3} with a 95.0 % confidence level. The only non-significant factor from a statistical point of view is "State", since its P-value is 0.9073 > 0.05, indicating no significant differences between NP and P elements. Consequently, this factor is omitted from subsequent analyses.

Table 69. ANOVA for f_{R3} to identify the influence on "State".

Source	Square Sum (SS)	DF	Mean Square	F-Ratio	P-Value
MAIN EFFECTS					
A: TIME OF EXPOSURE	6.73357	2	3.36678	10.92	0.0000
B: FIBER	60.3535	3	20.1178	65.24	0.0000
C: STATE	0.00418231	1	0.00418231	0.01	0.9073
D: TEMPERATURE	9.03115	5	1.80623	5.86	0.0000
E: fc	50.6755	12	4.22296	13.70	0.0000
RESIDUAL	119.951	389	0.308356		
TOTAL (CORR.)	330.021	412			

6.2.2. f_{R3}/N

Table 70 presents the results of the ANOVA test on f_{R3}/N. As in the previous case, the P-value in the ANOVA table for the "State" factor is 0.523 > 0.05, indicating that this factor is not statistically significant.

Table 70. ANOVA for f_{R3}/N to identify the influence on "State".

Source	Square Sum (SS)	DF	Mean Square	F-Ratio	P-Value
MAIN EFFECTS					
A: TIME OF EXPOSURE	0.000471199	2	0.000235599	6.28	0.0021
B: FIBER	0.000845864	3	0.000281955	7.52	0.0001
C: STATE	0.0000169116	1	0.0000169116	0.45	0.5023
D: TEMPERATURE	0.00136728	5	0.000273455	7.29	0.0000
E: fc	0.00408558	12	0.000340465	9.08	0.0000
RESIDUAL	0.0145155	387	0.0000375077		
TOTAL (CORR.)	0.0304985	410			

6.2.3. Summary of Results of Statistical Analysis for State.

The Analysis #1 has permitted to verify the influence of "State" on f_{R3} and f_{R3}/N from a statistical point of view, concluding that the factor "State" does not influence flexural strengths of FRCs under the extreme environmental conditions studied, regardless of whether normalization by N is considered or not.

6.3. Statistical Study of Flexural Strengths of MSFRC (PF1) at Extreme Environmental Conditions

Analysis #2 is performed to identify if the exposure to extreme environmental condition (temperature) over time is a significant factor on the flexural behavior of concrete reinforced with PF1 fibers (MSFRC-PF1). The variables analyzed were f_{LOP}, f_{R1}, f_{R1}/N, f_{R3} and f_{R3}/N.

6.3.1. f_{LOP}

Three factors were analyzed herein: time, temperature and fc. The results from this analysis are collected in Table 71.

Table 71. Analysis of Variance for f_{LOP}.

Source	Square Sum (SS)	DF	Mean Square	F-Ratio	P-Value
MAIN EFFECTS					
A: TIME OF EXPOSURE	4.07186	3	1.35729	3.99	0.0088
B: TEMPERATURE	46.8906	5	9.37811	27.59	0.0000
C:fc	6.83839	8	0.854799	2.52	0.0131
RESIDUAL	58.1184	171	0.339874		
TOTAL (CORR.)	151.332	187			

As observed, all the considered factors are significant. Temperature factor has a P-Value = 0.0000, lower than 0.05. After that, a multiple comparison procedure was applied on “Time” (short-term vs. long-term effects) and “Temperature”.

a) Inter-groups variability – short-term vs. long-term effects

Three homogeneous groups have been identified (Table 72), distinguished by the assigned letter (A, B, C) in columns for f_{LOP} per “Time”. No statistically significant differences are observed between levels sharing the same letter (90 and 180 days, and 3 days and 180 days). The results indicate that the variation on f_{LOP} due to the time of exposure, is already influential if only exposing for three days (0 vs. 3 days). There is significant difference between 3 and 90 days, but certain influences from the other groups can be detected at long-term (180 days). Moreover, Table 73 shows the estimated differences between each pair of levels. The asterisk indicates that these pairs show statistically significant differences with a 99.0 % confidence level.

Table 72. Multi-Range Test for f_{LOP} per “Time”.

TIME OF EXPOSURE	Cases	LS Mean	S Sigma	Homogeneous groups
0	83	3.54681	0.207818	A
3	42	3.90656	0.134992	B
90	21	4.30098	0.188674	C
180	42	4.25787	0.129684	BC

Table 73. Results from Method: 99.0 % Duncan.

Contrast	Sig.	Difference
0 - 3	*	-0.359744
0 - 90	*	-0.754172
0 - 180	*	-0.711059
3 - 90	*	-0.394428
3 - 180		-0.351315
90 - 180		0.0431128

* it indicates a significant difference.

b) Inter-groups variability – temperature effects

Table 74 shows four different groups for f_{LOP} per "Temperature". There are statistically significant differences between the levels that have different letter. This is in line with the previous hypothesis proposed, because the most influential temperature was -15 °C (it is the only group that is represented by the letter A in the column). Temperature of 5 °C may be considered in the same range of influence that 20 °C (in air conditioning as well as in immersion). Additionally, there is not statistically significant difference between 40 and 60 °C and the humidity is not an important factor (since 20=20S=60S). Additionally, Table 75 displays the estimated differences between each pair of levels. The asterisk indicates that these pairs show statistically significant differences with a 99.0 % confidence level.

Table 74. Multi-Range Test for f_{LOP} per "Temperature".

TEMPERATURE	Cases	LS Mean	S Sigma	Homogeneous groups
-15	21	5.46762	0.185486	A
5	14	4.04203	0.20574	B
20	104	3.92423	0.132371	BC
20S	14	3.98027	0.202236	BC
40	14	3.10448	0.213741	D
60S	21	3.49971	0.185486	CD

Table 75. Results from Method: 99.0 % Duncan.

Contrast	Sig.	Difference
-15 - 5	*	1.42559
-15 - 20	*	1.54339
-15 - 20S	*	1.48735
-15 - 40	*	2.36314
-15 - 60S	*	1.96791
5 - 20		0.117799
5 - 20S		0.0617566
5 - 40	*	0.937546
5 - 60S	*	0.542315
20 - 20S		-0.0560429
20 - 40	*	0.819746
20 - 60S		0.424516
20S - 40	*	0.875789
20S - 60S		0.480558
40 - 60S		-0.395231

* it indicates a significant difference.

6.3.2. f_{R1}

Secondly, a multi-factor ANOVA for f_{R1} is done (Table 76) to determine which factors have a statistically significant effect on this dependent variable. "Temperature" effect on f_{R1} is not statistically significant.

Table 76. Analysis of Variance for f_{R1}.

Source	Square Sum (SS)	DF	Mean Square	F-Ratio	P-Value
MAIN EFFECTS					
A: TIME OF EXPOSURE	2.19184	3	0.730615	3.25	0.0233
B: TEMPERATURE	1.43347	5	0.286694	1.28	0.2769
C: fc	7.37519	8	0.921899	4.10	0.0002
RESIDUAL	37.7721	168	0.224834		
TOTAL (CORR.)	65.8619	184			

Not considering the factor "Temperature", the results in Table 77 are obtained:

Table 77. Analysis of Variance for f_{R1}.

Source	Square Sum (SS)	DF	Mean Square	F-Ratio	P-Value
MAIN EFFECTS					
A: TIME OF EXPOSURE	3.04241	3	1.01414	4.48	0.0047
B: fc	9.03422	8	1.12928	4.98	0.0000
RESIDUAL	39.2056	173	0.226622		
TOTAL (CORR.)	65.8619	184			

In this ANOVA table (Table 77), “Time” and “fc” result to be significant factors with a P-Value = 0.047 and 0.0000 respectively. After that, for “Time”, Multiple Range Tests provided which means are significantly different from others (99.0 % Duncan).

a) Inter-groups variability – short-term vs. long-term effects

Two homogeneous groups have been identified according to the letters in columns, for “Time” factor (Table 78). Thus, it can be concluded that there are significant differences between short- and long-term results. In other words, 0 and 3 days make the group A (because they do not have significant differences) and 90 and 180 days make the group B. Table 79 shows the estimated differences between each pair of levels.

Table 78. Multi-Range Test for f_{R1} per “Time”.

TIME OF EXPOSURE	Cases	LS Mean	S Sigma	Homogeneous groups
0	83	1.8817	0.0652412	A
3	40	1.83462	0.108404	A
90	21	2.24033	0.144198	B
180	41	2.20508	0.0982454	B

Table 79. Results from Method: 99.0 % Duncan.

Contrast	Sig.	Difference
0 - 3		0.0470756
0 - 90	*	-0.358627
0 - 180	*	-0.323379
3 - 90	*	-0.405702
3 - 180	*	-0.370454
90 - 180		0.0352479

* it indicates a significant difference.

6.3.3. f_{R1}/N

ANOVA was performed on f_{R1}/N, considering the total number of fibers at the cross-section (N). The results are summarized in Table 80.

Table 80. Analysis of Variance for f_{R1}/N.

Source	Square Sum (SS)	DF	Mean Square	F-Ratio	P-Value
MAIN EFFECTS					
A: TIME OF EXPOSURE	0.000309839	3	0.00010328	5.38	0.0015
B: TEMPERATURE	0.0000660748	5	0.000013215	0.69	0.6329
C: fc	0.00024895	8	0.0000311187	1.62	0.1222
RESIDUAL	0.00320609	167	0.0000191982		
TOTAL (CORR.)	0.00458741	183			

“Temperature” and “fc” are not statistically significant. Not considering “Temperature” and “fc”, the results in Table 81 are obtained, with “Time” being a significant factor with a P-Value = 0.000.

Table 81. Analysis of Variance for f_{R1}/N.

Source	Square Sum (SS)	DF	Mean Square	F-Ratio	P-Value
MAIN EFFECTS					
A: TIME OF EXPOSURE	0.00105226	3	0.000350754	17.86	0.0000
RESIDUAL	0.00353514	180	0.0000196397		
TOTAL (CORR.)	0.00458741	183			

After that, for “Time” factor, Multiple Range Tests provides which means are significantly different from others (99.0 % Duncan).

a) Inter-groups variability – short-term vs. long-term effects

Two homogeneous groups have been identified in Table 82. There are not statistically significant differences between the results at 0 and 3 days, and there are not statistically significant between the results at 90 and 180 days. However, the time of exposition (short- or long-term periods) affects the response at f_{R1} since the results at 3 days are different from those obtained at 90 and 180 days. Table 83 shows the estimated differences between each pair of levels.

Table 82. Multi-Range Test for f_{R1}/N per “Time”.

TIME OF EXPOSURE	Cases	LS Mean	S Sigma	Homogeneous groups
0	82	0.0192024	0.000489396	A
3	40	0.01789	0.000700708	A
90	21	0.0244048	0.000967069	B
180	41	0.0233049	0.00069211	B

Table 83. Results from Method: 99.0 % Duncan.

Contrast	Sig.	Difference
0 - 3		0.00131244
0 - 90	*	-0.00520232
0 - 180	*	-0.00410244
3 - 90	*	-0.00651476
3 - 180	*	-0.00541488
90 - 180		0.00109988

* it indicates a significant difference.

6.3.4. f_{R3}

Table 84 collects the variability of f_{R3} into influences due to various factors (time and temperature). In this case, fc is not included as a factor since it is contemplated by the software as a linear combination of other factors.

Table 84. Analysis of Variance for f_{R3}.

Source	Square Sum (SS)	DF	Mean Square	F-Ratio	P-Value
MAIN EFFECTS					
A: TIME OF EXPOSURE	29.8544	2	14.9272	22.33	0.0000
B: TEMPERATURE	17.4068	5	3.48136	5.21	0.0002
RESIDUOS	116.342	174	0.668631		
TOTAL (CORR.)	163.94	181			

In the case, the “Time” factor has a P-value = 0.0000, and “Temperature” factor appears with a P-Value = 0.0002; therefore, their effects on f_{R3} are statistically significant. After that, as previously, multi-range tests were applied for f_{R3} per “Time” and “Temperature”, with a 99.0 % confidence level.

a) Inter-groups variability – short-term vs. long-term effects

Two homogeneous groups are detected per time of exposure, presenting significant differences between short-term and long-term results. Table 85 and Table 86 display the results obtained from the method Duncan's multiple comparison (99 % confidence level).

Table 85. Multi-Range Test for f_{R3} per “Time”.

TIME OF EXPOSURE	Cases	LS Mean	S Sigma	Homogeneous groups
3	79	2.11453	0.092021	A
90	35	3.0873	0.155804	B
180	68	2.89916	0.101058	B

Table 86. Results from Method: 99.0 % Duncan.

Contrast	Sig.	Difference
3 - 90	*	-0.972771
3 - 180	*	-0.784631
90 - 180		0.18814

* it indicates a significant difference.

b) Inter-groups variability – temperature effect

Table 87 and Table 88 present the outcomes of Duncan's multiple comparison test for f_{R3} concerning the “Temperature” factor. The influence of some level of temperature is combined with other levels since any factor is isolated in the placement of the letter. For instance, -15 could be considered similar to 20S, 40 and 60S. Moreover, -15 could be also considered similar to 5, 20 and 40.

Table 87. Multi-Range Test for f_{R3} per “Temperature”.

TEMPERATURE	Cases	LS Mean	S Sigma	Homogeneous groups
-15	40	2.79743	0.12932	AB
5	20	3.00042	0.192311	B
20	33	3.10088	0.143784	B
20S	27	2.35728	0.166991	A
40	21	2.65465	0.188393	AB
60S	41	2.29131	0.127721	A

Table 88. Results from Method: 99.0 % Duncan.

Contrast	Sig.	Difference
-15 - 20		-0.303448
-15 - 20S		0.440151
-15 - 40		0.142776
-15 - 5		-0.202992
-15 - 60S		0.506114
20 - 20S	*	0.743599
20 - 40		0.446224
20 - 5		0.100457
20 - 60S	*	0.809562
20S - 40		-0.297375
20S - 5	*	-0.643143
20S - 60S		0.0659626
40 - 5		-0.345768
40 - 60S		0.363338
5 - 60S	*	0.709105

* it indicates a significant difference.

6.3.5. f_{R3}/N

Lastly, this analysis of variance is performed to determine the significance of the factors on the dependent variable f_{R3}/N. As in the previous case, “fc” factor is not considered because it was interpreted by the software as a linear combination of other factors. Table 89 collects the results of the ANOVA tests. In this case, the “Time” factor has a P-value = 0.0000 and “Temperature” factor appears with a P-Value = 0.0077; therefore, their effects on f_{R3}/N are statistically significant.

Table 89. Analysis of Variance for f_{R3}/N.

Source	Square Sum (SS)	DF	Mean Square	F-Ratio	P-Value
MAIN EFFECTS					
A: TIME OF EXPOSURE	0.00212353	2	0.00106176	21.88	0.0000
B: TEMPERATURE	0.000790849	5	0.00015817	3.26	0.0077
RESIDUAL	0.00844288	174	0.0000485223		
TOTAL (CORR.)	0.0114374	181			

After that, the procedure of Duncan's multiple comparison at the 99 % confidence level was applied on “Time” and “Temperature”.

a) Inter-groups variability – short-term vs. long-term effects

Concerning the factor “Time”, two homogeneous groups have been identified in Table 90, for f_{R3}/N, differentiating the results obtained after 3 days of exposure with 90 and 180 days. There are no statistically significant differences between the levels of 90 and 180 days. Table 91 shows the estimated differences between each pair of levels.

Table 90. Multi-Range Test for f_{R3}/N per “Time”.

TIME OF EXPOSURE	Cases	LS Mean	S Sigma	Homogeneous groups
3	79	0.0243482	0.000783907	A
90	35	0.0307261	0.00132726	B
180	68	0.0317576	0.000860889	B

Table 91. Results from Method: 99.0 % Duncan.

Contrast	Sig.	Difference
3 - 90	*	-0.00637785
3 - 180	*	-0.0074094
90 - 180		-0.00103155

* it indicates a significant difference.

b) Inter-groups variability – temperature effects

Concerning the factor “Temperature”, two groups present differences between the levels, given by different alignment of the letters in column (in Table 92) or by those pairs in Table 93 that show statistically with a 99.0 % confidence level, indicated with an asterisk. These results are similar to those obtained for f_{R3}.

Table 92. Multi-Range Test for f_{R3}/N per "Temperature".

TEMPERATURE	Cases	LS Mean	S Sigma	Homogeneous groups
-15	40	0.0308204	0.00110165	AB
5	20	0.0324525	0.00163825	B
20	33	0.0297846	0.00122486	AB
20S	27	0.0270316	0.00142256	A
40	21	0.0267355	0.00160488	A
60S	41	0.0268391	0.00108803	A

Table 93. Results from Method: 99.0 % Duncan.

Contrast	Sig.	Difference
-15 - 5		-0.00163201
-15 - 20		0.00103582
-15 - 20S		0.00378883
-15 - 40		0.00408497
-15 - 60S		0.00398132
5 - 20		0.00266784
5 - 20S	*	0.00542084
5 - 40	*	0.00571699
5 - 60S	*	0.00561333
20 - 20S		0.00275301
20 - 40		0.00304915
20 - 60S		0.0029455
20S - 40		0.000296143
20S - 60S		0.00019249
40 - 60S		-0.000103653

* it indicates a significant difference.

6.3.6. Summary of Results of Statistical Study for MSFRC-PF1

Table 94 sums up the results obtained in this previous Section for MSFRC reinforced with PF1 fibers.

The time of exposure is a significant factor in the flexural behavior. Variations on f_{LOP}.are detected between 0 and any time of temperature exposure, however, no significant variations are detected between 3, 90 and 180 days of exposure. In the case of the residual strengths, f_{R1} and f_{R3}, short- and long-term results are differentiated (0 and 3 days are similar, 90 and 180 days are similar).

Temperature affects f_{LOP} and f_{R3}. At f_{LOP}, temperature of -15 °C is different from all the other levels, which have no differences between them. No clear differences are noticed between the levels for f_{R3}.

Table 94. Summary of statistical results for MSFRC-PF1.

Variables	f_{LOP}	f_{R1}	f_{R3}
Time of exposure	0 d ≠ (3 = 90 = 180d)	(0 = 3 d) ≠ (90 = 180 d)	3 d ≠ (90 = 180 d)
Temperature	M15 ≠ (5; 20; 20S; 40; 60S)	This parameter is not affected by this factor	Unclear differences (see Table 95)

Table 95 compares the previous obtained Ducan's results for the variable f_{R3} per temperature. It can be seen that not all the differences between the pair of means per temperature (if the N is considered or not), are coinciding. That suggests that the influence is not clear. Temperature of 60 °C could be, in this case, the most influential.

Table 95. Comparison of significance of pairs of means of f_{R3} and f_{R3}/N per "Temperature".

	f_{R3}		f_{R3}/N	
Contrast	**Sig.**	**Difference**	**Sig.**	**Difference**
-15 - 20		-0.303448		-0.00163201
-15 - 20S		0.440151		0.00103582
-15 - 40		0.142776		0.00378883
-15 - 5		-0.202992		0.00408497
-15 - 60S		0.506114		0.00398132
20 - 20S	*	0.743599		0.00266784
20 - 40		0.446224	*	0.00542084
20 - 5		0.100457	*	0.00571699
20 - 60S	*	0.809562	*	0.00561333
20S - 40		-0.297375		0.00275301
20S - 5	*	-0.643143		0.00304915
20S - 60S		0.0659626		0.0029455
40 - 5		-0.345768		0.000296143
40 - 60S		0.363338		0.00019249
5 - 60S	*	0.709105		-0.000103653

6.4. Statistical Study of Flexural Strengths of MSFRC (PF2) at Extreme Environmental Conditions

Analysis #3 is performed to identify if the extreme environmental conditions defined are a significant factor on the flexural behavior of concrete reinforced with PF2 fibers over time. The variables selected for this analysis are f_{LOP}, f_{R1}, f_{R1}/N, f_{R3} and f_{R3}/N.

6.4.1. f_{LOP}

The first dependent variable considered is the strength at limit of proportionality (f_{LOP}). Two factors were used to perform the analysis: time of exposure and temperature. Fc is not included as a factor since the software interpreted that it is a linear combination of the other factors. The results from this analysis are collected in Table 96.

Table 96. Analysis of Variance for f_{LOP}.

Source	Square Sum (SS)	DF	Mean Square	F-Ratio	P-Value
MAIN EFFECTS					
A: TIME OF EXPOSURE	6.65217	1	6.65217	15.64	0.0003
B: TEMPERATURE	45.0622	3	15.0207	35.32	0.0000
RESIDUAL	18.7096	44	0.425219		
TOTAL (CORR.)	69.3081	48			

All the considered factors are significant. “Time” factor has a P-Value = 0.0003 and “Temperature” factor has a P-Value = 0.0000, both lower than 0.05. After that, a multiple comparison procedure was applied on “Temperature” to determine which means significantly different from others, using Duncan's multiple comparison at the 99.0 % confidence level.

a) Inter-groups variability – temperature effects

Table 97 shows two different groups, according to the letters in columns for f_{LOP} per temperature. The results can be grouped in -15 °C and the rest of temperatures (in the range from 20 and 60 °C). Table 98 displays the estimated differences between each pair of levels.

Table 97. Multi-Range Test for f_{LOP} per “Temperature”.

TEMPERATURE	Cases	LS Mean	S Sigma	Homogeneous groups
-15	14	5.65644	0.174278	A
20	14	3.74306	0.174278	B
40	7	3.76624	0.266214	B
60S	14	3.29986	0.174278	B

Table 98. Results from Method: 99.0 % Duncan.

Contrast	Sig.	Difference
-15 - 20	*	1.91339
-15 - 40	*	1.8902
-15 – 60S	*	2.35659
20 - 40		-0.023181
20 – 60S		0.4432
40 – 60S		0.466381

6.4.2. f_{R1}

Table 99 shows the results of the multi-factor analysis of variance for f_{R1}, considering "Time" and "Temperature" as factors.

Table 99. Analysis of Variance for f_{R1}.

Source	Square Sum (SS)	DF	Mean Square	F-Ratio	P-Value
MAIN EFFECTS					
A: TIME OF EXPOSURE	1.77046	1	1.77046	17.57	0.0001
B: TEMPERATURE	0.966414	3	0.322138	3.20	0.0327
RESIDUAL	4.33358	43	0.100781		
TOTAL (CORR.)	7.54921	47			

In this ANOVA table, "Time" and "Temperature" result to be significant factors with a P-Value = 0.0001 and 0.0327 respectively. After that, for "Temperature" factor, Multiple Range Tests provided which means are significantly different from others (99.0 % Duncan).

a) Inter-groups variability – temperature effects

Table 100 shows the results obtained from the multi-range test for f_{R1} per temperature. According to the letters in columns, no significant differences can be detected between the different levels of temperatures. This suggests that temperature may have a minor effect (despite the fact that it is significant on the variability of f_{R1} of MSFRC-PF2), since the influence of the levels are similar. Table 101 shows the estimated differences between each pair of levels.

Table 100. Multi-Range Test for f_{R1} per "Temperature".

TEMPERATURE	Cases	LS Mean	S Sigma	Homogeneous groups
-15	13	1.37959	0.0881303	A
20	14	1.39876	0.0848448	A
40	7	1.3561	0.129846	A
60S	14	1.07087	0.0848448	A

Table 101. Results from Method: 99.0 % Duncan.

Contrast	Sig.	Difference
-15 - 20		-0.0191647
-15 - 40		0.0234902
-15 - 60S		0.308721
20 - 40		0.0426549
20 - 60S		0.327886
40 - 60S		0.285231

* it indicates a significant difference.

6.4.3. f_{R1}/N

The previous analysis of variance was repeated for f_{R1}/N, and the results are collected in Table 102.

Table 102. Analysis of Variance for f_{R1}/N.

Source	Square Sum (SS)	DF	Mean Square	F-Ratio	P-Value
MAIN EFFECTS					
A: TIME OF EXPOSURE	0.000254195	1	0.000254195	18.93	0.0001
B: TEMPERATURE	0.0000424011	3	0.0000141337	1.05	0.3792
RESIDUAL	0.000577475	43	0.0000134297		
TOTAL (CORR.)	0.000918079	47			

In this case, “Temperature” is not statistically significant. As mentioned in the analysis of the inter-groups’ variability, the variation on f_{R1}/N due to temperature seems to be in a minor extent. Not considering it, the results in Table 103 are obtained:

Table 103. Analysis of Variance for f_{R1}/N.

Source	Square Sum (SS)	DF	Mean Square	F-Ratio	P-Value
MAIN EFFECTS					
A: TIME OF EXPOSURE	0.000298203	1	0.000298203	22.13	0.0000
RESIDUAL	0.000619876	46	0.0000134756		
TOTAL (CORR.)	0.000918079	47			

In this ANOVA table, “Time” result to be significant factor with a P-Value = 0.000. Multiple Range Test (99.0 % Duncan) is not performed in this case because there are only two level for this factor (3 and 180 days).

6.4.4. f_{R3}

This analysis investigates the significant factors for f_{R3} in MSFRC with PF2 fibers (Table 104), considering time and temperature as factors. In this case, fc is not included as a factor since it is considered by the software as a linear combination of other factors.

Table 104. Analysis of Variance for f_{R3}.

Source	Square Sum (SS)	DF	Mean Square	F-Ratio	P-Value
MAIN EFFECTS					
A: TIME OF EXPOSURE	3.70989	1	3.70989	21.16	0.0000
B: TEMPERATURE	2.99408	3	0.998027	5.69	0.0022
RESIDUOS	7.71467	44	0.175333		
TOTAL (CORR.)	13.7054	48			

In the case, the “Time of exposure” factor has a P-value = 0.0000, and “Temperature” factor appears with a P-Value = 0.0022; therefore, their effects on f_{R3} are statistically significant. After that, as previously, multi-range tests were applied, herein for f_{R3} per temperature, with a 99.0% confidence level in each case.

a) Inter-groups variability – temperature effect

Per “Temperature”, Table 105 and Table 106 collect the results from Duncan's multiple comparison test for f_{R3} per temperature. In this case, it could be said that two range of temperatures can be defined: -15 to 20 °C and 20 to 60 ° C.

Table 105. Multi-Range Test for f_{R3} per “Temperature”.

TEMPERATURE	Cases	LS Mean	S Sigma	Homogeneous groups
-15	14	1.88899	0.11191	A
20	14	1.67068	0.11191	AB
40	7	1.25038	0.170945	B
60S	14	1.32778	0.11191	B

Table 106. Results from Method: 99.0 % Duncan.

Contrast	Sig.	Difference
-15 - 20		0.218307
-15 - 40	*	0.638605
-15 - 60S	*	0.561207
20 - 40		0.420298
20 - 60S		0.3429
40 - 60S		-0.0773976

* it indicates a significant difference.

6.4.5. f_{R3}/N

Lastly, this analysis of variance is performed on f_{R3}/N. As in the previous case, “fc” factor is not considered (Table 107). In this case, the “Time” factor has a P-value = 0.0001 and “Temperature” factor appears with a P-Value = 0.0014; therefore, their effects on f_{R3}/N are statistically significant.

Table 107. Analysis of Variance for f_{R3}/N.

Source	Square Sum (SS)	DF	Mean Square	F-Ratio	P-Value
MAIN EFFECTS					
A: TIME OF EXPOSURE	0.000474701	1	0.000474701	19.03	0.0001
B: TEMPERATURE	0.000461313	3	0.000153771	6.17	0.0014
RESIDUAL	0.00109745	44	0.000024942		
TOTAL (CORR.)	0.00188831	48			

After that, a multiple comparison procedure was applied to determine which averages significantly different from others on “Temperature”.

a) Inter-groups variability – temperature effects

Per “Temperature”, two groups present remarkable differences between the levels (Table 108 and Table 109). These results are the same to those obtained for f_{R3}.

Table 108. Multi-Range Test for f_{R3}/N per “Temperature”.

TEMPERATURE	Cases	LS Mean	S Sigma	Homogeneous groups
-15	14	0.0254786	0.00133475	A
20	14	0.0213357	0.00133475	AB
40	21	7	0.0161095	B
60S	14	0.0193143	0.00133475	B

Table 109. Results from Method: 99.0 % Duncan.

Contrast	Sig.	Difference
-15 - 20		0.00414286
-15 - 40	*	0.00936905
-15 - 60S	*	0.00616429
20 - 40		0.00522619
20 - 60S		0.00202143
40 - 60S		-0.00320476

* it indicates a significant difference.

6.4.6. Summary of Results of Statistical Analysis for MSFRC-PF2

Table 110 summarizes the results obtained in the previous Subsections for MSFRC-PF2.

The time of exposure is clearly an important factor in the flexural behavior of this MSFRC reinforced with PF2 fibers since short- and long-term (3 and 180 days respectively) present significant differences on the three parameters f_{LOP}, f_{R1} and f_{R3}.

Temperature also affects f_{LOP}, f_{R1} and f_{R3}. At f_{LOP}, temperature of -15 °C is different from all the other levels (which have no differences between them) as happened with PF1 fibers. At f_{R1}, the effect is not pronounced since the difference between levels are similar, despite the factor being identified as significant. At f_{R3}, the effect is more significant than in f_{R1} and two ranges of temperature can be defined: from -15 up to 20 °C and to 20 up to 60 °C.

Table 110. Summary of the results of Statistical Analysis for MSFRC-PF2.

Variables	f_{LOP}	f_{R1}	f_{R3}
Time of exposure	3 d ≠ 180d	3 d ≠ 180d	3 d ≠ 180d
Temperature	M15 ≠ (20 = 40 = 60S)	This parameter is affected in a minor extent (M15 = 20 = 40 = 60S)	Two ranges are distinguished: from -15 up to 20 °C, and to 20 up to 60 °C.

6.5. Statistical Study of Flexural Strengths of MSFRC (PF3) at Extreme Environmental Conditions

This statistical study (Analysis #4) is performed to identify mainly if the extreme environmental condition (temperature) is an important factor on the flexural behavior of MSFRC-PF3 over time. The variables analyzed are f_{LOP}, f_{R1}, f_{R1}/N, f_{R3} and f_{R3}/N.

6.5.1. f_{LOP}

In this Subsection, f_{LOP} is analyzed as dependent variable for MSFRC-PF3. The two factors used to perform the analysis were: time of exposure and temperature. The factor "fc" is not considered in this analysis since it is contemplated as a linear combination by the software. The results from the ANOVA test on f_{LOP} are collected in Table 111.

Table 111. Analysis of Variance for f_{LOP}.

Source	Square Sum (SS)	DF	Mean Square	F-Ratio	P-Value
MAIN EFFECTS					
A: TIME OF EXPOSURE	15.5495	1	15.5495	64.18	0.0000
B: TEMPERATURE	31.6226	3	10.5409	43.51	0.0000
RESIDUAL	10.4183	43	0.242287		
TOTAL (CORR.)	60.9493	47			

As shown in Table 111, all the considered factors are significant. "Temperature" and "Time" factors have a P-Value = 0.0000, both lower than 0.05. After that, a multiple comparison procedure (Duncan at the 99.0 % confidence level) was applied to determine which means significantly different from others on "Temperature".

a) Inter-groups variability – temperature effects

In Table 112, three different groups, according to the letters in columns for f_{LOP} per temperature are defined. Both levels of extreme temperatures show significant differences with 20 and 40 °C temperatures and no remarkable difference are noted between 20 and 40 °C. Table 113 displays the estimated differences between each pair of levels.

Table 112. Multi-Range Test for f_{LOP} per "Temperature".

TEMPERATURE	Cases	LS Mean	S Sigma	Homogeneous groups
-15	13	5.26684	0.136647	A
20	14	3.84413	0.131553	B
40	7	4.00497	0.201328	B
60S	14	3.13247	0.131553	C

Table 113. Results from Method: 99.0 % Duncan.

Contrast	Sig.	Difference
-15 - 20	*	1.42271
-15 - 40	*	1.26187
-15 - 60S	*	2.13437
20 - 40		-0.160841
20 - 60S	*	0.711657
40 - 60S	*	0.872498

* it indicates a significant difference.

6.5.2. f_{R1}

Secondly, a multi-factor analysis of variance for f_{R1} is performed (Table 114) to determine which factors have a statistically significant effect on this dependent variable. As in the previous Subsection, fc is not considered as an independent variable.

Table 114. Analysis of Variance for f_{R1}.

Source	Square Sum (SS)	DF	Mean Square	F-Ratio	P-Value
MAIN EFFECTS					
A: TIME OF EXPOSURE	2.32089	1	2.32089	20.29	0.0001
B: TEMPERATURE	2.64154	3	0.880513	7.70	0.0003
RESIDUAL	4.91777	43	0.114367		
TOTAL (CORR.)	10.2555	47			

"Time of exposure" and "Temperature" are statistically significant, with a P-Value = 0.0001 and 0.0003, respectively. After that, for "Temperature", Multiple Range Tests provided which means are significantly different from others (99.0 % Duncan).

a) Inter-groups variability – temperature effects

Table 115 shows the groups depending on the temperature level, and it can be said that both levels of extreme temperature (-15 and 60S) show differences between them, but similarities can be detected in both cases with 20 and 40 °C. Table 116 displays the estimated differences between each pair of levels, showing only significant differences when comparing the groups of -15 and 60 °C.

Table 115. Multi-Range Test for f_{R1} per "Temperature".

TEMPERATURE	Cases	LS Mean	S Sigma	Homogeneous groups
-15	13	1.91731	0.0938828	A
20	14	1.53988	0.0903828	AB
40	7	1.53548	0.138321	AB
60S	14	1.2958	0.0903828	B

Table 116. Results from Method: 99.0 % Duncan.

Contrast	Sig.	Difference
-15 - 20		0.377433
-15 - 40		0.381829
-15 - 60S	*	0.621512
20 - 40		0.00439605
20 - 60S		0.244079
40 - 60S		0.239683

* it indicates a significant difference.

6.5.3. f_{R1}/N

The previous analysis of variance was repeated for f_{R1}/N, and the results are included in Table 117.

Table 117. Analysis of Variance for f_{R1}/N.

Source	Square Sum (SS)	DF	Mean Square	F-Ratio	P-Value
MAIN EFFECTS					
A: TIME OF EXPOSURE	0.000156292	1	0.000156292	15.32	0.0003
B: TEMPERATURE	0.000175448	3	0.0000584825	5.73	0.0022
RESIDUAL	0.000428549	42	0.0000102035		
TOTAL (CORR.)	0.000781091	46			

"Time of exposure" and "Temperature" are statistically significant. After that, Multiple Range Tests is executed to solve which means are significantly different from others (99.0 % Duncan).

a) Inter-groups variability – temperature effects

In the case of groups depending on the “Temperature” factor, Table 118 shows that all the groups have effects from the 20°C group, except -15, as happened without considering the normalization by N. Table 119 displays the estimated differences between each pair of levels.

Table 118. Multi-Range Test for f_{R1}/N per “Temperature”.

TEMPERATURE	Cases	LS Mean	S Sigma	Homogeneous groups
-15	13	0.0173784	0.000886794	A
20	14	0.0134357	0.000853712	B
40	7	0.0142052	0.00130909	AB
60S	13	0.0125015	0.000886794	B

Table 119. Results from Method: 99.0 % Duncan.

Contrast	Sig.	Difference
-15 - 20	*	0.00394271
-15 - 40		0.00317321
-15 - 60S	*	0.00487692
20 - 40		-0.000769498
20 - 60S		0.000934214
40 - 60S		0.00170371

* it indicates a significant difference.

6.5.4. f_{R3}

Table 120 separates the variability of f_{R3} into influences due to various factors (time and temperature). In this case, fc is not included as a factor since it is considered by the software as a linear combination of other factors.

Table 120. Analysis of Variance for f_{R3}.

Source	Square Sum (SS)	DF	Mean Square	F-Ratio	P-Value
MAIN EFFECTS					
A: TIME OF EXPOSURE	3.75183	1	3.75183	14.94	0.0004
B: TEMPERATURE	7.78791	3	2.59597	10.34	0.0000
RESIDUOS	10.2973	41	0.251154		
TOTAL (CORR.)	21.2735	45			

In the case, the “Time” factor has a P-value = 0.0004, and “Temperature” factor appears with a P-Value = 0.0000; therefore, their effects on f_{R3} are statistically significant. After that, as previously, multi-range tests were applied, herein for f_{R3} per “Temperature”, with a 99.0 % confidence level.

a) Inter-groups variability – temperature effect

In the case of the “Temperature” factor, Table 121 and Table 122 collect the results from Duncan's multiple comparison test for f_{R3}. Remarkable differences are noticed between the extreme levels of temperature: -15 and high temperatures, 40 and 60 °C. For the rest, the influence of temperature is not clear.

Table 121. Multi-Range Test for f_{R3} per “Temperature”.

TEMPERATURE	Cases	LS Mean	S Sigma	Homogeneous groups
-15	12	2.87507	0.145294	A
20	13	2.38449	0.139133	AB
40	7	1.83099	0.205882	B
60S	14	1.89613	0.133939	B

Table 122. Results from Method: 99.0 % Duncan.

Contrast	Sig.	Difference
-15 - 20		0.490582
-15 - 40	*	1.04408
-15 - 60S	*	0.978945
20 - 40		0.553498
20 - 60S		0.488363
40 - 60S		-0.0651352

* it indicates a significant difference.

6.5.5. f_{R3}/N

Lastly, this analysis of variance is performed on MSFRC-PF3 to determine the significance of the factors on the dependent variable f_{R3}/N. As in the previous case, “fc” factor is not considered. Table 123 collects the results showing that, the “Time of exposure” factor has a P-value = 0.0007 and “Temperature” factor appears with a P-Value = 0.0000; therefore, their effects on f_{R3}/N are statistically significant.

Table 123. Analysis of Variance for f_{R3}/N.

Source	Square Sum (SS)	DF	Mean Square	F-Ratio	P-Value
MAIN EFFECTS					
A: TIME OF EXPOSURE	0.000218179	1	0.000218179	13.52	0.0007
B: TEMPERATURE	0.00056333	3	0.000187777	11.64	0.0000
RESIDUAL	0.000661579	41	0.0000161361		
TOTAL (CORR.)	0.00140738	45			

After that, a multiple comparison procedure was applied to determine which averages significantly different from others. The method Duncan's multiple comparison at the 99 % confidence level was applied on both significant factors.

a) Inter-groups variability – temperature effects

Per "Temperature", only one level of temperature shows remarkable differences between the other levels (see Table 124) or by those pairs in Table 125 that show statistically with a 99.0 % confidence level, indicated with an asterisk. These results present some differences with the obtained for the data without taking into account N. It is clear that -15 is the most influential level of temperature.

Table 124. Multi-Range Test for f_{R3}/N per "Temperature".

TEMPERATURE	Cases	LS Mean	S Sigma	Homogeneous groups
-15	12	0.0261787	0.0011646	A
20	13	0.0212094	0.00111522	B
40	7	0.0171651	0.00165024	B
60S	14	0.0177929	0.00107358	B

Table 125. Results from Method: 99.0 % Duncan.

Contrast	Sig.	Difference
-15 - 20	*	0.0049693
-15 - 40	*	0.00901362
-15 - 60S	*	0.00838585
20 - 40		0.00404432
20 - 60S		0.00341654
40 - 60S		-0.000627774

* it indicates a significant difference.

6.5.6. Summary of Results for MSFRC-PF3

Table 126 sums up the results obtained in the previous Subsections for MSFRC-PF3.

The time of exposure is a significant factor in the flexural behavior of this MSFRC reinforced with PF3 fibers. Short- and long-term exposures to temperatures (3 and 180 days respectively) produce significant differences on f_{LOP}, f_{R1} and f_{R3}.

Temperature also affects f_{LOP}, f_{R1} and f_{R3}. At f_{LOP}, temperature of -15 °C and 60 °C (extreme temperature) present significant differences from 20 and 40°C for MSFRC-PF3. At f_{R1}, a similar trend of f_{LOP} is detected, and the groups of -15 and 60S have clear differences. However, all the groups have certain similarities with the temperatures of 20 and 40°C (when not normalizing by N) or with 20°C (when normalizing by N). At f_{R3}, for the low temperature of -15 °C, the effect is greater than in f_{R1}, however, the rest of levels of temperature seem not to negatively affect this property, showing similar behavior between the groups 20, 40 and 60S.

Table 126. Summary of the results of Statistical Analysis for MSFRC-PF3.

Variables	f_{LOP}	f_{R1}	f_{R3}
Time of exposure	3 d ≠ 180d	3 d ≠ 180d	3 d ≠ 180d
Temperature	M15 ≠ (20 = 40) ≠ 60S	M15 ≠ 60S	M15 ≠ (20 = 40 = 60S)

6.6. Statistical Study of Flexural Strengths of SFRC at Extreme Environmental Conditions

Analysis #5 is executed to identify principally if the temperature is a main effect on SFRC's flexural behavior. The dependent variables analyzed are f_{LOP}, f_{R1}, f_{R1}/N, f_{R3} and f_{R3}/N.

6.6.1. f_{LOP}

First of all, the selected dependent variable is f_{LOP}. Three factors were selected to perform the analysis: time of exposure, temperature, and fc. The results from this analysis on f_{LOP} for SFRC-SF are collected in the form of table (Table 127). An effect of temperature, time of exposure and fc factors on f_{LOP} is observed.

Table 127. Analysis of Variance for f_{LOP}.

Source	Square Sum (SS)	DF	Mean Square	F-Ratio	P-Value
MAIN EFFECTS					
A: TIME OF EXPOSURE	9.39675	3	3.13225	16.52	0.0000
B: TEMPERATURE	26.5133	3	8.83776	46.62	0.0000
C: fc	4.95075	6	0.825126	4.35	0.0005
RESIDUAL	23.6977	125	0.189582		
TOTAL (CORR.)	119.293	137			

Additionally, as in the previous sections, Duncan's multiple comparison procedure is performed to determine which means are significantly different from others, with a 99% of confidence level.

a) Inter-groups variability – short-term vs. long-term effects

Table 128 shows two homogeneous groups that have been identified depending on the time of exposure. The results at 0, 3 and 90 days could be grouped the same homogeneous group and this group present a remarkable difference with the group formed by the results at 180 days. Table 129 shows the estimated differences between each pair of levels.

Table 128. Multi-Range Testing for f_{LOP} per "Time".

TIME OF EXPOSURE	Cases	LS Mean	S Sigma	Homogeneous groups
0	68	3.84562	0.107782	A
3	25	3.85371	0.102379	A
90	17	3.80574	0.126213	A
180	28	4.68773	0.0957571	B

Table 129. Results from Method: 99.0 % Duncan.

Contrast	Sig.	Difference
0 - 3		-0.00809117
0 - 90		0.0398816
0 - 180	*	-0.842115
3 - 90		0.0479728
3 - 180	*	-0.834024
90 - 180	*	-0.881997

* it indicates a significant difference.

b) Inter-groups variability – temperature effects

Table 130 shows the groups depending on the temperature, and it can be said that -15 °C is the most differentiated level. The rest of levels present certain similarities between them. The groups 20 and 20S show no differences between them. Regarding high temperatures, no differences were detected between 20 and 60S while some differences were detected between 20S and 60S. Table 131 shows the estimated differences between each pair of levels and corroborate numerically the results in Table 130. These results are in line with the results for MSFRCs, indicating that low temperatures affect f_{LOP} in a great extent.

Table 130. Results of Multi-Range Test for f_{LOP} per temperature.

TEMPERATURE	Cases	LS Mean	S Sigma	Homogeneous groups
-15	20	5.43847	0.1264	A
20	81	3.58636	0.097019	BC
20S	12	3.8223	0.167732	B
60S	25	3.34567	0.1355	C

Table 131. Results from Method: 99.0 % Duncan.

Contrast	Sig.	Difference
-15 - 20	*	1.85211
-15 - 20S	*	1.61617
-15 - 60S	*	2.0928
20 - 20S		-0.23594
20 - 60S		0.240687
20S - 60S	*	0.476627

* it indicates a significant difference.

6.6.2. f_{R1}

Table 132 and Table 133 summarize the results of applying the ANOVA analysis for SFRC-SF on the dependent variable f_{R1}. In this case, the “Time of exposure” factor appears with a P-Value = 0.0000, that is its effect on f_{R1} is statistically significant, as well as fc. “Temperature” factor is not considered influential for this variable.

Table 132. Analysis of Variance for f_{R1}.

Source	Square Sum (SS)	DF	Mean Square	F-Ratio	P-Value
MAIN EFFECTS					
A: TIME OF EXPOSURE	4.2249	3	1.4083	10.09	0.0000
B: TEMPERATURE	0.182241	3	0.0607471	0.44	0.7283
C: fc	6.23914	6	1.03986	7.45	0.0000
RESIDUAL	17.594	126	0.139635		
TOTAL (CORR.)	31.957	138			

Not considering temperature, this second ANOVA table is obtained. The ANOVA table decomposes the variability of f_{R1} in the effects of “Time” and “fc” since its P-Value is less than 0.05.

Table 133. Analysis of Variance for f_{R1}.

Source	Square Sum (SS)	DF	Mean Square	F-Ratio	P-Value
MAIN EFFECTS					
A: TIME OF EXPOSURE	4.56147	3	1.52049	11.03	0.0000
B: fc	7.86351	6	1.31058	9.51	0.0000
RESIDUAL	17.7762	129	0.1378		
TOTAL (CORR.)	31.957	138			

To determine which means are significantly different from others, Duncan’s Multiple Range Tests is performed in “Time of exposure”.

a) Inter-groups variability – short-term vs. long-term effects

The results from the analysis of multi-range test are tabulated in Table 134 and Table 135. It can be concluded that there are significant differences between results obtained after a short- period of time of exposure (0 and 3 days) and a long-term period (90 and 180 days).

Table 134. Results of Multi-Range Test for f_{R1} per "Time".

TIME OF EXPOSURE	Cases	LS Mean	S Sigma	Homogeneous groups
0	69	1.45257	0.0470831	A
3	27	1.31824	0.0792077	A
90	17	1.86917	0.0980701	B
180	26	1.81317	0.0806876	B

Table 135. Results from Method: 99.0 % Duncan.

Contrast	Sig.	Difference
0 - 3		0.134326
0 - 90	*	-0.416606
0 - 180	*	-0.360606
3 - 90	*	-0.550932
3 - 180	*	-0.494932
90 - 180		0.0559997

* it indicates a significant difference.

6.6.3. f_{R1}/N

Table 136 shows the ANOVA table for SFRC-SF to determine the significance of the factors on the dependent variable f_{R1}/N, showing that "Time of exposure" and "fc" have significant influences.

Table 136. Analysis of Variance for f_{R1}/N.

Source	Square Sum (SS)	DF	Mean Square	F-Ratio	P-Value
MAIN EFFECTS					
A: TIME OF EXPOSURE	0.00141895	3	0.000472984	9.07	0.0000
B: TEMPERATURE	0.000190466	3	0.000063488	61.22	0.3061
C: fc	0.00444728	6	0.000741213	14.22	0.0000
RESIDUAL	0.0064638	124	0.0000521274		
TOTAL (CORR.)	0.0150944	136			

Removing "Temperature" factor since this is not significant (P-value is equal to 0.3061), Table 137 is obtained. For f_{R1}/N, two factors are influential: time of exposure and fc, both with P-values = 0.0000 < 0.05.

Table 137. Analysis of Variance for f_{R1}/N.

Source	Square Sum (SS)	DF	Mean Square	F-Ratio	P-Value
MAIN EFFECTS					
A: TIME OF EXPOSURE	0.0015959	3	0.000531967	10.15	0.0000
B: fc	0.00519961	6	0.000866601	16.54	0.0000
RESIDUAL	0.00665426	127	0.0000523958		
TOTAL (CORR.)	0.0150944	136			

Additionally, to determine which means are significantly different from others, Multiple Range Tests was performed per "Time of exposure".

a) Inter-groups variability – short-term vs. long-term effects

In Table 138, two homogeneous groups have been identified clearly differentiating the groups of short- (0 and 3 days) and long-term (90 and 180 days) results. Table 139 displays the estimated differences between each pair of levels. The asterisk indicates that these pairs show statistically significant differences with a 99.0 % confidence level.

Table 138. Results of Multi-Range Test for f_{R1}/N per "Time".

TIME OF EXPOSURE	Cases	LS Mean	S Sigma	Homogeneous groups
0	67	0.0299863	0.000931497	A
3	27	0.0286826	0.00154611	A
90	17	0.0391701	0.00191424	B
180	26	0.0361259	0.00157483	B

Table 139. Results from Method: 99.0 % Duncan.

Contrast	Sig.	Difference
0 - 3		0.00130373
0 - 90	*	-0.00918381
0 - 180	*	-0.00613958
3 - 90	*	-0.0104875
3 - 180	*	-0.00744331
90 - 180		0.00304423

* it indicates a significant difference.

6.6.4. f_{R3}

Table 140 collects the results of the ANOVA test for f_{R3} of SFRC-SF. In this case, only fc factor has an effect on f_{R3} statistically significant.

Table 140. Analysis of Variance for f_{R3}.

Source	Square Sum (SS)	DF	Mean Square	F-Ratio	P-Value
MAIN EFFECTS					
A: TIME OF EXPOSURE	0.504265	2	0.252133	2.11	0.1251
B: TEMPERATURE	0.244755	3	0.081585	0.68	0.5634
C: fc	3.47293	6	0.578821	4.85	0.0002
RESIDUAL	14.7884	124	0.119262		
TOTAL (CORR.)	24.3011	135			

6.6.5. f_{R3}/N

Lastly, the analysis of variance is performed on SFRC-SF to determine the significance of the factors on the dependent variable f_{R3}/N (Table 141).

Table 141. Analysis of Variance for f_{R3}/N.

Source	Square Sum (SS)	DF	Mean Square	F-Ratio	P-Value
MAIN EFFECTS					
A: TIME OF EXPOSURE	0.000160961	2	0.0000804803	2.04	0.1343
B: TEMPERATURE	0.000138524	3	0.0000461748	1.17	0.3237
C: fc	0.00273107	6	0.000455178	11.54	0.0000
RESIDUAL	0.00481042	122	0.0000394297		
TOTAL (CORR.)	0.0107636	133			

6.6.6. Summary of Results for SFRC-SF

Table 142 sumps up the results of previous Subsections for SFRC.

The time of exposure is a significant factor in the flexural behavior of concrete reinforced with SF fibers. Short- (0 and 3 days) and long-term (180 days) exposures to temperatures produce significant differences on f_{LOP} and f_{R1} but not on f_{R3}. The results after 90 days of exposure are grouped with the short-term exposure for f_{LOP} and with the long term for f_{R1}.

Temperature effect is clearly important at f_{LOP}, especially for the temperature of -15 °C, and no clear differences have been detected for warm temperatures. On the contrary, for residual flexural strengths (f_{R1} and f_{R3}), temperature is not a significant factor.

Table 142. Summary of the results of Statistical Analysis for SFRC-SF.

Variables	f_{LOP}	f_{R1}	f_{R3}
Time of exposure	(0 = 3 = 90 d) ≠ 180 d	(0 = 3 d) ≠ (90 = 180 d)	This factor is not influential
Temperature	M15 ≠ (20; 20S; 60S) 20 = 20S	This factor is not influential	This factor is not influential

6.7. General Summary of the Statistical Study of Flexural Strengths of FRCs at Extreme Environmental Conditions over Time

In this Subsection, a global summary of the statistical analysis of all the results is carried out.

6.7.1. Effects of Extreme Environmental Conditions (temperature)

The ANOVA analysis showed the variability of $\boldsymbol{f_{LOP}}$ into contributions due to various factors in MSFRCs as well as SFRC. In both types of FRCs, temperature can be considered a statistically significant factor. For SFRC, only M15 (-15 °C) showed statistically significant differences between the studied temperature levels. For MSFRCs with fibers type PF1 and PF2, this analysis showed also statistically significant differences only between the extreme level of low temperature - 15 °C and the rest of temperatures. However, in the case of fiber type PF3, the level of 60°C could also be differentiated from the rest.

Temperature produces variations in $\boldsymbol{f_{R1}}$ for both type of FRCs, however, they are not significant since a statistical point of view for SFRC and MSFRC-PF1. Certain influence produced by temperature is detected for concretes reinforced with PF2 and PF3 fibers. In the case of MSFRC-PF2, the effect is only of a minor extent since the analysis of the applied multiple comparison procedure (99.0 % Duncan) did not show statistically significant differences in f_{R1} mean values (P-Values ≤ 0.01). In the case of PF3, it showed differences only between extreme temperatures (M15 ≠ 60S).

On the other hand, $\boldsymbol{f_{R3}}$ experienced the effects of temperature factor in its variability only for MSFRCs and not in SFRC, but in any case, the influence detected is limited from a general view. In MSFRC-PF1, according to the multiple comparison procedure applied, no groups whose means significantly different from others can be determined, thus the effect of all the levels can be considered as equal (unclear differences are shown in f_{R3}). In MSFRC-PF2, two range of responses are distinguished depending on temperature: from -15 up to 20 °C, and to 20 up to 60 °C. In MSFRC-PF3, M15 shows significant differences from the rest of conditions, which are all similar. Table 143 displays the percentage of reduction that the values of f_{R3} experiment for each type of MSFRC at 60 °C.

Table 143. Percentage of reduction at 60 °C for $\boldsymbol{f_{R3}}$.

MSFRCs	% of reduction for $\boldsymbol{f_{R3}}$ at 60 °C
PF1	-10
PF2	-17
PF3	-21

6.7.2. Other effects

In all these cases, the results from performing the ANOVA analyses are consistent either if the **normalization by the total number of fibers** at cross-section (N) is considered or not. Additionally, immersion conditions do not show statistically significant differences with air conditions for all the performed tests (20 vs 20S), thus the influence of the **humidity** at these temperatures does not seem to be relevant for the studied properties.

From this statistical study, it could be also said that the **presence of a crack** when exposing the elements to the extreme temperatures, that is, the "state" factor that differentiates non-pre-cracked and pre-cracked elements, affects only slightly the behavior of FRC subjected at temperatures, but these are not significant from a statistical point of view (as shown in Analysis #1). This analysis was performed on 413 specimens (non-pre-cracked and pre-cracked) and the P-Value obtained was 0.9073, higher than 0.05. Therefore, this factor (state) does not have an effect statistically significant on f_{R3} with a 95.0 % confidence level. Equal results are obtained for f_{R3}/N with a P-Value = 0.5023.

Regarding to the **time of exposure**, it is clear that there is a significant difference between 3- and 180- days' results for all the dependent variables studied. The results after 90 days, depending on the case, are grouped with 3- days' results or with 180-days' results. It is also important to point out that 3 days of exposure to the temperatures is enough time to see differences with results obtained without exposure (0 days).

Regarding to the **type of fibers**, they influence the results of f_{R1} and f_{R3} for certain values of temperatures (even among the different types of PP fibers). This result indicates that the selection of fibers is important to choose the most suitable material depending on the application and climate conditions.

To sum up, the exploratory data analysis tool has facilitated the identification of influences from different factors and the obtained information is the base for the equations proposals in the next Section.

6.8. Proposal of Simple Numerical Equations for Flexural Behavior of FRCs under Different Extreme Environment Conditions

In previous Sections, statistical analysis based on the experimental tests have confirmed the effect of temperatures on the flexural behavior of FRCs, as well as time of exposure or fiber type. In this Section 6.8, different equations (regression lineal models) are proposed to correlate the mechanical properties investigated (f_{LOP}, f_{R1}, f_{R1}/N, f_{R3} and f_{R3}/N) with the studied parameters that influence the flexural behavior of the tested FRCs, including temperature. As values of N, for each type of fiber (PF1, PF2, PF3 and SF), the mean value has been selected respectively (considering all the specimens, at short-term as well as long-term): 100, 70, 110, and 50.

The equations proposed in [24] require calibration for both SFRC and MSFRC to incorporate parameters that accurately represent their behavior in realistic scenarios, thereby improving prediction accuracy and material reliability. Drawing on the experiences of certain authors [162,238], it is evident that the existing FRC constitutive equations, which serve as a reference for design engineers and practitioners, need adjustments to properly capture post-cracking behavior, particularly in relation to temperature effects. Correction factors are required to precisely predict FRC behavior under varying environmental conditions, influenced by fiber type or quantity. Adjustments typically made in MSFRC formulations involve reducing residual strength at early stages (for CMOD < 0.5 mm) due to the tendency of constitutive equations to overestimate flexural strengths [162].

The objective of this Section is to propose straightforward equations that characterize the flexural strengths, both at peak load and residual, for FRC mixes (MSFRC and SFRC) under extreme temperature conditions. These equations encompass the effects of all significant factors identified in preceding Sections, without accounting for potential interactions among them.

6.8.1. Numerical Equations for Flexural Behavior of MSFRC-PF1

Equations to predict the flexural behavior for MSFRC-PF1 under different environmental conditions are presented in this Subsection. After determining the factors that have an effect statistically from a statistical point of view on the dependent variables studied (through ANOVA tests), the objective of this regression study is to obtain a mathematical expression that estimates the values of f_{LOP}, f_{R1}, f_{R1}/N, f_{R3} and f_{R3}/N respectively, from those factors. With this purpose, stepwise regressions were implemented by means of the commercial software Statgraphics Centurion 19. The method adopted is forward selection with an Alpha to enter of 0.05 and an Alpha to change of 0.05 for all the cases.

It is important to point out that the results obtained are applicable for fibers that have similar properties to those used in this study and the temperature range for these models is -15 to 60 °C.

a) f_{LOP}

Firstly, multiple regression analysis is performed for the dependent variable f_{LOP} in function on time of exposure, fiber, temperature, and fc. The number of observations is 188. All the data of MSFRC-PF1 are considered since no significative differences were detected depending on the state factor. The equation suggested for the strength at LOP (in MPa) in MSFRC-PF1 is Equation (7):

$$f_{LOP} = 5.43 + \frac{6.3}{1000} * \mathrm{t} - \frac{24}{1000} * \mathrm{T} - \frac{37}{1000} * f_c \qquad \textbf{Equation (7)}$$

where t –time of exposure to target temperature, in days; T – target temperature, in Celsius and fc – compressive strength, in MPa.

Estimates of coefficients in Equation (7) are shown in Table 144. In the Parameter column, the factors that have been considered in the regression study and a factor “Constant” of the equation are collected. The P-Values indicate the significance of introducing the factor in the model. Thus, those that appear with a p-value > 0.05 are those whose consideration or non-consideration in the model does not especially affect the level of adjustment obtained.

Table 144. Estimation of coefficients and significance test (Equation (7)).

Parameter	Estimate	Std. error	T Statistic	P-value
CONSTANT	5.4261	0.499407	10.8651	0.0000
TIME OF EXPOSURE	0.00630661	0.000713435	8.83978	0.0000
TEMPERATURE	-0.0245876	0.00258177	-9.52355	0.0000
fc	-0.036584	0.0132971	-2.75127	0.0065

In Table 145, the analysis of variance of the whole model is displayed. This indicates a significant relationship between factors and response variable which is worth the modelling since p-value is < 0.005. The R-Square value is 46.38 %.

Table 145. Analysis of Variance of the simple model presented in Equation (7).

Source	Square Sum (SS)	DF	Mean Square	F-Ratio	P-Value
Model	70.1901	3	23.3967	53.05	0.0000
Residual	81.1422	184	0.44099		
Total (Corr.)	151.332	187			

b) f_{R1}

Secondly, multiple regression analysis is performed for the dependent variable f_{R1} (in MPa) in MSFRC-PF1 in function on time of exposure since it was the only factor that had a significantly effect, according to the ANOVA test. The number of observations is 185. The model in Equation (8) is proposed:

$$f_{R1} = 1.69 + \frac{3.3}{1000} * \mathrm{t}$$ **Equation (8)**

where t –time of exposure to target temperature, in days.

Estimates of coefficients in Equation (8) are shown in Table 146. “Time of exposure” factor is included in the final equation proposed since it is significant. In Table 147, the analysis of variance of the whole model is displayed. The R-Square value is 17.54 %.

Table 146. Estimation of coefficients and significance test (Equation (8)).

Parameter	Estimate	Std. error	T Statistic	P-value
CONSTANT	1.68712	0.0484963	34.7886	0.0000
TIME OF EXPOSURE	0.00336237	0.000538783	6.24067	0.0000

Table 147. Analysis of Variance of the model presented in Equation (8).

Source	Square Sum (SS)	DF	Mean Square	F-Ratio	P-Value
Model	11.5571	1	11.5571	38.95	0.0000
Residual	54.3048	183	0.296747		
Total (Corr.)	65.8619	184			

c) f_{R1}/N

Multiple regression analysis is also performed for the dependent variable f_{R1}/N (in MPa) in MSFRC-PF1 (considering N = 100) in function on time of exposure, according to the ANOVA test. The number of observations is 184. The model in Equation (9) is proposed:

$$f_{R1} = 1.9 + \frac{2.8}{1000} * \mathrm{t}$$ **Equation (9)**

where t –time of exposure to target temperature, in days.

Estimates of coefficients in Equation (9) are shown in Table 148. “Time of exposure” factor is included in the final equation proposed since it is significant. In Table 149, the analysis of variance of the whole model is displayed. The R-Square value is 17.33 %.

Table 148. Estimation of coefficients and significance test (Equation (9)).

Parameter	Estimate	Std. error	T Statistic	P-value
CONSTANT	0.0190001	0.000408006	46.5681	0.0000
TIME OF EXPOSURE	0.000027922	0.00000452059	6.17663	0.0000

Table 149. Analysis of Variance of the model presented in Equation (9).

Source	Square Sum (SS)	DF	Mean Square	F-Ratio	P-Value
Model	0.000794969	1	0.000794969	38.15	0.0000
Residual	0.00379244	182	0.0000208376		
Total (Corr.)	0.00458741	183			

d) f_{R3}

Multiple regression analysis was performed for the dependent variable f_{R3} (in MPa) in MSFRC-PF1 in function on time and temperature since those factors had a significantly effect in the selected dependent variable, according to the ANOVA test. The number of observations is also 182. The simple model in Equation (10) is proposed:

$$f_{R3} = \quad 2.37 + \frac{4.3}{1000} * \mathrm{t} - \frac{7.4}{1000} * \mathrm{T}$$ **Equation (10)**

where t– time of exposure to target temperature, in days, and T – temperature of exposure, in Celsius.

Estimate of coefficients in Equation (10) are presented in Table 150. The analysis of variance of the whole model is displayed in Table 151. The R-Square value is 17.20 %.

Table 150. Estimation of coefficients and significance test (Equation (10)).

Parameter	Estimate	Std. error	T Statistic	P-value
CONSTANT	2.36558	0.109483	21.6067	0.0000
FIBER	0.00432734	0.00081359	5.31882	0.0000
TEMPERATURE	-0.00735082	0.0024468	-3.00426	0.0030

Table 151. Analysis of Variance of the model presented in Equation (10).

Source	Square Sum (SS)	DF	Mean Square	F-Ratio	P-Value
Model	28.2006	2	14.1003	18.59	0.0000
Residual	135.739	179	0.758318		
Total (Corr.)	163.94	181			

e) f_{R3}/N

Lastly, multiple regression analysis was performed for the dependent variable f_{R3}/N (in MPa) in MSFRC-PF1 (considering N = 100) in function on time and temperature since those factors had a significantly effect in the selected dependent variable, according to the ANOVA test. The number of observations is also 182. The model in Equation (11) is proposed:

$$f_{R3} = 2.6 + \frac{4.1}{1000} * \mathrm{t} - \frac{6.4}{1000} * \mathrm{T} \qquad \textbf{Equation (11)}$$

where t– time of exposure to target temperature, in days, and T – temperature of exposure, in Celsius.

Estimates of coefficients in Equation (11) are presented in Table 152. The analysis of variance of the whole model is displayed in Table 153. The R-Square value is 21.77 %.

Table 152. Estimation of coefficients and significance test (Equation (11)).

Parameter	Estimate	Std. error	T Statistic	P-value
CONSTANT	0.0261536	0.000888883	29.4231	0.0000
FIBER	0.0000414908	0.00000660544	6.28131	0.0000
TEMPERATURE	-0.0000644397	0.0000198653	-3.24384	0.0014

Table 153. Analysis of Variance of the model presented in Equation (11).

Source	Square Sum (SS)	DF	Mean Square	F-Ratio	P-Value
Model	0.00249004	2	0.00124502	24.91	0.0000
Residual	0.00894738	179	0.0000499854		
Total (Corr.)	0.0114374	181			

6.8.2. Numerical Equations for Flexural Behavior of MSFRC-PF2

The same process was done for obtaining the equations to predict the flexural behavior for MSFRC-PF2 under different environmental conditions.

a) f_{LOP}

Firstly, multiple regression analysis is performed for the dependent variable f_{LOP} in function on time of exposure and temperature. These factors were selected through the previous ANOVA tests. The number of observations is 49. The equation suggested for the strength at LOP (in MPa) in MSFRC-PF2 is the following (Equation (12)):

$$f_{LOP} = 4.49 + \frac{4.6}{1000} * \mathrm{t} - \frac{30}{1000} * \mathrm{T}$$ **Equation (12)**

where t – time of exposure to target temperature, in days, and T – target temperature, in Celsius.

Estimates of coefficients in Equation (12) are shown in Table 154 and in Table 155, the analysis of variance of the whole model is displayed. This indicates a significant relationship between factors and response variable which is worth the modelling since p-value is < 0.005. The R-Square value is 64.03 %.

Table 154. Estimation of coefficients and significance test (Equation (12)).

Parameter	Estimate	Std. error	T Statistic	P-value
CONSTANT	4.48653	0.181181	24.7627	0.0000
TIME OF EXPOSURE	0.00463257	0.00120432	3.84662	0.0004
TEMPERATURE	-0.0307053	0.00362697	-8.46581	0.0000

Table 155. Analysis of Variance of the simple model presented in Equation (12).

Source	Square Sum (SS)	DF	Mean Square	F-Ratio	P-Value
Model	44.3782	2	22.1891	40.94	0.0000
Residual	24.9299	46	0.541955		
Total (Corr.)	69.3081	48			

b) f_{R1}

Multiple regression analysis is performed for the dependent variable f_{R1} (in MPa) in MSFRC in function on time and temperature, since those factors had a significantly effect in the selected dependent variable, according to the ANOVA test. The number of observations is 48. The linear equation in Equation (13) is proposed:

$$f_{R1} = 1.15 + \frac{2.5}{1000} * \mathrm{t} - \frac{3.9}{1000} * \mathrm{T}$$ **Equation (13)**

where t – time of exposure to target temperature, in days, and T – target temperature, in Celsius.

Estimates of coefficients in the previous equation are shown in Table 156. “Time of exposure” and “Temperature” factors are included in the final equation proposed since both are significant. In Table 157, the analysis of variance of the whole model is displayed. The R-Square value is 37.83 %.

Table 156. Estimation of coefficients and significance test (Equation (13)).

Parameter	Estimate	Std. error	T Statistic	P-value
CONSTANT	1.1544	0.0826791	13.9625	0.0000
TIME OF EXPOSURE	0.00254135	0.000534762	4.7523	0.0000
TEMPERATURE	-0.00390543	0.00161905	-2.41218	0.0200

Table 157. Analysis of Variance of the model presented in Equation (13).

Source	Square Sum (SS)	DF	Mean Square	F-Ratio	P-Value
Model	0.00256239	2	0.00128119	72.82	0.0000
Residual	0.00341326	194	0.0000175941		
Total (Corr.)	0.00597565	196			

b) f_{R1}/N

Multiple regression analysis was performed for the dependent variable f_{R1}/N (in MPa) in MSFRC-PF2 (considering N = 70) in function time of exposure since this factor had a significantly effect in the selected dependent variable, according to the ANOVA test. The number of observations is also 48. The model in Equation (14) is proposed:

$$f_{R1} = \quad 1.05 + \frac{1.4}{1000} * \mathrm{t} \qquad \textbf{Equation (14)}$$

where t – time of exposure to target temperature, in days.

Estimates of coefficients in Equation (14) are presented in Table 158. The analysis of variance of the whole model is displayed in Table 159. The R-Square value is 32.48 %.

Table 158. Estimation of coefficients and significance test (Equation (14)).

Parameter	Estimate	Std. error	T Statistic	P-value
CONSTANT	0.0144943	0.000834836	17.3619	0.0000
TIME OF EXPOSURE	0.0000285634	0.00000607193	4.70416	0.0000

Table 159. Analysis of Variance of the model presented in Equation (14).

Source	Square Sum (SS)	DF	Mean Square	F-Ratio	P-Value
Model	0.00411089	3	0.0013703	33.25	0.0000
Residual	0.00795339	193	0.0000412093		
Total (Corr.)	0.0120643	196			

d) f_{R3}

Multiple regression analysis was performed for the dependent variable f_{R3} (in MPa) in MSFRC-PF2 in function on time and temperature since those factors had a significantly effect in the selected dependent variable, according to the ANOVA test. The number of observations is 49. The simple model in Equation (15) is proposed:

$$f_{R3} = \quad 1.5 + \frac{3}{1000} * \mathrm{t} - \frac{8}{1000} * \mathrm{T} \qquad \textbf{Equation (15)}$$

where t– time of exposure to target temperature, in days, and T – temperature of exposure, in Celsius.

Estimates of coefficients in Equation (15) are presented in Table 160. The analysis of variance of the whole model is displayed in Table 161. The R-Square value is 41.45 %.

Table 160. Estimation of coefficients and significance test (Equation (15)).

Parameter	Estimate	Std. error	T Statistic	P-value
CONSTANT	2.36558	0.109483	21.6067	0.0000
TIME OF EXPOSURE	0.00432734	0.00081359	5.31882	0.0000
TEMPERATURE	-0.00735082	0.0024468	-3.00426	0.0030

Table 161. Analysis of Variance of the model presented in Equation (15).

Source	Square Sum (SS)	DF	Mean Square	F-Ratio	P-Value
Model	28.2006	2	14.1003	18.59	0.0000
Residual	135.739	179	0.758318		
Total (Corr.)	163.94	181			

e) f_{R3}/N

Lastly, multiple regression analysis was performed for the dependent variable f_{R3}/N (in MPa) in MSFRC-PF2 (considering N = 70) in function on time and temperature since those factors had a significantly effect in the selected dependent variable, according to the ANOVA test. The number of observations is also 49. The model in Equation (16) is proposed:

$$f_{R3} \quad = \quad 1.4 + \frac{2.1}{1000} * \mathrm{t} - \frac{6.3}{1000} * \mathrm{T} \qquad \textbf{Equation (16)}$$

where t– time of exposure to target temperature, in days, and T – temperature of exposure, in Celsius.

Estimates of coefficients in Equation (16) are presented in Table 162. The analysis of variance of the whole model is displayed in Table 163. The R-Square value is 35.84 %.

Table 162. Estimation of coefficients and significance test (Equation (16)).

Parameter	Estimate	Std. error	T Statistic	P-value
CONSTANT	0.0205743	0.00126301	16.2899	0.0000
TIME OF EXPOSURE	0.0000319847	0.00000839531	3.80983	0.0004
TEMPERATURE	-0.0000918149	0.0000252836	-3.63141	0.0007

Table 163. Analysis of Variance of the model presented in Equation (16).

Source	Square Sum (SS)	DF	Mean Square	F-Ratio	P-Value
Model	0.000676849	2	0.000338424	12.85	0.0000
Residual	0.00121146	46	0.0000263361		
Total (Corr.)	0.00188831	48			

6.8.3. Numerical Equations for Flexural Behavior of MSFRC-PF3

The same process was done for obtaining the equations to predict the flexural behavior for MSFRC-PF3 under different environmental conditions.

a) f_{LOP}

Multiple regression analysis is performed for the dependent variable f_{LOP} in function on time of exposure and temperature. These factors were selected through the previous ANOVA tests. The number of observations is 48. The equation suggested for the strength at LOP (in MPa) in MSFRC-PF3 is Equation (17). Estimate of coefficients for this equation are shown in Table 164.

$$f_{LOP} = 4.02 + \frac{7.6}{1000} * \mathrm{t} - \frac{27}{1000} * \mathrm{T}$$ **Equation (17)**

where t– time of exposure to target temperature, in days, and T – temperature of exposure, in Celsius.

Table 164. Estimation of coefficients and significance test (Equation (17)).

Parameter	Estimate	Std. error	T Statistic	P-value
CONSTANT	4.01693	0.137885	29.1324	0.0000
TIME OF EXPOSURE	0.00761188	0.000891832	8.5351	0.0000
TEMPERATURE	-0.0269925	0.00270011	-9.99679	0.0000

In Table 165, the analysis of variance of the whole model is displayed. This indicates a significant relationship between factors and response variable which is worth the modelling since p-value is < 0.005. The R-Square value is 78.58 %.

Table 165. Analysis of Variance of the model presented in Equation (17).

Source	Square Sum (SS)	DF	Mean Square	F-Ratio	P-Value
Model	47.8963	2	23.9482	82.56	0.0000
Residual	13.053	45	0.290066		
Total (Corr.)	60.9493	47			

b) f_{R1}

Multiple regression analysis is performed for the dependent variable f_{R1} (in MPa) in MSFRC-PF3 in function on time and temperature, since those factors had a significantly effect in the selected dependent variable, according to the ANOVA test. The number of observations is 48. The model in Equation (18) is proposed:

$$f_{R1} = 1.51 + \frac{2.8}{1000} * \mathrm{t} - \frac{7.9}{1000} * \mathrm{T} \qquad \textbf{Equation (18)}$$

where t– time of exposure to target temperature, in days, and T – temperature of exposure, in Celsius.

Estimates of coefficients in Equation (18) are shown in Table 166. “Time of exposure” and “Temperature” factors are included in the final equation proposed since both are significant. In Table 167, the analysis of variance of the whole model is displayed. The R-Square value is 50.86 %.

Table 166. Estimation of coefficients and significance test (Equation (18)).

Parameter	Estimate	Std. error	T Statistic	P-value
CONSTANT	1.50803	0.0856768	17.6014	0.0000
TIME OF EXPOSURE	0.00283963	0.000554151	5.12428	0.0000
TEMPERATURE	-0.00795802	0.00167775	-4.74327	0.0000

Table 167. Analysis of Variance of the model presented in Equation (18).

Source	Square Sum (SS)	DF	Mean Square	F-Ratio	P-Value
Model	5.21584	2	2.60792	23.29	0.0000
Residual	5.03964	45	0.111992		
Total (Corr.)	10.2555	47			

c) f_{R1}/N

Multiple regression analysis was performed for the dependent variable f_{R1}/N (in MPa) in MSFRC-PF3 (considering N = 110) in function time of exposure and temperature since these factors had a significantly effect in the selected dependent variable, according to the ANOVA test. The number of observations is also 47. The model in Equation (19) is proposed:

$$f_{R3} = \quad 1.54 + \frac{2.2}{1000} * \mathrm{t} - \frac{6.6}{1000} * T \qquad \textbf{Equation (19)}$$

where t – time of exposure to target temperature, in days and T – target temperatures, in Celsius.

Estimates of coefficients in Equation (19) are presented in Table 168. The analysis of variance of the whole model is displayed in Table 169. The R-Square value is 41.34 %.

Table 168. Estimation of coefficients and significance test (Equation (19)).

Parameter	Estimate	Std. error	T Statistic	P-value
CONSTANT	0.0136634	0.000832051	16.4213	0.0000
TIME OF EXPOSURE	0.0000239737	0.00000543632	4.40992	0.0001
TEMPERATURE	-0.0000616348	0.0000164709	-3.74204	0.0005

Table 169. Analysis of Variance of the model presented in Equation (19).

Source	Square Sum (SS)	DF	Mean Square	F-Ratio	P-Value
Model	0.00411089	3	0.0013703	33.25	0.0000
Residual	0.00795339	193	0.0000412093		
Total (Corr.)	0.0120643	196			

d) f_{R3}

Multiple regression analysis was performed for the dependent variable f_{R3} (in MPa) in MSFRC-PF3 in function on time of exposure and time since those factors had a significantly effect in the selected dependent variable, according to the ANOVA test. The number of observations is 46. The simple model in Equation (20) is proposed:

$$f_{R3} = \quad 2.36 + \frac{3}{1000} * \mathrm{t} - \frac{13.8}{1000} * \mathrm{T} \qquad \textbf{Equation (20)}$$

where t– time of exposure to target temperature, in days, and T – temperature of exposure, in Celsius.

Estimates of coefficients in Equation (20) are presented in Table 170. The analysis of variance of the whole model is displayed in Table 171. The R-Square value is 49.20 %.

Table 170. Estimation of coefficients and significance test (Equation (20)).

Parameter	Estimate	Std. error	T Statistic	P-value
CONSTANT	2.36643	0.137223	17.2451	0.0000
TIME OF EXPOSURE	0.00308018	0.000855667	3.59974	0.0008
TEMPERATURE	-0.013805	0.00256512	-5.38183	0.0000

Table 171. Analysis of Variance of the model presented in Equation (20).

Source	Square Sum (SS)	DF	Mean Square	F-Ratio	P-Value
Model	10.4672	2	5.23361	20.83	0.0000
Residual	10.8063	43	0.251309		
Total (Corr.)	21.2735	45			

e) f_{R3}/N

Lastly, multiple regression analysis was performed for the dependent variable f_{R3}/N (in MPa) in MSFRC-PF3 (considering N = 110) in function on time and temperature since those factors had a significantly effect in the selected dependent variable, according to the ANOVA test. The number of observations is 46. The simple model in Equation (21) is proposed:

$$f_{R3} \; = \; 2.2 + \frac{2.5}{1000} * \mathrm{t} - \frac{13.2}{1000} * \mathrm{T}$$ **Equation (21)**

where t– time of exposure to target temperature, in days, and T – temperature of exposure, in Celsius.

Estimates of coefficients in Equation (21) are presented in Table 172. The analysis of variance of the whole model is displayed in Table 173. The R-Square value is 50.02 %.

Table 172. Estimation of coefficients and significance test (Equation (21)).

Parameter	Estimate	Std. error	T Statistic	P-value
CONSTANT	0.021832	0.00110711	19.7198	0.0000
TIME OF EXPOSURE	0.0000233313	0.00000690348	3.37964	0.0016
TEMPERATURE	-0.000116852	0.0000206953	-5.6463	0.0000

Table 173. Analysis of Variance of the model presented in Equation (21).

Source	Square Sum (SS)	DF	Mean Square	F-Ratio	P-Value
Model	0.00070398	2	0.00035199	21.52	0.0000
Residual	0.000703401	43	0.0000163582		
Total (Corr.)	0.00140738	45			

6.8.4. Numerical Equations for Flexural Behavior of SFRCs

The same process was done for obtaining the equations to predict the flexural behavior for SFRCs under different environmental conditions.

a) f_{LOP}

Firstly, multiple regression analysis is performed for the dependent variable f_{LOP} in function on time of exposure, temperature and fc. These factors are selected through the previous ANOVA tests. The number of observations is 138. The equation suggested for the strength at LOP (in MPa) in SFRC is Equation (22):

$$f_{LOP} = 2.32 + \frac{5.9}{1000} * \mathrm{t} - \frac{21.8}{1000} * \mathrm{T} + \frac{43}{1000} * \mathrm{fc}$$ **Equation (22)**

where t – time of exposure to target temperature, in days, T – temperature of exposure, in Celsius and fc – compressive strengths at 28 days at standard temperature, in MPa.

Estimates of coefficients and significance test in Equation (22) are presented in Table 174. The analysis of variance of the whole model is displayed in Table 175.The R-Square value is 53.74 %, similar to that obtained for MSFRCs for f_{LOP}.

Table 174. Estimation of coefficients and significance test (Equation (22)).

Parameter	Estimate	Std. error	T Statistic	P-value
CONSTANT	2.31542	0.527011	4.3935	0.0000
TIME OF EXPOSURE	0.00594791	0.000759491	7.83145	0.0000
TEMPERATURE	-0.0218755	0.00255007	-8.5784	0.0000

Table 175. Analysis of Variance of the model presented in Equation (22).

Source	Square Sum (SS)	DF	Mean Square	F-Ratio	P-Value
Model	64.1169	3	21.3723	51.90	0.0000
Residual	55.1758	134	0.41176		
Total (Corr.)	119.293	137			

b) f_{R1}

Multiple regression analysis is performed for the dependent variable f_{R1} in function on time of exposure and fc. These factors are selected through the previous ANOVA tests. The number of observations is 139. The equation suggested for f_{R1} (in MPa) in SFRC is Equation (23):

$$f_{R1} = -0.81 + \frac{2}{1000} * \mathrm{t} + \frac{59}{1000} * \mathrm{fc}$$ **Equation (23)**

where t – time of exposure to target temperature, in days, and fc – compressive strengths at 28 days at standard temperature, in MPa.

Estimates of coefficients and significance test in Equation (23) are presented in Table 176. The analysis of variance of the whole model is displayed in Table 177.The R-Square value is 37.22 %.

Table 176. Estimation of coefficients and significance test (Equation (23)).

Parameter	Estimate	Std. error	T Statistic	P-value
CONSTANT	-0.818073	0.313754	-2.60737	0.0101
TIME OF EXPOSURE	0.00210377	0.00046338	4.54005	0.0000
fc	0.0588727	0.00818206	7.19534	0.0000

Table 177. Analysis of Variance of the model presented in Equation (23).

Source	Square Sum (SS)	DF	Mean Square	F-Ratio	P-Value
Model	11.8929	2	5.94646	40.31	0.0000
Residual	20.0641	136	0.14753		
Total (Corr.)	31.957	138			

c) f_{R1}*/N*

Equation (24) is the simple numerical formulation calculated for the dependent variables f_{R1}/N (in MPa), considering N = 50. The number of observations is 137.The factors were previously determined through ANOVA tests.

$$f_{R1} = -1.45 + \frac{2.3}{1000} * \mathrm{t} + \frac{75}{1000} * fc \qquad \textbf{Equation (24)}$$

where t – time of exposure to target temperature, in days, T – temperature of exposure, in Celsius and fc – compressive strengths at 28 days at standard temperature, in MPa.

Estimates of coefficients and significance test in Equation (24) are presented in Table 178. The analysis of variance of the whole model is displayed in Table 179. The R-Square value is 48.32 %.

Table 178. Estimation of coefficients and significance test (Equation (24)).

Parameter	Estimate	Std. error	T Statistic	P-value
CONSTANT	-0.0292198	0.00628196	-4.65138	0.0000
TIME OF EXPOSURE	0.0000464384	0.00000922385	5.0346	0.0000
fc	0.00154146	0.000163499	9.42795	0.0000

Table 179. Analysis of Variance of the model presented in Equation (24).

Source	Square Sum (SS)	DF	Mean Square	F-Ratio	P-Value
Model	0.00729469	2	0.00364734	62.66	0.0000
Residual	0.00779971	134	0.0000582068		
Total (Corr.)	0.0150944	136			

d) f_{R3}

Multiple regression analysis was performed for the dependent variable f_{R3} (in MPa) in SFRC in function on fc since it had a significantly effect in the selected dependent variable, according to the ANOVA test. The number of observations is 136. The simple model in Equation (25) is proposed:

$$f_{R3} = -0.75 + \frac{58}{1000} * \text{fc}$$ **Equation (25)**

where fc – compressive strengths at 28 days at 20 °C, in MPa.

Estimate of coefficients in Equation (25) are presented in Table 180. The analysis of variance of the whole model is displayed in Table 181. The R-Square value is 30.28 %.

Table 180. Estimation of coefficients and significance test (Equation (25)).

Parameter	Estimate	Std. error	T Statistic	P-value
CONSTANT	-0.748414	0.293814	-2.54724	0.0120
fc	0.0581502	0.00762089	7.63037	0.0000

Table 181. Analysis of Variance of the model presented in Equation (25).

Source	Square Sum (SS)	DF	Mean Square	F-Ratio	P-Value
Model	7.36058	1	7.36058	58.22	0.0000
Residual	16.9405	134	0.126421		
Total (Corr.)	24.3011	135			

e) f_{R3}/N

Equation (26) is the simple numerical formulation calculated for the dependent variables f_{R3}/N (in MPa) in SFRC, considering N = 50. The number of observations is 136. The factors were previously determined through ANOVA tests. This equation is the following:

$$f_{R3} = -1.4 + \frac{75}{1000} * \text{fc}$$ **Equation (26)**

where fc – compressive strengths at 28 days at 20 °C, in MPa.

The coefficients predicted by these equations are tabulated in the following tables (see Table 182 and Table 183). The R-Square value is 47.75 %.

Table 182. Estimation of coefficients and significance test (Equation (26)).

Parameter	Estimate	Std. error	T Statistic	P-value
CONSTANT	0.0258776	0.00197826	13.081	0.0000
TIME OF EXPOSURE	0.0000789653	0.0000167164	4.72382	0.0000

Table 183. Estimation of coefficients and significance test (Equation (26)).

Parameter	Estimate	Std. error	T Statistic	P-value
CONSTANT	0.0259972	0.00146175	17.7849	0.0000
TIME OF EXPOSURE	0.000047962	0.0000124712	3.84583	0.0003

6.9. General Summary of the Regression Study

This regression study presented in the previous Subsections have allowed to evaluate the aging due to temperature in the pre- and post- flexural strengths on MSFRCs and SFRC. More than 400 specimens have been tested to detect whereas temperature is a potential parameter influencing the response of FRCs.

Table 184 and Table 185 sump up the obtained equations in the preceding Sections. In the former, N is not considered; in the second table, f_{LOP} is not included since this parameter is not divided by N. As can be seen, all the equations proposed are similar.

Table 184. Summary of the equations obtained for f_{LOP}, f_{R1} and f_{R3} for the different types of FRCs.

	f_{LOP}	f_{R1}	f_{R3}
MSFRC-PF1	$5.43 + \frac{6.3}{1000} * t - \frac{24}{1000} * T - \frac{37}{1000} * f_c$	$1.69 + \frac{3.3}{1000} * t$	$2.37 + \frac{4.3}{1000} * t - \frac{7.4}{1000} * T$
	R-Square 46.38%	*R-Square 17.54%*	*R-Square 17.20%*
MSFRC-PF2	$4.49 + \frac{4.6}{1000} * t - \frac{30}{1000} * T$	$1.15 + \frac{2.5}{1000} * t - \frac{3.9}{1000} * T$	$1.5 + \frac{3}{1000} * t - \frac{8}{1000} * T$
	R-Square 64.03%	*R-Square 37.83%*	*R-Square 41.45%*
MSFRC-PF3	$4.02 + \frac{7.6}{1000} * t - \frac{27}{1000} * T$	$1.51 + \frac{2.8}{1000} * t - \frac{7.9}{1000} * T$	$2.36 + \frac{3}{1000} * t - \frac{13.8}{1000} * T$
	R-Square 78.58%	*R-Square 50.86%*	*R-Square 41.34%*
SFRC	$2.32 + \frac{5.9}{1000} * t - \frac{21.8}{1000} * T + \frac{43}{1000} * fc$	$-0.81 + \frac{2}{1000} * t + \frac{59}{1000} * fc$	$-0.75 + \frac{58}{1000} * fc$
	R-Square 53.74%	*R-Square 37.22%*	*R-Square 30.28%*

In general terms, the “Temperature” factor affects f_{LOP} in great extent for all FRCs studied, but its effect on f_{R1} and f_{R3} is more limited. For f_{LOP}, the coefficients for T (Temperature) are between 21.8 and 30, they are in the same range of magnitude. For f_{R1}, MSFRC-PF1 and SFRC are not affected by T. MSFRC-

PF3 is the most affected by T (almost the double of MSFRC-PF2 that is also affected), but in a minor extent. The effect of T in f_{R3} can be seen comparing the coefficients of T para MSFRC-PF1, PF2 and PF3 (they are 7.4/1000, 8/1000 and 13.8/1000, respectively).

Regarding to R-square values, they may be considered relatively good in terms of prediction for the studied properties. The proposed equations can explain approximately 50 % of f_{LOP} in the cases of MSFRC- PF1 and SFRC. For MSFRC-PF2 and PF3, more than 50 % of the f_{LOP} is predicted by the independent variables. In terms of fitting, MSFRC-PF1 presents the lower results for the residual strengths.

Table 185. Summary of the equations obtained for f_{R1} and f_{R3} (considering N) for the different types of FRCs.

	f_{R1}	f_{R3}	N
MSFRC-PF1	$1.9 + \frac{2.8}{1000} * t$ *R-Square 17.33%*	$2.6 + \frac{4.1}{1000} * t - \frac{6.4}{1000} * T$ *R-Square 21.77%*	100
MSFRC-PF2	$1.05 + \frac{1.4}{1000} * t$ *R-Square 32.48%*	$1.4 + \frac{2.1}{1000} * t - \frac{6.3}{1000} * T$ *R-Square 35.84%*	70
MSFRC-PF3	$1.54 + \frac{2.2}{1000} * t - \frac{6.6}{1000} * T$ *R-Square 41.34%*	$2.2 + \frac{2.5}{1000} * t - \frac{13.2}{1000} * T$ *R-Square 50.02%*	110
SFRC	$-1.45 + \frac{2.3}{1000} * t + \frac{75}{1000} * fc$ *R-Square 48.32%*	$-1.4 + \frac{75}{1000} * fc$ *R-Square 47.75%*	50

The inclusion of the number of fibers (N) in the equations slightly reduce the temperature effect in all the studied cases. Comparing the coefficients of T in both previous tables, it can be observed that, for MSFRC-PF1, they change from 7.4/1000 to 6.4/1000 for f_{R3}. For MSFRC-PF2, they change from 3.9/1000 to not be affected by T for f_{R1}, and 8/1000 to 6.3/1000 for f_{R3}. For MSFRC-PF3, they change from 7.9/1000 to 6.6/1000 for f_{R1}, and 13.8/1000 to 13.2/1000 for f_{R3}.

It is important to remind that the results obtained are applicable for fibers that have similar properties to those used in this study and the temperature range for these models is -15 to 60 °C.

6.9.1. Response Surfaces

From the previous equations, the following response surfaces are generated for each dependent variable studied f_{LOP} , f_{R1} and f_{R3} for MSFRCs and SFRC. The response surfaces for the variables divided by N have not been included herein because they show many similarities.

Applying Equation (7), Equation (8) and Equation (10) for the different environmental conditions and fixing fc in 37 MPa, the surface for each variable dependent of MSFRC-PF1 over time are obtained (see Figure 105).

Applying Equation (12), Equation (13) and Equation (15) for the range of temperatures and time of exposure of this study, and fixing fc in 37 MPa, the following response surfaces are generated for each dependent variable studied for MSFRC with PF2 fibers (see Figure 106).

Applying Equation (17), Equation (18) and Equation (20) for the range of temperatures and time of exposure of this study, and fixing fc in 37 MPa, the following response surfaces are generated for each dependent variable studied for MSFRC-PF3 (see Figure 107).

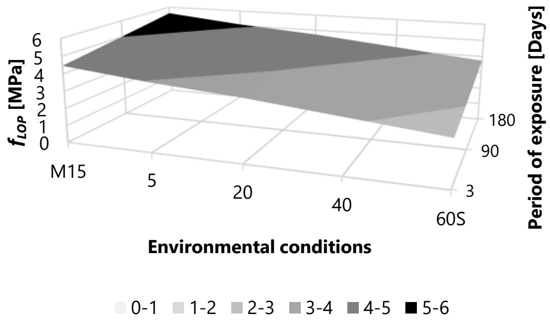

(a)

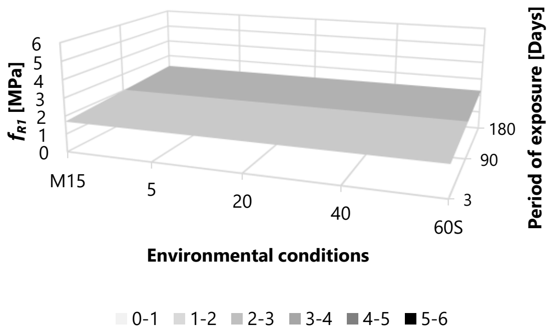

(b)

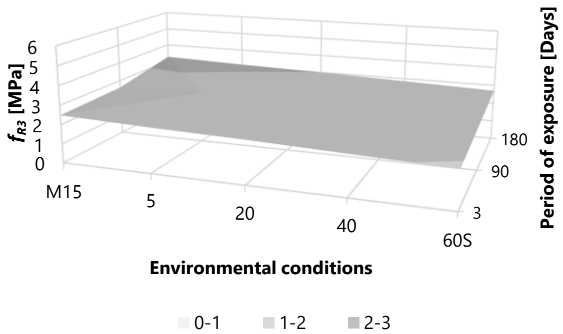

(c)

Figure 105. Response surface for MSFRC-PF1 over time: (a) f_{LOP}, (b) f_{R1}, and (c) f_{R3}.

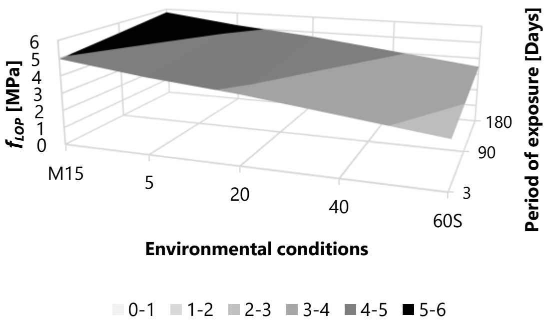

(a)

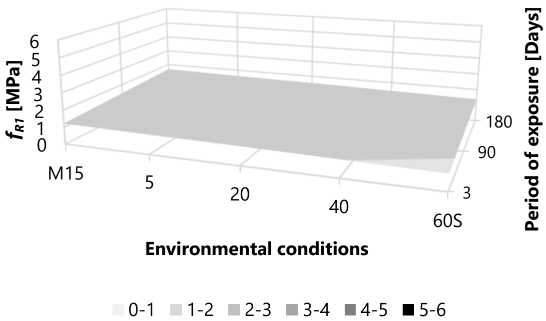

(b)

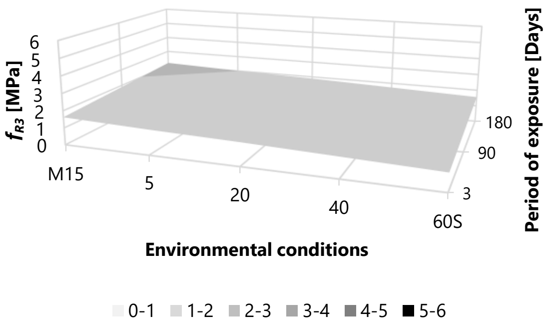

(c)

Figure 106. Response surface for MSFRC-PF2 over time: (a) f_{LOP}, (b) f_{R1} and (c) f_{R3}.

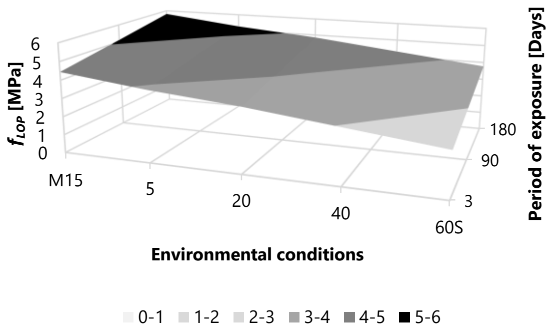

(a)

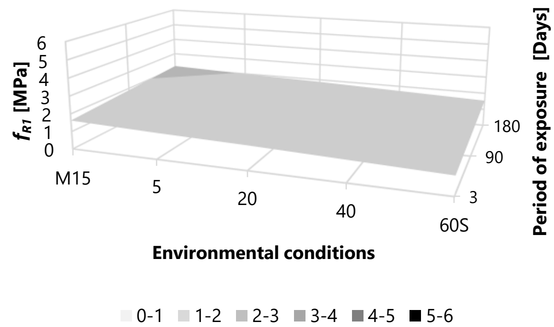

(b)

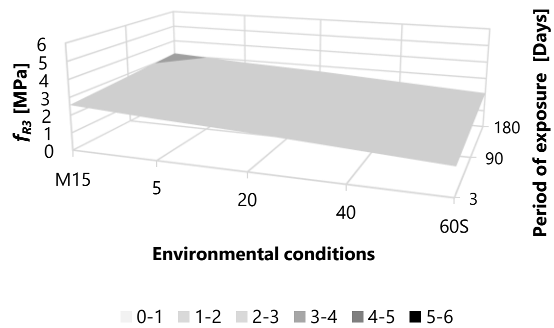

(c)

Figure 107. Response surface for MSFRC-PF3 over time: (a) f_{LOP}, (b) f_{R1} and (c) f_{R3}.

Applying Equations (16), (17) and (19) for the range of temperatures and time of exposure of this study, the graphics in Figure 108 are produced for each dependent variable studied (f_{LOP}, f_{R1} and f_{R3}) in SFRC, fixing fc in 37 MPa.

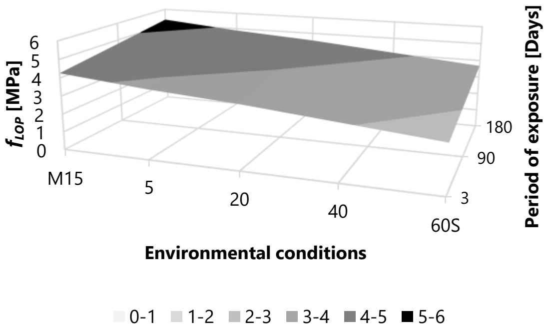

(a)

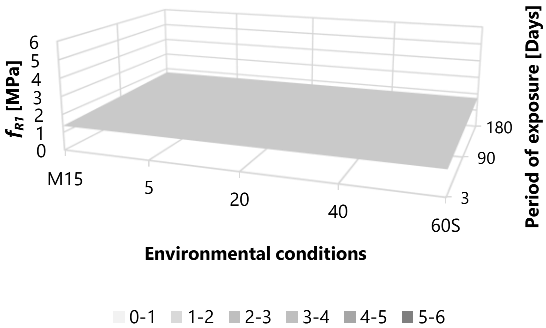

(b)

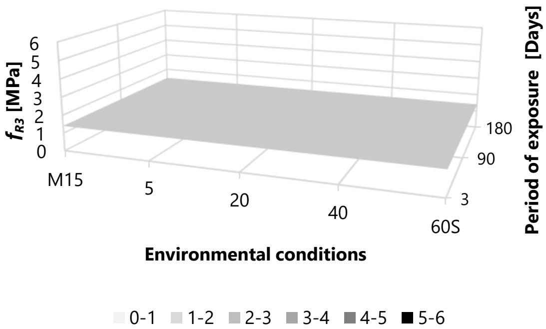

(c)

Figure 108. Response surface for SFRC over time: (a) f_{LOP}, (b) f_{R1} and (c) f_{R3}.

All the results obtained in this Chapter 6 aim to serve as a starting point for future validations of more advanced numerical models as those stated in [161,238].

The relationships obtained let predict each dependent variable in function the effect of the real environmental conditions over time, so that designers and practitioners will adequately predict structural behavior at temperatures after a period of time.

Additionally, it evaluates the mechanical performance of both MSFRC and SFRC under identical environmental scenarios and exposure durations, revealing comparable outcomes. This is an innovative approach which might make possible a better evaluation of the performance for engineering structures, since none of the previous Codes and Standards accounted for the influence of temperatures on flexural behavior.

To conclude this Subsection, and Chapter 6, Table 186 summarizes the predicted coefficient of the variation for each temperature (taking into account the time of exposure) and properties for the different FRCs. The condition 20S has not be included since there is not differences between the values obtained for those specimens submerged and those that were stored in air condition (20). N has not been also considered, given that it was seen that the effect of temperature is quite similar (a little bit more moderate).

Table 186. Summary of the predicted variation (in %) experienced by flexural and residuals strengths due to temperature for the different types of FRCs, according to the obtained equations.

Fiber	Property	f(M15)/f(20)	f(5)/f(20)	f(40)/f(20)	f(60S)/f(20)
PF1	f_{LOP}	18 %	8 %	-10 %	-21 %
	f_{R1}	0 %	0 %	0 %	0 %
	f_{R3}	9 %	4 %	-5 %	-10 %
PF2	f_{LOP}	23 %	10 %	-13 %	-26 %
	f_{R1}	9 %	4 %	-5 %	-10 %
	f_{R3}	15 %	15 %	-9 %	-17 %
PF3	f_{LOP}	19 %	8 %	-11 %	-22 %
	f_{R1}	15 %	6 %	-9 %	-17 %
	f_{R3}	18 %	8 %	-10 %	-21 %
SF	f_{LOP}	17 %	7 %	-10 %	-19 %
	f_{R1}	0 %	0 %	0 %	0 %
	f_{R3}	0 %	0 %	0 %	0 %

In conclusion, temperature affects f_{LOP} of all the FRCs in the same manner. Additionally, temperature effect is not significant for residual strengths of the studied SFRC. Similar results are obtained for MSFRC-PF1, since f_{R1} is not affected and the variation experienced on f_{R3} is less than 10 %. However, the influence of temperatures on the behavior of MSFRC with PF2 and PF3 fibers is more remarkable than in the previous cases, but the results are still reliable to be used with this approach in mind.

Chapter 7

Conclusions and Future Research

This chapter summarizes the contributions of this Thesis and presents a list of conclusions in Section 7.1 that can be drawn from the results obtained from Chapters 4, 5 and 6. Subsection 7.2 explores possible future lines of research that could be initiated from the results of this Thesis. Finally, Section 7.3 closes Chapter 7 with a list of publications derived by the research presented in this Thesis.

7.1. Conclusions

This Section summarizes the most significant final remarks derived from the results. The conclusions have been divided in three subsections: the first Subsection, conclusion extracted from the experimental works developed at short-term are presented. The second Subsection describes the conclusions reached from the experimental works carried out at long-term and finally, last Subsection draws the main conclusions from the deep statistical analysis of the current experimental results.

7.1.1. Conclusions Derived from Short-term Experimental Campaigns

Conclusions that can be shown from this work regarding short-term exposure (3 days of exposure) to temperatures are:

At fiber level:

- The UTS of the fibers, identified as the peak in stress-strain curves, decreased as temperature increased from 20 to 140 °C (by 50 %).

The elastic modulus decreased a 50 % in that same range of temperature. For a decrease of temperatures (from 20 up to -30 °C), an increased around 20 % was detected in both properties, UTS and E-modulus. Thus, low and moderate high (more noticeably from 60 °C) temperatures directly influenced the properties of the studied PP fiber.

- Changing the loading rate (from 1 MPa/s to 40 MPa/s) on tensile tests performed on single fibers at temperatures does not have significant effect in UTS and E-modulus (less than 10 %), but some minor cross-influences with the temperature were detected at temperatures from 20 to 80 °C.
- The number of fibers that broke instead of slipping was higher for below zero temperatures. Therefore, the failure mechanism of the tested macro synthetic fibers included inside the FRC matrix change when concrete is exposed temperatures, reflecting the viscoelastic nature of the fiber. In this case, the fiber showed embrittlement at low temperatures (higher number of broken fibers) and more ductile behavior at high temperature together with viscous slippage at the interface.

At material level:

- Temperatures affect the compressive strength of FRCs, in a similar manner to temperatures influence plain concrete. Temperatures below zero increased the compressive strength at short-term (around 30–50 %). For other above zero temperatures, when the temperature increased, the compressive strength was reduced (around 15–20 %). Temperatures also affect the mode of failure under compressive strengths of the FRC specimens.
- The mechanical properties of FRCs measured under saturation conditions are in same range to that of FRCs under the control scenario in this study, thus the influence of ambient humidity does not seem to be as relevant as those of temperature.
- Exposure to below zero temperatures led to a significant enhancement of f_{LOP} in both SFRC and MSFRC (around the double), but also more brittleness was detected. For f_{R1} values, an increase of a 30 % in average is shown at −15 °C for both FRCs. f_{R3} values were also quite similar for the analyzed FRCs, but the temperature effect was greater than for f_{R1} values in all the cases. When temperature increases from 5 to 60 °C, a decrease of f_{LOP} in both SFRC and MSFRC is detected (similar to this decrease obtained for compressive strengths). These temperatures (5 to 60 °C) had a relatively low influence after a period of 3 days of exposure in residual flexural strengths for both types of FRCs (15–20 %).

- Temperature affects the tensile direct behavior of the studied MSFRC at short-term. Low temperatures increase the peak load strength (15 % increase at -30 °C) and the residual tension strength (between 10 and 25 % increase for f^*_{R1}, f^*_{R2} and f^*_{R3} at -30 °C compared to 20 °C) although a more brittle behavior is also detected. At f^*_{R4}, a slight decrease is noted for all the temperatures compared to 20 °C. For high temperature, a reduction is detected, with a 20 % decrease at 40 °C, and also in the residual tension strengths (between 20 and 38 % decrease for f^*_{R1}, f^*_{R2}, f^*_{R3} and f^*_{R4}).
- Regarding to the interaction temperature and pre-cracking state at short-term, it can be said that the pre-cracking process did not influence the behavior of FRCs at the studied non-standard temperatures for short-term exposures.
- The exposition to temperature affects the bond strengths between fiber and concrete-matrix on MSFRCs. From the comparative study between the behavior at temperature of a single-fiber filament and the behavior of MSFRC in uniaxial and flexural bending tests, it is possible to affirm that the effect of temperature on the filament is less influential than in the residual strengths on the MSFRC specimens, and concretely, on tensile strengths. This indicates that temperatures affect the interaction between fiber and concrete-matrix.

7.1.2. Conclusions Derived from Long-term Experimental Campaigns

The following conclusions can be drawn from the experimental campaigns at long-term (90 and 180 days of exposure):

At 90 days:

- The tested FRCs, exposed to different temperatures, exhibited essentially the same compressive behavior at 90 days than at 3 days: an increase of 10-20 % after 90 days exposure to −15 °C and a decrease of 20-25 % after 90 days exposure to 60 °C.
- SFRC and MSFRC exhibited different behavior in flexure by 3PBTs at the studied temperatures. After 90 days exposure, SFRC experienced an increase in f_{R1} and f_{R3} of around 50-65 % for non-pre-cracked and pre-cracked specimens, with an increase of brittleness. On the contrary, low temperature seems to not affect the residual flexural strengths of MSFRC at 0.5 mm, but it does at 2.5 mm. After 90 days exposure to 60 °C, no significant effects are detected in f_{R1} nor f_{R3} for both type of FRCs and states (non-pre-cracked and pre-cracked). Values obtained are more disperse due to N than those obtained for 3 days. In general, it can be said that both FRCs shown

mechanical behavior that are compatible with engineering applications at high temperatures (60 °C) and, considering the different variation of properties detected, also at low temperatures (−15 °C).
- There was not a detectable synergy between the effect of pre-cracking and temperature on the flexural behavior of FRCs after 90 days of permanent exposure to different studied extreme environmental conditions.

At 180 days:

- Long-term exposure to temperatures affects the compressive strength and f_{LOP} of FRCs, reflecting a clear matrix effect. Temperatures below zero led to a significant an enhancement of f_{LOP} in both SFRC and MSFRC, but also more brittleness, that could mean that some structural requirements are not accomplished. At moderate-high temperatures, a decrease is detected compared to 20 °C, but nevertheless, the obtained values are satisfactory from a structural reliability level.
- The mechanical properties of FRCs measured in immersion conditions are similar to the properties of FRCs in air ambient in this study, thus the influence of the humidity does not seem to be as relevant as those of temperature or does not aggravate the temperature effect.
- Temperature and age affect the residual flexural strengths; nevertheless, their effects are limited, especially for the range of 0-60 °C. The values of f_{R1} and f_{R3} are quite constant for the tested conditions of this work, even more after 180 days compared to short-term (after 3 days).
- The interaction between pre-cracked and temperature is not influential at long-term, presenting similar results for all types of FRC studied.
- The aging after 180 days of the tested MSFRCs and SFRC have not demonstrated to be detrimental since the loss of flexural capability after 180 days is not evident and may have been partially compensated by maturing. The FRCs' durability is enough for a wide range of operational temperatures and applications.

7.1.3. Conclusions Derived from the Statistical Analysis

From the statistical analysis, the following conclusions can be drawn from the results obtained in the experimental campaigns on this Thesis:

- The ANOVA analysis showed the variability of f_{LOP} and residual flexural strengths into contributions due to various factors in both FRCs (considering N). In general, temperature can be considered a statistically significant factor; however, it is not a significant factor in f_{R1} or

f_{R1}/N (although temperature produces variations, they are not significant from a statistical point of view).

- The obtained information from ANOVA is forceful and has allowed to clarify and to verify the observed effects in the experimental campaigns on MSFRCs and SFRC.
- From the ANOVA results, it could be also said that the state (non-pre-cracked and pre-cracked) and humidity effects on the behavior of FRC subjected at temperatures, are not significant.
- A simple numerical approach to the mechanical properties of FRC when designing for extreme environmental conditions over time was proposed thanks to the previous exploratory data analysis. It allowed to analyze further the brittleness of FRCs at low temperatures and the degradation at moderate-high temperatures together with the influence of time.

7.2. Future Research

The present Thesis have tackled the mechanical behavior of FRCs (especially MSFRCs) under temperature and their aging, which this research observed in the temperature range of -30 to 60 °C. However, some aspects are still uncertain, and further investigation are needed in the near future. There are several challenging research lines that can be proposed after the work developed in this Thesis, such as:

- Investigating the performance of FRC structures under a wider range of temperatures in order to determine whether the loss in performance may harm the fiber reinforced concrete structures within the built environment.
- Studying the effect of temperature under other regimens (modifying the methodology) to know the response of MSFRCs under this evaluation. The behavior of MSFRCs under cycles or after being exposed to temperature after a long-term period but tested at 20 °C (residual conditions), should be studied.
- Studying single fiber pull-out tests at temperature to understand the mechanism causing the time-dependent crack mouth opening of MSFRC.
- Testing other periods of exposure and conditions in order to determine the durability and the degradation of the fibers and MSFRCs in these cases.
- Modifying the type and/or content of polymeric fibers in the matrix of the concrete, as well as the concrete-matrix.

- Encoding a numerical model that allows to simulate and predict the behavior of these composite materials giving a more realistic accuracy approach testing other regression.
- Promoting enlarging the public databases available on this topic with the support of scientific researchers interested in this topic to share their experimental results to make these results useful to obtain overall conclusions of the behavior of MSFRC material and promote guidelines that support its use.

7.3. Publications Derived from this Thesis

This section includes the list of publications from work derived from this Thesis up to 2023.

Refereed JCR journals

M. Caballero-Jorna, M. Roig-Flores, P. Serna, Influence of short-term operating temperatures on compression and flexural behaviour of Macro Synthetic and Steel Fibre Reinforced Concretes, Journal of Building Engineering 67 (2023). https://doi.org/10.1016/j.jobe.2023.105919

M. Caballero-Jorna, M. Roig-flores, P. Serna, A study of the flexural behavior of fiber-reinforced concretes exposed to moderate temperatures, Materials 14 (2021). https://doi.org/10.3390/ma14133522.

International conferences

G. Virgulto, M. Caballero-Jorna, N. Buratti, M. Roig-Flores, C. Mazzotti. Experimental Tests On The Effect Of Temperature On A Polypropylene Fiber And On A Macro-synthetic FRC. In FRC2023: Fiber Reinforced Concrete: from Design to Structural Applications ACI-fib-RILEM International Workshop. Tempe, Arizona, USA, 2023.

M., Caballero-Jorna, M. Roig-Flores, P. Serna, An Experimental Study on FRC Subjected to Low (-15 °C) and High (60 °C) Permanent Temperature Exposure. In FRC2023: Fiber Reinforced Concrete: from Design to Structural Applications ACI-fib-RILEM International Workshop. Tempe, Arizona, USA 2023.

M., Caballero-Jorna, M. Roig-Flores, P. Serna, Mechanical properties of macrosynthetic fiber reinforced concretes at moderate temperature. In Conference: fib International Congress 2022 Oslo, Norway, 2022.

M. Lerna, M. Caballero-Jorna, M. Roig-Flores, D. Foti, P. Serna. Influence of Recycled Materials on the Mechanical Properties of Macro Synthetic Fiber-Reinforced Concrete. In Conference: fib International Congress 2022 Oslo, Norway, 2022.

M., Caballero-Jorna, H. Doostkami, M. Roig-Flores, P. Serna, Autogenous Healing in Ultra High-Performance Fiber Reinforced Concrete: application in two reduced scale water reservoirs, MATEC Web of Conferences 361:01005 (2022) 10.1051/matecconf/202236101005

M. Caballero-Jorna, M. Roig-Flores, P. Serna, Effect of short-term exposure to moderate temperatures on the residual strength of cracked Fiber Reinforced Concretes, MATEC Web of Conferences 361 (2022). 10.1051/matecconf/202236105013

M. Caballero-Jorna, M. Roig-Flores, P. Serna, Short-Term Effects of Moderate Temperatures on the Mechanical Properties of Steel and Macrosynthetic Fiber Reinforced Concretes. In: Serna P., Llano-Torre A., Martí-Vargas J.R., Navarro-Gregori J. (eds) Fiber Reinforced Concrete: Improvements and Innovations II. BEFIB 2021. RILEM Bookseries, vol 36. Springer, Cham. (2022) https://doi.org/10.1007/978-3-030-83719-8_20

M. Caballero-Jorna, M. Roig-Flores, P. Serna, An Experimental Study of the Influence of Moderate Temperatures on the Behavior of Macrosynthetic Fiber Reinforced Concrete. In: Serna P., Llano-Torre A., Martí-Vargas J.R., Navarro-Gregori J. (eds) Fiber Reinforced Concrete: Improvements and Innovations. BEFIB 2020. RILEM Bookseries, vol 30. Springer, Cham. (2021) https://doi.org/10.1007/978-3-030-58482-5_30

References

[1] A. Bentur, S. Mindess, Fibre reinforced cementitious composites, Taylor & Francis, 2007.

[2] S. Yin, R. Tuladhar, F. Shi, M. Combe, T. Collister, N. Sivakugan, Use of macro plastic fibres in concrete: A review, Constr Build Mater 93 (2015) 180–188. https://doi.org/10.1016/j.conbuildmat.2015.05.105.

[3] M. Barman, Comparison of Performances of Structural Fibers and Development of a Specification for Using Them in Thin Concrete Overlays, 2018.

[4] ITAtech Activity Group Support, Guideline For Good Practice of Fibre Reinforced Precast Segment-Vol. 2 : Production Aspects, 2018. www.longrine.fr.

[5] ITA Working Group 2 Research, Twenty Years of FRC Tunnel Segments Practice: Lessons Learnt and Proposed Design Principles, 2016. www.longrine.fr.

[6] A E Richardson and P Jackson., Equating steel and synthetic fibre concrete post crack performance, in: International conference on current trends in technology, 'NUiCONE – 2011,' 2011: pp. 1–6.

[7] V. Marcos-Meson, A. Michel, A. Solgaard, G. Fischer, C. Edvardsen, T.L. Skovhus, Corrosion resistance of steel fibre reinforced concrete - A literature review, Cem Concr Res 103 (2018) 1–20. https://doi.org/10.1016/j.cemconres.2017.05.016.

[8] Y. Chen, G. Cen, Y. Cui, Comparative study on the effect of synthetic fiber on the preparation and durability of airport pavement concrete, Constr Build Mater 184 (2018) 34–44. https://doi.org/10.1016/j.conbuildmat.2018.06.223.

[9] P. Rossi, "Critique of synthetic-fiber FRS paper", TunnelTECH. (2020). https://www.tunneltalk.com/TunnelTECH-Sep2014-Rossi-critique-of-Bernard-WTC-synthetic-FRS-paper.php/ (accessed April 2020).

[10] S. H. Kosmatka, B. Kerkhoff, W. C. Panarese, Hot-Weather Concreting, in: Design and Control of Concrete Mixtures, 14th ed., Portland Cement Association, 2002.

[11] Australian Pre-mixed Concrete Association, Cold-Weather Concreting, 2002.

[12] R.H. Alasfar, S. Ahzi, N. Barth, V. Kochkodan, M. Khraisheh, M. Koç, A Review on the Modeling of the Elastic Modulus and Yield Stress of Polymers and Polymer Nanocomposites: Effect of Temperature, Loading Rate and Porosity, Polymers (Basel) 14 (2022) 1–31. https://doi.org/10.3390/polym.

[13] Anejo 7 Recomendaciones para la utilización de hormigón con fibras. In: Código Estructural. Real Decreto 470/2021 de 29 de junio. BOE-A-2021-13681. https://www.boe.es/eli/es/rd/2021/06/29/470.

[14] A. M. Neville, Properties of Concrete, 2011.

[15] M. Di Prisco, G. Plizzari, L. Vandewalle, Fibre reinforced concrete: New design perspectives, Materials and Structures/Materiaux et Constructions 42 (2009) 1261–1281. https://doi.org/10.1617/s11527-009-9529-4.

[16] M.F. Ashby, D.R.H. Jones, 21.7 Reinforcing Cement and Concrete, in: Engineering Materials 2, Elsevier, 2013: pp. 361–378. https://doi.org/10.1016/B978-0-08-096668-7.00021-8.

[17] A.E. Naaman, Fiber reinforced concrete: five decades of progress, in: ABEC Publicacoes, 2018: pp. 35–56. https://doi.org/10.21452/bccm4.2018.02.01.

[18] J.P. Romualdi, G.B. Batson, Behavior of Reinforced Concrete Beams with Closely Spaced Reinforcement, ACI Journal Proceedings 60 (1963) 775-790. https://doi.org/10.14359/7878.

[19] J.P. Romualdi, J.A. Mandel, Tensile Strength of concrete Affected by UnigormlyDistributed and Closely Spaced Short Lengths of wire Reinforcement, ACI Journal Proceedings 61 (1964) 657-672. https://doi.org/10.14359/7801.

[20] S. Kanalli, R. Palankar, B. Kumar, P. Kumar, Comparative study of polymer fibre reinforced concrete with conventional concrete pavement, IJRET 3 (2014) 139-143. http://www.ijret.org.

[21] O. Cengiz, L. Turanli, Comparative evaluation of steel mesh, steel fibre and high-performance polypropylene fibre reinforced shotcrete in panel test, Cem Concr Res 34 (2004) 1357–1364. https://doi.org/10.1016/j.cemconres.2003.12.024.

[22] D.T. Biddle, "Not Meshing Around", ForConstructionPros.Com. (2014). https://www.forconstructionpros.com/concrete/equipment-products/article/11355163/synthetic-fibers-are-safer-than-wire-mesh-in-slab-on-metal-deck-projects. (accessed May 2024).

[23] ACI Committee 544, Report on Fiber Reinforced Concrete, 2002.

[24] Fib, Model Code, Paris: Fédération Internationale du Béton fib/International Federation for Structural Concrete, 2010.

[25] S.B. Kunal Ahuja, Concrete Fibers Market - By Products (Steel, Synthetic (Polypropylene, Nylon, Polyester), Glass, Natural, Basalt), By Application (Pavement, Shotcrete, Precast, Slabs On Grade, Composite Metal Decks), By End Users & Global Forecast, 2023-2032, 2022. https://www.gminsights.com/industry-analysis/concrete-fiber-market (accessed May 2024).

[26] T.A. Söylev, T. Özturan, Durability, physical and mechanical properties of fiber-reinforced concretes at low-volume fraction, Constr Build Mater 73 (2014) 67–75. https://doi.org/10.1016/j.conbuildmat.2014.09.058.

[27] S.C. Paul, G.P.A.G. van Zijl, B. Šavija, Effect of fibers on durability of concrete: A practical review, Materials 13 (2020) 1–26. https://doi.org/10.3390/ma13204562.

[28] E.R.K. Chandrathilaka, S.K. Baduge, P. Mendis, P.S.M. Thilakarathna, Structural applications of synthetic fibre reinforced cementitious composites: A review on material properties, fire behaviour, durability and structural performance, Structures 34 (2021) 550–574. https://doi.org/10.1016/j.istruc.2021.07.090.

[29] A. Conforti, G. Tiberti, G.A. Plizzari, A. Caratelli, A. Meda, Precast tunnel segments reinforced by macro-synthetic fibers, Tunnelling and Underground Space Technology 63 (2017) 1-11. https://doi.org/10.1016/j.tust.2016.12.005.

[30] M.G. Alberti, A. Enfedaque, A. Picazo, Recent advances in structural fibre-reinforced concrete focused on polyolefin-based macro-synthetic fibres, Materiales de Construcción 70 (2020) 1–28. 10.3989/mc.2020.12418.

[31] S. Deb, N. Mitra, Swati Maitra, S.B. Majumdar, Comparison of Mechanical Performance and Life Cycle Cost of Natural and Synthetic Fiber-Reinforced Cementitious Composites, (2020) 04020150. https://doi.org/10.1061/(ASCE)MT.1943.

[32] C. Camille, O. Mirza, S. Senaratne, B. Kirkland, T. Clarke, Life cycle cost analysis of macro synthetic fibre reinforced concrete for railway sleeper applications, Structure and Infrastructure Engineering 20 (2024) 353–367. https://doi.org/10.1080/15732479.2022.2095408.

[33] J. Ahmad, Z. Zhou, Mechanical Properties of Natural as well as Synthetic Fiber Reinforced Concrete: A Review, Constr Build Mater 333 (2022) 127353. https://doi.org/10.1016/j.conbuildmat.2022.127353.

[34] P. Kaur, M. Talwar, Different types of Fibres used in FRC, International Journal of Advanced Research in Computer Science 8 (2017) 380–383. www.ijarcs.info.

[35] I. Elfaleh, F. Abbassi, M. Habibi, F. Ahmad, M. Guedri, M. Nasri, C. Garnier, A comprehensive review of natural fibers and their composites: An eco-friendly alternative to conventional materials, Results in Engineering 19 (2023). https://doi.org/10.1016/j.rineng.2023.101271.

[36] S.B. Kim, N.H. Yi, H.Y. Kim, J.H.J. Kim, Y.C. Song, Material and structural performance evaluation of recycled PET fiber reinforced concrete, Cem Concr Compos 32 (2010) 232–240. https://doi.org/10.1016/j.cemconcomp.2009.11.002.

[37] Z. Zheng, D. Feldman, Synthetic fiber-reinforced concrete, Program Polymer Sci 20 (1995) 185–210. https://doi.org/10.1016/0079-6700(94)00030-6.

[38] R. Sibaja, L. Ríos, M. Jiménez, J. Resumen, J.P. Montardo, The synthetics fibers effect in the concrete plastic properties, Revista Ingeniería de Construcción, 20 (2005). www.ing.puc.cl/ric.

[39] S.M. Abtahi, M. Sheikhzadeh, S.M. Hejazi, Fiber-reinforced asphalt-concrete - A review, Constr Build Mater 24 (2010) 871–877. https://doi.org/10.1016/j.conbuildmat.2009.11.009.

[40] H. Bolat, O. Şimşek, M. Çullu, G. Durmuş, Ö. Can, The effects of macro synthetic fiber reinforcement use on physical and mechanical properties of concrete, Compos B Eng 61 (2014) 191–198. https://doi.org/10.1016/j.compositesb.2014.01.043.

[41] S. Mukhopadhyay, S. Khatana, A review on the use of fibers in reinforced cementitious concrete, Journal of Industrial Textiles 45 (2015) 239–264. https://doi.org/10.1177/1528083714529806.

[42] C.C. Thong, D.C.L. Teo, C.K. Ng, Application of polyvinyl alcohol (PVA) in cement-based composite materials: A review of its engineering properties and microstructure behavior, Constr Build Mater 107 (2016) 172–180. https://doi.org/10.1016/j.conbuildmat.2015.12.188.

[43] L. Gu, T. Ozbakkaloglu, Use of recycled plastics in concrete: A critical review, Waste Management 51 (2016) 19–42. https://doi.org/10.1016/j.wasman.2016.03.005.

[44] H.R. Pakravan, T. Ozbakkaloglu, Synthetic fibers for cementitious composites: A critical and in-depth review of recent advances, Constr Build Mater 207 (2019) 491–518. https://doi.org/10.1016/j.conbuildmat.2019.02.078.

[45] T. Clarke, M. Ghiji, S. Fragomeni, M. Guerrieri, Mechanical properties of macro synthetic fiber reinforced concrete at elevated temperatures: A systematic review and meta-analysis, Structural Concrete 24 (2023) 1244–1270. https://doi.org/10.1002/suco.202100918.

[46] MSFA, Market-Update-September, (2021). https://msfassociation.com/msf-market-report-2021/ (accessed May 2024).

[47] ATS, “Australian Tunnelling Society-50 Years”, (2022). www.ats.org.au/wp-content/uploads/2023/01/ATS-50-Years-Journal_FINAL.pdf (accessed May 2024).

[48] “Macro Synthetic Fibres (MSF) for Concrete Reinforcement”. https://enviromesh.com.au/macro-synthetic-fibres/ (accessed May 2024).

[49] N. Banthia, R. Gupta, Influence of polypropylene fiber geometry on plastic shrinkage cracking in concrete, Cem Concr Res 36 (2006) 1263–1267. https://doi.org/10.1016/j.cemconres.2006.01.010.

[50] A.E. Richardson, K.A. Coventry, S. Wilkinson, Freeze/thaw durability of concrete with synthetic fibre additions, Cold Reg Sci Technol 83–84 (2012) 49–56. https://doi.org/10.1016/j.coldregions.2012.06.006.

[51] C.G. Han, Y.S. Hwang, S.H. Yang, N. Gowripalan, Performance of spalling resistance of high performance concrete with polypropylene fiber contents and lateral confinement, Cem Concr Res 35 (2005) 1747–1753. https://doi.org/10.1016/j.cemconres.2004.11.013.

[52] G. Park, G. Park, J. Park, N. Lee, S. Kim, Residual Tensile Properties and Explosive Spalling of High-Performance Fiber-Reinforced Cementitious Composites Exposed to Thermal Damage, Materials (2021) 1608. https://doi.org/10.3390/ma14071608.

[53] A. Conforti, R. Zerbino, G.A. Plizzari, Influence of steel, glass and polymer fibers on the cracking behavior of reinforced concrete beams under flexure, Structural Concrete 20 (2019) 133–143. https://doi.org/10.1002/suco.201800079.

[54] D. Visser, W.P. Boshoff, Shear behaviour of concrete V-shaped beams with and without steel fibres, Materials and Structures/Materiaux et Constructions 54 (2021). https://doi.org/10.1617/s11527-020-01589-3.

[55] S.J. Foster, T. Htut, T.S. NG, High performance fibre reinforced concrete: fundamental behaviour and modelling., in: Proceedings of the 8th International Conference on Fracture Mechanics of Concrete and Concrete Structures FraMCoS-8, Toledo, Spain, 2013: pp. 69–78.

[56] A.M. Brandt, Fibre reinforced cement-based (FRC) composites after over 40 years of development in building and civil engineering, Compos Struct 86 (2008) 3–9. https://doi.org/10.1016/j.compstruct.2008.03.006.

[57] G. Charan Behera, S. Panda, P. Kanda, Effect of Length of Fibers on Mechanical Properties of Normal Strength Concrete, in: IOP Conf Ser Mater Sci Eng, IOP Publishing Ltd, 2020. https://doi.org/10.1088/1757-899X/970/1/012020.

[58] M.O. Kaman, M.Y. Solmaz, K. Turan, Effects of ductile fiber size on the fracture toughness of copper/polyester composites, J Compos Mater 44 (2010) 3151–3164. https://doi.org/10.1177/0021998310371540.

[59] AENOR, UNE EN 14889-2:2018. Fibras para hormigón. Parte 2: Fibras poliméricas. Definiciones, especificaciones y conformidad., (2018).

[60] L.A. Pereira-De-Oliveira, J.P. Castro-Gomes, M.C.S. Nepomuceno, Effect of acrylic fibres geometry on physical, mechanical and durability properties of cement mortars, Constr Build Mater 27 (2012) 189–196. https://doi.org/10.1016/j.conbuildmat.2011.07.061.

[61] Y.F. Li, H.F. Wang, J.Y. Syu, G.K. Ramanathan, Y.K. Tsai, M.H. Lok, Mechanical properties of aramid/carbon hybrid fiber-reinforced concrete, Materials 14 (2021) 5881. https://doi.org/10.3390/ma14195881.

[62] L.P. Chaves, J. Cunha, Design of carbon fiber reinforcement of concrete slabs using topology optimization, Constr Build Mater 73 (2014) 688–698. https://doi.org/10.1016/j.conbuildmat.2014.10.011.

[63] M.G. Alberti, A. Enfedaque, J.C. Gálvez, On the mechanical properties and fracture behavior of polyolefin fiber-reinforced self-compacting concrete, Constr Build Mater 55 (2014) 274–288. https://doi.org/10.1016/j.conbuildmat.2014.01.024.

[64] T.A. Hajali Ahmed, Dr.O.M. Ahmed Daoud, Influence of Polypropylene Fibres on Concrete Properties, IOSR Journal of Mechanical and Civil Engineering 13 (2016) 09–20. https://doi.org/10.9790/1684-1305060920.

[65] T.Ch. Madhavi, L. Raju, D. Mathur, Polypropylene Fiber Reinforced Concrete-A Review, Materials Science, Engineering (2014) 114–119.

[66] D.C. Hughes, Stress transfer between fibrillated polyalkene films and cement matrices, Composites 15 (1984) 153–158. https://doi.org/10.1016/0010-4361(84)90728-6.

[67] EPC. Elasto Plastic Concrete., Advanced alkalinity testing, 2012.

[68] L. Xu, F. Deng, Y. Chi, Nano-mechanical behavior of the interfacial transition zone between steel-polypropylene fiber and cement paste, Constr Build Mater 145 (2017) 619–638. https://doi.org/10.1016/j.conbuildmat.2017.04.035.

[69] C. Zhang, V.S. Gopalaratnam, H.K. Yasuda, Plasma Treatment of Polymeric Fibers for Improved Performance in Cement Matrices, J Appl Polym Sci 76 (2000) 1985–1996. https://doi.org/10.1002/(SICI)1097-4628(20000628)76:14<1985::AID-APP1>3.0.CO;2-G.

[70] M. Mohammed, A.J. afar M. Jawad, A.M. Mohammed, J.K. Oleiwi, T. Adam, A.F. Osman, O.S. Dahham, B.O. Betar, S.C.B. Gopinath, M. Jaafar, Challenges and advancement in water absorption of natural fiber-

reinforced polymer composites, Polym Test 124 (2023). https://doi.org/10.1016/j.polymertesting.2023.108083.

[71] X. Liu, Y. Huang, C. Deng, X. Wang, W. Tong, Y. Liu, J. Huang, Q. Yang, X. Liao, G. Li, Study on the creep behavior of polypropylene, Polym Eng Sci 49 (2009) 1375–1382. https://doi.org/10.1002/pen.21330.

[72] P. Hughes, D. Fairhurst, I. Sherrington, N. Renevier, L.H.G. Morton, P.C. Robery, L. Cunningham, Microscopic examination of a new mechanism for accelerated degradation of synthetic fibre reinforced marine concrete, Constr Build Mater 41 (2013) 498–504. https://doi.org/10.1016/j.conbuildmat.2012.12.022.

[73] M. V Mohod, Performance of Polypropylene Fibre Reinforced Concrete, IOSR Journal of Mechanical and Civil Engineering (IOSR-JMCE 12 (2015) 28–36. https://doi.org/10.9790/1684-12112836.

[74] P. Di Maida, E. Radi, C. Sciancalepore, F. Bondioli, Pullout behavior of polypropylene macro-synthetic fibers treated with nano-silica, Constr Build Mater 82 (2015) 39–44. https://doi.org/10.1016/j.conbuildmat.2015.02.047.

[75] V. Guerini, A. Conforti, G. Plizzari, S. Kawashima, Influence of steel and macro-synthetic fibers on concrete properties, Fibers 6 (2018). https://doi.org/10.3390/fib6030047.

[76] M. Hsie, C. Tu, P.S. Song, Mechanical properties of polypropylene hybrid fiber-reinforced concrete, Materials Science and Engineering: A 494 (2008) 153–157. https://doi.org/10.1016/j.msea.2008.05.037.

[77] H. Rooholamini, A. Hassani, M.R.M. Aliha, Evaluating the effect of macro-synthetic fibre on the mechanical properties of roller-compacted concrete pavement using response surface methodology, Constr Build Mater 159 (2018) 517–529. https://doi.org/10.1016/j.conbuildmat.2017.11.002.

[78] P. Archana, A.N. Nayak, S.R. Nayak, H. Vaddar, D.S. Magnur, Study of Strength of Polypropylene Fiber Reinforced Concrete, International Journal of Engineering Research & Technology (IJERT) 6 (2017). www.ijert.org.

[79] R. Abad Khan, S. Khan, R. Abad Khan, A. Rahman Khan, M. Islam, S. Nayal, Mechanical Properties of Polypropylene fibre reinforced concrete for M25 and M 30 mixes: A Comparative Study, International Journal of Scientific Engineering and Applied Science (IJSEAS) (2015). www.ijseas.com.

[80] M.J. Hasan, M. Afroz, H.M.I. Mahmud, An Experimental Investigation on Mechanical Behavior of Macro Synthetic Fiber Reinforced Concrete, IJCEE-IJENS 11 (2011) 18–23.

[81] F. Ortiz Navas, J. Navarro-Gregori, G. Leiva Herdocia, P. Serna, E. Cuenca, An experimental study on the shear behaviour of reinforced concrete beams with macro-synthetic fibres, Constr Build Mater 169 (2018) 888–899. https://doi.org/10.1016/j.conbuildmat.2018.02.023.

[82] AENOR, UNE-EN 14651:2007+A1. Método de ensayo para hormigón con fibras metálicas. Determinación de la resistencia a la tracción por flexión (límite de proporcionalidad (LOP), resistencia residual), (2008).

[83] ASTM Committee, C1609 Standard Test Method for Flexural Performance of Fiber-Reinforced Concrete (Using Beam With Third-Point Loading), (2019).

[84] JSCE, G 552 Test method for bending strength and bending toughness of steel fiber reinforced concrete), (2013).

[85] ASTM, C1018 Standard Test Method for Flexural Toughness and First-Crack Strength of Fiber-Reinforced Concrete (Using Beam With Third-Point Loading), (1997).

[86] ASTM, C1399-Standard Test Method for Obtaining Average Residual-Strength of Fiber-Reinforced Concrete, (2015).

[87] ASTM, C1550-Standard Test Method for Flexural Toughness of Fiber Reinforced Concrete (Using Centrally Loaded Round Panel), (2020).

[88] AENOR, UNE-EN-14488 Ensayos de hormigón proyectado. Parte 2: Resistencia a compresión del hormigón proyectado a corta edad, (2007).

[89] M. Di Prisco, L. Ferrara, M.G.L. Lamperti, Double edge wedge splitting (DEWS): An indirect tension test to identify post-cracking behaviour of fibre reinforced cementitious composites, Materials and Structures/Materiaux et Constructions 46 (2013) 1893–1918. https://doi.org/10.1617/s11527-013-0028-2.

[90] R.P. Manfredi, F. de Andrade Silva, Test Methods for the Characterization of Polypropylene Fiber Reinforced Concrete: A Comparative Analysis, KSCE Journal of Civil Engineering 24 (2020) 856–866. https://doi.org/10.1007/s12205-020-0741-7.

[91] P. Kalifa, G. Chéné, C. Gallé, High-temperature behaviour of HPC with polypropylene fibres from spalling to microstructure, Cement and Concrete Research 31 (2001) 1487–1499. https://doi.org/10.1016/S0008-8846(01)00596-8.

[92] C.G. Han, Y.S. Hwang, S.H. Yang, N. Gowripalan, Performance of spalling resistance of high performance concrete with polypropylene fiber contents and lateral confinement, Cem Concr Res 35 (2005) 1747–1753. https://doi.org/10.1016/j.cemconres.2004.11.013.

[93] A. Karimipour, M. Ghalehnovi, J. de Brito, M. Attari, The effect of polypropylene fibres on the compressive strength, impact and heat resistance of

self-compacting concrete, Structures 25 (2020) 72–87. https://doi.org/10.1016/j.istruc.2020.02.022.

[94] A.M. Alani, D. Beckett, Mechanical properties of a large scale synthetic fibre reinforced concrete ground slab, Constr Build Mater 41 (2013) 335–344. https://doi.org/10.1016/j.conbuildmat.2012.11.043.

[95] M. Barman, B. Hansen, U. Arepalli, Performance Benefits of Fiber-reinforced Thin Concrete Pavement and Overlays, 2018.

[96] A. Peyvandi, P. Soroushian, S. Jahangirnejad, Enhancement of the structural efficiency and performance of concrete pipes through fiber reinforcement, Constr Build Mater 45 (2013) 36–44. https://doi.org/10.1016/j.conbuildmat.2013.03.084.

[97] X. Liu, Q. Sun, Y. Yuan, L. Taerwe, Comparison of the structural behavior of reinforced concrete tunnel segments with steel fiber and synthetic fiber addition, Tunnelling and Underground Space Technology 103 (2020) 103506. https://doi.org/10.1016/j.tust.2020.103506.

[98] A. Conforti, I. Trabucchi, G. Tiberti, G.A. Plizzari, A. Caratelli, A. Meda, Precast tunnel segments for metro tunnel lining: A hybrid reinforcement solution using macro-synthetic fibers, Eng Struct 199 (2019). https://doi.org/10.1016/j.engstruct.2019.109628.

[99] R. Serafini, S.R.A. Dantas, R.P. Salvador, R.R. Agra, D.A.S. Rambo, A.F. Berto, A.D. de Figueiredo, Influence of fire on temperature gradient and physical-mechanical properties of macro-synthetic fiber reinforced concrete for tunnel linings, Constr Build Mater 214 (2019) 254–268. https://doi.org/10.1016/j.conbuildmat.2019.04.133.

[100] A.G. Nitschke, R. Winterberg, Performance of Macro Synthetic Fiber Reinforced Tunnel Linings, 2016.

[101] J. Kaufmann, K. Frech, P. Schuetz, B. Münch, Rebound and orientation of fibers in wet sprayed concrete applications, Constr Build Mater 49 (2013) 15–22. https://doi.org/10.1016/j.conbuildmat.2013.07.051.

[102] A.M. Brandt, Fibre reinforced cement-based (FRC) composites after over 40 years of development in building and civil engineering, Compos Struct 86 (2008) 3–9. https://doi.org/10.1016/j.compstruct.2008.03.006.

[103] MSFA, Case Studies. https://msfassociation.com/case-studies/ (accessed May 2024).

[104] P. Balaguru, K. Slattum, Test methods for durability of polymeric fibers in concrete and UV light exposure, in: Testing of Fiber Reinforced Concrete, American Concrete Institute, Salt Lake City, United States, 1995: pp. 115–136.

[105] Z. Bayasi, M. Al Dhaheri, Effect of exposure to elevated temperature on polypropylene fiber-reinforced concrete, ACI Mater J 99 (2002) 22–26. https://www.concrete.org/publications/acimaterialsjournal.aspx.

[106] I. Soroka, Durability of concrete, in: Portland Cement Paste and Concrete, Palgrave, London, 1979: pp. 260–291. https://doi.org/doi.org/10.1007/978-1-349-03994-4_10.

[107] M.A. Hariri-Ardebili, L. Sanchez, R. Rezakhani, Aging of Concrete Structures and Infrastructures: Causes, Consequences, and Cures (C3), Advances in Materials Science and Engineering 2020 (2020). https://doi.org/10.1155/2020/9370591.

[108] S. Kaewunruen, L. Wu, K. Goto, Y.M. Najih, Vulnerability of structural concrete to extreme climate variances, Climate 6 (2018) 40. https://doi.org/10.3390/cli6020040.

[109] R. Madandoust, M. Kazemi, P.K. Talebi, J. de Brito, Effect of the curing type on the mechanical properties of lightweight concrete with polypropylene and steel fibres, Constr Build Mater 223 (2019) 1038–1052. https://doi.org/10.1016/j.conbuildmat.2019.08.006.

[110] F. Bouziadi, B. Boulekbache, M. Hamrat, The effects of fibres on the shrinkage of high-strength concrete under various curing temperatures, Constr Build Mater 114 (2016) 40–48. https://doi.org/10.1016/j.conbuildmat.2016.03.164.

[111] M. Çiflikli, M. Sarıdemir, F. Soysat, Adverse effects of high temperatures and freeze-thaw cycles on properties of HFRHSCs containing silica fume and metakaolin, Constr Build Mater 174 (2018) 507–519. https://doi.org/10.1016/j.conbuildmat.2018.04.150.

[112] V.D. Pizzol, L.M. Mendes, H. Savastano, M. Frías, F.J. Davila, M.A. Cincotto, V.M. John, G.H.D. Tonoli, Mineralogical and microstructural changes promoted by accelerated carbonation and ageing cycles of hybrid fiber-cement composites, Constr Build Mater 68 (2014) 750–756. https://doi.org/10.1016/j.conbuildmat.2014.06.055.

[113] V. Pacáková, J. & Virt, PLASTICS, in: Encyclopedia of Analytical Science (Second Edition), 2005: pp. 180–187. https://doi.org/https://doi.org/10.1016/B0-12-369397-7/00467-2.

[114] ASTM, D794 Determining Permanent Effect of Heat on Plastics, (1993).

[115] L. McKeen, The Effect of Temperature and other Factors on Plastics and Elastomers, Elsevier, 2014. https://doi.org/10.1016/C2013-0-18393-6.

[116] A.G. Gibson, M.E.O. Torres, T.N.A. Browne, S. Feih, A.P. Mouritz, High temperature and fire behaviour of continuous glass fibre/polypropylene laminates, in: Compos Part A Appl Sci Manuf, 2010: pp. 1219–1231. https://doi.org/10.1016/j.compositesa.2010.05.004.

[117] C. Hall, POLYMER MATERIALS: An introduction for technologists and scientist, 1981.

[118] NV Bekaert SA., Dramix ® Steel-and Synthetic Fibre Reinforced Concrete Which fibre to use for which application and why? (2011). http://dramix.bekaert.com (accessed May 2024).

[119] E.M. Arruda, M.C. Boyce, R. Jayachandran, Effects of strain rate, temperature and thermomechanical coupling on the finite strain deformation of glassy polymers, Mechanics of Materials 19 (1995) 193–212. https://doi.org/10.1016/0167-6636(94)00034-E

[120] J. Johnsen, F. Grytten, O.S. Hopperstad, A.H. Clausen, Influence of strain rate and temperature on the mechanical behaviour of rubber-modified polypropylene and cross-linked polyethylene, Mechanics of Materials 114 (2017) 40–56. https://doi.org/10.1016/j.mechmat.2017.07.003.

[121] Y. Ding, C. Azevedo, J.B. Aguiar, S. Jalali, Study on residual behaviour and flexural toughness of fibre cocktail reinforced self compacting high performance concrete after exposure to high temperature, Constr Build Mater 26 (2012) 21–31. https://doi.org/10.1016/j.conbuildmat.2011.04.058.

[122] E.A. Campos, Thermal Properties of Polymeric Materials, in: Selection of Polymeric Materials, 2008: pp. 103–140. https://doi.org/10.1016/B978-0-8155-1551-7.50005-X.

[123] S. Kurtz, P. Balaguru, Postcrack creep of polymeric fiber-reinforced concrete in flexure, Cement and Concrete Research, 30 (2000) 183–190. https://doi.org/10.1016/S0008-8846(99)00228-8.

[124] N. Segre, E. Tonella, I. Joekes, Evaluation of the stability of polypropylene fibers in environments aggressive to cement-based materials, Cement and Concrete Research, 28 (1998) 75-81. https://doi.org/10.1016/S0008-8846(97)00220-2.

[125] M.R. Gohel, N. Neithalath, Creep of Cracked Fiber Reinforced Concrete, Master dissertation, ASU,2017.

[126] R. Vrijdaghs, M. di Prisco, L. Vandewalle, Creep deformations of structural polymeric macrofibers, in: RILEM Bookseries, Kluwer Academic Publishers, 2017: pp. 53–61. https://doi.org/10.1007/978-94-024-1001-3_5.

[127] A. Takaku, Effect of Temperature on Creep Fracture of Polypropylene Fibers, J Appl Polym Sci 25 (1980) 1861–1866. https://doi.org/0021-8995/80/0025-1981.

[128] P. Serna, A. Llano-Torre, S.H.P. Cavalaro Editors, Creep Behaviour in Cracked Sections of Fibre Reinforced Concrete, in: RILEM Bookseries

(Ed.), Proceedings of the International RILEM Workshop FRC-CREEP, 2016. http://www.springer.com/series/8781.

[129] ADFIL Construction Fibres, Durability assessment Durus ® S500, (2017). 2021-Technical-Note-Durability-assessment-Durus-S500.pdf (accessed May 2024).

[130] AENOR, UNE-EN ISO 13438. Geosintéticos. Método de ensayo para la determinación de la resistencia a la oxidación de geotextiles y productos relacionados, (2020).

[131] M. Hunger, J. Bokern, S. Cleven, R. Vrijdaghs, Creep in FRC – From Material Properties to Composite Behavior, in: RILEM Bookseries, Springer Science and Business Media B.V., 2021: pp. 402–413. https://doi.org/10.1007/978-3-030-58482-5_37.

[132] D. H. Hannat, Durability of polypropylene fibers in portland cement-based composites: eighteen years of data, Cem Concr Res 28 (1998) 1809–1817. https://doi.org/10.1016/S0008-8846(98)00155-0.

[133] R. Brown, A. Shukla, K.R. Natarajan, Fiber Reinforcement of Concrete Structures - URITC PROJECT NO. 536101, (2002).

[134] H. Malhotra, The effect of temperature on the compressive strength of concrete, Magazine of Concrete Research 8 (1956) 85. https://doi.org/10.3989/mc.1957.v07.i080.2138

[135] M. Mastali, A. Dalvand, A.R. Sattarifard, Z. Abdollahnejad, M. Illikainen, Characterization and optimization of hardened properties of self-consolidating concrete incorporating recycled steel, industrial steel, polypropylene and hybrid fibers, Compos B Eng 151 (2018) 186–200. https://doi.org/10.1016/j.compositesb.2018.06.021.

[136] D.R. Gardner, R.J. Lark, B. Barr, Effect of conditioning temperature on the strength and permeability of normal- and high-strength concrete, Cem Concr Res 35 (2005) 1400–1406. https://doi.org/10.1016/j.cemconres.2004.08.012.

[137] C. Del Prete, N. Buratti, C. Mazzotti, Experimental Investigation on the Influence of Temperature Variations on Macro-synthetic Fibre Reinforced Concrete Short and Long Term Behaviour, in: RILEM Bookseries, Springer Science and Business Media B.V., 2022: pp. 331–341. https://doi.org/10.1007/978-3-030-83719-8_29.

[138] P. Navarro, M.N. Sánchez, E. Martín, I. Segura, J. De la Cruz, A. De la Fuente, Dovelas innovadoras de alta durabilidad reforzadas solo con fibras no metálicas, ROP 3613 (2019) 16–25.

[139] Y.F. Chang, Y.H. Chen, M.S. Sheu, G.C. Yao, Residual stress-strain relationship for concrete after exposure to high temperatures, Cem Concr

Res 36 (2006) 1999–2005. https://doi.org/10.1016/j.cemconres.2006.05.029.

[140] G. Pachideh, M. Gholhaki, An experimental study on the effects of adding steel and polypropylene fibers to concrete on its resistance after different temperatures, J Test Eval 47 (2019) 1606–1620. https://doi.org/10.1520/JTE20170145.

[141] B.G. C Lee, T.S. Shih, K.C. Chang, A. Member, Mechanical properties of concrete at low temperature, Journal of Cold Regions Engineering 2 (1988). http://opjs.aip.org/cro

[142] P. Duthil, Material properties at low temperature, CAS-CERN Accelerator School: Superconductivity for Accelerators - Proceedings (2014) 77–95. https://doi.org/10.5170/CERN-2014-005.77.

[143] S. Chai, H. Zheng, D. Hou, M. Wang, Y. Zhang, B. Yin, P. Wang, Understanding the filling effect of ice on the mechanical properties of calcium silicate hydrate gel, Case Studies in Construction Materials 20 (2024) e03109. https://doi.org/10.1016/j.cscm.2024.e03109

[144] L. Dahmani, A. Khenane, S. Kaci, Behavior of the reinforced concrete at cryogenic temperatures, Cryogenics (Guildf) 47 (2007) 517–525. https://doi.org/10.1016/j.cryogenics.2007.07.001.

[145] L.A. Montejo, S.M. Asce, J.E. Sloan, A.M. Asce, ; Mervyn, J. Kowalsky, T. Hassan, Cyclic Response of Reinforced Concrete Members at Low Temperatures, Journal of Cold Regions Engineering 22 (2007) 79–102. https://doi.org/10.1061/ASCE0887-381X200822:379.

[146] S.N. Shoukry, G.W. William, B. Downie, M.Y. Riad, Effect of moisture and temperature on the mechanical properties of concrete, Constr Build Mater 25 (2011) 688–696. https://doi.org/10.1016/j.conbuildmat.2010.07.020.

[147] T. Drzymała, W. Jackiewicz-Rek, M. Tomaszewski, A. Kuś, J. Gałaj, R. Šukys, Effects of High Temperature on the Properties of High Performance Concrete (HPC), in: Procedia Eng, Elsevier Ltd, 2017: pp. 256–263. https://doi.org/10.1016/j.proeng.2017.02.108.

[148] X.P. Cai, W.C. Yang, J. Yuan, Y. Ge, B.S. Zhang, Effect of low temperature on mechanical properties of concrete with different strength grade, in: Key Eng Mater, Trans Tech Publications Ltd, 2011: pp. 308–312. https://doi.org/10.4028/www.scientific.net/KEM.477.308.

[149] J. Xie, J.B. Yan, Experimental studies and analysis on compressive strength of normal-weight concrete at low temperatures, Structural Concrete 19 (2018) 1235–1244. https://doi.org/10.1002/suco.201700009.

[150] F.S. Rostásy, K.H. Sprenger, Strength and deformation of steel fibre reinforced concrete at very low temperature, International Journal of Ce-

ment Composites and Lightweight Concrete 6 (1984) 47–51. https://doi.org/10.1016/0262-5075(84)90059-9

[151] W. Li, H. Liu, B. Zhu, X. Lyu, X. Gao, C. Liang, Mechanical properties and freeze-thaw durability of basalt fiber reactive powder concrete, Applied Sciences (Switzerland) 10 (2020). https://doi.org/10.3390/app10165682.

[152] R. Madandoust, M. Kazemi, P.K. Talebi, J. de Brito, Effect of the curing type on the mechanical properties of lightweight concrete with polypropylene and steel fibres, Constr Build Mater 223 (2019) 1038–1052. https://doi.org/10.1016/j.conbuildmat.2019.08.006.

[153] J.-K. Kim, S.H. Han, Y.C. Song, Effect of temperature and aging on the mechanical properties of concrete Part I. Experimental results, Cem Concr Res 32 (2002) 1087–1094. https://doi.org/10.1016/S0008-8846(02)00744-5.

[154] Z. Mi, Q. Li, Y. Hu, C. Liu, Y. Qiao, Fracture properties of concrete in dry environments with different curing temperatures, Applied Sciences (Switzerland) 10 (2020). https://doi.org/10.3390/app10144734.

[155] A. Richardson, R. Ovington, Temperature related steel and synthetic fibre concrete performance, Constr Build Mater 153 (2017) 616–621. https://doi.org/10.1016/j.conbuildmat.2017.07.101.

[156] A. Lau, M. Anson, Effect of high temperatures on high performance steel fibre reinforced concrete, Cem Concr Res 36 (2006) 1698–1707. https://doi.org/10.1016/j.cemconres.2006.03.024.

[157] M. Elices, J. Planas, P. Maturana, Fracture of concrete at cryogenic temperatures, in: S. Shah, S. Swartz (Eds.), SEM/RILEM International Conference on Fracture of Concrete and Rock, Houston, Texas, 1987: pp. 106–107.

[158] P. Maturana, J. Planas, M. Elices, Evolution of fracture behaviour of saturated concrete in the low temperature range, Engineering Fracture Mechanics 35 (1990) 827–834. https://doi.org/10.1016/0013-7944(90)90167-F.

[159] C. Rocco, J. Planas, GV. Guinea, M. Elices, Fracture properties of concrete under cryogenic conditions, ECF13, San Sebastian (2001) 1–8. http://www.gruppofrattura.it/ocs/index.php/esis/ECF13/paper/download/8513/4955.

[160] M.M. Mirzazadeh, M. Noel, M.F. Green, Effect of low temperature on the shear-fatigue performance of reinforced concrete beams, Proceedings, Annual Conference - Canadian Society for Civil Engineering 4 (2016) 2682–2691.

[161] M. Pigeon, R. Cantin, Flexural properties of steel fiber-reinforced concretes at low temperatures, Cem Concr Compos 20 (1998) 365–375. https://doi.org/10.1016/S0958-9465(98)00017-1.

[162] S. Aidarov, A. Nogales, I. Reynvart, N. Tošić, A. de la Fuente, Effects of Low Temperatures on Flexural Strength of Macro-Synthetic Fiber Reinforced Concrete: Experimental and Numerical Investigation, Materials 15 (2022). https://doi.org/10.3390/ma15031153.

[163] J.-K. Kim, Y.-W. Mai, High Strength, High Fracture Toughness Fibre Composites with Interface Control A Review, Composites Science and Technology 41 (1991) 333-378. https://doi.org/10.1016/0266-3538(91)90072-W

[164] N. Buratti, C. Mazzotti, Temperature effect on the long term behaviour of macro-synthetic-and-steel–fibre reinforced concrete, 8th RILEM International Symposium on Fibre Reinforced Concrete: Challenges and Opportunities (2012).

[165] C. Del Prete, N. Buratti, C. Mazzotti, Experimental analysis of time dependent phenomena and temperature effects on macro-synthetic fibre reinforced concretes in different loading conditions, Constr Build Mater 326 (2022). https://doi.org/10.1016/j.conbuildmat.2022.126904.

[166] A. Llano Torre, P. Serna Ros, J. Rocío Martí Vargas, IMPROVEMENTS IN TEST METHODOLOGY AND CHARACTERISATION OF LONG-TERM FLEXURE BEHAVIOUR OF FIBRE-REINFORCED CONCRETE, 2023.

[167] M. Caballero-Jorna, M. Roig-flores, P. Serna, A study of the flexural behavior of fiber-reinforced concretes exposed to moderate temperatures, Materials 14 (2021). https://doi.org/10.3390/ma14133522.

[168] Z. Bayasi, M. Al Dhaheri, Effect of exposure to elevated temperature on fibrillated polypropylene fiber-reinforced concrete, ACI Mater J 99 (2022) 22–26.

[169] F.B. Varona, F.J. Baeza, D. Bru, S. Ivorra, Influence of high temperature on the mechanical properties of hybrid fibre reinforced normal and high strength concrete, Constr Build Mater 159 (2018) 73–82. https://doi.org/10.1016/j.conbuildmat.2017.10.129.

[170] U. Schneider, Concrete at High Temperatures-A General Review*, Fire Safety Journal, 13 (1988) 55-68. https://doi.org/10.1016/0379-7112(88)90033-1.

[171] N. Tošić, S. Aidarov, A. de la Fuente, Systematic Review on the Creep of Fiber-Reinforced Concrete, Materials 13 (2020). https://doi.org/10.3390/ma13225098.

[172] M. Caballero-Jorna, M. Roig-Flores, P. Serna, Influence of short-term operating temperatures on compression and flexural behaviour of Macro Synthetic and Steel Fibre Reinforced Concretes, Journal of Building Engineering 67 (2023). https://doi.org/10.1016/j.jobe.2023.105919.

[173] F.B. Varona, F.J. Baeza, S. Ivorra, D. Bru, Análisis experimental de la pérdida de adherencia hormigón-acero en hormigones sometidos a altas temperaturas, Dyna (Spain) 90 (2015) 78–86. https://doi.org/10.6036/7184.

[174] H. Cifuentes, J.D. Ríos, C. Leiva, F. Medina, Influencia del tiempo de exposición a altas temperaturas en el comportamiento en fractura de hormigones autocompactantes reforzados con fibras, Anales de Mecánica de Fractura (2016) 1–6.

[175] M. Caballero-Jorna, M. Roig-Flores, P. Serna, Short-Term Effects of Moderate Temperatures on the Mechanical Properties of Steel and Macro-synthetic Fiber Reinforced Concretes, in: RILEM Bookseries, Springer Science and Business Media B.V., 2022: pp. 220–231. https://doi.org/10.1007/978-3-030-83719-8_20.

[176] N. Buratti, C. Mazzotti, Experimental tests on the effect of temperature on the long-term behaviour of macrosynthetic Fibre Reinforced Concretes, Constr Build Mater 95 (2015) 133–142. https://doi.org/10.1016/j.conbuildmat.2015.07.073.

[177] J. Planas, H. Corres, M. Elices, Thermal deformation of loaded concrete during thermal cycles from 20°C to -165°C., Cem Concr Res 14 (1984) 639–644.

[178] A. El-Zohairy, H. Hammontree, E. Oh, P. Moler, Temperature effect on the compressive behavior and constitutive model of plain hardened concrete, Materials 13 (2020) 1–18. https://doi.org/10.3390/ma13122801.

[179] F.-P. Cheng, V K R Kodur, T.-C. Wang, Stress-Strain Curves for High Strength Concrete at Elevated Temperatures, Journal of Materials in Civil Engineering 16 (2004) 84–90. https://doi.org/10.1061/ASCE0899-1561200416:184.

[180] R. Gettu, Z. Zerbino, S. Jose, Factors Influencing Creep of Cracked Fibre Reinforced Concrete: What We Think We Know & What We Do Not Know, in: P. Serna et al. (eds.) (Ed.), Creep Behaviour in Cracked Sections of Fibre Reinforced Concrete, 2017.

[181] K.L. Scrivener, A.K.C. Lyon, F.P. Laugesen, The Interfacial Transition Zone (ITZ) Between Cement Paste and Aggregate in Concrete, Interface Science 12 (2004) 411–421. 10.1023/B:INTS.0000042339.92990.4c

[182] Y.M. Abbas, M. Iqbal Khan, Fiber–Matrix Interactions in Fiber-Reinforced Concrete: A Review, Arab J Sci Eng 41 (2016) 1183–1198. https://doi.org/10.1007/s13369-016-2099-1.

[183] C. Lin, T. Kanstad, S. Jacobsen, G. Ji, Bonding property between fiber and cementitious matrix: A critical review, Constr Build Mater 378 (2023). https://doi.org/10.1016/j.conbuildmat.2023.131169.

[184] K.Y. Liao, P.K. Chang, Y.N. Peng, C.C. Yang, A study on characteristics of interfacial transition zone in concrete, Cem Concr Res 34 (2004) 977–989. https://doi.org/10.1016/j.cemconres.2003.11.019.

[185] A. Bentur, I. Odler, Development and nature of interfacial microstructure., in: Interfacial Transition Zone in Concrete, 1996: pp. 18–44.

[186] S. Zhao, W. Sun, Nano-mechanical behavior of a green ultra-high performance concrete, Constr Build Mater 63 (2014) 150–160. https://doi.org/10.1016/j.conbuildmat.2014.04.029.

[187] L. Xu, F. Deng, Y. Chi, Nano-mechanical behavior of the interfacial transition zone between steel-polypropylene fiber and cement paste, Constr Build Mater 145 (2017) 619–638. https://doi.org/10.1016/j.conbuildmat.2017.04.035.

[188] E. Adili, A. Kheyroddin, Fiber Interfacial Transition Zone Concept for Steel Fiber-Reinforced Concrete by SEM Observation, Journal of Applied Research and Technology 19 (2021) 294–307. https://doi.org/10.22201/icat.24486736e.2021.19.4.1024.

[189] P.A. Bentur, M.G. Alexander, O. Buyukozturk, J. Elsen, D. Hooton, H. Jennings, A. Katz, K.O. Kjellsen, A. Kronlof, B. Laggerblad, S. Mindess, J. OUivier, A review of the work of the RILEM TC 159-ETC: Engineering of the interfacial transition zone in cementitious composites, 2000.

[190] M.G. Alberti, A. Enfedaque, J.C. Gálvez, A. Ferreras, Pull-out behaviour and interface critical parameters of polyolefin fibres embedded in mortar and self-compacting concrete matrixes, Constr Build Mater 112 (2016) 607–622. https://doi.org/10.1016/j.conbuildmat.2016.02.128.

[191] A.J. Babafemi, W.P. Boshoff, Pull-out response of macro synthetic fibre from concrete matrix: Effect of loading rate and embedment length, Constr Build Mater 135 (2017) 590–599. https://doi.org/10.1016/j.conbuildmat.2016.12.160.

[192] S. Garcia, A.E. Naamanl, J. Pera, Experimental investigation onthe potential use of poly(vinyl alcohol) short fibers in fiber-reinforced cement-based composites, Materials and Structures 30 (1997) 43–52. 10.1007/BF02498739.

[193] S. Abdallah, M. Fan, D.W.A. Rees, Effect of elevated temperature on pull-out behaviour of 4DH/5DH hooked end steel fibres, Compos Struct 165 (2017) 180–191. https://doi.org/10.1016/j.compstruct.2017.01.005.

[194] S. Abdallah, M. Fan, K.A. Cashell, Pull-out behaviour of straight and hooked-end steel fibres under elevated temperatures, Cem Concr Res 95 (2017) 132–140. https://doi.org/10.1016/j.cemconres.2017.02.010.

[195] S. Singh, A. Shukla, R. Brown, Pullout behavior of polypropylene fibers from cementitious matrix, Cem Concr Res 34 (2004) 1919–1925. https://doi.org/10.1016/j.cemconres.2004.02.014.

[196] J.O. Lerch, H.L. Bester, A.S. Van Rooyen, R. Combrinck, W.I. de Villiers, W.P. Boshoff, The effect of mixing on the performance of macro synthetic fibre reinforced concrete, Cem Concr Res 103 (2018) 130–139. https://doi.org/10.1016/j.cemconres.2017.10.010.

[197] AENOR, UNE-EN-12504-3: Ensayos de hormigón en estructuras. Parte 3: Determinación de la fuerza de arrancamiento, (2006).

[198] A. Abrishambaf, M. Pimentel, S. Nunes, A meso-mechanical model to simulate the tensile behaviour of ultra-high performance fibre-reinforced cementitious composites, Compos Struct 222 (2019). https://doi.org/10.1016/j.compstruct.2019.110911.

[199] A. Amin, S.J. Foster, R.I. Gilbert, W. Kaufmann, Material characterisation of macro synthetic fibre reinforced concrete, Cem Concr Compos 84 (2017) 124–133. https://doi.org/10.1016/j.cemconcomp.2017.08.018.

[200] A. Blanco, P. Pujadas, A. De La Fuente, S. Cavalaro, A. Aguado, Application of constitutive models in European codes to RC-FRC, Constr Build Mater 40 (2013) 246–259. https://doi.org/10.1016/j.conbuildmat.2012.09.096.

[201] European Committee for Standarisation, UNE-EN 1992-1-2:2011/A1:2021 Eurocódigo 2: Proyecto de estructuras de hormigón. Parte 1-2: Reglas generales. Proyecto de estructuras sometidas al fuego.

[202] E.S. Bernard, Age-dependent changes in post-crack performance of fibre reinforced shotcrete linings, Tunnelling and Underground Space Technology 49 (2015) 241–248. https://doi.org/10.1016/j.tust.2015.05.006.

[203] G. Plizzari, P. Serna, Structural effects of FRC creep, Materials and Structures/Materiaux et Constructions 51 (2018) 1–11. https://doi.org/10.1617/s11527-018-1290-0.

[204] P. Pujadas, A. Blanco, S. Cavalaro, A. de la Fuente, A. Aguado, The need to consider flexural post-cracking creep behavior of macro-synthetic fiber reinforced concrete, Constr Build Mater 149 (2017) 790–800. https://doi.org/10.1016/j.conbuildmat.2017.05.166.

[205] AENOR, EN 14889-1:2008: Fibras para hormigón. Parte 1: Fibras de acero. Definiciones, especificaciones y conformidad, (2008).

[206] AENOR, UNE-EN-14845-1: Métodos de ensayo para fibras para hormigón. Parte 1: Hormigones de referencia, (2008).

[207] AENOR, UNE-EN-14649: Productos prefabricados de hormigón. Método de ensayo para la determinación de la resistencia remanente de las fibras de vidrio en el cemento y el hormigón (ensayo SIC), (2006).

[208] C. Del Prete, B. Buratti, C. Mazzotti, Influence of moderate temperature variation on fibers for MSFRCs, in: Atti Italian Concrete Conference 2022 Edizione PDF, 2022: pp. 842–846.

[209] AENOR, UNE-EN 12350-2. Ensayos de hormigón fresco. Parte 2: Ensayo de asentamiento, (2009).

[210] AENOR, UNE-EN 12350-7. Ensayos de hormigón fresco. Parte 7: Determinación del contenido de aire. Métodos de presión., (2010).

[211] AENOR, UNE-EN 12350-6. Ensayos de hormigón fresco Parte 6: Densidad, (2020).

[212] AENOR, UNE-EN 12390-3:2009. Determinación de la resistencia a compresión de probetas, (2009).

[213] M. Caballero-Jorna, M. Roig-Flores, P. Serna, An Experimental Study of the Influence of Moderate Temperatures on the Behavior of Macrosynthetic Fiber Reinforced Concrete, RILEM Bookseries 30 (2021) 322–332. https://doi.org/10.1007/978-3-030-58482-5_30.

[214] N. Banthia, J.-F. Trottier, Micromechanics of Steel Fiber Pull-Out: Rate Sensitivity at Very Low Temperatures, Cement and Concrete Composite 14 (1992) 119–130. https://doi.org/10.1016/0958-9465(92)90005-G

[215] R. Castellanos Castellón, Comportamiento mecánico del hormigón reforzado con fibras de poliolefina bajo la acción de temperatura elevada, Thesis Dissertation, Universidad Politécnica de Madrid, 2018.

[216] K.K. Sideris, P. Manita, E. Chaniotakis, Performance of thermally damaged fibre reinforced concretes, Constr Build Mater 23 (2009) 1232–1239. https://doi.org/10.1016/j.conbuildmat.2008.08.009.

[217] Y. Bai, T. Keller, T. Vallée, Modeling of stiffness of FRP composites under elevated and high temperatures, Compos Sci Technol 68 (2008) 3099–3106. 10.1016/j.compscitech.2008.07.005

[218] A. Cwirzen, The effect of the heat-treatment regime on the properties of reactive powder concrete, Advances in Cement Research 19 (2007) 25–33. https://doi.org/10.1680/adcr.2007.19.1.25.

[219] L. Jin, X. Du, G. Ma, Macroscopic effective moduli and tensile strength of saturated concrete, Cem Concr Res 42 (2012) 1590–1600. https://doi.org/10.1016/j.cemconres.2012.09.012.

[220] B. Bhusan Das, D. Narain Singh, B. Das, D. Singh, S. Pandey, Influence of initial curing humidity on compressive strength and ultrasonic properties of concrete, 2014. https://www.researchgate.net/publication/286193465.

[221] S. Calavaro, A. Aguado, Intrinsic scatter of FRC: an alternative philosophy to estimate characteristic values, Mater Struct 48 (2015) 3537–3555. https://doi.org/10.1617/s11527-014-0420-6.

[222] P. Acharya, C. Mazzotti, N. Buratti, C. Del Prete, Study of temperature variation effects on the mechanical behaviour of polypropylene fibers in macro-synthetic fiber reinforced concrete, Master Dissertation, Università di Bologna, 2021.

[223] A.E. Richardson, Bond characteristics of structural polypropylene fibres in concrete with regard to post-crack strength and durable design, Structural Survey 23 (2005) 210–230. https://doi.org/10.1108/02630800510610143.

[224] Y. Chen, P. Liu, Z. Yu, Effects of environmental factors on concrete carbonation depth and compressive strength, Materials 11 (2018). https://doi.org/10.3390/ma11112167.

[225] J. Komonen, V. Penttala, Effects of High Temperature on the Pore Structure and Strength of Plain and Polypropylene Fiber Reinforced Cement Pastes, Fire Technology 39 (2003) 23-34.

[226] Fib, Model Code for Concrete Structures 2020 (MC2020), 2021.

[227] A. De la Fuente, A. Monserrat-López, N. Tosic, P. Serna, Design of Steel Fibre Reinforced Concrete Structures According to the Annex L of the Eurocode-2 2023, Hormigón y Acero (2023). https://doi.org/10.33586/hya.2023.3124.

[228] I. Soroka, CONCRETE IN HOT ENVIRONMENTS, First edition 1993, London, 2004.

[229] F.T. Al Rikabi, S.M. Sargand, I. Khoury, H.H. Hussein, Material Properties of Synthetic Fiber–Reinforced Concrete under Freeze-Thaw Conditions, Journal of Materials in Civil Engineering 30 (2018). https://doi.org/10.1061/(asce)mt.1943-5533.0002297.

[230] Zdenëk P. Bazant, Pere C. Prat, Effect of Temperature and Humidity on Fracture Energy of Concrete, ACI Mater J 85 (1988) 262–271. http://worldcat.org/issn/0889325X

[231] ACI, “What is the effect of aging on concrete?”, Technical Questions. https://www.concrete.org/tools/frequentlyaskedquestions.aspx?faqid=646 (accessed May 2024)

[232] E.S. Bernard, Changes in long-term performance of fibre reinforced shotcrete due to corrosion and embrittlement, Tunnelling and Underground Space Technology 98 (2020). https://doi.org/10.1016/j.tust.2020.103335.

[233] T.E. Teixeira Buttignol, M. Colombo, M. di Prisco, Long-term aging effects on tensile characterization of steel fibre reinforced concrete, Structural

Concrete 17 (2016) 1082–1093. https://doi.org/10.1002/suco.201500149.

[234] A. Llano-Torre, P. Serna, eds., Round-Robin Test on Creep Behaviour in Cracked Sections of FRC: Experimental Program, Results and Database Analysis, Springer International Publishing, Cham, 2021. https://doi.org/10.1007/978-3-030-72736-9.

[235] STATGRAPHICS ® Centurion XVII Manual de Usuario, (2014). www.STATGRAPHICS.com.

[236] R.L. Wasserstein, N.A. Lazar, The ASA's Statement on p-Values: Context, Process, and Purpose, American Statistician 70 (2016) 129–133. https://doi.org/10.1080/00031305.2016.1154108.

[237] E.J. García Taengua, Bond of Reinforcing Bars to Steel Fiber Reinforced Concrete (SFRC), Thesis Dissertation, Universitat Politècnica de València, 2013.

[238] C. Del Prete, R. Wan-Wendner, N. Buratti, C. Mazzotti, Parametric study of the Lattice Discrete Particle Model (LDPM) constitutive law for fiber reinforced concretes (FRCs), in: Computational Modelling of Concrete and Concrete Structures, CRC Press, 2022: pp. 525–532. https://doi.org/10.1201/9781003316404-62.